Universidad de Santiago de Compostela
Facultad de Farmacia
Departamento de Farmacia y Tecnología Farmacéutica

Desarrollo de micro- y nanopartículas de polisacáridos para la administración pulmonar y nasal de macromoléculas terapéuticas

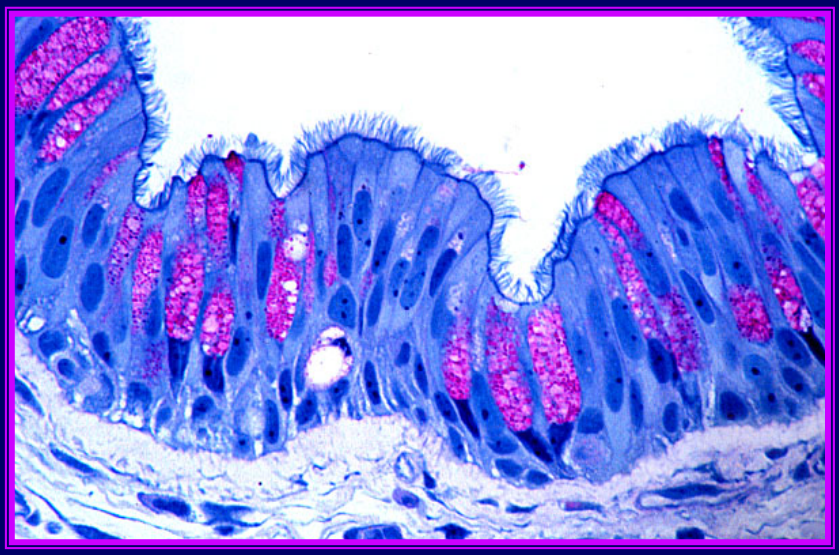

Desirée Teijeiro Osorio

Santiago de Compostela, 2007

UNIVERSIDAD DE SANTIAGO DE COMPOSTELA

FACULTAD DE FARMACIA

Departamento de Farmacia y Tecnología Farmacéutica

DESARROLLO DE MICRO- Y NANOPARTÍCULAS DE POLISACÁRIDOS PARA LA ADMINISTRACIÓN PULMONAR Y NASAL DE MACROMOLÉCULAS TERAPÉUTICAS

Desirée Teijeiro Osorio

Santiago de Compostela, 2007

AGRADECIMIENTOS

Y por fin llegó el día de agradecer y dedicar... Una buena señal, ya que significa que el trabajo de estos años se ha visto culminado... aunque bueno, he de reconocer que no esperé al último día para escribir estas palabras, porque no quisiera que las prisas me hiciesen olvidar a alguien, a buen seguro importante.

Me gustaría dividir este apartado en dos grupos; el de aquellos que me han dirigido, orientado o ayudado a nivel profesional y el de todos los que me apoyaron y han estado a mi lado a nivel personal. Sin embargo, y me siento muy afortunada por ello, en parte ambos han conseguido converger y solaparse, y así, puedo decir que entre los que empezaron siendo compañeros he encontrado verdaderos amigos. Ellos lo saben.

Así, por contribuir en la realización de esta Tesis Doctoral, debo expresar mi profundo agradecimiento:

- *A mis Directoras de tesis, Carmen Remuñán López y María José Alonso, por su orientación, esfuerzo y apoyo durante estos años.*
- *A los demás profesores del grupo de investigación: Alejandro Sánchez, Begoña Seijo y Dolores Torres, por la ayuda brindada ante cualquier duda o problema.*
- *A la Dra. Hanne Mørck Nielsen, de la "Faculty of Pharmaceutical Sciences" de Copenhague, por su amistosa acogida a mi llegada a Dinamarca y su preocupación por hacerme sentir en casa, por su enorme y cercano apoyo en el desarrollo de nuestro proyecto y por su contagiososo entusiasmo. También a A S. Sørensen y B. Dinitzen, técnicos de células del departamento y, en general, a todo el grupo de investigación, por hacerme sentir una más y compartir conmigo esos maravillosos seminarios-desayuno con sabor danés.*
- *A Miro, Merche y Raquel, del Servicio de Microscopía, por su ayuda y su paciencia en el trabajo de Microscopía Electrónica y Confocal.*
- *A Mónica, Pepo y Salva, del Departamento de Farmacología, por ayudarme con mis últimos experimentos con células.*

- *A Carlos y Kim, por su entusiasta colaboración en la realización experimental de parte de los artículos 1 y 2 recogidos en esta memoria.*
- *A Rafa, por su valiosa ayuda en los estudios con animales y siempre que lo he necesitado.*
- *A los compañeros del Departamento que he sentido más cerca durante estos años y que de uno u otro modo me han brindado su ayuda y apoyo: tanto a los que ya eran más o menos veteranos cuando empecé: Dayamí, Ana Vila, Ana Gómez, Noemi y Marcos; como a los que se han ido incorporando a lo largo de este tiempo: Vicky, Nela, Sascha, Francisco, Yolanda e Ivana. Mención especial para María Alonso y María de la Fuente, con quienes he compartido el inicio, los logros y tropiezos del transcurso y la satisfacción del final...gracias por su infinita paciencia, sus consejos y su confianza, siempre.*

Y ahora, de un modo más personal, por estar siempre a mi lado y formar parte de mi vida, agradezco y dedico esta Tesis:

- *A Bea Lantero, siempre cercana en la distancia.*
- *A Ana, Natalia, Pili, Amayita, Lorena, Rocío, Álvaro y Juan.*
- *A mis amigos de Chantada: Laura, Elena, Meju, María, Patri, Bea y Mónica.*
- *A Ada y Diego, por hacer inolvidable mi estancia en Dinamarca, y a Lyse, Ulrik, Thomas y Casper, mi "familia" danesa.*
- *A la pandi de mis Marías, y sus respectivos Pedrito y David, a Ruth, Fran, Noemi y Marcos.*
- *A mi FAMILIA, y en especial: a mi tía Isa, por su entusiasmo a cada paso, por sentir mis logros suyos; a mis tíos Jose y Oti y mis primas Estela y Carolina, por confiar en mis posibilidades seguro que más que yo misma; a mis padrinos y mi tía Balbi, por su cariño y apoyo constante aún en la distancia; a mis abuelos Rodrigo y Maruja, por no necesitar saber para creer; a mi tía Jesusa, que cada día reza por mi y los míos; y a mis abuelos Lisardo y Elvira y mi tío Segundo, a los que, estén donde estén, siento y sentiré siempre a mi lado.*

- *Mención especial se merecen mis PADRES, a quienes dedico especialmente esta Tesis y a quienes no bastaría una vida para agradecer. Ellos me han enseñado todo lo que de verdad importa y que cada día es más difícil aprender: el valor del trabajo, el sacrificio, la lealtad, la humildad, el amor y la verdad. Gracias por su cariño y apoyo incondicional.*
- *A mi hermana Alba, la eterna "peque" de la casa, por su confianza y comprensión, sus abrazos y mimos, y su alegría y optimismo, a veces inevitable y afortunadamente contagiosos ;-).*
- *A mi particular "niño" Jesús, al que conocí al inicio de esta aventura y que me ha acompañado y apoyado incondicionalmente, con mucha paciencia, complicidad y amor, tanto en los momentos de descacharradas risas como en el llanto del desánimo y las despedidas. A él debo buena parte de esto y con él espero compartir todo lo que esté por venir...*

A todos, GRACIAS

DÑA CARMEN REMUÑÁN LÓPEZ Y DÑA MARÍA JOSÉ ALONSO FERNÁNDEZ, PROFESORA TITULAR Y CATEDRÁTICA, RESPECTIVAMENTE, DEL DEPARTAMENTO DE FARMACIA Y TECNOLOGÍA FARMACÉUTICA DE LA UNIVERSIDAD DE SANTIAGO DE COMPOSTELA

INFORMAN:

Que la presente memoria titulada "**DESARROLLO DE MICRO- Y NANOPARTÍCULAS DE POLISACÁRIDOS PARA LA ADMINISTRACIÓN PULMONAR Y NASAL DE MACROMOLÉCULAS TERAPÉUTICAS"** elaborada por la Licenciada en Farmacia **Dña. Desirée Teijeiro Osorio,** ha sido realizada bajo su dirección en el Departamento de Farmacia y Tecnología Farmacéutica y, hallándose concluida, autorizan su presentación, a fin de que pueda ser juzgada por el tribunal correspondiente.

Y para que así conste, expiden y firman el presente informe en Santiago de Compostela, a 21 de Julio de 2007.

Fdo: C. Remuñán López

Fdo: M.J. Alonso Fernández

ÍNDICE

Introducción

INTRODUCCIÓN

1. Interés de las vías pulmonar y nasal para la administración de macromoléculas terapéuticas

Los avances producidos en los últimos años en el campo de la biotecnología han dado lugar a la obtención de nuevas macromoléculas, tales como péptidos, proteínas, antígenos y ADN plasmídico, que poseen un enorme potencial terapéutico. La mayor parte de estos compuestos comparten, sin embargo, una serie de limitaciones para su administración por la vía oral, dada su inestabilidad e intensa degradación proteolítica en los fluidos gastrointestinales, y su elevado peso molecular e hidrofilia, características que dificultan su paso a través del epitelio intestinal. Es por ello que la mayoría de los tratamientos establecidos para este tipo de macromoléculas recurren a administración parenteral, la cual conlleva una serie de inconvenientes a diversos niveles, principalmente un elevado coste de producción, el requerimiento de personal especializado para su administración y la baja aceptación y el consiguiente incumplimiento de la pauta posológica por parte del paciente.

En los últimos años, las vías nasal y pulmonar han adquirido un gran interés como rutas alternativas a la parenteral para la administración de nuevas macromoléculas terapéuticas con efecto sistémico. Esto es debido, principalmente, a que los epitelios nasal y alveolar constituyen zonas de absorción relativamente permeables y altamente irrigadas, que evitan el efecto de primer paso hepático y que poseen una baja actividad enzimática en comparación a la gastro-intestinal[1,2] (**Figura 1**).

[1] **Arora P., Sharma S., Garg S.**, Permeability issues in nasal drug delivery, DDT, 7 (2002) 967-975.

[2] **Patton J.S., Platz R.M.**, Routes of delivery: case studies. 2. Pulmonary delivery of peptides and proteins for systemic action, Adv. Drug. Del. Rev., 8 (1992) 179-196.

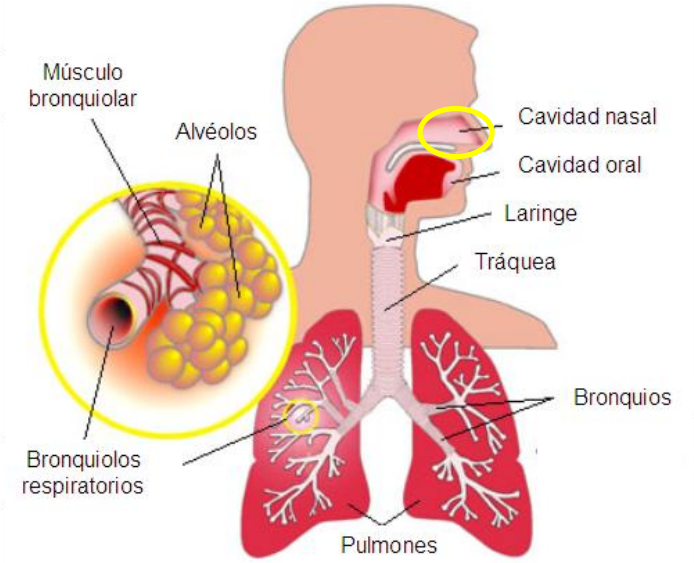

Figura 1. Dibujo de las distintas partes que componen el tracto respiratorio. Especialmente señaladas se hallan las zonas nasal y alveolar, donde la absorción sistémica es más importante (adaptado de http://www.medicinenet.com).

Sin embargo, también presentan una serie de limitaciones relacionadas con los propios mecanismos de defensa del organismo. Estos son, en el caso de la vía pulmonar: a) el *recodo orofaríngeo*, donde se depositan las partículas inhaladas mayores de 8 μm[3]; b) el *ascensor mucociliar*, en el que se ven implicados la capa de mucus y los cilios epiteliales, que envuelven, atrapan y expulsan hacia el exterior las partículas extrañas ($\approx$4-6 μm) que hayan podido penetrar en la región traqueobronquial[4]; c) los *macrófagos alveolares*, que constituyen la principal línea de defensa del pulmón y capturan las partículas inhaladas (virus, bacterias,

[3] **Hanes J., Dawson M., Har-el Y., Suh J., Fiegel J.**, Gene delivery to the lung. En: Hickey A.J. (Ed.), Pharmaceutical inhalation aerosol technology, Marcel Dekker, New York, (2004) pp. 489-539.

[4] **Altiere R.J., Thompson D.C.**, Physiology and Pharmacology of the airways. En: Hickey A.J. (Ed.), Inhalation aerosols: physical and biological basis for therapy, Marcel Dekker, New York, (1996) pp. 85-138.

polvo,...) que han escapado previamente al aclaramiento mucociliar[5]; y d) la propia eliminación con el aire exhalado de las partículas que, por su extremadamente pequeño tamaño, no han llegado a depositarse en la zona alveolar.

En el caso de la vía nasal, de más fácil acceso que la pulmonar, destaca el intenso y rápido aclaramiento mucociliar[6], que da lugar a la completa renovación del mucus cada 12-15 minutos[7,8] y que, obviamente, limita el tiempo de contacto de los fármacos con el epitelio de absorción[9].

En las **Tablas 1** y **2** se reflejan las principales características de las vías pulmonar y nasal, agrupadas en una serie de ventajas y limitaciones, que dejan patentes, asimismo, unos requerimientos de formulación específicos a la hora de administrar sistémicamente macromoléculas por cada una de ellas. De este modo, mientras para la vía nasal es de extrema importancia conseguir incrementar el tiempo de residencia de la formulación en la cavidad nasal (reduciendo así el proceso de aclaramiento mucociliar) y aumentar la permeabilidad de las macromoléculas a través del epitelio; el éxito de la administración por vía pulmonar radica, fundamentalmente, en conseguir que la formulación evite los mecanismos de defensa y alcance la región adecuada del pulmón[10].

[5] **Ahsan F., Rivas I.P., Khan M.A., Torres-Suárez A.I.**, Targeting to macrophages: role of physicochemical properties of particulate carriers-liposomes and microspheres- on the phagocytosis by macrophages, J. Control. Rel., 79 (2002) 29-40.

[6] **Türker S., Onur E., Özer Y.**, Nasal route and drug delivery systems, Pharm. World Sci., 26 (2004) 137-142.

[7] **Martín E., Schipper N.G.M., Verhoef J.C., Merkus W.H.M.**, Nasal mucociliary clearance as factor in nasal drug delivery, Adv. Drug Del. Rev., 29 (1998) 13-38.

[8] **Gizurarson S.**, Animal models for intranasal drug delivery studies, Acta. Pharm. Nord., 2 (1990) 105-122.

[9] **Mygind N., Dahl R.**, Anatomy, physiology and function of the nasal cavities in health and disease, Adv. Drug Del. Rev., 29 (1998) 3-12.

[10] **Davis S.S**., Delivery of peptide and non-peptide drugs through the respiratory tract, PSTT, 2 (1999) 450-456.

Tabla 1. Principales ventajas e inconvenientes de la administración sistémica de macromoléculas por vía pulmonar[11]

Ventajas		Limitaciones
Ruta de administración no invasiva		Estructura del tracto respiratorio que actúa como filtro de partículas
Gran superficie de absorción alveolar (100 m^2)	↑permeabilidad	Aclaramiento mucociliar
Elevada irrigación		Macrófagos alveolares
Bajo grosor del epitelio alveolar (0.1-0.2 μm)[12]		Eliminación de partículas por exhalación
Baja actividad proteolítica en comparación con la vía oral		Absorción muy influenciada por las condiciones fisiológicas y patológicas
No efecto de primer paso hepático		Dificultad de manipulación de inhaladores
Rápida absorción y comienzo del efecto		Diversos problemas de reproducibilidad

Tabla 2. Principales ventajas e inconvenientes de la administración sistémica de macromoléculas por vía nasal[13,14]

Ventajas	Limitaciones
Ruta de administración no invasiva y de fácil acceso	Limitado volumen de administración (≈150μL/fosa nasal)[15]
Relativamente elevada superficie de absorción (150cm^2)[16]	Rápido aclaramiento mucociliar (≈15 min)
Elevada irrigación	Baja absorción de moléculas con PM >1 kDa
Baja actividad proteolítica en comparación con la vía oral	Gran variabilidad inter-especie, dificultad de extrapolación de resultados
No efecto de primer paso hepático	Absorción influenciada por condiciones fisiológicas y patológicas
Rápida absorción y comienzo del efecto	Irritación de la mucosa nasal

[11] **Grenha A., Carrión-Recio D., Teijeiro-Osorio D., Seijo B., Remuñán-López C.**, 2007 (ver **Anexo I** de la presente memoria)

[12] **Patton J.S.**, Mechanisms of macromolecule absorption by the lungs, Adv. Drug Del. Rev., 19 (1996) 3-36.

[13] **Arora P., Sharma S., Garg S.**, Permeability issues in nasal drug delivery, DDT, 7 (2002) 967-975.

[14] **Davis S.S.**, Delivery of peptide and non-peptide drugs through the respiratory tract, PSTT, 2 (1999) 450-456.

[15] **Gizurarson S.**, Animal models for intranasal drug delivery studies, Acta. Pharm. Nord., 2 (1990) 105-122.

[16] **Sharma P., Chaudhari P., Kolsure P., Ajab A., Varia N.**, Recent trends in nasal drug delivery - an overview, http://www.pharmainfo.net (consultada el 21/03/07).

2. Administración de macromoléculas terapéuticas por vía pulmonar: sistemas microparticulares

Así pues, el mayor reto de la administración sistémica de fármacos por vía pulmonar reside en que éstos, una vez inhalados, alcancen la región alveolar del tracto respiratorio, donde la elevada irrigación y permeabilidad del epitelio, así como la gran superficie expuesta y la ausencia de mucus, van a favorecer su absorción.

Entre los factores tecnológicos que condicionan el lugar de depósito de los fármacos inhalados se encuentran: naturaleza del material, distribución de tamaños, densidad y morfología de las partículas y contenido en humedad. En este sentido, es sabido que la disminución de la densidad de las partículas acompañada de un aumento de su tamaño, consigue mejorar el comportamiento del aerosol, al verse disminuida su tendencia a la aglomeración en comparación a las partículas convencionales pequeñas y compactas o no porosas[17]. Recientemente se ha propuesto un importante parámetro, el diámetro aerodinámico, que combina la influencia del tamaño físico con la inercia de la partícula, condicionada por su densidad[18]. Las partículas que poseen un diámetro aerodinámico de entre 1 y 5 μm son capaces de llegar a las zonas más profundas del pulmón y depositarse[19]. Esta fracción de partículas se denomina "fracción respirable".

Los trabajos más recientes en el campo de la administración pulmonar de moléculas activas se centran en el diseño y formulación de sistemas de inhalación microparticulares, que pueden ser preparados con diferentes características morfológicas (forma y porosidad) y aerodinámicas (tamaño y densidad) mediante la modificación de distintas variables en el proceso de producción.

---

[17] **Li W.-I., Perlz M., Heyder J., Langer R., Brain J.D., Englmeier K.-H., Niven R.W., Edwards D.A.**, Aerodynamics and aerosol particle deaggregation phenomena in model oral-pharyngeal cavities, J. Aerosol Sci., 27 (1996) 1269-1286.

[18] **Edwards D.A., Ben-Jebria A., Langer R**., Recent advances in pulmonary drug delivery using large, porous inhaled particles, J. Applied Physiol., 85 (1998) 379-385.

[19] **Vanbever R., Ben-Jebria A., Mintzes J. D., Langer R., Edwards D. A.**, Sustained release of insulin from insoluble inhaled particles, Drug Deliv. Research, 48 (1999) 178-185.

El desarrollo de un sistema microparticular que garantice que la práctica totalidad del fármaco llegue a su correspondiente lugar de acción, permitiría disminuir los efectos secundarios asociados a un depósito prematuro, el número de dosis y, en definitiva, mejoraría la eficacia del tratamiento. Este hecho reviste una importancia adicional cuando se trata de macromoléculas, como péptidos y proteínas, cuyo coste hace que un dispositivo ineficaz convierta la terapia en prohibitiva a nivel económico[20].

Existen diversos estudios *in vivo* en los que se han obtenido prometedores resultados tras la administración pulmonar de distintos tipos de micropartículas o microsferas con diferentes fines terapéuticos. De una forma más específica, en la **Tabla 3** se muestran aquellos que han sido realizados con sistemas microparticulares, compuestos por polímeros de origen sintético o natural, destinados a la administración pulmonar de macromoléculas de acción sistémica.

Adicionalmente, en el **ANEXO I** de esta memoria se adjunta una completa revisión general de los trabajos *in vitro* e *in vivo* relacionados con la administración pulmonar de fármacos, abarcando, además de las micropartículas, otros sistemas propuestos, tales como nanopartículas y sistemas combinados de nano- y micropartículas. Asimismo, en dicha revisión, se incluye una amplia introducción que abarca, de un modo más extenso, los factores que afectan la administración de moléculas activas por vía pulmonar, así como sus distintas aplicaciones terapéuticas, mencionando además aquellas formulaciones ya comercializadas o recientemente aprobadas para su próxima comercialización.

[20] **Cryan S.-A**., Carrier-based strategies for targeting protein and peptide drugs to the lungs, The AAPS J., 7 (2005) E20-E41 (http://www.aapsj.org)

Tabla 3. Estudios *in vivo* correspondientes a la administración pulmonar de macromoléculas de acción sistémica encapsuladas en sistemas microparticulares poliméricos.

Polímero	Macromolécula	Modelo animal	Parámetro investigado
PLGA (Air™, Alkermes)	Insulina	Rata	Descenso glucemia y biodisponibilidad[21]
PLGA	Insulina	Rata	Descenso de glucemia[22]
PLGA	Insulina[a]	Rata	Descenso glucemia[23]
PEG-fosfato cálcico	Insulina	Rata	Parámetros farmacocinéticos y farmacodinámicos[24]
Derivados de diketopiperazina (Technospheres™)	Insulina	—[b]	Descenso de glucemia, biodisponibilidad[25,26]
Ácido hialurónico e hidroxipropilcelulosa	Insulina	Perro raza *Beagle*	Parámetros farmacocinéticos[27]
Quitosano	Insulina	Rata	Descenso de glucemia[28]

[a] Complejo con ciclodextrina; [b] Voluntarios humanos

PLGA: ácido poliláctico-co-glicólico; PEG: polietilenglicol.

[21] **Edwards D.A., Hanes J., Caponetti G., Hikach J., Ben-Jebria A., Eskew M.L., Mintzes J., Deaver D., Lotan N., Langer R.**, Large porous particles for pulmonary drug delivery, Science, 276 (1997) 1868-1871.

[22] **Kawashima Y., Yamamoto H., Takeuchi H., Fujioka S., Hino T.**, Pulmonary delivery of insulin with nebulized DL-lactide/glycolide copolymer (PLGA) nanospheres to prolong hypoglycemic effect, J. Control. Rel., 62 (1999) 279-287.

[23] **Aguiar M.M.G., Rodríguez J.M., Silva C.A.**, Encapsulation of insulin-cyclodextrin complex in PLGA microspheres: a new approach for prolonged pulmonary insulin delivery, J. Microencapsul., 21 (2004) 553-564.

[24] **García-Contreras L., Morcol T., Bell S.J., Hickey A.J.**, Evaluation of novel particles as pulmonary delivery systems for insulin in rats, AAPS Pharm. Sci., (2003) 1-11 (http://www.aapsj.org)

[25] **Pfutzner A., Mann A.E., Steiner S.,** Technosphere™/insulin- a new approach for effective delivery of human insulin via the pulmonary route, Diabetes Tech. Ther., 4 (2002) 589-594.

[26] **Steiner S., Pfutzner A., Harzer O., Heineman L., Rave K.**, Technosphere™/insulin- Proof of concept study with a new insulin formulation for pulmonary delivery, Exp. Clin. Endocrinol. Diabetes, 110 (2002) 17-21.

[27] **Surendrakumar K., Martín G.P., Hodgers E.C.M., Jansen M., Blair J.A.**, Sustained release of insulin from sodium hyaluronate based dry powder formulations after pulmonary delivery to beagle dogs, J. Control. Rel., 91 (2003) 385-394.

[28] **Carrión-Recio D., Taboada-Montero C., Vila-Jato J.L., Remuñán-López C.**, Enhancement of protein lung absorption using chitosan microspheres, *(sometida a evaluación)*

De entre estos trabajos, cabe destacar la interesante aportación de nuestro grupo de investigación, a través del desarrollo de microsferas de quitosano para la administración pulmonar de macromoléculas terapéuticas y la evaluación de su potencial *in vivo*. Para ello, se encapsuló insulina como molécula modelo y se midió la respuesta hipoglucémica tras la administración intratraqueal a ratas de las microsferas en forma de polvo seco. Como se puede observar en la **Figura 2** los resultados fueron muy satisfactorios. Obviamente, este hecho generó un interés adicional por continuar trabajando en esta línea, concretamente en el desarrollo y caracterización de nuevos sistemas polisacarídicos para la administración pulmonar de macromoléculas, de lo cual es objeto la primera parte de la presente memoria.

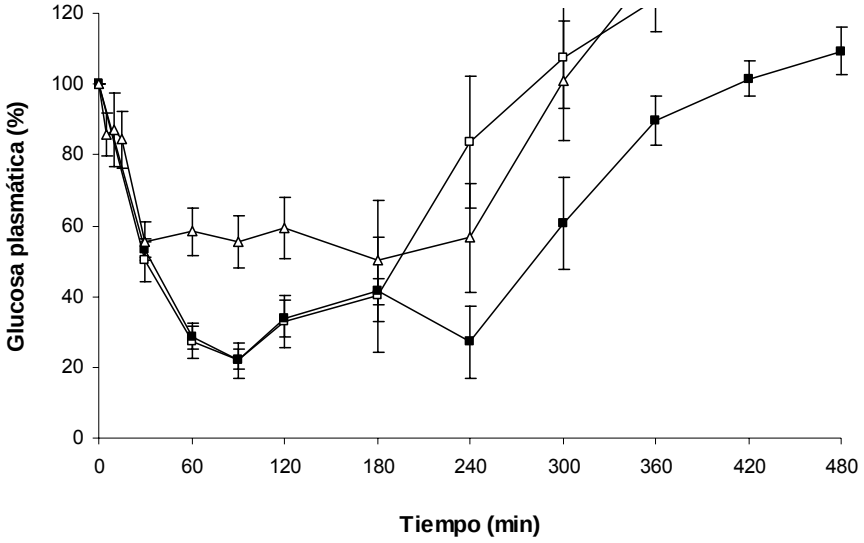

Figura 2. Efecto hipoglucémico obtenido tras la administración intratraqueal de: (Δ) solución de insulina en PBS pH 7.4; (□) 750 μg de microsferas de quitosano (15% de carga de insulina); y (■) 1500 μg de microsferas de quitosano (7.5% de carga de insulina) a ratas (media ± SEM, *n* = 5-6). Dosis de insulina = 13.1 U/Kg.

3. Administración de macromoléculas por vía nasal: sistemas nanoparticulares

A la hora de diseñar una formulación dirigida a la administración de macromoléculas por vía nasal existen tres limitaciones principales que solventar: (1) el rápido aclaramiento mucociliar; (2) la baja permeabilidad del epitelio nasal para aquellas moléculas mayores de 1KDa; y (3) la posible degradación enzimática de las mismas. Así pues, entre las diversas estrategias propuestas con el fin de aumentar significativamente la biodisponibilidad de péptidos y proteínas por vía nasal se encuentra el empleo de inhibidores enzimáticos[29] y, sobretodo, de promotores de la absorción, tales como surfactantes, sales biliares, ácidos grasos, fosfolípidos, glucósidos o disacáridos modificados y ciclodextrinas[30,31,32,33]. Sus principales mecanismos de acción se resumen en: (a) incrementar la permeabilidad de la membrana celular, principalmente mediante la extracción de alguno de sus componentes o la alteración/desorden de sus fosfolípidos; (b) aumentar la lipofilia del fármaco; (c) formar poros acuosos intracelulares; y (d) abrir las uniones íntimas o uniones "tight" intercelulares[34].

Sin embargo, algunos de estos promotores de la absorción provocan daños irreversibles en la mucosa nasal y, además, su administración en solución, junto con el compuesto activo, no solventa el problema del rápido aclaramiento mucociliar. En consecuencia, algunas de las estrategias dirigidas específicamente a

[29] **Dondeti P., Zia H., Needham T.E.**, Bioadhesive and formulation parameters affecting nasal absorption, Int. J. Pharm., 127 (1996) 115-133.

[30] **Gordon G.S., Moses A.C., Silver R.D., Flier J.S., Carey M.C**., Nasal absorption of insulin: enhancement by hydrophobic bile salts, Proc. Natl. Acad. Sci. USA, 82 (1985) 7419-7423.

[31] **Merkus F.W., Verhoef J.C., Marttin E., Romeijn S.G., van der Kuy P.H.M., Hermens W.A.J.J., Schipper N.G.M.**, Cyclodextrins in nasal drug delivery, Adv. Drug Deliv. Rev., 36 (1999) 41-57.

[32] **Pillion D.J., Ahsan F., Arnold J., Balasubramaniam B.M, Piraner O., Meezan E**., Synthetic long chain alkyl maltosides and alkyl sucrose esters as enhancers of nasal insulin absorption, J. Pharm. Sci., 91 (2002) 1456-1462.

[33] **Hirai S., Yashiki T., Mima H.**, Effect of surfactants on the nasal absorption of insulin in rats, Int. J. Pharm., 9 (1981) 165-172.

[34] **Sharma P., Chaudhari P., Kolsure P., Ajab A., Varia N.**, Recent trends in nasal drug delivery - an overview, http://www.pharmainfo.net (consultada el 21/03/07).

incrementar el tiempo de residencia de las macromoléculas en la cavidad nasal se refieren al uso de geles termosensibles, como el gel de etil(hidroxietil) celulosa[35], o soluciones, geles y microsferas de polímeros mucoadhesivos como el quitosano[36,37,38]. Pero sin duda, el desarrollo de partículas poliméricas bioadhesivas y de tamaño nanométrico (10-1000 nm) ha suscitado un enorme interés en los últimos años y ha abierto un gran abanico de posibilidades en el campo de la administración de macromoléculas a través de mucosas[39,40].

Existen numerosos trabajos que evidencian la importancia de la composición y el tamaño de partícula en la eficacia de los sistemas micro- y nanoparticulares tanto *in vitro* como *in vivo* [41,42,43]. Así, actualmente no existe duda acerca de que el tamaño es un parámetro crítico que determina la capacidad de los sistemas para atravesar las barreras biológicas y, de un modo general, puede concluirse que son las partículas inferiores a 1 μm, y por tanto consideradas nanopartículas, las que pueden hacerlo en mayor medida. Otro de los factores a destacar son las propiedades superficiales de las partículas, y el efecto de las mismas sobre su

[35] **Pereswetoff-Morath L., Bjurstrom S., Khan R., Dhalin M., Edman P.**, Toxicological aspects of the use of dextran microspheres and thermogelling ethyl (hysroxyethyl) cellulose (EHEC) as nasal drug delivery systems, Int. J. Pharm., 128 (1996) 9-21.

[36] **Aspden T.J., Illum L., Skaugrud Ø.**, Chitosan as nasal delivery system: evaluation of insulin absorption enhancement and effect on nasal membrane integrity using rat models, Eur. J. Pharm. Sci., 4 (1996) 23-31.

[37] **Varhosaz J., Sadrai H., Heidari A.**, Nasal delivery of insulin using bioadhesive chitosan gels, Drug Delivery, 13 (2006) 31-38.

[38] **Farraj N.F., Johansen B.R., Davis S.S., Illum L.**, Nasal administration of insulin using bioadhesive microspheres as a delivery system, J. Control. Rel., 13 (1990) 253-261.

[39] **Janes K.A., Calvo P., Alonso M.J.**, Polysaccharide colloidal particles as delivery systems for macromolecules, Adv. Drug Del. Rev., 47 (2001) 83-97.

[40] **Alonso M.J.**, Nanomedicines for overcoming biological barriers, Biomedicine and Pharmacotherapy, 58 (2004) 168-172.

[41] **Desai, P-M., Labhasetwar, V., Walter, E., Levy, R.J. y Amidon, G.L.**, The mechanism of uptake of biodegradable microparticles in Caco-2 cells is size dependent, Pharm. Res., 14 (1997) 1568-1573.

[42] **Win, K. Y. y Feng, S.S.,** Effects of the particle size and surface coating on the cellular uptake of polymeric nanoparticles for oral delivery of anticancer drugs, Biomaterials, 26 (2005) 2713-2722.

[43] **Florence A.T**., The oral absorption of micro- and nanoparticulates: neither exceptional nor unusual, Pharm. Res., 14 (1997) 259-266.

interacción con las mucosas, así como sobre su internalización por las células epiteliales que las conforman[44,45]. Dentro de este apartado, merecen especial mención la carga superficial de los sistemas y la presencia de ligandos específicos en la superficie de las nanopartículas, que pueden incrementar significativamente su interacción con la superficie celular.

En cuanto a los mecanismos de transporte de las nanopartículas a través del epitelio nasal, se ha de tener en cuenta que las células epiteliales se hallan unidas íntimamente por las denominadas uniones "tight". El diámetro de las mismas se encuentra en torno a los 3.9-8.4 Å, e incluso tras su apertura transitoria por acción de promotores de la absorción, no supera los 15 nm[46]. Esto hace que, en general, se deba hablar de transporte de nanopartículas por vía transcelular y no paracelular. No así las macromoléculas asociadas, que una vez liberadas, y ayudadas por la apertura de uniones intercelulares, atraviesan el epitelio por vía paracelular. Ambos mecanismos se representan esquemáticamente en la **Figura 3**.

[44] **Behrens I., Vila A., Alonso M.J., Kissel T**., Comparative uptake studies of bioadhesive nanoparticles in human intestinal cell lines and rats: The effect of mucus on particle adsorption and transport, Pharm. Res., 19 (2002) 1185-1193.

[45] **Brooking J., Davis S.S., Illum L.**, Transport of nanoparticles across the rat nasal mucosa, J. Drug Target., 9 (2001) 267-279.

[46] **Illum L.**, Nanoparticulate systems for nasal delivery of drugs : a real improvement over simple systems ?, J. Pharm. Sci., 96 (2007) 473-483.

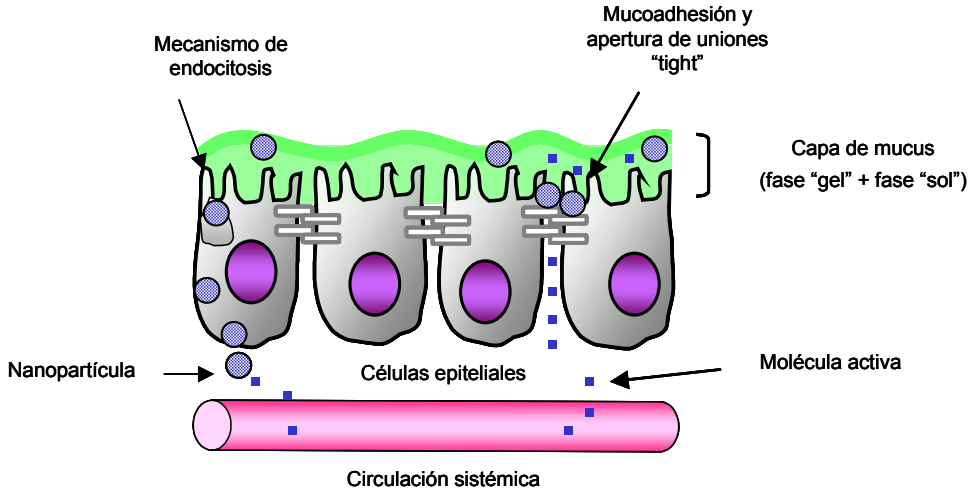

Figura 3. Nanopartículas como vehículos de macromoléculas a través del epitelio nasal.

El paso transcelular de las partículas se encuentra mediado por un proceso de endocitosis, que consiste en la invaginación de la membrana plasmática formando vesículas que liberan su contenido en el citoplasma celular. Este proceso puede ocurrir de forma pasiva, pero mayoritariamente se produce de una manera activa y saturable, bien por endocitosis "adsortiva"[32] o bien a consecuencia de la interacción específica de un determinado ligando presente en la superficie de las partículas con receptores que se expresan en la membrana celular[47]. En general, se asume que el proceso de endocitosis va seguido de un proceso de salida de las partículas internalizadas hacia los espacios subepiteliales, agrupándose este conjunto de procesos bajo la denominación de transcitosis[48]. Como consecuencia de este proceso de transcitosis las nanopartículas pueden atravesar el epitelio nasal y llegar a la circulación sistémica, actuando así como verdaderos vehículos

[47] **Cui, Z., Hsu, C.H. y Mumper, R.J.**, Physical characterization and macrophage cell uptake of mannan-coated nanoparticles, *Drug Develop. Ind. Pharm.* 29, 689-700 (2003).

[48] **Jung T., Kamm W., Breitenbach A., Kaiserling E., Xiao J.X., Kissel T.**, Biodegradable nanoparticles for oral delivery of peptides: is there a role for polymers to affect mucosal uptake?, Eur. J. Pharm. Biopharm., 50 (2000) 147-160.

transportadores de macromoléculas[49], a la vez que se consigue evitar la degradación presistémica de las mismas.

En el caso específico de la administración de antígenos, hay que destacar el papel de las células M y, en general, del NALT (tejido linfoide asociado al epitelio nasal). Estas células se caracterizan por no presentar moco y poseer una gran capacidad de captura de antígenos particulados (virus, bacterias, nanopartículas...), los cuales, una vez han atravesado el epitelio nasal, pueden alcanzar directamente los vasos sanguíneos y nódulos linfáticos cervicales o ser procesados en las células linfoides del NALT, dando lugar a la respuesta inmune[50].

En las **tablas 4** y **5**, correspondientes a nanopartículas preparadas con polímeros sintéticos y naturales, respectivamente, se recogen una serie de estudios realizados *in vivo* en distintos modelos animales, los cuales han puesto de manifiesto la capacidad de las nanopartículas administradas por vía nasal de generar importantes respuestas terapéuticas o inmunes, según la molécula encapsulada.

Como se puede observar, son muy numerosos los trabajos dirigidos a la demostración del potencial de las nanopartículas poliméricas para la obtención de respuesta inmune. En este sentido cabe destacar que la administración nasal de vacunas encapsuladas en nanopartículas ha permitido obtener interesantes respuestas inmunológicas, tanto a nivel sistémico como local [51,52]. Adicionalmente, en la última década ha suscitado un gran interés la denominada vacunación genética, un concepto basado en el uso de plásmidos codificantes de antígenos[53].

---

[49] **Almeida A.J., Alpar H.O., Brown M.R.W.**, Immune response to nasal delivery of antigenically intact tetanus toxoid associated with poly(L-lactic acid) microspheres in rats, rabbits and guinea pigs, J. Pharm. Pharmacol., 45 (1993) 198-203.

[50] **Partidos C.D**., Intranasal vaccines: fothcoming challenges, PSTT, 3 (2000) 273-280.

[51] **Vila A., Sánchez A., Janes K., Behrens I., Kissel T., Vila-Jato J.L., Alonso M.J.**, Low molecular weight chitosan nanoparticles as new carriers for nasal vaccine delivery in mice, Eur. J. Pharm. Biopharm., 57 (2004) 123-131.

[52] **Csaba N., García-Fuentes M., Alonso M.J**., The performance of nanocarriers for transmucosal drug delivery, Expert Opin. Drug Deliv., 3 (2006) 463-478.

[53] **Lowrie D.B.**, DNA vaccination exploits normal biology, Nature Med., 4 (1998) 147-148.

Las vacunas genéticas son muy seguras y poseen la capacidad de generar respuestas inmunes fuertes y eficaces[54]. Aunque, hasta el momento, existen pocos estudios *in vivo* en donde se haya investigado el potencial de las nanopartículas poliméricas como vectores sintéticos de estos plásmidos, los resultados obtenidos resultan muy prometedores[55].

Por otro lado, el potencial de los sistemas nanoparticulares poliméricos como vehículos para la administración nasal de péptidos ha sido recientemente evaluado por nuestro grupo de investigación. Concretamente, el estudio se llevó a cabo con nanopartículas de quitosano conteniendo insulina como molécula modelo, y demostró el efecto promotor de este sistema en la absorción sistémica de insulina, que se tradujo en una mayor respuesta hipoglucémica en comparación con soluciones control de insulina y quitosano e insulina[56].

[54] **Friede M., Aguado M.T.**, Need for new vaccine formulations and potential of particulate antigen and DNA delivery systems, Adv. Drug Deliv. Rev., 57 (2005) 325-331.

[55] **Csaba N., Sánchez A., Alonso M.J.**, PLGA:Poloxamer and PLGA:Poloxamine blen nanostructures as carriers for nasal gene delivery, J. Control. Rel., 113 (2006) 164-172.

[56] **Fernández-Urrusuno R., Calvo P., Remuñán-López C., Vila-Jato J.L., Alonso M.J.**, Enhancement of nasal absorption of insulin using chitosan nanoparticles, Pharm. Res., 16 (1999) 1576-1581.

Tabla 4. Estudios *in vivo* correspondientes a la administración nasal de macromoléculas encapsuladas en sistemas nanoparticulares (polímeros sintéticos).

Polímero	Macromolécula	Modelo animal	Parámetro investigado
Polimetilmetacrilato	VIH-2	Ratón	Respuesta inmune[57]
PLA	Ovoalbúmina	Ratón	Respuesta inmune[58]
PLA	Toxoide tetánico	Cobayas	Respuesta inmune[59,60]
PLA-PEG	Toxoide tetánico	Rata	Absorción y biodistribución[61]
PLA-PEG	Toxoide tetánico y ADN plasmídico	Rata y ratón	Biodistribución y respuesta inmune (transfección) [62]
PLA y PEG-PLA	Toxoide tetánico	Ratón	Respuesta inmune[63,31]
SB-PVAL-g-PLGA	Toxoide tetánico	Ratón	Respuesta inmune[64]
PLG	Antígeno toxoplasmosis	Oveja	Respuesta inmune[65]
Poly-ε-caprolactona	Toxoide diftérico	Ratón	Respuesta inmune[66]
PLGA:poloxámero y PLGA:poloxamina	ADN plasmídico	Ratón	Transfección-Respuesta inmune[67]

[57] **Stieneker F., Kreuter J., Löwer J.**, High antibody titres in mice with polymethylmethacrylate nanoparticles as adjvants for HIV vaccines, AIDS, 5 (1991) 431-435.

[58] **Somavarapu S., Alpar H.O., Song C.Y.S.**, Biodegradable nanoparticles in nasal vaccine delivery: effect of particle size and loading, Proceed. Inter. Symp. Control. Rel. Bioact. Mater., 25 (1998) 451-452.

[59] **Almeida A.J., Alpar H.O., Brown M.R.W.**, Immune response to nasal delivery of antigenically intact tetanus toxoid associated with poly(L-lactic acid) microspheres in rats, rabbits and guinea pigs, J. Pharm. Pharmacol., 45 (1993) 198-203.

[60] **Alpar H.O., Almeida A.J.**, Identification of some of the physico-chemical characteristics of microspheres which influence the induction of the immune response following mucosal delivery, Eur. J. Pharm. Biopharm., 40 (1994) 198-202.

[61] **Tobío M., Gref R., Sánchez A., Langer R., Alonso M.J.**, Stealth PLA-PEG nanoparticles as nasal protein delivery systems, Pharm. Res., 15 (1998) 274-279.

[62] **Vila A., Sánchez A., Pérez C., Alonso M.J**., PLA-PEG nanospheres: new carriers for transmucosal delivery of proteins and plasmid DNA, Polym. Adv. Technol.,13 (2002) 851-858.

[63] **Vila A., Sánchez A., Évora C., Soriano I., Vila-Jato J.L., Alonso M.J.**, PEG-PLA nanoparticles as carriers for nasal vaccine delivery, Journal of Aerosol Medicine, 17 (2004) 174-185.

[64] **Jung T., Kamm W., Breitenbach A., Hungerer K.D., Hundt E., Kissel T.**, Tetanus toxoid loaded nanoparticles from sulfobutylated poly(vinilalcohol)-graf-poly(lactide-co-glycolide): evaluation of antibody response after oral and nasal application in mice, Pharm. Res., 18 (2001) 352-360.

[65] **Stanley A.C., Buxton D., Innes E.A., Huntley J.F.**, Intranasal immunization with Toxoplasma gondii tachyzoite antigen encapsulated into PLG microspheres induces humoral and cell-mediated immunity in sheep, Vaccine, 22 (2004) 3929-3941.

[66] **Singh J., Pandit S., Bramwell V.W., Alpar H.O.**, Diphteria toxoid loaded poly-(ε-caprolactone) nanoparticles as mucosal vaccine delivery systems, Methods, 38 (2006) 96-105.

Tabla 5. Estudios *in vivo* correspondientes a la administración nasal de macromoléculas encapsuladas en sistemas nanoparticulares (polímeros naturales y derivados).

Polímero	Macromolécula	Modelo animal	Parámetro investigado
Quitosano	Insulina	Conejo	Descenso de glucemia[68]
Quitosano	Toxoide tetánico	Ratón	Respuesta inmune[69,70]
Quitosano	Ovoalbúmina y toxina colérica	Rata	Respuesta inmune[71]
Quitosano	Toxoide Tat	Ratón	Respuesta inmune[72]
Quitosano y Quitosano-PEG	ADN plasmídico	Ratón	Transfección-Respuesta inmune[73]
N-Trimetil-Quitosano	Antígeno gripe	Ratón	Respuesta inmune[74]
Maltodextrina[a]	Antígeno hepatitis B y β-galactosidasa	Ratón	Respuesta inmune[75]

[a] Biovectors™: Sistema compuesto por un núcleo polisacarídico catiónico reticulado rodeado de una bicapa lipídica

Claves tablas 4 y 5: PLA: ácido poliláctico; PLGA: ácido poliláctico-co-glicólico; PEG: polietilenglicol; PLG: poliláctico-co-glicólico; PVAL: polivinilalcohol.

[67] **Csaba N., Sánchez A., Alonso M.J.**, PLGA:Poloxamer and PLGA:Poloxamine blen nanostructures as carriers for nasal gene delivery, J. Control. Rel., 113 (2006) 164-172.

[68] **Fernández-Urrusuno R., Calvo P., Remuñán-López C., Vila-Jato J.L., Alonso M.J.**, Enhancement of nasal absorption of insulin using chitosan nanoparticles, Pharm. Res., 16 (1999) 1576-1581.

[69] **Vila A., Sánchez A., Tobío M., Calvo P., Alonso M. J.**, Design of biodegradable particles for protein delivery, J. Control. Rel. 78 (2002) 15-24.

[70] **Vila A., Sánchez A., Janes K., Behrens I., Kissel T., Vila-Jato J.L., Alonso M.J.**, Low molecular weight chitosan nanoparticles as new carriers for nasal vaccine delivery in mice, Eur. J. Pharm. Biopharm., 57 (2004) 123-131.

[71] **Nagamoto T., Hattori Y., Takayama K., Maitani Y.**, Novel chitosan particles and chitosan-coated emulsions inducing immune response via intranasal vaccine delivery, Pharm. Res., 21 (2004) 671-674.

[72] **Le Buanec H., Vetu C., Lachgar A., Benoit M.A., Gillard J., Paturance S., Aucouturier J., Gane V., Zagury D., Bizzini B.**, Induction in mice of anti-Tat mucosal immunity by the intranasal and oral routes, Biomed. Pharmacother., 55 (2001) 316-320.

[73] **Csaba N., Koping-Hoggard M., Fernández-Megía E., Novoa-Carballal R., Riguera R., Alonso M.J.**, Ionically Crosslinked chitosan nanoparticles as gene delivery systems: effect of PEGylation on in vitro and in vivo gene transfer, *submitted*

[74] **Amidi M., Romeijn S.G., Verhoef J.C., Junginger H.E., Bungener L., Huckriede A., Crommelin D.J.A., Jiskoot W.**, N-Trymethyl chitosan (TMC) nanoparticles loaded with influenza subunit antigen for intranasal vaccination: biological properties and immunogenicity in a mouse model, Vaccine, 25 (2007) 144-153.

[75] **Debin A., Kravtzoff R., Santiago J.V., Cazales L., Sperandio S., Melber K., Janowicz Z., Betbeder D., Moynier M.**, Intranasal immunization with recombinant antigens associated with new cationic particles induces strong mucosal as well as systemic antibody and CTL responses, Vaccine, 20 (2002) 2752-2763.

4. Interés del quitosano, glucomanano y ciclodextrinas en la preparación de sistemas micro- y nanoparticulares

Entre los biopolímeros utilizados en la preparación de sistemas de liberación de fármacos, los polisacáridos han suscitado un gran interés en los últimos años. Se trata de polímeros generalmente hidrofílicos con gran potencial no solo para la preparación de micro- y nanopartículas como tales, sino también como materiales de recubrimiento de las mismas, debido a sus interesantes propiedades como mucoadhesividad, baja toxicidad y presencia de grupos que pueden facilitar su interacción con las superficies biológicas o incluso ser reconocidos específicamente por receptores de células diana.

Quitosano

Entre los polisacáridos destaca especialmente el quitosano (CS) ((1-4) 2 amino-2deoxi-β-D-glucano) (**Figura 4**), el cual se obtiene a partir de la quitina, principalmente de crustáceos, por un proceso de desacetilación en medio básico[76]. Sus monómeros, N-acetilglucosamina y N-glucosamina, se encuentran aleatoriamente distribuidos, y su porcentaje relativo da lugar a lo que se conoce como el grado de desacetilación (% de grupos amino libres). A diferencia de la quitina, el CS es soluble en soluciones ácidas diluidas, mientras que las sales comercializadas de CS son solubles en agua.

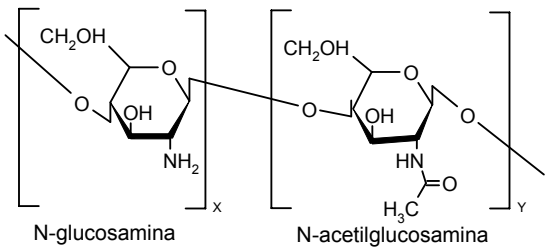

Figura 4. Estructura química del quitosano (CS)

[76] **Paul W., Sharma C.,** Chitosan, a durg carrier for the 21th century, STP Pharma Sci., 10 (2000) 5-22.

El interés creciente suscitado por este polisacárido como vehículo de moléculas activas se debe a su biocompatibilidad, biodegradabilidad y baja toxicidad. Pero además, el CS es un polímero hidrofílico con propiedades mucoadhesivas, mediadas, principalmente por su carácter catiónico, que le confiere la capacidad de interaccionar de forma electrostática con los restos de ácido siálico del mucus, cargados negativamente[77].

Asimismo, son numerosos los trabajos que demuestran su capacidad para promover la absorción de macromoléculas a través de distintos epitelios[78,79,80,81], principalmente mediante la apertura reversible de las uniones "tight" intercelulares[82,83].

En los últimos años, se ha propuesto un elevado número de sistemas de liberación de fármacos compuestos en parte o en su totalidad por CS, dejando así patente el gran interés que suscita este polisacárido. Entre ellos destacan diferentes tipos de micropartículas y nanopartículas, preparadas por muy diversas

[77] **Lehr C.M., Bowstra J.A., Schacht E.H., Junginger H.E.,** In vitro evaluation of mucoadhesive properties of chitosan and some other natural polymers, Int. J. Pharm.. 78 (1992) 43-48.

[78] **Portero A., Remuñán-López C., Nielsen H.M.,** The potential of chitosan in enhancing peptide and protein absorption across the TR146 cell culture model- an in vitro model of buccal epithelium, Pharm. Res., 19 (2002) 169-174.

[79]**Aspden T.J., Illum L., Skaugrud, O.,** Chitosan as a nasal delivery system: evaluation of the absorption enhancement and effect on nasal membrane integrity using rats models, Eur. J. Pharm. Sci., 22 (1996) 23-31.

[80]**Artursson P., Lindmark T., Davis S.S., Illum L.**, Effect of chitosan on permeability of monolayers of intestinal epithelial cells (Caco-2), Pharm. Res., 11 (1994) 1358-1361.

[81] **Florea B.I., Thanou M., Junginger H.E., Borchard G.**, Enhancement of bronchial octreotide absorption by chitosan and N-trimethyl chitosan shows linear in vitro/in vivo correlation, J. Control. Rel., 110 (2006) 353-361.

[82] **Dodane V., Khan M.A., Merwin J.R.**, Effect of chitosan on epithelial permeability and structure, Int. J. Pharm., 182 (1999) 21-32.

[83] **Smith J., Wood E., Dornish M.,** Effect of chitosan on epithelial cell tight junctions, Pharm. Res., 21 (2004) 43-49.

técnicas[84],[85], así como sistemas coloidales recubiertos de CS (liposomas, nanopartículas)[86,87,88,89].

Glucomanano

Por otra parte, el glucomanano (GM) es un polímero lineal constituido por residuos de D-glucosa y D-manosa unidos por enlaces β-(1,4) (**Figura 5**), con un alto grado de polimerización. Extraído principalmente de los tubérculos del *Amorphophallus konjac*, es un polisacárido de carácter hidrofílico que pertenece a la familia de los mananos[90]. Se considera, además, que no es tóxico, puesto que es tradicionalmente utilizado en los países asiáticos como complemento dietético[91] y, recientemente, se le han atribuido propiedades anticolesterolémicas e hipoglucemiantes[92,93].

En el **ANEXO II** de la presente memoria, se adjunta una revisión específica sobre este polímero. En ella se recogen importantes y variados aspectos,

[84] **Calvo P., Remuñán-López C., Vila-Jato J.L., Alonso M.J.,** Novel hydrophilic chitosanpolyehtylene-oxide nanoparticles as protein carriers, J. Appl. Polym. Sci., 63 (1997) 125-132.

[85] **Agnihotri S.A., Mallikarjuna N.N., Aminabhavi T.M.**, Recent advances on chitosan-based micro- and nanoparticles in drug delivery, J. Control. Rel., 100 (2004) 5-28.

[86] **Sinha V.R., Singla A.K., Wadhawan S., Kaushik R., Kumria R., Bansal K., Dhawan S**., Chitosan microspheres as a potential carrier for drugs, Int. J. Pharm., 274 (2004) 1-33.

[87] **Takeuchi H., Yamamoto H., Niwa T., Hino T., Kawashima Y.,** Enteral absorption of insulin in rats from mucoadhesive chitosan coated liposomes, Pharm. Res., 13 (1996) 896-901.

[88] **Janes K.A., Calvo P., Alonso M.J.,** Polysaccharide colloidal particles as delivery systems for macromolecules, Avd. Drug Del. Rev., 47 (2001) 83-97.

[89] **García-Fuentes M., Prego C., Torres D., Alonso M.J.,** A comparative study of the potential of solid triglyceride nanostructures coated with chitosan or poly(ethylene glycol) as carriers for oral calcitonin delivery. Eur. J. Pharm. Sci., 25 (2005) 133-143.

[90] **Maeda M., Shimahara H., Sugiyama N.,** Detailed examination of the branched Structure of konjac glucomannan, Agric. Biol. Chem., 44 (1980) 245-252.

[91] **Nishinari K.,** Konjac Glucomannan, En Doxastakis G. y Kiosseoglou V. (Eds.), Novel Macromolecules in Food Systems, Elsevier Science (2000).

[92] **Avrill A. y Bodin L.,** Effect of short-term ingestion of konjac glucomannan on serum cholesterol in healthy men, Am. J. Clin. Nutr., 61 (1995) 585-589.

[93] **McCarty M.F.,** Glucomannan minimizes the postprandial insulin surge: a potential adjuvant for hepatothermic therapy, Medical hipotheses, 58 (2002) 487-490.

estrechamente relacionados con su prometedora utilidad en el diseño y desarrollo de nuevos sistemas de liberación de fármacos. Así, primeramente se describen todas aquellos propiedades físico-químicas que lo caracterizan y, asimismo, condicionan su comportamiento (estructura, peso molecular, viscosidad, solubilidad, gelificación...). A continuación, se revisan aspectos relativos a su degradación *in vitro* e *in vivo*, interacción con otros polímeros, y preparación de derivados semisintéticos. Finalmente, y dada la perspectiva desde la que se realizó esta revisión bibliográfica, se recogen las aplicaciones investigadas hasta el momento en el campo de la medicina y el diseño de sistemas de liberación de fármacos. Estos sistemas han sido, principalmente, beads, hidrogeles y films.

Recientemente, nuestro grupo de investigación ha desarrollado nanopartículas de CS y GM destinadas a la liberación de macromoléculas por vía oral. Interesantemente, se demostró que la presencia de GM conseguía aportar a estos sistemas una mayor estabilidad y control de la liberación de la molécula encapsulada (ver **ANEXO III** de la presente memoria), así como un mayor grado de interacción con el epitelio intestinal, mediada por los receptores de manosa existentes en las células M de las placas de Peyer[94,95].

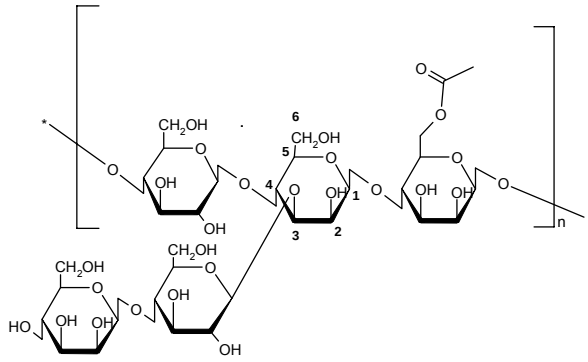

Figura 5. Estructura química del glucomanano (GM).

[94] **Alonso-Sande M., Remuñán-López C., Alonso-Lebrero J.L., Alonso M.J**, Proc. 32nd Meeting of the Controlled Release Society, Miami 2005.

[95] **Alonso-Sande M., des Rieux A., Schneider Y.J., Remuñán-López C., Alonso M.J., Préat V.**, Proc. 33rd Meeting of the Controlled Release Society, Vienna 2006.

Ciclodextrinas

Las ciclodextrinas (CDs) son oligosacáridos cíclicos, producidos a partir del almidón y compuestos por 6, 7 u 8 unidades (según sean α-, β- o γ-ciclodextrinas) de D-(+) glucopiranosa unidas por enlaces α-(1, 4)[96] (**Figura 6**).

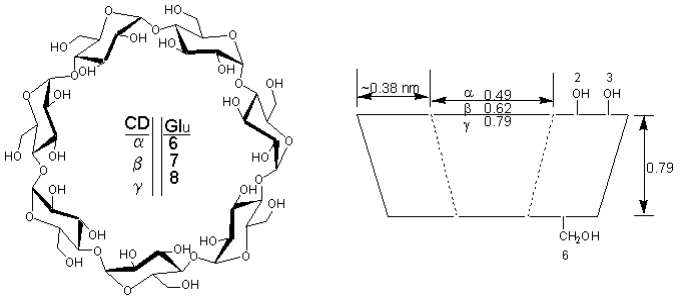

Figura 6. Estructura química (general) de las ciclodextrinas (CDs).

Generalmente, debido a su peculiar forma y estructura molecular, las CDs poseen una habilidad única de albergar diferentes moléculas (generalmente hidrofóbicas) en su interior, dando lugar a complejos de inclusión que presentan una serie de ventajas en formulaciones farmacéuticas, tales como: protección frente a degradación física, química y enzimática; estabilización y aumento de la solubilidad; control de la liberación; reducción de irritación; y enmascaramiento de olores y sabores desagradables[97,98].

Aunque las macromoléculas presentan un tamaño e hidrofilia que no les permite ser incluidos en su totalidad en el interior de las ciclodextrinas, sí se ha

[96] **Uekama K., Hirayama F., Irie T.**, Cyclodextrin drug carrier systems, Chem. Rev., 98 (1998) 2045-2076.

[97] **Loftsson T., Brewster M.E.**, Pharmaceutical applications of cyclodextrins. 1. Drug solubilization and stabilization, J. Pharm. Sci., 85 (1996) 1017-1025.

[98] Cyclodextrins for pharmaceutical applications [International Specialty Products, **Technical Brochure**] (2000), Disponible en: http://www.ispcorp.com/products/pharma/content/forwhatsnew/cyclodex/cyclodex.pdf. (consultada el 25/08/06).

descrito que pueden hacerlo parcialmente, mediante interacciones con sus cadenas hidrofóbicas[99], siendo esta inclusión parcial suficiente para mejorar su estabilidad[100].

Además, algunas ciclodextrinas han demostrado una gran eficacia como promotoras de la absorción de macromoléculas, tales como la insulina o la calcitonina, a través de los epitelios nasal[101,102,103] y pulmonar[104,105], siendo además capaces de desactivar ciertos enzimas proteolíticos[106].

Entre otros muchos promotores de la absorción, las CDs resultan de especial interés dado el alto grado de conocimiento existente acerca de sus propiedades farmacéuticas y toxicológicas. Así por ejemplo, las β-CDs naturales ya han sido aprobadas como excipiente GRAS en Estados Unidos y existen monográficos acerca de ellas tanto en la Farmacopea americana (USP) como en la europea y japonesa. Interesantemente, mediante modificación química de las CDs naturales se han conseguido compuestos más hidrosolubles e incluso con mejores perfiles de toxicidad. De este modo, existen en la actualidad derivados de CD comercializados en diferentes formulaciones y para distintas vías de administración[107]. Es el caso, por ejemplo, de las CDs sulfatadas (sulfobutil-β-CD o

[99] **Irie T., Uekama K.**, Cyclodextrins in peptide and protein delivery, Adv. Drug Deliv. Rev., 36 (1999) 101-123.
[100] **Dotsikas Y., Loukas Y.L.**, Kinetic degradation study of insulin complexed with methyl-beta cyclodextrin. Conformation of complexation with electrospray mass spectroscopy and ^{1}H NMR, J. Pharm. Biomed. Anal., 29 (2002) 487-494.

[101] **Merkus F.W., Verhoef J.C., Marttin E., Romeijn S.G., van der Kuy P.H.M., Hermens W.A.J.J., Schipper N.G.M.**, Cyclodextrins in nasal drug delivery, Adv. Drug Deliv. Rev., 36 (1999) 41-57.

[102] **Yu S., Zhao Y., Wu F., Zhang X., Lü W., Zhang H., Zhang Q.**, Nasal insulin delivery in the chitosan solution : in vitro and in vivo studies, Int. J. Pharm., 281 (2004) 11-23.

[103] **Rajewski R., Stella V.J.**, Pharmaceutical applications of cyclodextrins. 2. In vivo drug delivery, J. Pharm. Sci., 85 (1996) 1142-1169.

[104] **Kobayashi S., Kondo S., Juni K.**, Pulmonary delivery of salmon calcitonin dry powders containing absoption enhancers in rats, Pharm. Res., 13 (1996) 80-83.

[105] Hussain A., Yang T., Zaghloul A.A., Ahsan F., Pulmonary absorption of insulin mediated by tetradecyl-beta-maltoside and dimethyl-beta-cyclodextrin, Pharm. Res., 20 (2003) 1551-1557.

[106] **Matsubara M., Ando Y., Irie T., Uekama K.**, Protection afforded by maltosyl-β-cyclodextrin against α-chymotrypsin-catalyzed hydrolysis of a luteinizing-releasing hormone agonist, bserelin acetate, Pharm. Res., 14 (1997) 1401-1405.

[107] **Challa R., Ahuja A., Ali J., Khar R.K.**, Cyclodextrins in drug delivery: an updated review, AAPS PharmSciTech, 6 (2005) E329-E357. (http://www.aapspharmscitech.org).

Captisol®) ya comercializadas por Pfizer en Europa y EEUU en formulaciones para administración intramuscular de ziprasidona (Geodon®, Zeldox®) e intravenosa de voriconazol (Vfend®)[108].

.

[108] **Cydex Inc. website**, disponible en: http://www.cydexinc.com, Consultada el 04/05/07.

PARTE I: Antecedentes, hipótesis y objetivos

PARTE I

ANTECEDENTES

1. La administración por vía pulmonar de macromoléculas terapéuticas (péptidos, proteínas) con fines sistémicos ha sido, en los últimos años, objeto de gran atención como una interesante alternativa a la administración parenteral de las mismas. Entre las ventajas inherentes a esta vía cabe destacar la elevada irrigación, permeabilidad y superficie de absorción del epitelio alveolar, que determinan el rápido comienzo de la acción del fármaco, mientras se evita, además, el efecto de primer paso hepático y la degradación gastrointestinal asociados a la vía oral[1,2,3]. Todo ello se traduce en la obtención de una elevada biodisponibilidad de las macromoléculas administradas por vía pulmonar[4].

2. Desde el punto de vista de su estabilidad y manipulación por parte del paciente, la formulación de macromoléculas terapéuticas en forma de polvos secos con características adecuadas para inhalación resulta más ventajosa que las disoluciones de las mismas[5].

---

[1] **Folkesson H.G., Westrom B.R., Karlsson B.W.**, Permeability of the respiratory tract to different-sized macromolecules after intratracheal instillation in young and adult rats, Acta Physiol. Scand., 139 (1990) 347-354.

[2] **Smith P.L.**, Peptide delivery via the pulmonary route: avalid approach for local and systemic delivery, J. Control. Rel., 46 (1997) 90-106.

[3] **Clark A.**, Formulation of proteins and peptides for inhalation, Drug Deliv. Syst. Sci., 2 (2002) 73-77.

[4] **Patton J.S., Trinchero P., Platz R.M.,** Bioavailability of pulmonary delivered peptides and proteins: α-interferon, calcitonins and parathyroid hormones, J. Control. Rel., 28 (1994) 79-85.

[5] **Cryan S.-A.**, Carrier-based strategies for targeting protein and peptide drugs to the lungs, The AAPS J., 7 (2005) E20-E41 (http://www.aapsj.org).

3. Las micropartículas/microsferas presentan un notable interés como vehículos para la administración pulmonar de fármacos. El desarrollo de un sistema microparticular con características morfológicas y aerodinámicas adecuadas, que garantice la llegada de la máxima cantidad de dosis de principio activo a la zona apropiada y libere durante un tiempo controlado el fármaco, permitirá disminuir y espaciar las dosis, reducir los efectos secundarios y, en definitiva, aumentar la eficacia del tratamiento. Si el objetivo final de la administración es conseguir una absorción sistémica de la molécula activa encapsulada, el diámetro aerodinámico de estas partículas debe situarse entre 1 y 5 μm, lo que permitirá que alcancen y se depositen en la región alveolar[6,7].

4. El quitosano es un polisacárido cuyas características de biodegradabilidad, biocompatibilidad, mucoadhesión y efecto promotor de la absorción a través de diferentes epitelios, lo convierten en un candidato único para el desarrollo de nuevos sistemas de liberación de macromoléculas terapéuticas a nivel de mucosas[8]. El grado de desacetilación, indicativo de la proporción de grupos amino libres (no acetilados) presentes en la molécula de quitosano, es una característica especialmente relevante debido a que determina el carácter catiónico del polímero, el cual puede modular gran parte de sus características. El quitosano es, además, un material muy versátil para la preparación de microsferas, que pueden ser producidas mediante muy distintas técnicas[9] y con muy diversas aplicaciones[10].

---

[6] **Vanbeber R., Ben-Jebria A., Mintzes J.D., Langer R., Edwards D.A.**, Sustained release of insulin from insoluble inhaled particles, Drug Dev. Res., 48 (1999) 178-185.

[7] **Taylor G., Kellaway I.**, Pulmonary drug delivery, in: Hillery A., Lloyd A., Swarbrick J. (Eds.), Drug delivery and targeting for pharmacists and pharmaceutical scientists, Taylor & Francis, New York, (2001) pp. 269-300.

[8] **van der Lubben I.M., Verhoef J.C., Borchard G., Junginger H.E.**, Chitosan and its derivatives in mucosal drug and vaccine delivery, Eur. J. Pharm. Sci., 14 (2001) 201-207.

[9] **Aghinotri S.A., Mallikarjuna N.N.**, Recent advances on chitosan-based micro- and nanoparticles in drug delivery, J. Control. Rel., 100 (2004) 5-28.

5. Muy recientemente, nuestro grupo de investigación ha demostrado el potencial de las microsferas de quitosano como vehículos para la administración pulmonar de macromoléculas terapéuticas. Más específicamente, las microsferas, producidas por las técnicas de atomización y doble emulsificación/evaporación del disolvente encapsulando insulina como molécula modelo, fueron administradas intratraquealmente a ratas en forma de polvo seco. Interesantemente, la respuesta hipoglucémica obtenida fue muy satisfactoria mejorando, de manera significativa, el perfil correspondiente al péptido en solución[11].

6. El glucomanano es un polisacárido con gran potencial en el diseño de sistemas de liberación de fármacos debido, principalmente, a sus características de solubilidad, gelificación y no toxicidad, así como a su capacidad de interaccionar con otros polisacáridos, lo que puede contribuir a mejorar o simplemente modular las propiedades de los sistemas e incrementa su versatilidad en este campo[12].

7. Recientemente, la combinación de glucomanano y quitosano ha permitido la obtención de nuevos sistemas nanoparticulares con interesantes propiedades, entre las que se halla una excelente capacidad de asociar y liberar macromoléculas terapéuticas. Además, se demostró que la presencia de glucomanano aporta a estos sistemas una mayor estabilidad y control de

[10] **Sinha V.R., Singla A.K., Wadhawan S., Kaushik R., Kumria R., Bansal K., Dhawan S.**, Chitosan microspheres as a potential carrier for drugs, Int. J. Pharm., 274 (2004) 1-33.

[11] **Carrión-Recio D., Taboada-Montero C., Vila-Jato J.L., Remuñán-López C**., Enhancement of protein lung absorption using chitosan microspheres, *sometida a evaluación.*

[12] **Alonso-Sande M., Teijeiro-Osorio D., Remuñán-López C., Alonso M.J.**, Glucomannan, a promissing plysaccharide for pharmaceutical and biomedical purposes, *Anexo III*.

la liberación de la molécula encapsulada[13], así como un mayor grado de interacción con el epitelio intestinal[14,15].

HIPÓTESIS

1. Los polisacáridos hidrofílicos quitosano y glucomanano son materiales particularmente interesantes para la administración pulmonar de macromoléculas terapéuticas con fines sistémicos, dada su baja toxicidad y, en el caso del quitosano, debido a sus propiedades mucoadhesivas y de promoción de la absorción de fármacos.

2. El quitosano y el glucomanano permitirán obtener, mediante una técnica adecuada para la asociación de principios activos lábiles como es la atomización, microsferas con características morfológicas y aerodinámicas adecuadas (diámetro aerodinámico comprendido entre 1 y 5 μm) para ser administradas por vía pulmonar y alcanzar la región alveolar, donde se espera que se libere la macromolécula terapéutica asociada.

3. El empleo de quitosanos de distinto grado de desacetilación, así como la combinación de quitosano y glucomanano en diferentes proporciones, permitirá la obtención de una serie de formulaciones con distintas características adicionales - tales como toxicidad, mucoadhesión, perfil de liberación de la macromolécula asociada y promoción de la absorción -, que determinarán la selección de unas variables de formulación óptimas.

[13] **Alonso-Sande M., Alonso-Sande M., Cuña M., Remuñán-López C., Teijeiro-Osorio D., Alonso-Lebrero J.L., Alonso, M.J.**, Formation of new glucomannan-chitosan nanoparticles and study of their ability to associate and deliver proteins, Macromolecules, 39 (2006) 4152-4158.

[14] **Alonso-Sande M., Remuñán-López C., Alonso-Lebrero J.L., Alonso M.J**, Proc. 32nd Meeting of the Controlled Release Society, Miami 2005.

[15] **Alonso-Sande M., des Rieux A., Schneider Y.J., Remuñán-López C., Alonso M.J., Préat V.**, Proc. 33rd Meeting of the Controlled Release Society, Vienna 2006.

OBJETIVOS

Teniendo en cuenta los antecedentes expuestos y las hipótesis de partida, el objetivo global de la primera parte de esta memoria se ha dirigido al desarrollo de sistemas microparticulares basados en quitosano destinados a la administración pulmonar de macromoléculas terapéuticas. Desde un punto de vista práctico, el trabajo experimental llevado a cabo para alcanzar este objetivo global, se han recogido en los apartados que se detallan a continuación:

1. Preparación y caracterización de microsferas utilizando quitosano de distintos grados de desacetilación solo o en combinación con glucomanano. Investigación del efecto del grado de desacetilación del quitosano y proporción de glucomanano sobre las características morfológicas y aerodinámicas de las microsferas. Evaluación de su capacidad para asociar y liberar macromoléculas terapéuticas.

   Los resultados han sido recogidos en los **Artículos 1 y 2**.

2. Investigación *in vitro* en líneas celulares modelo de los epitelios bucal y respiratorio de la citotoxicidad del quitosano (distintos grados de desacetilación) y del glucomanano; evaluación de la influencia del grado de desacetilación del quitosano sobre sus propiedades como promotor de la absorción de macromoléculas de distinto peso molecular y estudio de la interacción/mucoadhesión de los sistemas microparticulares con el epitelio respiratorio.

   Los resultados han sido recogidos en los **Artículos 2 y 3**.

Artículo 1: “Preparation and *in vitro* evaluation of different deacetylation degree chitosan microspheres for pulmonary protein delivery”.

Artículo 2: “Preparation and characterization of chitosan/glucomannan microspheres for pulmonary delivery of macromolecules”.

Artículo 3: “Chitosan nanoparticles and solutions as absorption enhancers for peptides and proteins – *in vitro* studies with the TR146 and Calu-3 cell culture models”.

PARTE I: Trabajo experimental

ARTÍCULO 1

Preparation and In Vitro Evaluation of Different Deacetylation Degree Chitosan Microspheres for Pulmonary Protein Delivery

Desirée Teijeiro-Osorio and Carmen Remuñán-López

ABSTRACT

Chitosans with different degrees of deacetylation (DD) were prepared from a highly deacetylated commercial chitosan by reacetylation with acetic anhydride in an aqueous medium. Polymer DDs were assessed by nuclear magnetic resonance (NMR) and changes in their mucoadhesivity properties as function of DD were also determined. The effect of the chitosan DD on the morphological and aerodynamic properties of microspheres produced by spray drying was investigated. Morphology was highly influenced by chitosan reacetylation level, thus the reacetylated microspheres showing an increasing distorted surface, as opposite to the good sphericity and smooth surface showed by non-reacetylated chitosan microspheres. Aerodynamic properties resulted to be adequate for lung delivery. A protein model (insulin) was efficiently encapsulated in order to determine the influence of chitosan reacetylation on the drug release behavior of different formulations. In general, the release of insulin from microspheres was fast, and accompanied by a burst effect.

KEY WORDS: Chitosan, deacetylation degree, insulin, microspheres, mucoadhesion, peptide/protein lung delivery, spray-drying.

1. INTRODUCTION

Recently, pulmonary delivery has emerged as an interesting possibility for the non-invasive administration of peptides, proteins and other macromolecular drugs (Yu and Chien, 1997). The features of the lung favouring the systemic absorption of drugs include a large absortive surface area (≈100 m^2), extensive vascularization and thin alveolar epithelium (0.1-0.5 μm). In addition, pulmonary drug delivery avoids first-pass hepatic metabolism and gastrointestinal degradation associated with the oral administration (Patton and Platz, 1992; Edwards et al., 1998; Courier et al., 2002). As a consequence, evidence of acceptable bioavailability following pulmonary administration has been reported for several peptide and protein drugs such as calcitonin, human growth and parathyroid hormones, interferons and insulin (Patton et al., 1994; Kobayashi et al., 1994; Colthorpe et al., 1995; Sakr, 1996; Patton et al., 1999). In this sense, it must be mention that insulin is already available in the market (in Europe and USA) in a formulation from Pfizer, Nektar and Aventis called Exubera®; and a growing number of other peptides/proteins are in various phases of clinical trials (Cryan, 2005).

However, the success of pulmonary protein administration could be reinforced by incorporating the drug in an adequate carrier system to improve its aerosolization, alveolar deposition and, definitively, its therapeutic efficacy. Moreover, particulate drug carriers may protect the drug from degradation, enhance its transport through the epithelium, and even act as a controlled release system, resulting in prolonged blood concentrations (van der Lubben et al., 2001; Cryan et al., 2005).

An interesting approach in this field has focused on the design and formulation of microspheres, since they can be tailored with the desired morphologic and aerodynamic characteristics by simply modifying the composition and process variables. Microspheres can be produced using a wide range of naturally occurring or synthetic polymers. Among natural polymers, the polysaccharide chitosan (CS) is being widely investigated in drug delivery due to its biodegradability, biocompatibility, low toxicity and other desirable properties, such as

mucoadhesiveness and the ability to enhance the absorption of macromolecules through different epithelia (van der Lubben et al., 2001). CS is a deacetylated product of chitin, which is commercially derived from crustacean shells. CS is a linear polymer that consists of N-acetyl glucosamine and glucosamine units. Its deacetylation degree (DD), which reflects the balance between these two kind of residues (percentage of N-acetyl glucosamine units relative to the total units number), plays a very important role on CS physical, physicochemical, and biological properties (Mima et al., 1983; Schipper et al., 1996; Varum et al., 1997). CS is a polycation at acidic pH values, with an intrinsic pKa of approximately 6.5 (Domard, 1987). Besides pH, the charge density of the polymer is also determined by the DD, since only the glucosamine units are positively charged. In this sense, there are several characteristics of CS that seem to be related to its DD and, consequently, to its positive charge, such as solubility, biodegradability, toxicity and mucoadhesiveness (Schipper et al., 1996; Tomihata and Ikada, 1997; Zhang and Neau, 2001; Huang et al., 2004). More specifically, it has been reported that decreasing DD favours the polymer degradation by enzymes (e.g. lisozyme) and decreases polymer toxicity. The decrease in the CS DD is also associated with a reduction in its water solubility and an important loss in the polymer mucoadhesive properties, this latter given by the decreased presence of positively charged amino groups able to electrostatically interact with mucus or a negatively charged mucosal surface.

Different processing techniques for the preparation of CS microspheres have been extensively developed since the 1980's (Kas et al., 1997). Among them, spray-drying is a well-known technique, which is commonly used to prepare dry powders from drug-excipient solutions and suspensions. Our research group has proposed the application of CS microspheres, obtained by spray-drying, for the pulmonary delivery of peptides and proteins (Congreso), demonstrating their compatibility with the hydrofluoroalkane propellant P134a and, hence, their suitability for lung delivery via pressurized dose inhalers (pMDI) (Williams et al., 1998). Besides, we have recently demonstrated that insulin-loaded CS microspheres with adequate

aerodynamic properties are able to reach the alveolar region after intratracheal administration of the dry powder to rats, inducing a significantly improved hypoglycemic response than those corresponding to the peptide solution (Carrión-Recio et al., *submitted*).

In order to reach the lower respiratory tract and optimize systemic drug absorption, it has been reported that dry powder aerosols need to present aerodynamic diameters between 1 and 5 μm (Vanbeber et al., 1999). Larger particles impact in the oro-pharynx while sub-micron particles remain suspended in air and are exhaled. Additionally, a certain number of particles will be transported away from the lung by mucociliary clearance. Although there is no consensus concerning the ideal size range to avoid or delay macrophages phagocytosis, it has been reported that particles beyond 2 μm can more easily escape from this defense mechanism (Roser et al., 1998). Furthermore, it has been reported that microspheres having primary amino groups on their surfaces were most effectively engulfed by the macrophages (Makino et al., 2003). Therefore, it is possible to hypotesize that partial acetylation of CS amino groups could reduce the macrophages uptake.

Bearing all this in mind, the aim of the present work was to develop microspheres with appropriate morphological and aerodynamic characteristics for pulmonary protein delivery using CS of different DD. First, CS of different DD were prepared from a commercial CS sample by reacetylation with acetic anhydride and conveniently characterized (DD, mucoadhesiveness). Afterwards, microspheres were prepared by spray-drying the corresponding CS solutions/dispersions and the effect of CS DD on surface morphology, size, density and aerodynamic diameter of the particles was investigated. Finally, the potential of these micospheres as peptide/protein carriers was studied by incorporating insulin as a peptide model.

2. MATERIALS AND METHODS

2.1. Materials

The following chemicals were obtained from commercial suppliers and used as received: chitosan glutamate (Sea Cure G210, supplier´s specification: Mw of 300 kDa and deacetylation degree > 80%) (Pronova Lab., Norway); acetic anhydride (AA), mucin type III (1% sialic acid), insulin from bovine pancreas, deuterium acetic acid (CD_3COOD) (Sigma-Aldrich, Spain) and deuterium oxide (D_2O) (Merck, Germany). Ultrapure water (Milli-Q plus, Millipore Ibérica, Spain) was used throughout. All other reagents were of the highest grade available and were used without further purification.

2.2. Preparation of chitosans of different deacetilation degree

To prepare the CS derivatives with different DD, a variable volume of AA (ratios: 1.25, 2.5, 5, and 10 µl AA/mg of CS) was added to CS solutions (1% w/w in water) and allowed to react under magnetic stirring for 24 h (room temperature). Then, the reacetylated polymer solutions were dialyzed (Dialysis tubing 100 FT, Sigma-Aldrich, Spain) until elimination of the acetic acid remaining in the medium, which was controlled by pH measurements until no pH change. Finally, the polymeric solutions were freeze dried (Labconco Co., USA) to obtain CS powders. Production yield of reacetylated CS (R_{CS}-yield) were calculated using the formula:

$$R_{CS}\text{-yield (\%)} = (\text{mg of reacetylated CS powder / mg of native CS}) \times 100$$

2.3. Determination of chitosan deacetylation degree by ^{1}H NMR (proton nuclear magnetic resonance)

The chemical structures of the different CS DD samples obtained as indicated above were characterized by ^{1}H NMR. CS samples were dissolved in CD_3COOD/D_2O solution and NMR spectra (500 MHz) were obtained at 80ºC with a Bruker DRX500 instrument (Bruker DRX500, Germany). CS DD were obtained using the formula indicated below (Hirai et al., 1991).

$$DD = 1 - \left(\frac{1/3\ I_{CH_3}}{1/6\ I_{H_2\text{-}H_6}} \right) \times 100$$

where “DD” is the degree of deacetylation of CS expressed as the percentage, “I_{CH3}” is the integral intensity of CH_3 (protons of the N-acetylglucosamine residues) and “$I_{H2\text{-}H6}$” is the summation integral intensities of H_2, H_3, H_4, H_5 and H_6 (protons of both glucosamine and N-acetylglucosamine residues).

2.4. *In vitro* evaluation of chitosan mucoadhesive properties in aqueous solution

Mucoadhesive properties of the aqueous solutions of CS with different DD were evaluated by measuring its interaction with mucin by a turbidimetric method (He et al., 1998). Stock polymer (reacetylated CS and non-reacetylated CS as control) and mucin solutions (2 mg/ml, in acetate buffer pH 4.5) were prepared, filtered and stored at 4ºC until their use. The mucin and CS solutions were mixed in different ratios (mucin:CS ratio = 1:3; 1:1; 3:1) and incubated under horizontal stirring (200 oscillations/min, Heidolph Promax 2020, Germany) during 30 min at room temperature. The absorbances of these samples (A_{exp}) were assayed for turbidimetry by UV spectroscopy at 500nm (UV-1603 Shimadzu, Japan). The absorbances of the individual polymers and mucin solutions in acetate buffer were measured as controls to give the theoretical values (A_t) for a non-interacting system. Calculations were performed as follows:

$$A_t = A_{mucin} \times P_{mucin} + A_{polymer} \times P_{polymer}$$

where “A_{mucin}” and “$A_{polymer}$” are the absorbances obtained for the mucin and polymer solutions individually, and “P_{mucin}” and “$P_{polymer}$” are the proportion of mucin and polymer, respectively, present in the mixture. The absorbance difference between the measured experimentally and the calculated theoretically (A_{exp} - A_t) represents the mucoadhesion strength. All samples were analyzed in triplicate (n = 3).

2.5. Preparation of CS microspheres

CS microspheres were produced by spray-drying polysaccharide solutions (0.5% w/w or 1% w/w, depending on CS DD), which were prepared by dissolving CS in a diluted acidic solution (acetic acid, 1% v/v) at room temperature, using a Büchi 290 Mini Spray-drier (Afora, Spain). The spray drying conditions were: feed rate of 2.8 mL/min (nozzle size = 0.7 mm), air flow rate of 473-550 Nl/h, and inlet and outlet temperatures of 160-162 ºC and 107-114 ºC, respectively. For CS microspheres containing insulin, the corresponding amount of peptide (15% w/w based on CS) was previously dissolved in HCl 0.1 M and then, added to the CS solution, obtaining a final polymer concentration of 0.5% w/w (for CS DD < 30%), or 1% w/w (for CS DD > 30%). Differences in concentration of the feedstock solutions to spray-dry were due to the solubility and handling limitations inherent to the lowest CS DD. The solutions were maintained under continuous mechanical stirring during all the process. Spray-drying production yields (SPD-yield) were determined according the following expression:

SPD-yield (%) = (microspheres weight /total components weight) x 100

2.6. Characterization of CS microspheres

2.6.1. FT-IR (Fourier Transform Infrared spectra) of chitosan microspheres

The IR spectra of reacetylated and non-reacetylated CS microspheres were recorded using the KBr technique (1 mg sample in 50 mg KBr) (Bruker model IFS-66v, Germany) with a frequency range of 4000-400 cm^{-1}. The DD of the samples was calculated from the ratio of absorbance at 1655 cm^{-1} (ascribed to amide I band) and the hydroxyl band at 3450 cm^{-1} using two different baselines, baseline (a), which was proposed by Domszy and Roberts and baseline (b) by Baxter et al. (Domszy and Roberts, 1985; Baxter et al., 1992). The computation equations for the two baselines are given below:

$$DD = 100 - [(A_{1655} / A_{3450}) \times 100 / 1.33] - baseline \qquad \textbf{(a)}$$

where the factor '1.33' denoted the value of the ratio A_{1655} / A_{3450} for fully N-deacetylated chitosan, and

$$DD = 100 - [(A_{1655} / A_{3450}) \times 115] - baseline \qquad \textbf{(b)}$$

The amide and hydroxyl bands absorbances can further be represented by the simple mathematical expressions as proposed by Sabnis and Block (Sabnis and Block, 1997).

$$A_{1655} = Log_{10} (DF_1/DE) \quad or \quad A_{1655} = Log_{10} (DF_2/DE), \text{ and}$$

$$A_{3450} = Log_{10} (AC/AB)$$

where DF_1 (for the baseline 'a') or DF_2 (for the baseline 'b'), DE, AC, and AB depicted the absolute heights of the absorption bands of the functional groups at their respective wavelengths (see **Figure 1**).

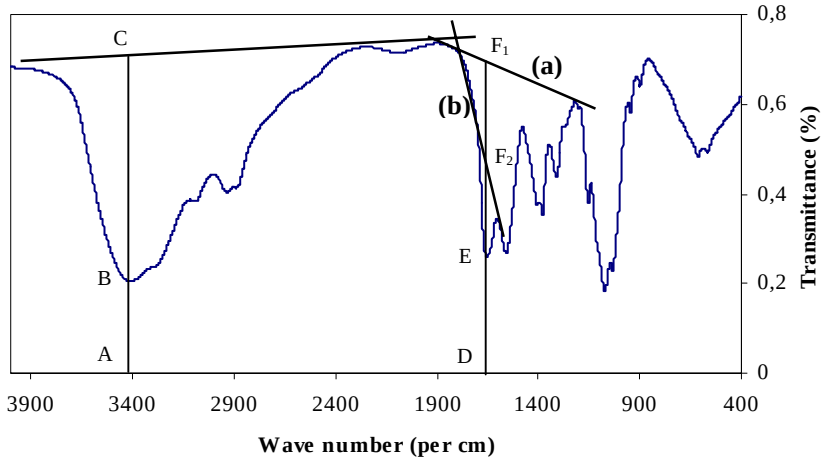

Figure 1. IR spectrum of chitosan showing the two baselines ('a' and 'b') for calculating the amide I band absorbance ratio A_{1655}/A_{3450} (Tanveer et al., 2002).

2.6.2. Characterization of microspheres size and morphology

The morphology and surface appearance of the microspheres were examined by scanning electron microscopy (SEM). The particles were freeze-dried (Labconco Co., USA), coated with gold palladium to achieve films of 60 nm thickness (Polaron SC7640 High Resolution Sputter-coater, Thermo VG Scientific, England) and observed with a scanning electron microscope (SEM Leica S440, England).

The particle size was estimated as the Feret´s diameter (the measured distance between parallel lines that are tangent to the particle profile and perpendicular to the ocular scale) and was directly measured with an optical microscope (Olympus BH-2, Japan) on 100 particles, (n = 100).

2.6.3. Determination of real and apparent densities

Real densities of microspheres were determined by Helium pycnometry (Micropycnometer, Quanta Chrome, MPY-2 model, USA) (n = 6). The apparent (tap) densities were obtained by measuring the volume of a known weight of powder in a 10 mL graduated cylinder. After registering the initial volume, the cylinder was mechanically tapped (30 taps/min, Tecnociencia, Spain) until a constant volume was achieved (El-Gibaly, 2002). The apparent density was calculated as the mass divided by the volume (n = 3).

2.6.4. Measurement of aerodynamic properties

Aerodynamic diameters (d_{aer}) of microspheres were determined using a TSI Aerosizer® LD analyzer equipped with an Aerodisperser® (*Amherst Process Instrument Inc*., USA) (n = 3), whose measuring principle is based on direct time-of-flight measurements according to the following equation:

$$C_d \frac{\pi d^2}{4} \rho_a \frac{(V_a - V_p)^2}{2} = 1/6\, \pi d^3 \rho_p \frac{dV_p}{dt}$$

where C_d: particle drag coefficient, d: particle Feret´s diameter, ρ_a: air density, ρ_p: particle real density, V_a: air velocity and V_p: particle velocity.

2.6.5. Determination of insulin association to the microspheres

Protein content of formulations was determined following the microspheres incubation (1.25 mg of microspheres, test tubes of 10 mL) in 6 mL of PBS pH 7.4 under horizontal shaking (105 oscillations/min, *Heidolph Promax 2020,* Germany) at 22°C, until the complete protein release (4 h). The microspheres dispersions were filtered (0.45 µm filters unit *MILLEX®-HV*, low protein binding, USA) and the supernatants assayed for insulin content by measuring their absorbances at 562 nm (*Micro BCA Protein Assay Reagent Kit, Pierce*, USA; *UV-1603 Shimadzu*, Japan) (*n* = 3).

The association efficiency (A.E.) to the microspheres was determined as follows:

A.E. (%) = (Weight of associated protein/Total protein weight) x 100

2.6.6. In vitro release studies

In vitro release studies of protein-loaded microspheres were performed as follows. Microspheres (2.5 mg) were incubated (10 mL test tubes) in 6 mL of PBS pH 7.4 under horizontal shaking (105 oscillations/min, *Heidolf promax 2020*, Germany) at 37ºC. At pre-determined times (15, 30, 45, 60 and 120 min) the microparticles dispersions supernatants were filtered (0.45 µm filters unit *MILLEX®-HV*, low protein binding, USA) and assayed for drug release by measuring their absorbances at 562 nm (*Micro BCA Protein Assay Reagent Kit, Pierce*, USA; *UV-1603 Shimadzu*, Japan) (*n* = 3-6).

2.7. Statistical Analysis

Statistical differences were investigated by using one-way ANOVA followed by the Student-Newman-Keuls method for multiple comparissons. All analysis were run using the SigmaStat statistical program (version 3.1) and differences between groups were judged significant at $P < 0.05$.

RESULTS AND DISCUSSION

A total of 4 samples of CS with DD ranging between 23 and 47% were prepared by reacetylation of the commercial polymer of DD > 80% (according to the supplier´s specifications). The reaction of acetylation was performed with acetic anhydride in an aqueous medium at room temperature. After dialysis and freeze-drying, the final dry products were characterized by ^{1}H NMR spectrometry; the corresponding spectra are reported in **Figure 2**. CS DD was easily estimated from the ratio of the integral intensity of the N-acetyl protons to the sum of integral intensities of the H_2, H_3, H_4, H_5 and H_6 (protons of both glucosamine and N-acetylglucosamine residues), as reported by Hirai et al. (Hirai et al., 1991). The yields of reacetylation process ([mg of reacetylated CS powder / mg of native CS] x 100), as well as the determined CS DDs are represented in **Table 1**.

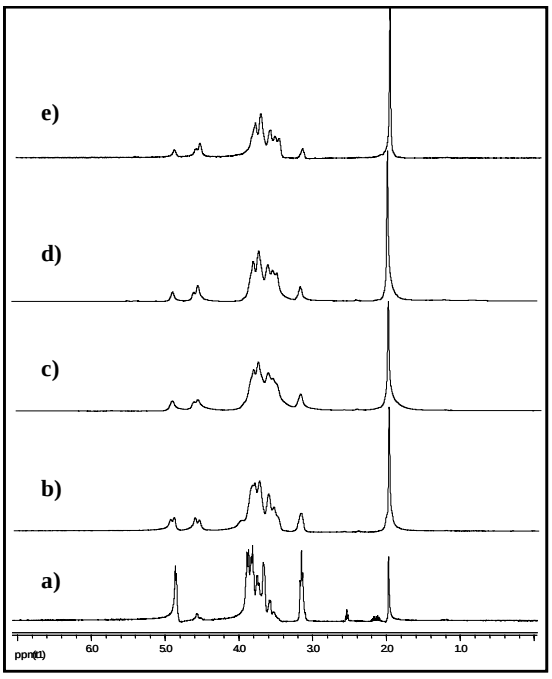

Figure 2. ^{1}H NMR spectra of: (a) non-reacetylated chitosan, and (b) R-1.25, (c) R-2.5, (d) R-5, (e) R-10 reacetylated chitosans; corresponding the values 1.25, 2.5, 5 and 10 to the ratios AA/CS (μl/mg) used for the CS reacetylation processes.

Table 1. Reacetylation process yields and experimental deacetylation degrees of CS solutions obtained by ^{1}H NMR.

CS	Reacetylation yield (%)[b]	DD (*^{1}H NMR*) (%)
R-0	-	83.47
R-1.25[a]	66.86	46.66
R-2.5	62.58	37.56
R-5	62.29	25.97
R-10	63.60	23.07

[a] AA/CS (μL/mg) ratios used for the CS reacetylation processes

[b] Reacetylation yield (%) = (mg of reacetylated CS powder / mg of native CS) x 100

It is known that the cationic polyelectrolyte nature of CS could provide a strong electrostatic interaction with mucus or a negatively charged mucosal surface. For this reason, we evaluated the influence of the positive charge loss, inherent to the acetylation of free amino groups, over polymer mucoadhesive properties. The results of the turbidimetric studies on the mucin/CS mixed systems are depicted in **Figure 3.** The absorbances (A) of the mixtures of mucin/polymer and of the individual mucin and the individual polymer sample at 500 nm were measured. The theoretical absorbance (A_t) for the mixture was calculated from the individual ones, as explained in the methodology section. The absorbance differences (A_{exp}-A_t) between the measured and theoretical values represent the mucoadhesion strength. Thus, when no interaction occurs, "A_{exp}-A_t" is zero, whereas the higher is the "A_{exp}-A_t" value, the higher is the polymer-mucin interaction (He et al., 1998). In general, these absorbance differences were high for all the samples, suggesting a strong interaction between the different DD CS and mucin, and thus probing the mucoadhesive properties of all the prepared CSs (with DD as low as 23%). As expected, the maximum values corresponded to non-reacetylated CS (DD 83%). This absorbance, around 0.7, decreased gradually as the DD decreases, as

correspond to the fall in the number of positively charged amino groups able to interact with the negatively charged groups on mucin.

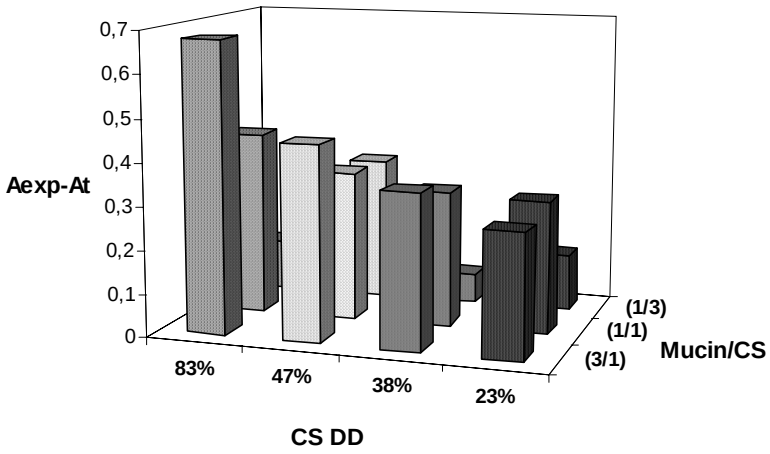

Figure 3. Turbidimetric measurements of the interaction between mixtures of CS with different deacetylation degrees and mucin in different ratios. "A_{exp}-A_t" is the absorbance difference between the measured experimentally (λ = 500 nm) and the calculated theoretically, and represents the mucoadhesion strength (*n* = 3).

In order to obtain a suitable CS carrier for lung delivery of peptides/proteins, CS microspheres were prepared by spray-drying the CS solutions of different degrees of acetylation, as indicated in the methodology section. Microspheres were named as function of the CS from they were made of. Thus, the assigned names (particle code) are listed in **Table 2**, together with the corresponding production yields ([microspheres weight /total solids weight] x 100), which in all cases were high (64-75%).

Table 2. Particle code and production yields of the spray-dried microspheres

CS	Particle code	SPD-yield[b] (%)
R-0	MS DD 83%	72.50
R-1.25[a]	MS DD 47%	66.75
R-2.5	MS DD 38%	63.68
R-5	MS DD 26%	75.00
R-10	MS DD 23%	71.05

[a] AA/CS (μL/mg) ratios used for the CS reacetylation processes

[b] Spray-drying yield (%) = (microspheres weight /total solids weight) x 100

As an additional study, DD of the CS microspheres, as a dry powder, was also determined by FT-IR. Spectroscopic methods based on IR spectra are commonly used for the estimation of CS DD values, since they are relatively fast and do not require dissolution of the CS samples (Baxter et al., 1992). FT-IR spectra of microspheres prepared from non-modified or native CS and N-acetylated chitosans are represented in **Figure 4**. The absorption peaks at 1654 cm^{-1} can be assigned to the carbonyl stretching of secondary amides (amide I band), at 1576 cm^{-1} to the N-H bending vibration of non-acylated 2-aminoglucose primary amines, and at 1555 cm^{-1} to the N-H bending vibrations of the amide II band (Xu et al., 1996). After N-acetylation, the vibrational band corresponding to primary amino groups at 1576 cm^{-1}, which is characteristic of CS with DD > 50% (Dong et al., 2001), dissapeared, while gradually prominent amide I and amide II bands at 1654 cm^{-1} and 1555 cm^{-1} were observed (Le Tien et al., 2003). Over the last two decades, improvements in the IR methods have been proposed by making use of new absorption bands and/or baselines for the measurement of DD. Among the different proposals, use of the amide I absorption band (1655 cm^{-1}) combined with the hydroxyl absorption band (3450 cm^{-1}) as internal reference appears to provide the best results (Lavertu et al.,

2003). The concentration of N-acetyl groups is given by the absorbance of the amide I band at 1655 cm^{-1}, but it is necessary to have an internal reference standard in order to compensate for differences in sample concentration in the KBr disc. The selection of the band at 3450 cm^{-1} as reference is given by two main advantages: it is prominent and relatively isolated, and its intensity is approximately constant from chitosan to the fully N-acetylated chitosan or chitin (Moore and Roberts, 1980).

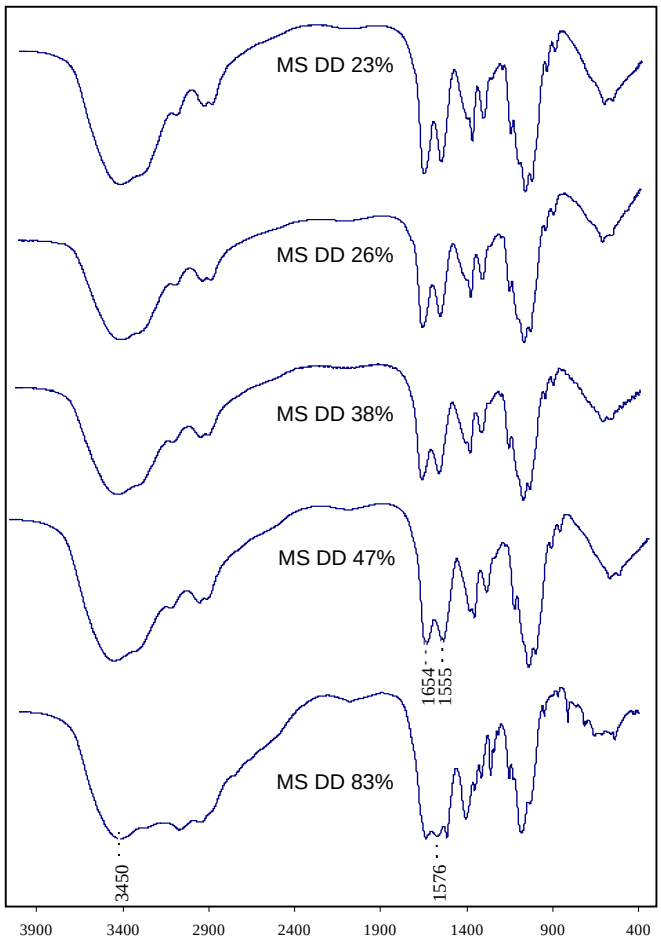

Figure 4. FT-IR spectra of microspheres prepared from CS of different deacetylation degrees.

Thus, as previously described into the Methodology, CS DD was calculated by applying two equations, based on the ratio of absorbances A_{1655}/A_{3450} and using two different baselines (Domszy and Roberts, 1985; Baxter et al., 1992). As can be observed in **Table 3**, similar DD were obtained by both equations, these values being also similar to those obtained by NMR of the polymer solutions, demonstrating the accuracy of the techniques employed for the characterization/determination of DD. Reacetylation yields ([mg of reacetylated CS / mg of native CS] x 100) were very reproducible (SD < 2%) and high, varying within 63 and 67 %.

Table 3. Experimental deacetylation degrees of CS, obtained by FT-IR spectroscopy of microspheres powder.

	DD (*FT-IR*) (%)	
Particle code	A_{1655} / A_{3450} (baseline a)	A_{1655} / A_{3450} (baseline b)
MS DD 83%	n.d	86.01
MS DD 47%	40.18	43.69
MS DD 38%	36.86	38.02
MS DD 26%	32.72	30.88
MS DD 23%	30.46	27.83

SEM studies were performed at both low and high magnifications (20000x and 50000x) in order to obtain information about general powder characteristics (predominant particle size and shape) and particle surface (texture, roughness). SEM photographs revealed the great influence of CS DD on the surface morphology of blank microspheres. Clear changes in particle morphology and surface roughness are showed in representative photos in **Figures 5** and **6**. It is very outstanding the evolution from the spherical shape and smooth suface of non-reacetylated CS

microspheres (MS DD 83%) to the very characteristic irregular shape and convoluted/wrinkled surface corresponding to the most reacetylated CS particles (MS DD 26% and MS DD 23%).

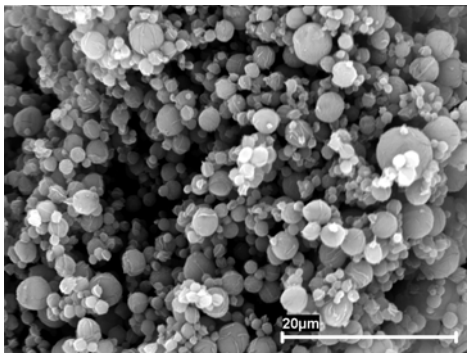

Figure 5. SEM microphotograph of the microspheres obtained by spray-drying non-reacetylated CS solution (1% w/w): MS DD 83%.

Similar morphologycal characteristics have been shown in the literature for spray-dried particles obtained from other polymers, e.g. hyaluronic acid (Surendrakumar et al., 2003); polymeric mixtures, e.g. CS-gelatin (Huang et al., 2002); and pure proteins, e.g. bovin serum albumin or human anti-IgE antibodies (Ameri and Maa, 2006). Huang et al. explained this phenomenon as a consequence of an explosion produced by high heat (170 ºC) during the spray drying process, probably due to a lack of rigidity in the polymeric matrix (Huang et al., 2002). As reported by Ameri et Maa, the liquid composition to be spray dried prescribes the shape of the resulting particles, i.e., some materials tend to form solid spherical particles while others form holow, deformed or even disintegrated particles. They hypothesized that, as the droplet dries, a polymer film formed at the external surface could hinder the outward diffusion of water and cause the water vapor pressure inside the droplet to increase. At a critical pressure, the film bursts, deforming the particle shape from its original sphericity. Certainly, the extent of such hinderance in diffusion will be dictated by the film properties (flexibility, mechanical strength, porosity) (Ameri and Maa, 2006), but also by the affinity between the spray-dried material and the solvent. In this sense, a reduced polymer-solvent interaction (caused by low solubility of the polymer) led to

a more difficult diffusion of the solvent through the outer polymer wall (Zhang et al., 2000), as it may occur for reacetylated CSs.

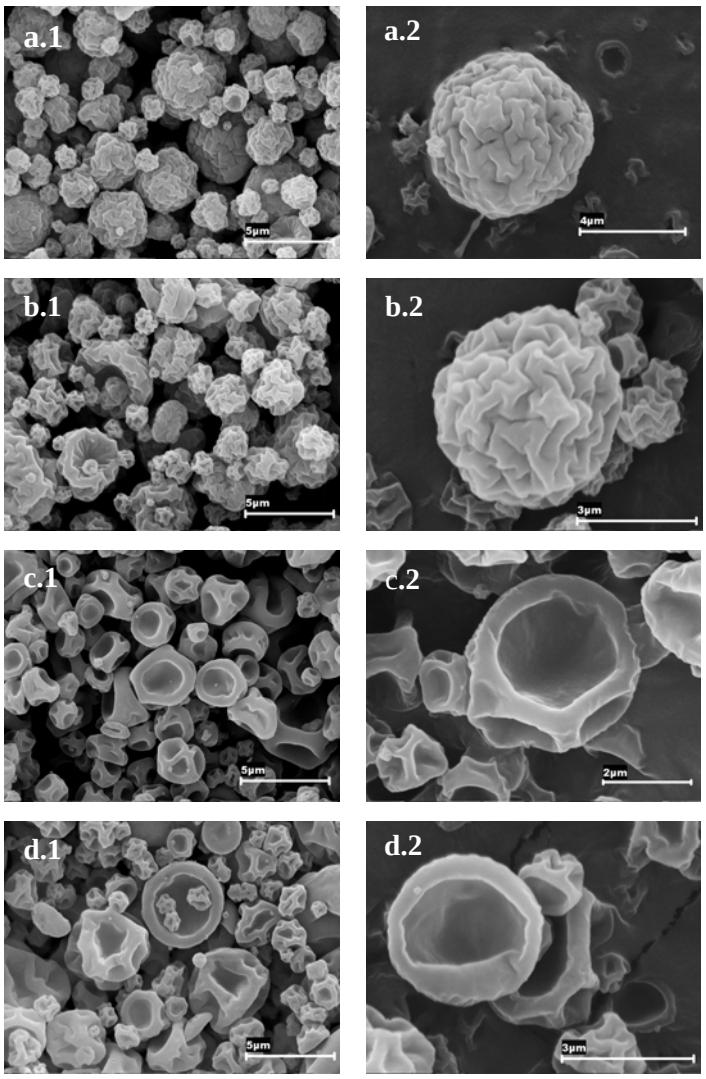

Figure 6. SEM microphotographs of the microspheres obtained by spray-drying CS solutions of different DD: (a) MS DD 47%; (b) MS DD 38%; (c) MS DD 26% and (d) MS DD 23%. Magnifications: (a) 20000x and (b) 50000x (except a.2 at 30000x).

Finally, it must be mentioned that the increase in surface rugosity, directly related with the decrease in CS DD of microspheres, may have a profitable impact on the agglomeration properties of the dispersed particles, as it has been reported that asperities prevent close approach of particles, thus avoiding van der Waals contact (Tarara et al., 2004).

The particle size of a powder formulation intended for inhalation is, together with density, a key factor in its therapeutic success because both strongly influence the particle aerosolization and *in vivo* deposition properties (Taylor and Kellaway, 2001; Courier et al., 2002). Spray dried microspheres obtained in this study have a small size, around 2 μm, being the differences between formulations not significant. Their specifical values, expressed as mean Feret diameters, and respective standard deviations are listed in **Table 4**.

Table 4. Micromeritic properties of microspheres obtained by spray-drying from CS with different deacetylation degree.

Particle code	Feret diameter (μm)	Real density (g/cm^3)	Apparent density (g/cm^3)	d_{aer} (μm)[a]
MS DD 83%	2.04 ± 0.93	1.48 ± 0.09	0.48 ± 0.01	1.96 ± 1.53
MS DD 47%	2.04 ± 1.24	1.47 ± 0.07	0.47 ± 0.02	1.53 ± 1.48
MS DD 38%	1.93 ± 1.37	1.43 ± 0.09	0.42 ± 0.02	1.56 ± 1.49
MS DD 26%	1.85 ± 0.65	1.37 ± 0.04	0.40 ± 0.01	1.56 ± 1.45
MS DD 23%	1.79 ± 1.16	1.36 ± 0.04	0.38 ± 0.03	1.46 ± 1.45

[a] d_{aer} : aerodynamic diameter determined with an Aerosizer® analyzer

In contrast, real and apparent density values, shown also in **Table 4**, resulted to be depending on CS DD. Thus, microsphere densities decreased with the decrease in CS DD, ranging from 1.48 to 1.36 g/cm^3 and from 0.48 to 0.38 g/cm^3 for real and apparent densities, respectively. This fact could be explained by the obvious morphologycal/surface differences mentioned above, although the contribution of

CS reacetylation to form less compact polymeric matrixs should not be discarded. The tendency resulted to be signifficant for the different apparent density values ($P < 0.05$).

The experimental aerodynamic diameters (d_{aer}) of the microspheres, measured using the Aerosizer® - Aerodisperser® equipment, are shown in **Table 4**. Results could be grouped in two significatively different values: 2 μm for MS DD 83%, and around 1.5 μm for the formulations prepared from reacetylated chitosans (DD < 50%). According to these aerodynamic diameter data, the developed microspheres are in the adequate range for optimal alveolar deposition, which must be of approximately 1-5 μm (Vanbever et al., 1999).

In order to investigate the suitability of CS microspheres to associate therapeutic proteins, insulin was selected as model. Insulin-loaded microspheres were prepared from three representative CS samples with DD of 83%, 38% and 23%. At this point, it must be mentioned that the high temperature used, inherent to the spray-drying processes, is not expected to compromise the stability of the associated protein (Broadhead et al., 1992). The association of insulin to the microspheres (theoretical 15% w/w based on CS) did not produce morphological differences compared to the unloaded particles. As can be observed in SEM microphotographs (**Figure 7**), the insulin loaded particles show similar shape to their respective blank particles (see **Figure 6**).

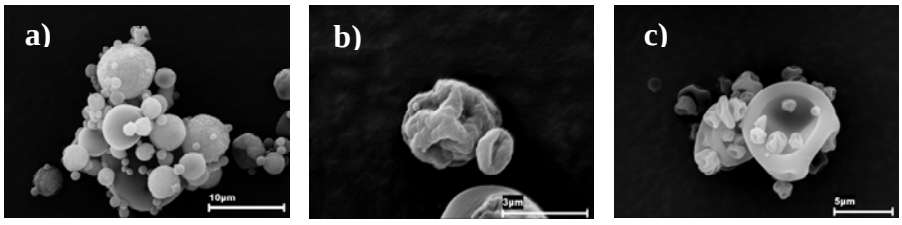

Figure 7. SEM microphotographs of the different CS DD microspheres containing 15% w/w insulin (based on polymer) obtained by spray-drying: (a) MS DD 83%; (b) MS DD 38%, and (c) MS DD 23%.

Association efficiencies were experimentally calculated as described in the methodology section. The determination of association efficiencies was performed at 22ºC rather than at 37ºC (physiological temperature), in order to minimize the insulin self-aggregation tendency occurring at higher temperatures (Sluzky, Klibanov & Langer, 1992; Reithmeier et al., 2001) and thus, to obtain the total amount of associated insulin. High insulin association efficiencies were obtained, ranging from 71%, for MS DD 83%, to 90-91%, for MS DD 38 and 23%. These high association efficiencies are usually associated with the spray drying processes (Surendrakumar et al., 2003). However, a decrease in the percent of associated insulin was observed for the microspheres prepared with the most deacetylated CS (DD 83%). In order to know if these differences were due to a real decrease in the insulin association during the spray-drying process or only to a decrease in the amount of insulin able to be quantified, we incubated the corresponding microspheres components (theoretical proportion of CS of different DD and insulin physically mixtured as before spray-drying) and determined the percent of recovered insulin. Since the differences found were less than a 5% (n = 3), as compared with the reported association efficiencies, we could conclude that there is some factor that hinders insulin quantification. Taking into account that the amount of quantified insulin decrease as the DD increases, the most feasible factor is an interaction between CS primary amino groups (non-acetylated) and insulin. Besides, a certain insulin self-aggregation should not be discarded.

Figure 8 depicts the release profiles of insulin from the spray-dried microspheres (MS DD 23%, MS DD 38%, and MS DD 83%) in PBS pH 7.4. Unlike association efficiency, *in vitro* release studies were carried out at 37ºC to mimic the physiological temperature. A clear `burst effect´ was observed during the first 15 minutes in contact with the medium, when most of the drug was released, irrespective of the formulation assayed. In general, after these first 15 minutes and until the maximum of insulin released is reached (at 1 hour), profiles resulted to be significantly different for the reacetylated CS formulations, MS DD 23% and MS DD

38%, with respect to MS DD 83% ($P < 0.05$). Specifically, the insulin release from the reacetylated CS formulations was faster and higher. The factors affecting this unexpected release behavior would be, basically: (a) the particular convoluted surface showed by MS DD 23% and MS DD 38% (as opposed to the spherical shape and smooth surface of non-reacetylated CS microspheres), that provides a higher specific surface area in contact with the release medium; and (b) their lower particle density, that suggest a less-compact internal structure, which may facilitate the diffusion of insulin through the polymeric matrix. However, taking into account that reacetylated CSs are less soluble, it could be expected that, once the microspheres are administered *in vivo* in a dry way, the insulin release will be slower.

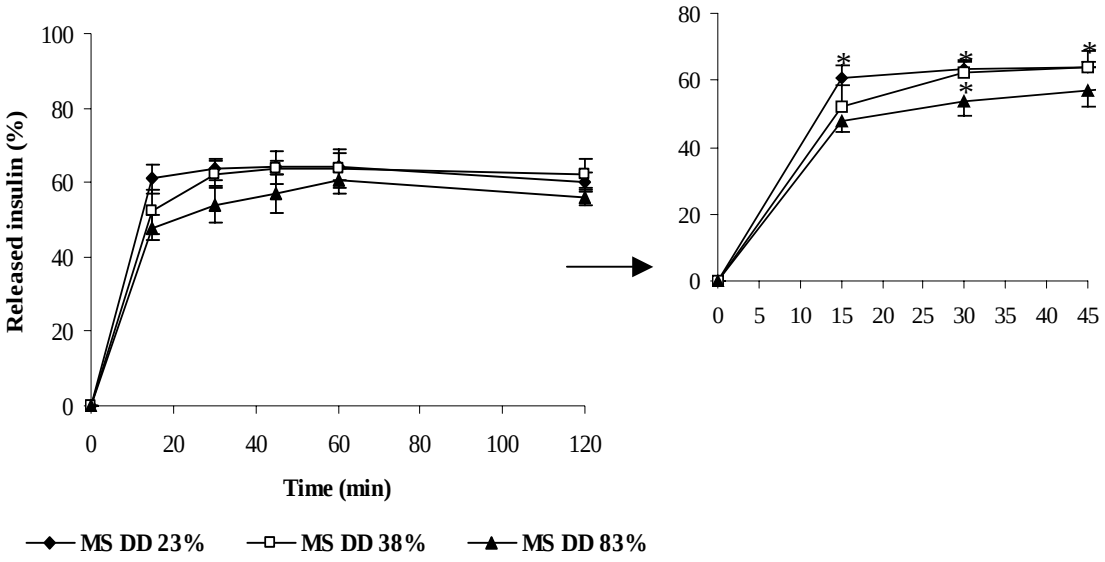

Figure 8. Release profiles of insulin from CS microspheres of different DD (23, 38, and 83%) in PBS pH 7.4 at 37ºC (insulin = 15% w/w based on CS; mean ± S.D., n = 3-6). (*) denotes significant differences ($P < 0.05$).

In summary, different CS DD microspheres were prepared by spray-drying in an entirely aqueous medium. Morphological and aerodynamic properties were dependent on CS DD, in all cases being suitable for drug delivery to the deep lung. The microspheres present a great potential as peptide/protein carriers, since high insulin (peptide model) association efficiencies were obtained. Based on previous studies performed by our group, we hypothesized that the microspheres, once inhaled, would reach the deep lung and adhere to the alveolar epithelium, where the protein would be released and CS could promote its absorption. By decreasing CS DD, it is expected that the formulations are significatively less toxic and more biodegradable, while preserving part of the favourable mucoadhesive and absorption-enhancing properties inherent to high deacetylated CS.

In order to find the optimum formulation for being administered *in vivo* to rats, further experiments will be aimed to extensively investigate the influence of CS DD on the polymer cytotoxicity and its ability to enhance the absorption of macromolecules across a cell culture model of the pulmonary epithelium.

ACKNOWLEDGEMENTS

This work was financially supported by the Spanish Government (CI-CYT, SAF2002-03314), FEDER (cofinanced) and Xunta de Galicia (PGIDIT03PXIC20301PN: Incentivo del proyecto SAF 2002-03314).

REFERENCES:

1. Ameri M., Maa Y. –F., Spray drying of biopharmaceuticals: stability and process considerations, Drying Technology, 24 (2006) 763-768.
2. Baxter A., Dillon M., Taylor K. D. A. and Roberts G. A. F., Improved method for i.r determination of the degree of N-acetylation of chitosan, Int. J. Biol. Macromol., 14 (1992) 166-169.
3. Broadhead J., Edmond-Rouan S. K., Rhodes C. T., The spray-drying of pharmaceuticals, Drug Dev. Ind. Pharm., 18 (1992) 1169-1206.
4. Carrión-Recio D., Taboada-Montero C., Vila-Jato J.L., Remuñán-López C., Enhacement of protein lung absorption using chitosan microspheres, *submitted*.
5. Colthorpe P., Farr S. J., Smith I. J., Wyatt D., Taylor G., The influence of regional deposition on the pharmacokinetics of pulmonary-delivered human growth hormone in rabbits, Pharm. Res., 12 (1995) 356-359.
6. Courier H. M., Butz N., Vandamme T. F., Pulmonary drug delivery systems: recent developments and prospects, Crit. Rev. Ther. Drug Carrier Syst., 19 (2002) 425-498.
7. Cryan S.-A., Carrier-based strategies for targeting protein and peptide drugs to the lungs, AAPS J., 7 (2005) E20-E45.
8. Domard A., pH and c.d. measurements on a fully deacetylated chitosan: application to Cu^{II}-polymer interactions, Int. J. Biol. Macromol., 9 (1987) 98-104.
9. Domszy J. G. and Roberts G. A. F., Evaluation of infrared spectroscopic techniques for analyzing chitosan, Makromol. Chem., 186 (1985) 1671-1677
10. Dong Y., Xu C., Wang J., Wang M., Wu Y. and Ruan Y., Determination of degree of substitution for N-acylated chitosan using IR spectra, Science in China (Series B), 44 (2001) 216-224.

11. Edwards D.A., Ben-Jebria A., Langer R., Recent advances in pulmonary drug delivery using large, porous inhaled particles, J. Applied Physiol., 85 (1998) 379-385.

12. El-Gibaly I., Development and in vitro evaluation of novel floating chitosan microcapsules for oral use: comparisson with non-floating chitosan microspheres, Int. J. Pharm., 294 (2002) 7-21.

13. He P., Davis S. S., Illum L., In vitro evaluation of the mucoadhesive properties of chitosan microspheres, Int. J. Pharm., 166 (1998) 75-68.

14. Hirai A., Odani H., Nakajima A., Determination of degree of deacetylation of chitosan by ^{1}H NMR spectroscopy, Polym. Bull., 26 (1991) 87-94.

15. Huang M., Khor E., and Lim L. –Y., Uptake and cytotoxicity of chitosan molecules and nanoparticles: effects of molecular weight and degree of deacetylation, Pharm. Res., 21 (2004) 344-353.

16. Huang Y. -C., Yeh M. -K., Chiang C. -H., Formulation factors in preparing BTM-chitosan microspheres by spray drying method, Int. J. Pharm., 242 (2002) 239-242.

17. Kas H. S., Chitosan: properties, preparation and application to microparticulate systems, J. Microencapsulation, 14 (1997) 659-711.

18. Kobayashi S., Kondo S., Juni K., Study on pulmonary delivery of salmon calcitonin in rats: effects of protease inhibitors and absorption enhancers, Pharm. Res., 11 (1994) 1239-1243.

19. Lavertu M., Xia Z., Serreqi A. N., Berrada M., Rodrígues A., Wang D., Buschmann M.D. and Gupta A., A validated ^{1}H NMR method for the determination of the degree of deacetylation of chitosan, J. Pharm. Biomed. Anal., 32 (2003) 1149-1158.

20. Le Tien C., Lacroix M., Ispas-Szabo P., and Mateescu M.-A., N-acylated chitosan: hydrophobic matrices for controlled drug release, J. Control. Rel., 93 (2003) 1-13.

21. Mima S., Miya M., Iwamoto R. and Yoshikawa S., Highly deacetylated chitosan and its properties, J. Appl. Polym. Sci., 28 (1983) 1909-1917.

22. Moore G. K. and Roberts G. A. F., Determination of the degree of N-acetylation of chitosan, Int. J. Biol. Macromol., 2 (1980) 115.

23. Patton J.S., Bukar J., Nagarajan S., Inhaled insulin, Adv. Drug Del. Rev., 35 (1999) 235-247.

24. Patton J.S., Platz R.M., Routes of delivery: case studies. 2. Pulmonary delivery of peptides and proteins for systemic action, Adv. Drug Deliv. Rev., 8 (1992) 179-196.

25. Patton J.S., Trinchero P., Platz R.M., Bioavailability of pulmonary delivery of peptides and proteins: α-interferon, calcitonins and parathyroid hormones, J. Control. Rel., 28 (1994) 79-85.

26. Reithmeier H., Herrman J., Göpferich A., Lipid microparticles as a parenteral controlled release device for peptides, J. Control. Rel., 73 (2001) 339-350.

27. Roser M., Fisher D., Kissel T., Surface modified biodegradable albumin nano- and microspheres. II: effect of surface charges on in vitro phagocytosis and biodistribution in rats, Eur. J. Pharm. Biopharm., 4 (1998) 255-263.

28. Sabnis S. and Block L. H., Improved infrared spectroscopic method for the analysis of degree of N-acetylation of chitosan, Polym. Bull., 39 (1997) 67-71

29. Sakr F. M., The pharmacokinetics of pulmonary nebulizer insulin and its effect on glucose tolerance in streptozotocin-induced diabetic rabbit, Int. J. Pharm., 128 (1996) 215-222.

30. Schipper N.G.M., Varum K.M., Artursson P., Chitosans as absorption enhancers for poorly water absorbable drugs. I. Influence of molecular weight and degree of acetylation on drug transport across human intestinal epithelial (Caco-2) cells, Pharm. Res., 13 (1996) 1686-1692.

31. Sluzky V., Klibanov A.M., Langer R., Mechanism of insulin aggregation and stabilization in agitated aqueous solutions, Biotechnology and Bioengineering, 40 (1992) 1-9.

32. Surendrakumar K., Martín G.P., Hodgers E.C.M., Jansen M., Blair J.A., Sustained release of insulin from sodium hyaluronate based dry powder formulations after pulmonary delivery to beagle dogs, J. Control. Rel., 91 (2003).

33. Tanveer A.K., Kok K.P., Hung S.C., Reporting degree of deacetylation values of chitosan: the influence of analytical methods, J. Pharm. Pharmaceut. Sci., 5 (2002) 205-212.

34. Tarara T. E, Hartman M. S., Gill H., Kennedy A. A., and Weers J. G., Characterization of suspension-based metered dose inhaler formulations composed of spray-dried budesonide microcrystals dispersed in HFA-134a, Pharm. Res., 21 (2004) 1607-1614.

35. Taylor G., Kellaway I. In: Hillery M., Lloyd A. W., Swerbrick J. (Ed.), Pulmonary drug delivery. Drug delivery and targeting for pharmaceutical scientists, Taylor & Francis, London (2001) pp. 269-300.

36. Tomihata K., and Ikada Y., In vitro and in vivo degradation of films of chitin and its deacetylated derivatives, Biomaterials, 18 (1997) 567-575.

37. van der Lubben I. M., Verhoef J. C., Borchard G., and Junginger H. E., Chitosan and its derivatives in mucosal drug and vaccine delivery, Eur. J. Pharm. Sci., 14 (2001) 201-207.

38. Vanbever R., Ben-Jebria A., Mintzes J. D., Langer R., Edwards D. A., Sustained release of insulin from insoluble inhaled particles, Drug Deliv. Research, 48 (1999) 178-185.

39. Varum K.M., Myhr M.M., Hjerde R.J., Smidrod O., In vitro degradation rates of partially N-acetylated chitosans in human serum, Carbohydrate Researh, 299 (1997) 99-101.

40. Williams R. O., Barron M. K., Alonso M. J., Remuñán-López C., Investigation of a pMDI formulation containing chitosan microspheres, Int. J. Pharm., 174 (1998) 209-222.

41. Xu J., McCarthy S. P., Gross R. A., and Kaplan D. L., Chitosan film acylation and effects on biodegradability, Macromolecules, 29 (1996) 3436-3440.

42. Yu J., Chien Y.W., Pulmonary drug delivery: physiologic and mechanistic aspects, Crit. Rev. Ther. Drug Carrier Syst., 14 (1997) 395-453.

43. Zhang Z.-Y., Ping Q.-N., Xiao B., Microencapsulation and characterization of tramadol-resin complexes, J. Control. rel., 66 (2000) 107-113.

44. Zhang H., Neau S.H., In vitro degradation of chitosan by a commercial enzyme preparation: effect of molecular weight and degree of deacetylation, Biomaterials, 22 (2001) 1653-1658.

ARTÍCULO 2

Preparation and Characterization of Chitosan/Glucomannan Microspheres for Pulmonary Delivery of Macromolecules

Desirée Teijeiro-Osorio[a,b], Carlos J. Lamela[a], Hanne Mørck Nielsen[b], Carmen Remuñán-López[a]

[a] Department of Pharmacy and Pharmaceutical Technology, Faculty of Pharmacy, University of Santiago de Compostela, Santiago de Compostela, Spain.

[b]Department of Pharmaceutics and Analytical Chemistry, Faculty of Pharmaceutical Sciences, University of Copenhagen, Copenhagen, Denmark.

ABSTRACT

Chitosan:glucomannan (CS:GM) microparticles intended for pulmonary drug delivery have been prepared by spray-drying. The results have shown that the morphology and surface appearance of the microspheres, as well as their densities and aerodynamic diameters, are closely dependent on their composition (presence and amount of GM), and suggested the adequacy of these particles to be delivered to the deep lung. A protein model (insulin) was efficiently encapsulated, and the influence of the CS:GM ratio on the drug release behavior of the particles was investigated. In general, the release of insulin from the microspheres was fast and accompanied by a burst effect, this fact being mainly related with the particle morphology, the polymeric matrix structure and the own drug model, as well as the non-employment of crosslinking agents in their preparation. However, it is expected a different behavior *in vivo*, when the particles, administered as dry powders, reach the mucosal/alveolar surfaces and release the entrapped drug more gradually, after a humectation and swelling process. In these sense, *in vitro* studies performed in well-differentiated Calu-3 cells, showed the ability of these CS:GM microspheres to closely interact with the mucus and remain adhered to the epithelium.

KEY WORDS: Chitosan, glucomannan, microspheres, mucoadhesion, pulmonary delivery, spray-drying.

1. INTRODUCTION

Drug delivery to the lungs by inhalation has attracted tremendous scientific and biomedical interest over the last few years. Inhaled drugs can be absorbed, after deposition, in various parts of the respiratory tract, but the highest absorption occurs in the alveolar region owing to its large surface, extensive vasculature and very thin epithelium (Taylor and Kellaway, 2001). However, important barriers to deep lung deposition of particulate delivery systems are the impaction of delivered material at the throat and major bifurcations and rapid particle removal from the lungs by mucociliary and phagocytic clearance mechanisms (Edwards et al., 1998; Groneberg et al., 2003). The avoidance of these obstacles depends on shape, size and density (aerodynamic properties) as well as surface characteristics of the particles. In this sense, numerous estudies have demonstrated that particles of mean aerodynamic diameter of 1-5 μm (Clark and Egan, 1994; Vanbever et al., 1999), deposit minimally at the mouth ant throat and maximally in the alveolar or deep lung region, thus being optimal for inhalation therapy. Additionally, it must be taken into account that an excessive particle aggregation in the inhaler can lead also to an inefficient drug delivery. In this sense, major improvements in aerosol particle performance have been reported by lowering particle mass density and increasing particle size, since these particles display less tendency to agglomerate than conventional small and nonporous (compact) particles (Edwards et al., 1998).

For all the mentioned above, it can be deduced that the design of an adequate drug carrier system becomes in an essential prerequisite for the successfull delivery of macromolecules to the systemic circulation by inhalation.

Several research works have been focusing in the design and formulation of microspheres as carriers for pulmonary administration. Among the different techniques used to prepare microparticles for aerosol delivery (supercritical fluid technology, emulsion-solvent evaporation, spray-drying, emulsion-solvent diffussion, and phase separation) (Cryan, 2005), spray-drying has the advantage of allowing the preparation of microspheres in an entirely aqueous medium from the mixture of drug and excipient solutions as well as suspensions (Sinha et al., 2004; Agnihotri et

al., 2004). Furthermore, the high temperature inherent to all spray-dried processes, is known not to compromise the stability of the associated protein (Broadhead et al., 1992). These systems can be prepared by using a wide range of naturally occurring or synthetic polymers, while desired morphologic (shape and porosity) and aerodynamic (size and density) characteristics can be achieved by simply modifying the composition and/or the processing parameters (Cryan, 2005).

Chitosan (CS) is a natural polysaccharide with great potential for pharmaceutical applications, mainly due to its well-documented biodegradability, biocompatibility and low-toxicity (Hirano et al., 1989; Knapczyc et al., 1989; Tomihata and Ikada, 1997). Indeed, the polymeric cationic nature and gel-forming capability of CS play an effective role on the opening of intercellular tight junctions, thereby favoring mucoadhesion and permeation of hydrophilic macromolecules across the well-organized epithelium (van der Lubben et al., 2001; Portero et al., 2002).

In this sense, we have recently demonstrated that insulin-loaded CS microspheres prepared by spray-drying are adequate for lung protein delivery, since they are able to reach the alveolar region after intratracheal administration of the dry powder to rats and provide a significantly lower glucose levels (60 and 90 min after administration) than those corresponding to the insulin solution (Carrión-Recio et al., *submitted*).

Glucomannan (GM) is a hydrocolloidal polysaccharide, very abundant in nature, which consists in β-1,4 linked mannose and glucose residues and that has been lately introduced in the drug delivery field; mainly as a pharmaceutical excipient in tablets, films, beads and hydrogels, due to its gelling, solubility and biodegradable properties, but also for the targeting of nanocarriers to specific receptors on the cell surface, such as the mannose receptors (Alonso-Sande et al., *submitted*). In this sense, we would like to underline the development of CS:GM-based nanoparticles, which have shown attractive features as carriers for transmucosal drug delivery applications. The main role of GM in this system was to improve the stability of the CS nanoparticles and to control the release of the encapsulated proteins (Du et al., 2005; Cuña et al., 2006; Alonso-Sande et al., 2006a). Furthermore, the introduction

of GM in the nanoparticles demonstrated to increase their interaction with the intestinal epithelium both *in vitro*, in Caco-2 cells, and *in vivo*, after oral administration to rats (Alonso-Sande et al., 2005; 2006b).

Taking into account all this previous information, in the present work we decided to introduce GM as a "modifying" factor in the composition of the CS microspheres, which were proposed for pulmonary drug delivery, thus investigating the effect of GM type (different viscosity) and content (different ratios CS:GM) on the morphological and aerodynamic characteristics of the particles, as well as on their mucoadhesive properties and drug release patterns. Therefore, the aim of the present work was to develop, using a spray-drying technique, CS:GM-based microspheres with appropriate morphological and aerodynamic characteristics to reach the deep lung, where the associated protein is expected to be delivered and absorbed. The potential of these microspheres as protein carriers was investigated using insulin and FITC-BSA as model compounds.

2. MATERIALS AND METHODS

2.1. Materials

The following chemicals were obtained from commercial suppliers and used as received: chitosan (Sea Cure 223, supplier´s specification: Mw of 150 KDa and deacetylation degree > 80%) (Pronova Lab., Norway); Ultrapure chitosan (Protasan UP G113, supplier´s specification: Mw of 128 KDa and deacetylation degree = 86%) (FMC Biopolymers, Norway); glucomannan (Propol RX-L, Propol RS and Propol A, supplier´s specifications: viscosity of a 1% GM solution at 25ºC: 15000, 35000 and 100000 cps, respectively) (Shimizu Chemical Co., Japan); mucin type III (1% sialic acid), insulin from bovine pancreas, fluorescein isothiocyanate labelled bovine serum albumin (FITC-BSA), phenazine methosulphate (PMS) and penicillin/streptomycin (Sigma-Aldrich, Germany); 3-(4,5-dimethylthiazol-2-yl)-5-(3-carboxymethoxyphenyl)-2-(4-sulfophenyl)-2H-tetrazolium (MTS) (Promega, USA); Dulbecco's modified Eagles medium (DMEM), Hanks' balanced salt solution (HBSS)

and trypsin-EDTA (Gibco BRL, UK); morpholino-ethanesulphonic acid anhidrous (MES) (Applichem GmbH, Germany); Bodipy® Phalloidin 650/665 (Molecular Probes, USA); Triton® X (Fluka, Switzerland); fetal bovine serum (FBS) (Biotech Line A/S, Denmark). Ultrapure water (Milli-Q plus, Millipore Ibérica, Spain) was used throughout. All other reagents were of the highest grade available and were used without further purification.

2.2. Cell culture

Calu-3 cells were purchased from American Type Culture Collection ATCC (Rockville, USA) and cultured as previously referred (Tréhin et al, 2004) with slight modifications. Briefly, cells were detached from culturing flasks by trypsin-EDTA and subcultivated at 37ºC with a 5% CO_2 humidified atmosphere for studies with proliferating cells or a well-differentiated epithelium. For studies with proliferating cells, the cells were seeded in flat-bottomed 96-well culture plates (0.33 cm^2/well, Costar®, Corning Inc., USA) in a density of 8.2 x 10^4 cells/well and cultured for 24 h. To obtain a differentiated epithelium, Calu-3 cells (passage 27-28) were cultured on inserts with a constant density of 2 x 10^5 cells/cm^2 (Falcon® 12-well tissue culture plates, 0.9 cm^2/insert, 0.4 μm pore size, Becton Dickinson Labware, USA). Cell culture medium was removed from the apical compartment 24 h after seeding, in order to allow the cells to form a monolayer at an air-liquid interface. Calu-3 differentiated monolayers were used after 15 days.

2.3. Evaluation of cytotoxicity and mucoadhesive properties of polymers

2.2.1. Cytotoxicity of GM

The dehydrogenase activity in the Calu-3 proliferating cells was used to estimate the cells sensitivity to different GM concentrations and measured according to the MTS/PMS assay (Eirheim et al., 2004). Thus, cells grown in 96-well culture plates were incubated with 100 μL of GM (RX-L) solutions in concentrations ranging from 0.01 to 5 mg/mL (20mM MES in HBSS, pH 6) for 4 h. At the end of the incubation

time, samples were discarded and replaced by the MTS/PMS solution. Incubation was done under stirring and protected from light for 2 h at 37ºC. The absorbance was measured at 492 nm using a microplate reader (FluoStar Optima, BMG Labtech GmbH, Germany). The enzyme activity in untreated cells was set at 100%, and the effect of the GM solutions was measured as the relative decrease in enzyme activity. Analysis of three replicates was conducted in three different passages of cells.

2.2.2. Mucoadhesive properties of polymer solutions

Mucoadhesive properties of the aqueous solutions of CS (223), GM (Propol RX-L and Propol RS) and different ratios of CS:GM mixtures (75:25, 50:50 and 25:75, for both GM types) were evaluated by measuring its interaction with mucin by a turbidimetric method (He et al., 1998). Stock polymer (CS and the two different GM) and mucin solutions (2 mg/mL, acetate buffer pH 4.5) were prepared, filtered and stored at 4ºC until their use. The mucin and polymer solutions were mixed in different ratios (mucin:polymer ratio = 1:3; 1:1; 3:1) and incubated under horizontal shaking (200 oscillations/min, *Heidolph Promax 2020,* Germany) during 30 min at room temperature. The absorbances of these samples (A_{exp}) were assayed for turbidimetry by UV spectroscopy at 500 nm (*UV-1603 Shimadzu,* Japan). The absorbances of the individual polymers and mucin solutions in acetate buffer were measured as controls to give the theoretical values (A_t) for a non-interacting system. Calculations were performed as follows:

$$A_t = A_{mucin} \times P_{mucin} + A_{polymer} \times P_{polymer}$$

where A_{mucin} and $A_{polymer}$ are the absorbances obtained for the mucin and polymer solutions individually, and P_{mucin} and $P_{polymer}$ are the proportion of mucin and polymer, respectively, present in the mixture. The absorbance difference between the measured experimentally and the calculated theoretically ($A_{exp} - A_t$) represents the mucoadhesion strength. All samples were analyzed in triplicate (n = 3).

2.4. Preparation of drug-unloaded (blank) CS:GM microspheres

CS solutions (CS 223, 3% w/w) were prepared by dissolving the polymer in a diluted acidic solution (1.5M acetic acid) and centrifuged (21100 g, 15 min) (*Beckman Avanti ^{TM} 30,* USA) in order to eliminate possible CS impurities. GM solutions (1% w/w in Milli-Q water) were prepared in three main steps, which duration was fixed depending on the native GM viscosity. First, the powder was humected under magnetical stirring at room temperature, followed by refrigeration (4ºC) and lastly, magnetical stirring at room temperature again. Polysaccharide solutions to spray dry were prepared by diluting and/or mixing the solutions previously obtained in order to get the different concentrations and ratios depicted in **Table 1**. The solutions, maintained under continuous mechanical stirring, were spray-dried using a feed rate of 2.8 mL/min (nozzle size = 0.7 mm) and an air flow rate of 473-550 Nl/h, at inlet and outlet temperatures of 159-163 ºC and 108-116 ºC, respectively (*Büchi Mini Spray-drier B-290, Büchi Labortechnik AG,* Switzerland).

The spray-drying production yields (SPD-yield) were calculated as follows:

SPD-yield (%) = (Microspheres weight/Total solids weight) x 100

2.5. Infrared spectra of CS:GM microspheres

The infrared (IR) spectra of microspheres containing different CS:GM ratios (100:0, 50:50, 0:100) were recorded using the KBr technique (1 mg sample in 50 mg KBr) (Bruker model IFS-66v, Germany) with a frequency range of 4000-400 cm^{-1}.

2.6. Characterization of microspheres size and surface morphology

The morphology and surface appearance of the microspheres were examined by scanning electron microscopy (SEM). The particles were freeze-dried (*Labconco apparatus, Labconco Co.,* USA), coated with gold palladium to achieve films of 60 nm thickness (*Polaron SC7640 High Resolution Sputter-coater, Thermo VG Scientific,* England) and observed with a scanning electron microscope (*SEM Leica S440,* England).

The particle size was estimated as the Feret´s diameter (the measured distance between parallel lines that are tangent to the particle profile and perpendicular to the ocular scale) and was directly determined with an optical microscope (*Olympus BH-2*, Japan) on 100 particles.

2.7. Determination of microspheres density

Real densities of blank microspheres were determined by Helium pycnometry (*Micropycnometer, Quanta Chrome*, *model MPY-2*, USA) (*n* = 6). Apparent (tap) densities were obtained by measuring the volume of a known weight of powder in a 10 mL graduated cylinder. After registering the initial volume, the cylinder was mechanically tapped (30 tap/min, *Tecnociencia,* Spain) until a constant volume was achieved (El-Gibaly, 2002). The apparent density was calculated as the mass divided by the volume (*n* = 3).

2.8. Evaluation of microspheres aerodynamic diameter

Aerodynamic diameters (d_{aer}) of microspheres were determined using a TSI Aerosizer® LD analyzer equipped with an Aerodisperser® (*Amherst Process Instrument Inc*., USA) (*n* = 3), whose measuring principle is based on direct time-of-flight measurements according to the following equation:

$$C_d \frac{\pi d^2}{4} \rho_a \frac{(V_a - V_p)^2}{2} = 1/6\, \pi d^3 \rho_p \frac{dV_p}{dt}$$

where C_d: particle drag coefficient, d: the particle Feret´s diameter, ρ_a: air density, ρ_p: particle real density, V_a: air velocity and V_p: particle velocity.

2.9. Association of macromolecules to microspheres

The potential of CS, GM and CS:GM microspheres as carriers of therapeutic macromolecules was investigated using insulin (15% w/w based on CS 223 and/or GM) as protein model. Additionally, for cell studies, an ultrapure CS was used in the preparation of CS and CS:GM fluorescent microsphere encapsulating FITC-BSA (30% w/w based on CS and/or GM). Insulin and FITC-BSA were dissolved in 0.1M HCl and water, respectively. Afterwards, protein solutions were mixed with the corresponding polymeric solutions by magnetic stirring to form final 1% w/w solutions, which were spray-dried following the same operating conditions described for unloaded microspheres.

2.9.1. Determination of insulin content

Protein content of formulations was determined following the microspheres incubation (1.25 mg of microspheres, test tubes of 10 mL) in 6 mL of PBS pH 7.4 under horizontal shaking (105 oscillations/min, *Heidolph Promax 2020,* Germany) at 22°C, until the complete protein release (4 h). The microspheres dispersions were filtered (0.45 µm filters unit *MILLEX®-HV*, low protein binding, USA) and the supernatants assayed for insulin content by measuring their absorbances at 562 nm (*Micro BCA Protein Assay Reagent Kit, Pierce*, USA; *UV-1603 Shimadzu*, Japan) (*n* = 3). The association efficiency (A.E.) to the microspheres was determined as follows:

$$\text{A.E. (\%)} = (\text{Weight of associated protein}/\text{Total protein weight}) \times 100$$

2.9.2. In vitro release studies

In vitro release studies of protein-loaded microspheres were performed as follows. Microspheres (2.5 mg) were incubated (10 mL test tubes) in 6 mL of PBS pH 7.4 under horizontal shaking (105 oscillations/min, *Heidolf promax 2020*, Germany) at 37ºC. At pre-determined times (15, 30, 45, 60 and 120 min) the microparticles dispersions supernatants were filtered (0.45 µm filters unit *MILLEX®-HV*, low protein

binding, USA) and assayed for drug release by measuring their absorbances at 562 nm (*Micro BCA Protein Assay Reagent Kit, Pierce*, USA; *UV-1603 Shimadzu*, Japan) (*n* = 3).

2.10. *In vitro* evaluation of microspheres mucoadhesive properties

2.10.1. Microspheres incubation with mucin

Cualitative mucoadhesive properties were evaluated by a slightly modified method reported by Genta et al. (Genta et al., 1998). The experiment was carried out in triplicate as follows: samples of 3 mg of unloaded microspheres were dispersed in 3 mL of an aqueous solution containing mucin (1 mg/mL) and incubated at room temperature for 2 min under horizontal shaking (200 oscillations/min, *Heidolph Promax 2020,* Germany). The dispersions were then centrifuged at 4000 rpm (*Sigma Laborzentrifugen*, Germany) for 2 min and the supernatants removed afterwards. Finally, pellets containing the microspheres were freeze-dried and samples were prepared, as previously described, in order to be observed by SEM (*Leica S440,* England).

2.10.2. Cualitative bioadhesion/interaction of microspheres with Calu-3 cells

Calu-3 cells were grown as confluent monolayers at an air-liquid interface on filter inserts, as described above. On day 15 after seeding, transepithelial electric resistance (TEER) values measured with a Millicell®-ERS (Millipore, Bedford, USA) were between 1100-1200 Ω x cm^2. These confluent, polarized Calu-3 cell monolayers, which are an *in vitro* model of the bronchial human epithelium, were used to assess the adhesion of microspheres. For these bioadhesion studies, dry CS and CS:GM microspheres encapsulating FITC-BSA were applied to the apical surface of cells. An special device (*DP-4 Dry Powder Insufflator, Penn Century Inc.*, USA) was used in order to ensure the homogeneous dry powder distribution on the cells (**Figure 1**). Upon incubation of fluorescent microspheres with the cells (1 h, 37ºC), 250 μL of HBSS was added to the apical compartment. The filter was swirled

gently and the HBSS collected to remove poorly adhering microspheres. Thereafter, cells were fixed with 4% paraformaldehyde for 10 min and washed, and cell membranes were stained with Bodipy® Phalloidin 650/665 (60 μL/mL in HBSS containing 0.2% w/v Triton X®) for 30 min. Finally, the filters were washed, cut and examined under Confocal Laser Scanning Microscopy (CLSM, *Zeiss 501*, Jena, Germany) at 488 nm and 633 nm excitation wavelenghts for FITC and Bodipy® Phalloidin, respectively. Experiments were performed in triplicate.

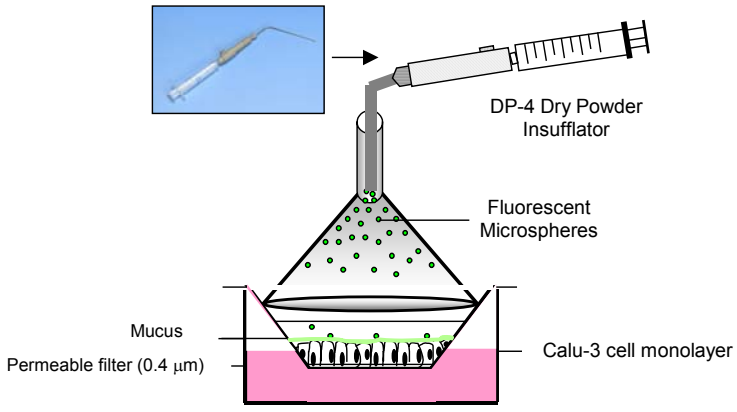

Figure 1. Escheme of microsphere´s release from a dry powder insufflator on the Calu-3 epithelium.

3. RESULTS AND DISCUSSION

The goal of the present work was to prepare CS:GM microspheres suitable for pulmonary delivery of therapeutic proteins. As a first step, we evaluated the cytotoxicity and mucoadhesive properties of the polymers. Then, the influence of several formulation variables on morphology and aerodynamic properties of the CS:GM microspheres was investigated and the ability of some selected formulations to associate and deliver the therapeutic macromolecule model (insulin) was evaluated. In addition, the bioadhesion/interaction of fluorescein-labelled microspheres with Calu-3 differentiated cells, an *in vitro* model of the airways epithelium, was investigated by confocal microscopy.

3.1. Evaluation of cytotoxicity and mucoadhesive properties of polymers

3.1.1. *Cytotoxicity studies*

Taking into account that the toxicity of CS (different Mw and deacetylation degree, and different salt) was previously and extensively studied by our group in different cell lines (Portero et al., 2002; Teijeiro-Osorio et al., *submitted*), we decided to focus our attention in the study of GM toxicity.

It is well known that GM has been traditionally used as a food additive in China and Japan, most specifically as a dietary fibre and, hence, considered good for health (Nishinari, 2000). In this sense, only a few works have been aimed at studying the toxicity of GM, most of them focused on their acute, sub-acute and sub-chronic intestinal toxicity following oral administration, and founding no significant signs of toxicity at high doses (Alonso-Sande et al., *submitted*). However, the recent incursion and interest of GM in the drug delivery field makes also necessary the study of polymer toxicity by other alternative routes. Since our interest lies in the application of GM by the pulmonary route and no studies have been reported on this topic until now, we considered specially interesting to evaluate the cytotoxic effects of GM (Propol RX-L) in Calu-3 cells, an *in vitro* model of the airways epithelium. The

dehydrogenase activity in the Calu-3 proliferating cells was used to estimate the cells sensitivity to GM doses within 3 and 1515 μg/cm^2, and measured according to the MTS/PMS assay. Interestingly, the cell viability remained around 80%, even for a polymer dose as high as 606 μg/cm^2 (**Figure 2**), no reaching the IC_{50} value for any of the tested doses. This fact is specially outstanding if we consider that the IC_{50} values reported for different CS (Mw 128 and 300 kDa), in the Calu-3 cell line and under similar assay conditions, were around 6-7.5 μg/cm^2 (Teijeiro-Osorio et al., 2005).

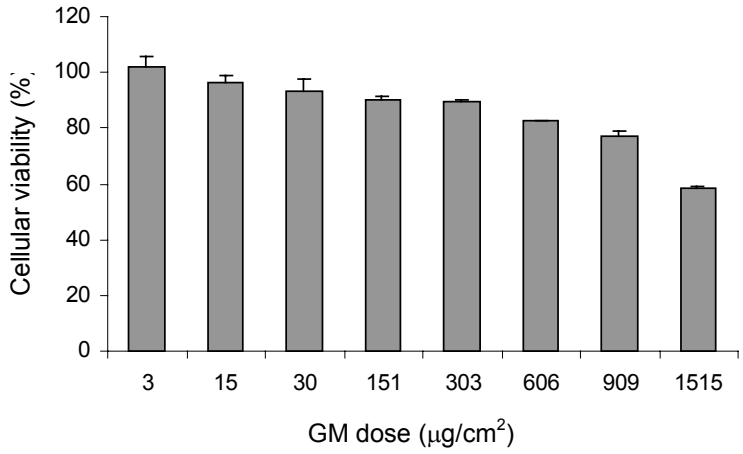

Figure 2. Sensitivity of Calu-3 proliferating cells toward various concentrations of GM in solution determined by the MTS/PMS assay (means ± SD, *n=3*).

3.1.2. *Mucoadhesive properties of polymer solutions*

It is known that the cationic polyelectrolyte nature of CS provide a strong electrostatic interaction with mucus or a negatively charged mucosal surface. In this sense, it could be expected that the presence of increasing amounts of the neutral polysaccharide GM in the CS:GM formulations could led to lose a part of this mucoadhesion behaviour. In a first attempt of evaluating the effect of GM content on

mucoadhesive properties, we performed turbidimetric studies on polymer mixtures (CS and/or GM in different ratios) incubated with different amounts of mucin (He et al., 1998). The absorbances (A) of the polymer mixtures and mucin were first measured separately and used for calculating theoretical absorbance values (A_t), and then measured together (A_{exp}), following incubation, as explained in the Methodology section. The absorbance difference (A_{exp} - A_t) between the measurement and the theoretical value is the parameter that represents the mucoadhesion strength. Thus, when no interaction occurs, A_{exp} - A_t is zero, whereas the higher is the "A_{exp} - A_t" value, the higher is the interaction between the polymer mixture and mucin and, consequently, the mucoadhesion strength. This parameter is depicted in **Figure 3**, as function as the composition of polymer mixtures and the ratio mucin/polymer used in the incubation processes.

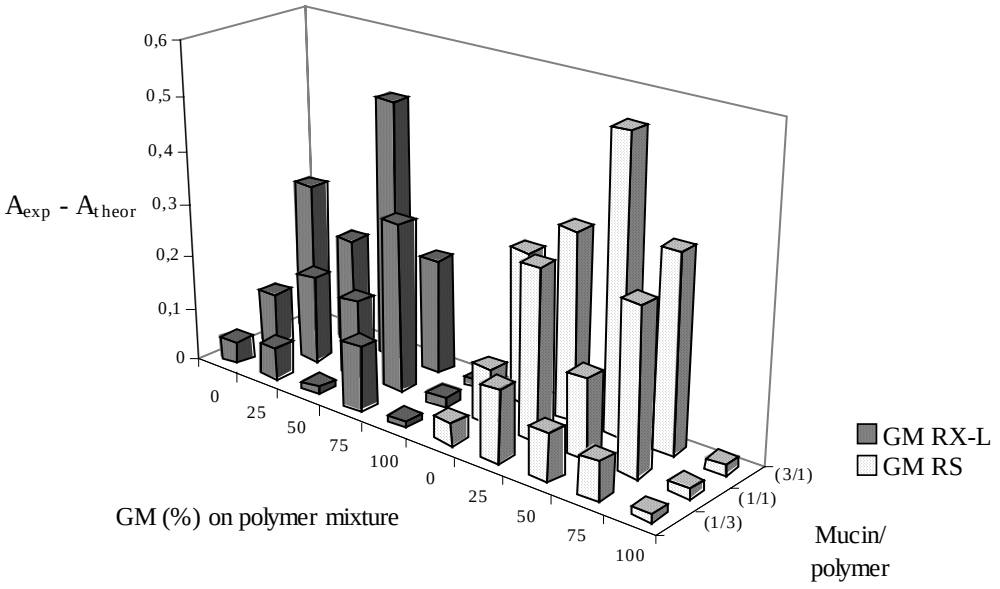

Figure 3. Turbidimetric measurement of the interaction between CS:GM polymeric solutions and mucin.

As expected, no mucoadhesion was found for those solutions composed only by GM, whereas high "A_{exp} - A_t" values were found for all the CS/GM mixtures. Surprisingly, these values resulted to be even higher than those corresponding to CS solutions, thus suggesting an interesting synergistic effect for CS/GM mixtures. The highest effect was found for the 50:50 ratio (CS:GM), with an "A_{exp} - A_t" value around 0.50-0.55. Very similar results were obtained for both types of GM tested, Propol RX-L and Propol RS, thus revealing the non-influence of GM viscosity and, hence, molecular weight.

3.2. Preparation of unloaded CS:GM microspheres by spray drying

As mentioned in the Methodology section, microspheres were prepared by spray-drying different polymeric solutions, composed by CS (223) and GM (Propol RX-L and RS) at different ratios (CS:GM= 75:25, 50:50 or 25:75) as well as by only both polymers (CS:GM= 100:0 and 0:100). In addition, the effect of the polymer concentration (0.1 and 1% w/w) was also investigated in two selected formulations (CS:GM RX-L= 25:75 and 0:100). The employment of GM Propol A was limitted by its own extremely high viscosity (100000 cps), being used only at a low concentration (0.1% w/w) to facilitate its handling. All the formulations prepared are shown in **Table 1**, as well as their corresponding spray-drying production yields [(Microspheres weight/Total solids weight) x 100]. As it can be noted, the higher was the CS content in the microspheres, the higher was the production yield, ranging from 30-35% for GM microspheres to 64% for CS microspheres.

Table 1. Formulations prepared by spray-drying from different chitosan:glucomannan ratios, type of glucomannan (15000, 35000 and 100000 cps) and polymer concentration (0.1 and 1% w/w), and resulting process yields.

Composition	CS:GM ratio	Polymer concentration (% w/w)	Spray-drying process yield (%)
CS 223	100:0	1	64.02
CS 223:GM RX-L	75:25	1	63.10
	50:50	1	61.81
	25:75	1	56.70
		0.1	51.73
GM RX-L	0:100	1	35.82
		0.1	33.04
CS 223:GM RS	75:25	1	58.53
	50:50	1	47.50
	25:75	1	37.84
GM RS	0:100	1	30.21
CS 223: GM A	25:75	0.1	n.d
GM A	0:100	0.1	n.d

3.3. Infrared spectra of CS:GM microspheres

IR spectra of CS:GM microspheres (0:100, 50:50, 100:0), which were recorded as explained in the methodology, are shown in **Figure 4**. The stretching peak of the carbonyl at 1730 cm^{-1} was assigned to the aceto groups in GM (Maeda et al., 1980) while the characteristic absorption bands of mannose in GM appeared at 871 and 802 cm^{-1}, in agreement with literature (Xiao et al., 2000). On the other hand, the peak at 1570 cm^{-1} was assigned to the characteristic bending absorption band of primary amino groups in CS (Xu et al., 1996). As it can be observed, for the CS:GM (50:50) microspheres, the stretching of carbonyl at 1730 cm^{-1} of GM disappeared, and the stretching of intramolecular hydrogen bonds at 1633 cm^{-1} in GM tended to couple and shift to around 1565 cm^{-1}, suggesting that new hydrogen bonds between CS and GM molecules ocurred. Moreover, the absorption band around 3400 cm^{-1} (data not shown) broadened with the increase of GM, indicating the gradual increase of intermolecular hydrogen bonds between CS and GM. However, no dissappearance of the intensive band at 1082 cm^{-1} took place, as it has been decribed for another kind of interactions (do not specified) between CS and GM in blend films (Xiao et al., 2000). Based upon these findings, it could be concluded that CS-GM miscibility before the spray drying process (in solution) was due to the intermolecular hydrogen bonds between –OH in CS and $–COCH_3$ in GM and between $–NH_2$ groups in CS and –OH groups in GM. Thus, the composition of the microspheres, as well as the matrix formed by both CS and GM polymers, were presumably homogeneus.

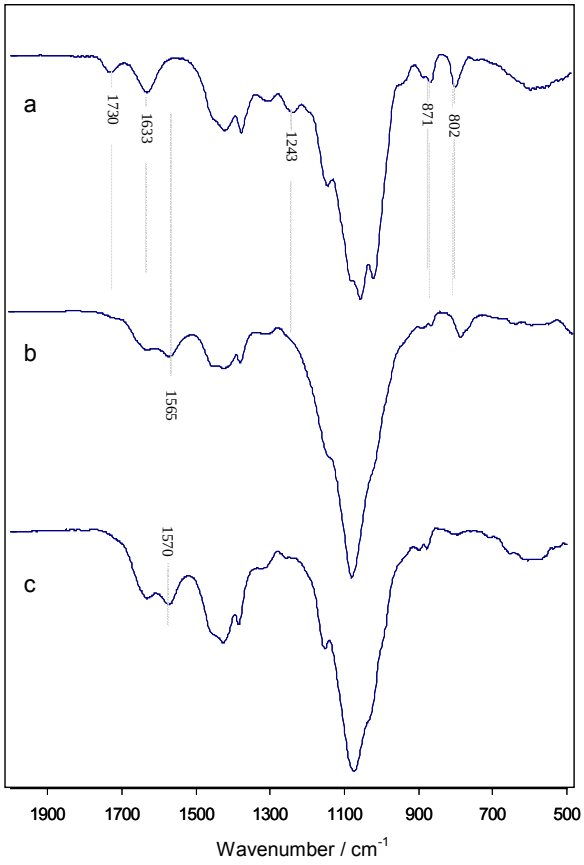

Figure 4. Infrared spectra in the region 500-2000 cm^{-1} for (a) GM microspheres; (b) CS:GM (50:50) microspheres; (c) CS microspheres.

3.4. Morphological and aerodynamic characterization of unloaded CS:GM microspheres

3.4.1. *Morphological characterization by SEM*

SEM studies were performed in order to obtain information about general powder characteristics (predominant particle size and shape) and particle surface (texture, roughness) of the microsphere formulations. Representative SEM photographs revealed the great influence of GM on the surface morphology of blank microspheres. Thus, microspheres composed only by CS presented a smooth surface and spherical shape (**Figure 5**) whereas the incorporation of GM to the formulations produced spheroidal and wrinkled particles. As it can be clearly noted in **Figure 6**, increasing amounts of GM led to the obtaining of more convoluted surfaces and irregular shapes. As reported by Ameri et Maa, the liquid composition to be spray dried prescribes the shape of the spray dried particles, e.g., some materials tend to form solid spherical particles while others form holow, deformed or even disintegrated particles. They hypothesized that, as the droplet dries, a polymer film formed at the external surface could hinder the outward diffusion of water and cause the water vapor pressure inside the droplet to increase. At a critical pressure, the film bursts, deforming the particle shape from its original sphericity. Certainly, the extent of such hinderance in diffusion will be dictated by the film properties, such as flexibility, mechanical strength, porosity, etc. (Ameri and Maa, 2006), which, in their turn, will depend on the microspheres composition. Similarly, Huang et al. related a reduction of polymeric rigidity caused by gelatin with the presence of large holes on the structure of CS:gelatin particles. The mixture of CS and gelatin was more susceptible to the explosion produced by high heat (170 ºC) during the spray drying process than the polymer composition containing only CS (Huang et al., 2002).

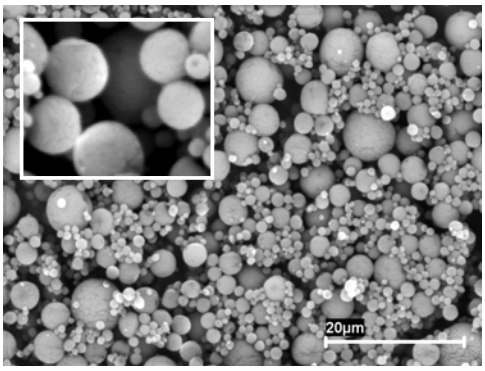

Figure 5. SEM photographs of chitosan microspheres obtained by spray-drying of 1% w/w solution.

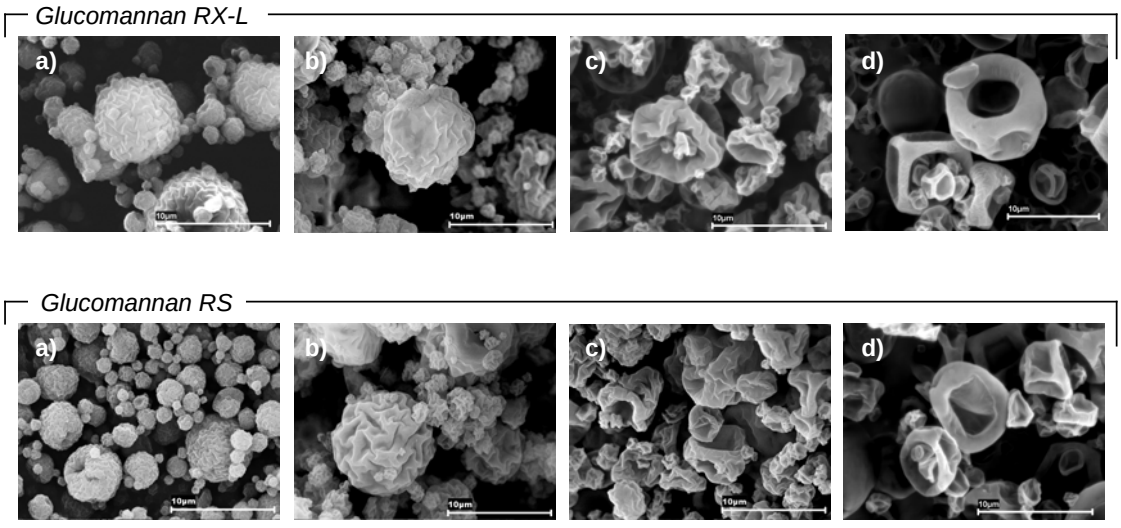

Figure 6. SEM photographs of microspheres obtained by spray-drying of CS and/or GM polymer solutions (1% w/w). Ratio CS:GM: (a) 75:25; (b) 50:50; (c) 25:75 and (d) 0:100, from both GM Propol RX-L and Propol RS. Scale bars = 10 μm.

With regard to the SEM photographs of CS:GM microspheres produced from 0.1% w/w polymeric solutions, it must be noted that the particles also presented very convoluted surfaces, being this effect more pronounced for GM RX-L (**Figure 7**). When compared these photos with those corresponding to microspheres prepared from 1% polymeric solutions (**Figure 6**), we observed that surface convolutions were also more pronounced, while borders delimiting the large holes seemed to be thinner.

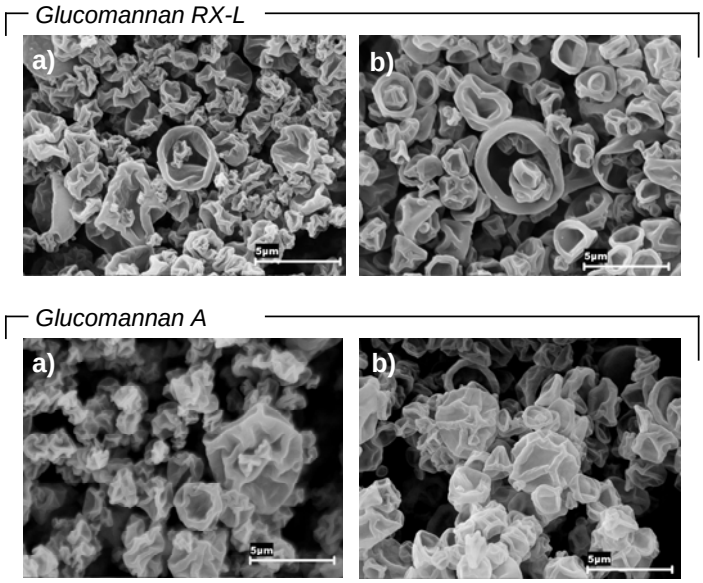

Figure 7. SEM photographs of microspheres obtained by spray-drying of CS and/or GM polymer solutions (0.1% w/w). Ratio CS:GM: (a) 25:75 and (b) 0:100, from both GM Propol RX-L and Propol A.

Finally, it must be mentioned that the increase in surface rugosity may have a significant impact on the agglomeration properties of the dispersed particles, as it has been reported that asperities prevent close approach of particles, thus avoiding van der Waals contact. In fact, these morphologic features (convolutions, roughness) have demonstrated to contribute to the excellent suspension stability of

spray dried budesonide particles in hydrofluoroalkane 134a propellant (Tarara et al., 2004).

3.4.2. Aerodynamic characterization

The particle size of a powder formulation intended for inhalation is, together with density, a key factor in its therapeutic success because both strongly influence the particle dispersion and *in vivo* sedimentation properties (Taylor and Kellaway, 2001; Courier et al., 2002). As it has been previously mentioned, the aerodynamic diameter of particles for optimal lung administration should be of approximately 1-5 μm (Clark and Egan, 1994; Vanbever et al., 1999).

Aerodynamic properties (size, density and aerodynamic diameter) of blank CS:GM microspheres produced from the 1% w/w polymeric solutions are summarized in **Table 2**. Mean particle size (expressed as Feret´s diameter) varied between approx. 1.8 and 4 μm, and shown a tendency to increase as the amount of GM forming the microspheres increased. This fact would be related with the correlative increase in the polymeric solution viscosity, since droplets formed from more viscous solutions would be larger, thus producing larger microspheres (He et al., 1999).

Apparent and real densities resulted to be also dependent on the GM content, significantly decreasing as the presence of GM in the polymeric matrix was increased. Apparent densities ranged from 0.48 g/cm^3, for CS microspheres, to 0.17-0.20 g/cm^3, for those particles composed solely by GM. Similarly, real densities ranged from 1.49 g/cm^3 to 0.97-0.99 g/cm^3. This fact must be explained not only by the obvious morphological and surface differences observed by SEM, but also by the contribution of GM to form less compact matrixs. In this sense, as previously mentioned in the introduction section, it has been reported that noncompact particles display less tendency to agglomerate than those conventional small and nonporous (Edwards et al., 1998).

The experimental aerodynamic diameters, measured using the Aerosizer® - Aerodisperser® equipment, ranged from 1.5 to 1.7 μm. According to these

aerodynamic diameter data, these microspheres should be considered adequate for alveolar deposition.

Table 2. Micromeritic properties of CS:GM microspheres obtained by spray-drying of 1% w/w polymeric solutions (means ± S.D., *n*=3-6).

Composition	CS:GM ratio	Feret´s diameter (µm)	Apparent density (g/cm^3)	Real density (g/cm^3)	d_{aer} (µm)
CS 223	100:0	2.15 ± 1.05	0.48 ± 0.02	1.49 ± 0.21	1.35 ± 1.44
	75:25	1.92 ± 1.07	0.53 ± 0.03	1.47 ± 0.06	1.49 ± 1.51
CS 223:GM RX-L	50:50	2.21 ± 1.04	0.46 ± 0.04	1.42 ± 0.08	1.56 ± 1.50
	25:75	2.69 ± 1.10	0.30 ± 0.02	1.20 ± 0.08	1.64 ± 1.46
GM RX-L	0:100	3.19 ± 1.52	0.20 ± 0.02	0.97 ± 0.09	1.61 ± 1.54
	75:25	1.80 ± 1.45	0.55 ± 0.03	1.42 ± 0.02	1.63 ± 1.54
CS 223: GM RS	50:50	2.50 ± 1.85	0.44 ± 0.02	1.37 ± 0.24	1.58 ± 1.55
	25:75	2.84 ± 1.82	0.28 ± 0.01	1.27 ± 0.05	1.60 ± 1.53
GM RS	0:100	4.00 ± 3.31	0.17 ± 0.01	0.99 ± 0.06	1.49 ± 1.47

d_{aer} = aerodynamic diameter

The influence of polymer concentration was also investigated by determining the aerodynamic properties of the microspheres produced from 0.1% w/w polymeric solutions (CS:GM ratio= 25:75 and 0:100) **(Table 3)**. In general, smaller particle size and slighty lower apparent density were obtained for the microspheres prepared from the less concentrated solutions. These results could be easily explained by the lower viscosity of the sprayed polymeric solutions, that produced smaller droplets, as well as by the morphological characteristics mentioned above. Very similar results were obtained for microspheres prepared from GM Propol A as compared with GM RX-L. Despite of the aerodynamic properties of these microspheres were also adequate for lung delivery, it seems that they not bring forward any additional advantage. For this reason, the following experiments were focused on selected formulations prepared from the 1% polymeric solutions.

Table 3. Micromeritic properties of CS:GM microspheres obtained by spray-drying of 0.1% w/w polymeric solutions (means ± S.D., *n*=3-6).

Composition	CS:GM ratio	Feret´s diameter (µm)	Apparent density (g/cm^3)	Real density (g/cm^3)	d_{aer} (µm)
CS 223:GM RX-L	25:75	2.20 ± 1.08	0.23 ± 0.02	n.d	n.d
GM RX-L	0:100	2.53 ± 1.04	0.20 ± 0.01	n.d	n.d
CS 223:GM A	25:75	2.25 ± 0.92	0.25 ± 0.02	1.43 ± 0.11	1.03 ± 1.34
GM A	0:100	2.83 ± 1.25	0.16 ± 0.01	1.10 ± 0.04	1.13 ± 1.42

n.d = not determined; d_{aer} = aerodynamic diameter

3.5. Association of insulin to CS:GM microspheres and *in vitro* release behavior

As explained in the methodology section, insulin (previously dissolved in 0.1M HCl) was incorporated in the CS and/or GM solutions before the spray-drying process. SEM photographs shown that the morphologycal appearance of microspheres was not affected by the incorporation of the model peptide (15% w/w based on polymer) (**Figure 8**). Process yields, particle sizes and insulin association efficiencies are shown in **Table 4**. Spray drying process yields were similar to those obtained for unloaded microspheres while mean particle sizes were increased by the insulin loading. Despite of this fact, which has been previously reported, sizes remain in the appropriate range for lung delivery. The determination of association efficiencies was performed at 22ºC rather than at 37ºC, to minimize the insulin self-aggregation tendency occurring at higher temperatures (Sluzky, Klibanov & Langer, 1992; Reithmeier et al., 2001). As it can be observed, the association efficiency of insulin to GM microspheres was 98%. These high association efficiencies are usually associated with the spray drying processes (Surendrakumar et al., 2003). However, a decrease in the percent of associated insulin was observed for those formulations containing CS, which was proportional to the CS content, ranging from 91% (for

CS:GM = 25:75) to 63% (for CS microspheres). In order to know if these differences were due to a real decrease in the insulin association during the spray-drying process or only to a decrease in the amount of insulin able to be quantified, we incubated the corresponding microspheres components (theoretical proportion of polymers and insulin physically mixtured as before spray-drying) and determined the percent of insulin recovered. Since the differences found were less than a 5%, as compared with the reported association efficiencies, we could conclude that the obtained association efficiencies are due to some factor that hinders insulin quantification. Taking into account that the quantified insulin decrease as the presence of CS increases, the most feasible factor is an interaction between CS and insulin. Moreover, a certain insulin self-aggregation should not be discarded.

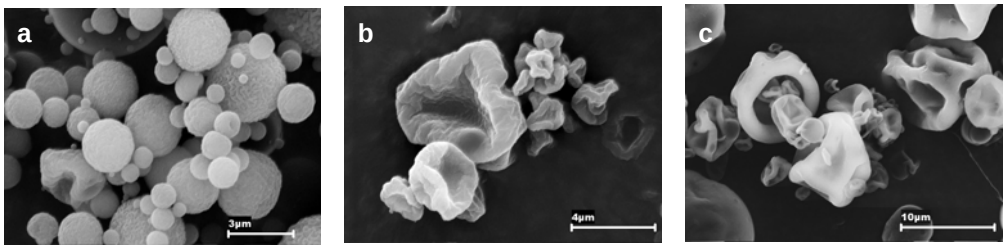

Figure 8. SEM microphotographs of insulin loaded microspheres (15% w/w, based on polymers): (a) CS microspheres; (b) CS:GM (25:75) microspheres; and (c) GM microspheres.

Table 4. Process yields, paticle size and association effieciency of microspheres prepared by spray drying of CS:GM solutions containing insulin (15% w/w, based on polymers).

Polymeric composition	CS:GM ratio	Protein	Spray-drying process yield (%)	Feret´s diameter (µm)	Association Efficiency (%)
CS 223	100:0	Insulin (15%)	64.70	1.78 ± 1.07	62.80 ± 1.82
CS 223:GM RX-L	50:50		50.31	2.93 ± 1.70	77.70 ± 2.19
	25:75		37.60	3.01 ± 1.52	91.41 ± 7.75
GM RX-L	0:100		22.32	3.98 ± 2.50	98.42 ± 4.73

Unlike association efficiency, *in vitro* release studies were carried out at 37ºC to mimic the physiological temperature. The *in vitro* release profiles of insulin from CS, CS:GM and GM microspheres are plotted in **Figure 9**.

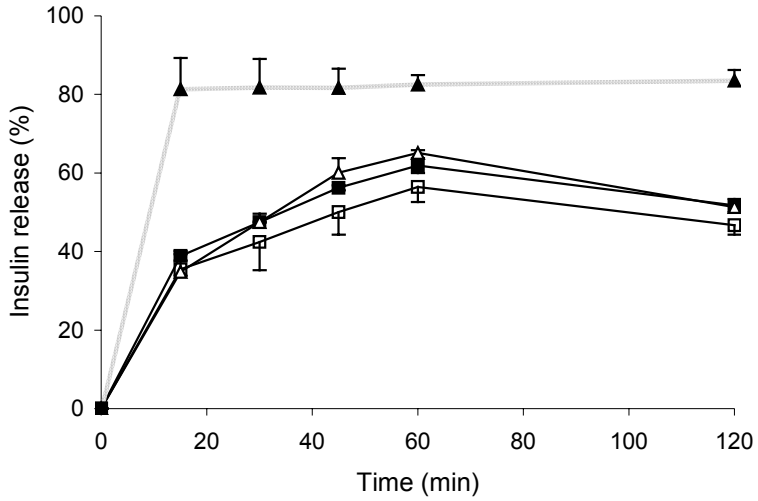

Figure 9. In vitro release of insulin from: (■) CS; (□) CS:GM (50:50); (∆) CS:GM (25:75); and (▲) GM microspheres in PBS pH 7.4 at 37ºC (insulin = 15% w/w based on polymers; mean ± S.D., *n* = 3).

Insulin release from GM microspheres was very fast and accompanied by a marked "burst" effect. Almost the total of the protein (82%) was released in the first 15 min, showing a plateau from this point. Two main factors can contribute to this fact: (a) the high specific surface area of these wrinkled particles in contact with the release medium; and (b) the non-compact internal structure suggested by low particle density, which may facilitate the diffusion of insulin through the GM matrix. On the other hand, CS and CS:GM microspheres presented a significatively slower release, with less than 40% after the first 15 min, as well as a lower amount of total protein released (57-65%). Taking into account the fast insulin release from GM microspheres, it could be expected a similar behavior for CS:GM microspheres, since they are composed by a high amount of GM (50-75%) and present similar morphologic characteristics. In this sense, the interaction between CS and GM,

previously demonstrated by IR spectroscopy, could play an important role in delay of insulin release.

Finally, the decrease in the drug concentration observed at 120 min may be due to the aready mentioned phenomenon of aggregation of insulin at 37ºC or surface readsorption (Brange et al., 1997; Reithmeier et al., 2001).

3.6. *In vitro* evaluation of microspheres mucoadhesive properties

3.6.1. *Microspheres interaction with mucin*

As explained in the methodology section, CS:GM microspheres were briefly incubated with mucin, centrifuged and examined by SEM. Representative microphotographs of completely mucin-coated CS:GM microspheres (100:0 and 50:50) are shown in **Figure 10**. This fact supported the previous results obtained in the study of the interaction of the corresponding polymeric solutions with mucin.

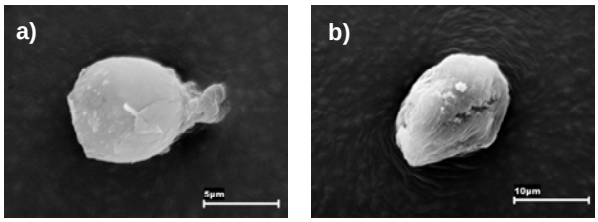

Figure 10. Representative SEM photographs of microspheres after incubation with the mucin (1/1) in aqueous solution: (a) CS microsphere, (b) CS:GM (50:50) microsphere.

3.6.2. *Cualitative bioadhesion/interaction of microspheres with Calu-3 cells*

Fluorescent microspheres (CS and CS:GM) were prepared by encapsulating FITC-BSA (30% w/w based on polymer) with the aim of investigating their ability to interact with the mucus layer and remain adhered to Calu-3 cells. An ultrapure CS (G113; Mw 128 KDa), with similar Mw than the previosly used CS (223; Mw 150 KDa), was selected for the preparation of those microspheres aimed to be tested in

cell culture studies. FITC-BSA release from the particles was almost inexixtent (10% after 24 h, PBS pH 7.4), mainly due to its strong interaction with CS (data not shown). Therefore, no release was expected for the microspheres administered in a dry way, at least during the duration of the study. The spray drying process yields of unloaded particles ranged between 64.60%, for CS microspheres, and 51.42%, for CS:GM (50:50) microspheres. For microspheres encapsulating FITC-BSA very similar yield values were obatined (64.15 and 49.38%, respectively).

As explained in the methodology section, CS and CS:GM fluorescent microspheres were aerosolized on the Calu-3 epithelium by means of a PennCentury™ insufflator (DP-4). This device was selected as a simple, commercially available system that could aerosolize dry powders to animal lungs (Surendrakumar et al., 2003; Grainger et al., 2004), and was simply adapted to the administration on cells. Although it was previously shown that the microspheres possess adequate aerodynamic diameters for inhalation, the suitability of the powders was once again evidenced by their correct emission from the insufflator. Particles were easily dispersed from the device, whathever the shape and polymeric composition, thus providing a homogeneous deposition on the cell surface. As shown in **Figures 11** and **12**, CS and CS:GM microspheres showed the ability to closely interact with the mucus layer and remain adhered to the epithelium, where it is expected that the systems release the protein and promote its absorption.

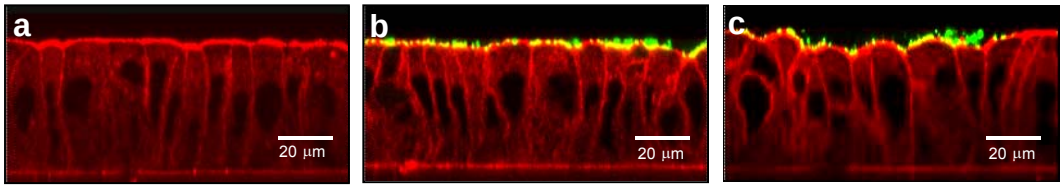

Figure 11. Confocal fluorescence images (x-z cross sections) of Calu-3 differentiated cells after incubation with FITC-BSA loaded microspheres administered in a dry way (PennCentury™ dry powder insufflator): (a) control, (b) CS:GM microspheres, and (c) CS microspheres, (*n* = 3).

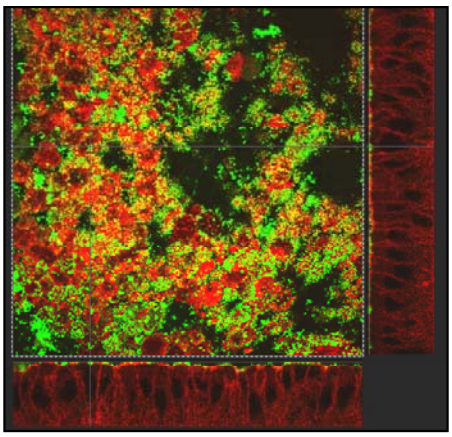

Figure 11. Representative confocal fluorescence image (x-y-z) of Calu-3 differentiated cells after incubation with FITC-BSA loaded CS:GM microspheres administered in a dry way (PennCentury™ dry powder insufflator).

In summary, protein-loaded CS:GM microspheres with suitable morphological and aerodynamic properties for pulmonary drug delivery were prepared by a spray-drying technique. From our results, we suggest that the incorporation of GM may contribute to significantly reduce the formulation toxicity and even increase the mucoadhesive properties of microspheres, as compared with the formulations composed solely by CS. Moreover, it is expected that the demonstrated interaction between both polymers, as well as their swelling capacity, can play an important role in slowing down the insulin release when microspheres are administered *in vivo* in a dry way. Since CS:GM microspheres shown adequate aerodynamic properties and a positive behavior in cell bioadhesion studies, we expect they could reach the deep lung and adhere to the alveolar epithelium, where the protein would be released and CS can promote its absorption. In terms of biodegradation, it is known that CS can be degraded by enzymes, such as lysozime, while glucomannan and partially-dissintegrated microspheres could be removed by the macrophages, since they

present specific mannose receptors and an increased phagocytosing activity for those smaller particles.

Further experiments will be aimed to explore the capacity of the CS:GM microspheres at decreasing glucose levels *in vivo* (in rats) following intratraccheal administration.

ACKNOWLEDGEMENTS

This work was supported by the Spanish Government (CICYT, SAF 2002-03314), FEDER (cofinanced) and Xunta de Galicia (PGIDIT03PXIC20301PN: Incentivo del proyecto SAF 2002-03314). The first author acknowledges a Marie Curie Fellowship of the European Community program “Improving the Human Research Potential and the Socio-Economic Knowledge Base” under contract number HPMT-CT-2001-00403.

REFERENCES:

1. Agnihotri S.A., Nadagouda N., Mallikarjuna N., Aminabhavi T.M., Recent advances on chitosan-based micro- and nanoparticles in drug delivery, J. Control. Rel., 100 (2004) 5-28.
2. Alonso-Sande, M.; Remuñán-López, C.; Alonso-Lebrero, J.L. and Alonso, M.J, Proc. 32nd Meeting of the Controlled Release Society, Miami 2005.
3. Alonso-Sande M., Cuña M., Remuñán-López C., Teijeiro-Osorio D., Alonso-Lebrero J.L., Alonso, M.J., Formation of new glucomannan-chitosan nanoparticles and study of their ability to associate and deliver proteins, Macromolecules, 39 (2006a) 4152-4158.
4. Alonso-Sande, M.; des Rieux, A.; Schneider, Y.J. ; Remuñán-López, C. ; Alonso, M.J. and Préat, V., Proc. 33rd Meeting of the Controlled Release Society, Vienna 2006b
5. Alonso-Sande M., Teijeiro-Osorio D., Remuñán-López C., Alonso M.J., Glucomannan, a promissing polysaccharide for pharmaceutical and biological purposes, *submitted*
6. Alpar H.O., Somavarapu S., Atuah K.N., Bramwell V.W., Biodegradable mucoadhesive particulates for nasal and pulmonary antigen and DNA delivery, Advanced Drug Delivery Reviews, 57 (2005) 411-430.
7. Ameri M., Maa Y.–F., Spray drying of biopharmaceuticals: stability and process considerations, Drying Technology, 24 (2006) 763-768.
8. Brange J., Andersen L., Laursen E.D., Meyn G., Rasmussen E., Toward understanding insulin fibrillation, J. Pharm. Sci., 86 (1997) 517-525.
9. Broadhead J., Edmond-Rouan S. K., Rhodes C. T., The spray-drying of pharmaceuticals, Drug Dev. Ind. Pharm., 18 (1992) 1169-1206.

10. Carrión-Recio D., Taboada-Montero C., Vila-Jato J.L., Remuñán-López C., Enhacement of protein lung absorption using chitosan microspheres, *submitted.*

11. Cheng Y. S., Barr E. B., Marshall I. A., and Mitchell J. P., Calibration and performance of an API* Aerosizer, J. Aerosol. Sci., 24 (1993) 501-514.

12. Clark A.R., Egan M., Modelling the deposition of inhaled powdered drug aerosols, J. Aerosol Sci., 25 (1994) 175-186.

13. Courier H.M., Butz N., Vandamme T.F., Pulmonary drug delivery systems: recent developments and prospects, Crit. Rev. Ther. Drug Carrier Syst., 19 (2002) 425-498.

14. Cryan S.-A., Carrier-based strategies for targeting protein and peptide drugs to the lungs, AAPS J., 7 (2005) E20-E45.

15. Cuña M., Alonso-Sande M., Remuñan-López C., Pivel J.P., Alonso-Lebrero J.L., Alonso M.J., J. Nanosci. Nanotechnol., 8 (2006) 1-9.

16. Du J., Sun R., Zhang S., Zhang L. F., Xiong Ch. D., Peng Y. X., Biopolymers, 18 (2005) 1-8.

17. Edwards D.A., Ben-Jebria A., Langer R., Recent advances in pulmonary drug delivery using large, porous inhaled particles, J. Applied Physiol., 85 (1998) 379-385.

18. Eirheim H.U., Bundgaard C., Nielsen H.M., Evaluation of different toxicity assays applied to proliferating cells and to stratified epithelium in relation to permeability enhancement with glycocholate, 18 (2004) 649-657.

19. El-Gibaly I., Development and in vitro evaluation of novel floating chitosan microcapsules for oral use: comparisson with non-floating chitosan microspheres, Int. J. Pharm., 294 (2002) 7-21.

20. Genta I., Pavanetto F., Conti B., Giunchedi P., Conte U., Improvement of dexamethasone dissolution rate from spray-dried chitosan microspheres, S. T. P. Pharma Sci., 5 (1995) 202-207.

21. Grainger C.I., Alcock R., Gard T.G., Quirk A.V., van Amerongen G., de Swart R.L., Hardy J.G., Administration of an insulin powder to the lungs of cynomolgus monkeys using a Penn Cantury insufflator, Int. J. Pharm., 269 (2004) 523-527.

22. Groneberg D.A., Witt C., Wagner U., Chung K.F., Fisher A., Fundamentals of pulmonary drug delivery, Respir. Med., 97 (2003) 382-387.

23. Hastings R.H., Folkesson H.G., Mathay M.A., Mechanisms of alveolar protein clearance in the intact lung, Am. J. Physiol. Lung Cell. Mol. Physiol., 286 (2004) L679-L689.

24. He P., Davis S.S., Illum L., In vitro evaluation of the mucoadhesive properties of chitosan microspheres, Int. J. Pharm., 166 (1998) 75-68.

25. Hirano S., Tsuchida H., Nagao N., N-acetylation in chitosan and the rate of its enzymic hydrolysis, Biomaterials, 10 (1989) 574-576.

26. Huang Y. -C., Yeh M. -K., Chiang C. -H., Formulation factors in preparing BTM-chitosan microspheres by spray drying method, Int. J. Pharm., 242 (2002) 239-242.

27. Knapczyc J., Krowczynski L., Krzck J., Brzeki M., Nirnberg E., Schenk D., Struscyk H., Requirements of chitosan and pharmaceutical and biomedical applications. In: Skak-Braek B., Anthonsen T., Sandford P. (Ed.), Chitin and chitosan: sources, chemistry, biochemistry, physical properties and applications, Elsevier, London, (1989) pp. 657-663.

28. Maeda M., Shimahara H., Sugiyama N., Agric. Biol.. Chem., 44 (1980) 245-252.

29. Nishinari K., Developments in Food Science, 41 (2000) 309-330.

30. Portero A., Remuñán-López C., Nielsen H.M., The potential of chitosan in enhancing peptide absorption across the TR146 cell culture model- an in vitro model of the buccal mucosa, Pharm. Res., 19 (2002) 169-174.

31. Reithmeier H., Herrman J., Göpferich A., Lipid microparticles as a parenteral controlled release device for peptides, J. Control. Rel., 73 (2001) 339-350.

32. Sinha V.R., Singla A.K., Wadhawan S., Kaushik R., Kumria R., Bansal K., Dhawan S., Chitosan microspheres as a potential carrier for drugs, Int. J. Pharm., 274 (2004) 1-33.

33. Sluzky V., Klibanov A.M., Langer R., Mechanism of insulin aggregation and stabilization in agitated aqueous solutions, Biotechnology and Bioengineering, 40 (1992) 1-9.

34. Surendrakumar K., Martín G.P., Hodgers E.C.M., Jansen M., Blair J.A., Sustained release of insulin from sodium hyaluronate based dry powder formulations after pulmonary delivery to beagle dogs, J. Control. Rel., 91 (2003).

35. Tarara T. E, Hartman M. S., Gill H., Kennedy A. A., and Weers J. G., Characterization of suspension-based metered dose inhaler formulations composed of spray-dried budesonide microcrystals dispersed in HFA-134a, Pharm. Res., 21 (2004) 1607-1614.

36. Taylor G., Kellaway I. In: Hillery M., Lloyd A. W., Swerbrick J. (Ed.), Pulmonary drug delivery. Drug delivery and targeting for pharmaceutical scientists, Taylor & Francis, London (2001) pp. 269-300.

37. Teijeiro-Osorio D., Remuñán-López C., Nielsen H.M., Proc. 32nd Meeting of the Controlled Release Society, Miami 2005, 378.

38. Tomihata K., Ikada Y., In vitro and in vivo degradation of films of chitin and its deacetylated derivatives, Biomaterials, 18 (1997) 567-575.

39. Tréhin R., Krauss U., Beck-Sickinger A.G., Merkle H.P. and Nielsen H.M., Cellular uptake but low permeation of human calcitonin-derived cell penetrating peptides and Tat(47-57) through well-differentiated epithelial models, Pharm. Res., 21 (2004) 1248-1256.

40. van der Lubben I. M., Verhoef J. C., Borchard G., Junginger H. E., Chitosan and its derivatives in mucosal drug and vaccine delivery, Eur. J. Pharm. Sci., 14 (2001) 201-207.

41. Vanbever R., Ben-Jebria A., Mintzes J. D., Langer R., Edwards D. A., Sustained release of insulin from insoluble inhaled particles, Drug Deliv. Research, 48 (1999) 178-185.

42. Xiao C., Gao S., Wang H. and Zhang L., Blend films from chitosan and konjac glucomannan solutions, J. Appl. Polym. Sci., 76 (2000) 509-515.

43. Xu J., McCarthy S. P., Gross R. A., and Kaplan D. L., Chitosan film acylation and effects on biodegradability, Macromolecules, 29 (1996) 3436-3440.

ARTÍCULO 3

Chitosan Nanoparticles and Solutions as Absorption Enhancers for Peptides and Proteins – In Vitro Studies with the TR146 and Calu-3 Cell Culture Models -

---

Desirée Teijeiro-Osorio[a,b], Carmen Remuñán-López[a], Hanne Mørck Nielsen[b]

[a] Department of Pharmacy and Pharmaceutical Technology,
Faculty of Pharmacy, University of Santiago de Compostela,
Santiago de Compostela, Spain.

[b] Department of Pharmaceutics and Analytical Chemistry,
Faculty of Pharmaceutical Sciences, University of Copenhagen,
Copenhagen, Denmark.

ABSTRACT

In the present work our goal was to evaluate the efficiency of several chitosan (CS)-based formulations to enhance the transport of macromolecular drugs across two different cell culture models, TR146 and Calu-3, which are in vitro models of the human buccal and bronchial epithelium, respectively.

Changes in intracellular dehydrogenase activity (MTS/PMS assay) were used to assess the cytotoxicity of CS solutions (different Mw and deacetylation degree) and nanoparticle (NP) suspensions in proliferating as well as fully-differentiated cells. Permeability studies were performed to determine the enhancing effect of the different formulations on permeation of fluorescein isothiocyanate labeled dextrans (FD) of different Mw across the cell culture models. Apparent permeability coefficient (P_{app}) and absorption enhancement ratio (ER) were calculated and related to changes in TEER values and cytotoxicity.

Sensitivity of TR146 and Calu-3 cells to CS-based formulations was increased with CS dose, deacetylation degree, solution relative to NP and with proliferating compared to differentiated cells. In general, the effects of the formulations on epithelial permeability of hydrophilic molecules were clearly dependent on CS deacetylation degree, with the highest deacetylated CSs performing as the most effective absorption enhancers in both cell culture models. CS NP were able to significantly increase the permeability of model substances with Mw up to 20 kDa across the TR146 cell model, reaching similar values to those obtained with the highly deacetylated CS solution. The enhancement effect attained with CS NP and low deacetylated CS solutions was lower in the Calu-3 cell model, which could be partially atributted to the presence of extracellular mucus on the apical surface.

KEY WORDS: chitosan, deacetylation degree, nanoparticles, macromolecules absorption, permeability enhancement, toxicity, TR146 cells, Calu-3 cells.

INTRODUCTION

Nowadays, several non-invasive routes of delivery, such as the buccal, nasal or pulmonary route, are being extensively studied as alternatives to the parenteral route for the systemic delivery of macromolecular drugs. Both pulmonary and buccal routes have the main advantage of avoiding hepatic fist-pass metabolism and gastrointestinal degradation, which follow oral administration. Furthermore, pulmonary and buccal epithelia contain less proteolytic enzymes than the epithelium of the gastrointestinal tract (Lee, 1989). The lung alveoli offer a large absorptive surface area, whereas the buccal mucosa offers an extraordinary easy access of the drug to the absorption site and an excellent patient acceptance.

Nevertheless, permeability of these mucosae to peptides and proteins is limited because of the high molecular weight (Mw) and the hydrophilic nature of the macromolecules. Therefore, for successful absorption of peptides and proteins, the use of drug delivery systems with excipients such as permeability enhancers is required, but drug absorption enhancement is generally accompanied by mucosal damage. An exceptional behavior has, however, been observed for the cationic polysaccharide chitosan (CS), which is known to facilitate drug absorption across mucosal barriers, such as the nasal, buccal, intestinal, and vaginal (Fernández-Urrusuno et al., 1999; Portero et al., 2002; Artursson et al., 1994; Rossi et al., 2003). Physical and biological properties of CS, such as mucoadhesiveness and biocompatibility, are dependent on its Mw and deacetylation degree (DD) (Mima et al., 1983; Shipper et al., 1996; Tomihata et al., 1997). With regard to CS biocompatibility, it has been reported that relatively low Mw and low DD favour CS degradation by enzymes (Zhang and Neau, 2001). In this sense, CS with a DD below 70% were found to be readily degraded when implanted subcutaneously in rats, in contrast to a DD above 70% (Tomihata et al., 1997). However, the decrease in the DD is also associated with an important loss of the polymer mucoadhesive properties, given by the decreased amount of positively charged amino groups able to electrostatically interact with mucus or a negatively charged mucosal surface. This fact is especially interesting since it has been suggested that one of the most

important enhancing mechanism of CS is a combination of mucoadhesion and a transient widening of the junctions between epithelial cells (Artursson et al., 1994). In this sense, the study of the influence of Mw and DD on CS toxicity and its ability to promote the absorption of macromolecules is essential to reach a compromise between biocompatibility and permeability-enhancing properties.

Due to the favourable biological properties, significant efforts are being dedicated to design CS-based micro- and nanoparticles (NP) as mucosal drug delivery vehicles, since they may (1) provide additional protection to the encapsulated labile molecules against degradation, (2) release the active compounds in a controlled manner if desired, and (3) present even greater mucosal retention than CS solutions. A particular interest lies in the comparative study of CS particules and solutions in terms of absorption enhancement and cytotoxicity.

Fully organized epithelial barriers represent relevant *in vitro* models to study the benefits of the enhancers in improving the absorption of biomacromolecular therapeutics. The cell culture models TR146 and Calu-3 represent two distinct types of epithelia featuring specialized properties in terms of cell-to-cell junctions, cell morphology, and function as physiologic absorption barrier (**Table 1**). The TR146 cell line originates from a neck node metastasis of a human buccal carcinoma (Rupniak et al., 1985) and, when subcultured on filters, express ultrastructural characteristics similar to normal human buccal epithelium. Thus, TR146 differentiated cells represent an *in vitro* model of the human buccal epithelium (Jacobsen et al., 1995) and potentially may act as a barrier model for other stratified squamous epithelia. Calu-3 is a human bronchial submucosal adenocarcinoma cell line that forms tight, polarized, and well differentiated monolayers with apical microvilli and tight-junctional complexes (Shen et al., 1994). In this sense, Calu-3 cells have been suggested as an appropriate model for the nasal and bronchotracheal airway epithelium (Witschi and Mrsny, 1999; Winton et al., 1998).

Table 1. Main characteristics of the TR146 and Calu-3 cell culture models.

Cell line	**TR146** 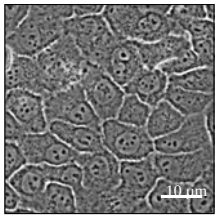	**CALU-3** 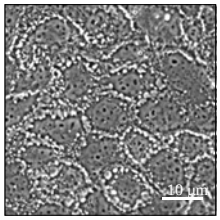
***In vitro* model**	Buccal epithelium	Bronchial epithelium
Origin	Human buccal carcinoma	Human bronchial adenocarcinoma
Characteristics:	Stratified and non-keratinised epithelium	Well-differentiated monolayers
Microvilli	No	Yes
Extracellular mucus	No	Yes
Tight junctions	No	Yes

Compiled from Jacobsen et al., 1995; Foster et al., 2000; Tréhin et al., 2004

The aim of the present study was to investigate the potential of CS with different Mw and DD and CS NP to enhance peptide and protein absorption across the TR146 and Calu-3 cell culture models. The effect on viability and integrity was related to the efficiency of the CS-based formulations to mediate the transport of macromolecules across the cell layer(s). For this purpose, fluorescein isothiocyanate labeled dextrans (FD) of different Mw were chosen as macromolecular model substances, and ^{3}H-mannitol as an integrity marker. To our knowledge, no studies exploring the permeability enhancement and cytotoxicity of CS as function as the DD and its formulation into NP have been performed neither in the TR146 nor the Calu-3 cell culture model.

MATERIALS AND METHODS

Materials

The following chemicals were obtained from commercial suppliers and used as received: Chitosan (CS): Sea cure G210 (Mw of 300 kD and DD 83%) (Pronova Lab., Norway), and Protasan CS G113 Ultrapure (Mw of 128 kD and DD 86%) (FMC Novamatrix, Norway); acetic anhydride (AA), and sodium tripolyphosphate (TPP) (Sigma-Aldrich, Germany); morpholino-ethanesulphonic acid anhydrous (MES) (Applichem GmbH, Germany); D-mannitol-[(1-^{3}H-(N)] 17.00 Ci/mmol (Amersham, UK); phenazine methosulphate (PMS), and fluorescein isothiocyanate labeled dextrans (FD) FD4, FD20, and FD40 with average Mw (kD)/FITC contents (molecule FITC/molecule glucose) of 4.4/0.004, 19.5/0.006, and 40/0.020, respectively (Sigma, MO, USA); 3-(4,5-dimethylthiazol-2-yl)-5-(3-carboxymethoxyphenyl)-2-(4-sulfophenyl)-2H-tetrazolium (MTS) (Promega, WI, USA); Ultima Gold™ MV scintillation cocktail (Packard Instruments BV, The Netherlands); Falcon® 12-well tissue culture plates and cell culture inserts (0.9 cm^2, 0.4 μm pore size, polyethylene terephthalate filter inserts) (Falcon, Becton Dickinson Labware, NJ, USA) and Transwell® 12-well plates and cell culture inserts (1.1 cm^2, 0.4 μm pore size) (Corning Inc., Corning, NY); Costar® flatbottomed 96-well cell culture cluster (tissue culture treated, polystyrene) (Corning Inc., Corning, NY); vitrogen collagen (Nutacon, Belgium); Hanks' balanced salt solution (HBSS); Dulbecco's modified Eagles medium (DMEM), penicillin, streptomycin, and trypsin-EDTA (Gibco BRL, UK); fetal bovine serum (FBS) (Biotech Line A/S, Denmark).

Methods

Preparation of CS solutions

Polymers of different DD were prepared from a highly deacetylated CS (G210) by a reacetylation procedure of the polymer with acetic anhydride, followed by dialysis and freeze-drying (Labconco Co., MI, USA), as previously described

(Teijeiro-Osorio and Remuñán-López, *submitted*). CS samples with a DD of 47% (CS G210-R47) and 38% (CS G210-R38) were obtained. DD was determined by ^{1}H-*NMR* spectroscopy (Bruker DRX500, Germany) (Hirai et al., 1991). Solutions of CS G210, CS G210-R47, CS G210-R38 and an ultra pure CS G113 UP were prepared by dissolving them in HBSS supplemented with 20 mM MES (mHBSS). Just before the experiments, the CS solutions were adjusted to pH 6.0 with NaOH.

Preparation and characterization of CS NP

CS NP were prepared according to the procedure previosly developed by our group (Calvo et al., 1997) based on the ionotropic gelation of CS with TPP anions. The particles formed spontaneously upon addition of 1.2 mL of an aqueous TPP solution (0.84 mg/mL) to 3 mL of CS G113 UP solution (2 mg/mL) under magnetic stirring. NP were isolated by centrifugation at 10.000 g on a glycerol bed for 40 min (Mikro 22R, Hettich, DJB Labcare Ltd., UK). Supernatants were discarded and NP were resuspended in MQ-water. Particle sizes and zeta potentials were determined by photon correlation spectroscopy (PCS) and Laser Doppler Anemometry (LDA), using a Zetasizer 4® and Zetamaster® (Malvern Instruments, UK), respectively. For the cell experiments NP suspended in MQ water were diluted (1:1) in double concentrated HBSS. The resultant NP suspension, with a final pH of 6.3, was incubated at 37ºC for 24 h, and size measurements were periodically performed in order to evaluate the NP stability.

Cell culture

The cell line TR146 was kindly provided by Imperial Cancer Research Technology (UK) and cultivation was assessed as previously described (Jacobsen et al., 1995) with modifications (Nielsen and Rassing, 1999). Calu-3 cells were purchased from American Type Culture Collection ATCC (MD, USA) and cultured as previously referred (Tréhin et al, 2004). Cells were detached from culturing flasks by trypsin-EDTA and subcultivated for studies with proliferating cells or well-differentiated epithelium. For studies with proliferating cells the cells were seeded in flat-bottomed 96-well culture plates in a density of 2×10^4 and 4×10^4 cell/well for

TR146 and Calu-3 cells, respectively, and cultured for 22-24 h. To obtain a differentiated epithelium, cells were cultured on inserts with a seeding density of 2.2×10^4 cells/cm^2 for TR146 (on 0.9 cm^2 insert) and 8.2×10^4 cells/cm^2 for Calu-3 (on 1.1 cm^2 insert). For Calu-3, the filters were initially coated with collagen (290 ng/mL, 200 μl). The TR146 cells were cultured submerged. Post seeding onto the filter, the Calu-3 cells attached to the filter overnight and the medium was then removed from the apical compartment to allow the cells to form a monolayer at an air-liquid interface. Apart from the absence of liquid in the apical chamber, the Calu-3 cells were cultured as the TR146 cells. TR146 multilayers (passages 19-28) and Calu-3 monolayers (passages 38-47) were used after 28 and 21 days, respectively.

MTS/PMS assay in proliferating cells

The dehydrogenase activity in the TR146 and Calu-3 proliferating cells was used to estimate the cells sensitivity to different CS solutions and CS NP suspensions and measured according to the MTS/PMS assay (Jacobsen et al., 1996; Eirheim et al., 2004), optimized for each cell line. Thus, cells grown in 96-well culture plates were incubated for 4 h with 100 μL of CS solutions and NP in concentrations ranging from 0.001 mg/mL to 5 mg/mL CS. At the end of the incubation time, samples were discarded and replaced by the MTS/PMS solution. Incubation was done under stirring protected from light for 1-2 h at 37ºC. The absorbance was measured at 492 nm using a microplate reader (FluoStar Optima, BMG Labtech GmbH, Germany). The effect of the CS solutions and NP was measured as the relative decrease in enzyme activity compared to the negative control (cells exposed to buffer), and the IC_{50} was defined as the sample concentration inhibiting cell viability with 50%. Analysis of three replicates was conducted in three different passages of cells.

Permeability, TEER and cytotoxicity studies in differentiated cells

The permeability experiments were performed at 37ºC and 150 rpm by using a temperated horizontal shaker (Edmund Bühler, Germany), as previously described (Portero et al., 2002). Prior to permeability measurements, following standard

protocols, differentiated TR146 and Calu-3 cells were equilibrated for 15 min at room temperature in HBSS (pH 7.4), and the transepithelial electrical resistance (TEER) was measured (Endohm™ culture cup connected to EVOM™ voltohmmeter). Permeability of the different FITC-labeled molecules, alone or in co-administered with an enhancer (**Table 2**), across the epithelia was assessed at 150 rpm to ensure mixing and in order to minimize the aqueous boundary layer. ^{3}H-mannitol permeability was also determined to validate the cellular integrity of the epithelial cell layer(s) at pH 6.0 (in mHBSS) and pH 6.3 (with NP in HBSS, **Table 2**).

Table 2. Formulations assayed for permeability experiments in the TR146 and Calu-3 cells culture models.

Tested formulations			
Enhancer	Mw (kDa); DD[b] (%)	Concentration (mg/mL)	Labeled substance
CS[a] G113 UP	128 kDa; 86%	0.015, 1	FD[c] 4, FD20, FD40
CS G210	300 kDa; 83%	0.015, 1	FD 4, FD20, FD40
CS G210-R47	300 kDa; 47%	1, 5	FD 4, FD20, FD40
CS G210-R38	300 kDa; 38%	1, 5	FD 4, FD20, FD40
CS G113 UP-NP [d]		1	^{3}H-mannitol FD 4, FD20, FD40

[a] CS = chitosan; [b] DD = degree of deacetylation; [c] FD = FITC-labelled dextran; [d] NP = nanoparticles

Test substance donor solution (0.9 mL in TR146 and 0.7 mL in Calu-3) was applied to the apical side of the cell layers, and the inserts were immediately placed in wells containing 2.1 mL receptor solution (HBSS, pH 7.4) and 100 µl samples were withdrawn from both the receptor and the donor solution. Hereafter, samples

were collected from the basal side and replaced with HBSS buffer, every 15 min for 1 h and every 30 min up to 4 h. At the end of the experiments, 100 μL samples were taken from the donor and the receptor solutions. The concentrations of the test substances were 0.2 μCi/mL ^{3}H-mannitol, 0.45 mM FD4, 0.50 mM FD20 or FD40. Studies were carried out in three replicates and in three different passages of cells. Radiotracer samples were mixed with 2.0 mL scintillation cocktail (Ultima Gold, MD, USA) and measured by liquid scintillation (Packard Instruments, CT, USA). The assessment of FD was performed using black 96-well plates in a microplate reader (FluoStar Optima, BMG Labtech GmbH, Germany) at excitation/emission wavelenghts of 491 nm/520 nm.

After the permeability experiment, cells were washed and equilibrated with HBSS and TEER was measured again. Finally, MTS/PMS dye was applied to cells grown on filters to evaluate the cellular viability after exposure to CS NP and solutions. The assay was carried out as previously described (Eirheim et al., 2004). A volume of 320 μL MTS/PMS reagent was added to the apical side of the epithelium, and 1 mL HBSS was added to the basal side. The cells were incubated under conditions described as for studies of cytotoxicity in proliferating cells. 100 μL was the withdrawn from the apical side of each filter and transferred to a clear 96-well plate and the absorbance was measured at 492 nm. The mitochondrial dehydrogenase activity was calculated relative to buffer-exposed cells.

Data analysis

Enzyme activity of TR146 and Calu-3 cells toward different CS solutions and NP suspensions were determined relative to cells exposed to the corresponding buffer and calculated according to Eq. (1):

$$\text{Relative enzyme activity (\%)} = [(Abs_{treated} - Abs_{blank}) / (Abs_{control} - Abs_{blank})] \times 100 \quad (1)$$

where $Abs_{treated}$ is the absorbance of cells treated with the test samples; Abs_{blank} is the absorbance of wells without cells and without samples; and $Abs_{control}$ is the absorbance of buffer-treated cells. Individual data points of the concentration–

response data curves are presented relative to the control ±SD (*n*), where *n* is the number of replicates.

IC_{50} values were calculated from curves fitted by a non-linear four parameter logistic equation with estimation of the correlation coefficient (R^2).

$$\text{Relative enzyme activity} = \min + \frac{(\max - \min)}{1 + \left(\text{conc}/\text{IC}_{50}\right)^s} \quad (2)$$

where min is the minimum value measures, max the maximum value measured, conc the concentration, and s the slope of the curve.

The apparent permeability coefficients (P_{app}) for the permeability of test substances across the TR146 and Calu-3 models were calculated according to Eq. (3):

$$P_{app} = dQ/dt \times 1/(A \times C_0) \quad (3)$$

where *dQ/dt* is the steady-state rate of permeation, *A* is the cross-sectional area of the filter membrane, and C_0 is the initial concentration of test substance in the donor compartment.

The enhancement ratio (ER) for each test sample was determined as described in Eq. (4):

$$ER = P_{app} \text{ (enhancer)}/ P_{app} \text{ (control)} \quad (4)$$

where P_{app} (enhancer) and P_{app} (control) are the apparent permeability coefficients of the test compounds (^{3}H-mannitol, FD4, FD20, FD40) across the TR146 and Calu-3 model in the presence and in the absence of the absorption enhancers (CS, CS NP), respectively.

Statistical Evaluation

Statistical differences were investigated by using one-way ANOVA followed by the Student-Newman-Keuls method for multiple comparissons. Differences between groups were judged significant at $P < 0.05$.

RESULTS AND DISCUSSION

Characterization of CS NP

In an attempt to evaluate the effect of the physical condition of CS (presented as a solution or in a particulate form) on its cellular toxicity and permeability enhacing properties, CS NP were prepared as described in the methodology section. The formation of CS NP occurs spontaneously upon incorporation of the counter anion sodium TPP into the CS solution (CS G113 UP) (Calvo et al., 1997). As shown in **Table 3**, CS NP had an average size of 292 nm and a positive surface charge of +35 mV. The stability of NP is a crucial issue, since it is broadly accepted that the size of the particles plays an important role in their ability to interact with mucosal surfaces (De Campos et al., 2004). In fact, one of the major problems encountered with colloidal systems is their tendency to aggregate after exposure to high ionic strength biological media. In this sense, an immediate aggregation of CS NP at pH > 6.5 was observed. This pH limit is probably due to the pK_a of CS, which value is of approximately 6.5, independently of DD (Domard, 1987). Consequently, CS NP stability was determined by means of periodical particle size measurements upon incubation in HBSS pH 6.3 at 37ºC. The results, presented in **Table 3,** indicate that the size was slighty, but not significantly, increased even after 24 h, which led us to consider that the NP were stable under these conditions.

Table 3. Physico-chemical properties and stability of chitosan nanoparticles (CS G113 UP-NP). Values are means ± SD (n = 3).

Formulation	Size (nm)	Zeta Potential (mV)	Stability [a]	
			4 h	24 h
CS G113 UP- NP	292 ± 22	35 ± 1	315 ± 34	330 ± 43

[a] Measured as nanoparticle size after incubation in HBSS (pH 6.3) at 37ºC.

MTS/PMS Assay in proliferating cells

To assess whether CS (different Mw and DD) and CS NP are cytotoxic, the effects of several concentrations on intracellular dehydrogenase activity of TR146 and Calu-3 cells were evaluated by the MTS/PMS assay. It should be emphasized that the experiment was carried out by using TR146 and Calu-3 cells that were in the exponential growth phase (proliferating cells), which might be more sensitive to the formulations than well-differentiated cells grown on permeable inserts for 3-4 weeks.

The relative enzyme activity of TR146 cells exposed to various sample concentrations was plotted in **Figure 1**. A very similar profile was found for Calu-3 cells (Figure not shown). The adverse effects of CS in both cell lines, varied between clear concentration-dependent toxicity, for the highly deacetylated CS (G113 and G210) and CS NP, to almost no effect at all in the concentration ranges studied, for the reacetylated CS (G210-R47 and -R38).

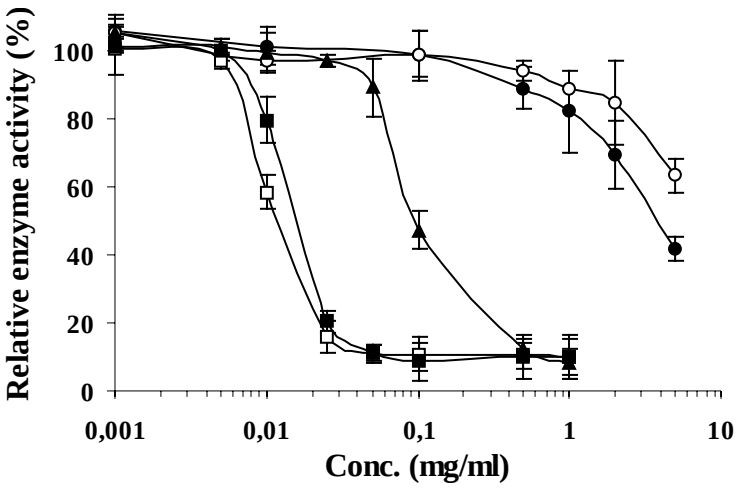

Figure 1. Sensitivity of TR146 proliferating cells toward various concentrations of different types of chitosan (different Mw and DD) and nanoparticles: (□) CS G113 UP, (■) CS G210, (▲) CS G113 UP-NP, (●) CS G210-R47, (○) CS G210-R38, determined by the MTS/PMS assay (means ± SD, n = 3-4).

From the IC_{50} values in **Table 4**, it is evident that the Calu-3 cell culture model was slightly more resilient than the TR146 cell culture model. With regard to the effect of Mw, it was found that CS toxicity slighty decreased as its Mw increased. This variation may be explained by the greater solubility of lower Mw CS, which may facilitate closer interaction with the surface of epithelial cells. A similar finding was observed by Portero et al. with CS glutamate and hydrochloride salts (Portero et al., 2002).

Table 4. Estimated IC_{50} (μg/mL) values obtained for different types of chitosan and chitosan nanoparticles in proliferating TR146 and Calu-3 cells.

Formulation	Mw (kDa) DD[a] (%)	IC_{50} [b,c] (TR146 cells)	IC_{50} [b,c] (Calu-3 cells)
CS G113 UP	128; 86	12.8 ± 4.6	15.7 ± 4.4
CS G113 UP-NP	128; 86	83.2 ± 12.2	166.3 ± 8.0
CS G210	300; 83	15.6 ± 4.0	21.2 ± 1.5
CS G210-R47	300; 47	~ 3500	> 5000 [d]
CS G210-R38	300; 38	> 5000 [d]	> 5000 [d]

[a] DD = degree of deacetylation
[b] IC_{50} values were estimated by using a four-parameter logistic model (Eirheim et al., 2004)
[c] Values are means ± SD, n = 3-4, except for CS G113 UP-NP in Calu-3, where n=2
[d] IC_{50} values not reached, even at a polymer concentration of 5 mg/mL

For the CS with low DD (CS G210-R47 and -R38), an extraordinaryly higher cell viability was obtained, even at the maximum concentration assayed (5 mg/mL). For a 2 mg/mL polymer concentration, the relative enzyme activity remained around 60-70% for both CS G210-R47 and G210-R38 in TR146 cells, and over 80% in Calu-3 cells. This finding concurs with previous studies performed in different cell lines, Caco-2 and A549 cells, in which the key factor in CS toxicity was attributted to its DD, being not or only slighty affected by Mw (Schipper et al., 1996; Huang et al., 2004). Thus, the toxicity of CS appears to be more related to the DD and, consequently, the positive charge density of the polymer, which is in agreement with the well-known cell lytic and toxic properties of other cationic polymers with high

charge density, such as poly-L-lysine, poly-L-arginine, and protamine (Chang et al., 1987; Ekrami and Shen, 1995).

Transformation of soluble CS G113 into a nanoparticulate form led also to a significant decrease of cytotoxity. Specifically, the IC_{50} values of CS NP were 7-fold higher in TR146 cells, and 11-fold higher in Calu-3 cells, than the corresponding CS solutions. This finding could be related with the crosslinking of CS with TPP that occurs during NP formation, process by which the possitive charge density of CS is reduced. In disagreement with our results, Huang et al. reported no differences in cytotoxicity between CS in solution and NP toward the A549 cells (Huang et al., 2004). However, the existence of free CS molecules (which had not interacted with TPP during NP formation) in the CS NP suspensions could explain this fact, as the authors did not specify if NP were isolated or not. Although TPP is considered a non-toxic crosslinking agent, its possible adverse effects were evaluated in TR146 and Calu-3 cells as an additional control, and for the concentration range assayed (0.01 - 2 mg/mL no cytotoxicity was observed, data not shown).

Permeability Studies

Based on the cytotoxicity results obtained in proliferating cells and previous studies performed by our group, three CS concentrations were chosen for the following permeability studies in differentiated cells: (a) a fixed concentration of 1 mg/ml for all the formulations, CS and NP, in terms of comparability; (b) a low concentration (0.015 mg/mL) for the highly deacetylated CS (G113 and G210), since a similar concentration (0.020 mg/mL) resulted to be the most effective for absorption enhancement in previously reported studies (Portero et al., 2002); and (c) a very high concentration (5 mg/mL) for the reacetylated CS (G210-R47 and G210-R38), in order to investigate the effects of a high polymer concentration and taking advantage of their extremely low cytotoxicity.

From the permeability profiles of ^{3}H-mannitol, FD4, FD20, and FD40, the apparent permeability coeffiecient (P_{app}) and absorption enhacement ratio (ER) after incubation with the different CS and CS NP were calculated and related to changes in TEER values and cellular viability measured on the well-differentiated cell layers.

It must be pointed out that the different pH of CS solutions (pH 6.0) and NP (pH 6.3) resulted in comparable TEER values and ^{3}H-mannitol permeability on both TR146 and Calu-3 layer(s). In addition, it has been reported that TR146 cell layers are not sensitive to pH changes in the range 5-9 (Nielsen and Rassing, 1999).

Permeability studies with the TR146 cell culture model

The TR146 cell culture model has been previously used to study the permeability enhancing effect of chitosans (different salts and Mw) (Portero et al., 2002), bile salts (Nielsen et al., 1999), and glycocholate (Eirheim et al., 2004). After culturing for 28 days, the mean TEER value of TR146 epithelium, corrected for filter background, was 260 ± 54 $\Omega \times cm^2$ (n=100), which is in the range of those TEER values reported for TR146 differentiated cells used previously (Nielsen et al., 1999; Portero et al., 2002).

Permeability results in the absence and presence of CS and NP are summarized in **Table 5**. As expected, in the absence of enhancers, the highest permeability was obtained for ^{3}H-mannitol (14.46×10^{-7} cm/s), whereas permeability of FD4, FD20, and FD40 decreased with increasing Mw of the test substance, from 2.53×10^{-7} to 0.21×10^{-7} cm/s. Decreased permeability rates of hydrophilic substances with increasing Mw have also been previously reported for the TR146 cell culture and *in vitro* buccal porcine models (Nielsen et al., 1999; Junginger et al., 2001; Portero et al., 2002). With regard to the results obtained in presence of test enhancers, the highly deacetylated CS (G113 and G210) were able to significantly increase the permeability of all the model substances ($P < 0.05$). In general, this effect tended to be higher for the lowest CS concentration (0.015 mg/mL versus 1 mg/mL), although significant differences were found only for FD20 permeability values ($P < 0.05$). This dependence on concentration of the CS effect concurs with other studies performed in TR146 and Caco-2 cells (Portero et al., 2002; Schipper et al., 1996; Dodane et al., 1999), where a plateu level was reached at a determined CS concentration (between 0.020 mg/mL and 1 mg/mL). When the CS concentration is increased, the solutions become more viscous, and the diffusion of the test substances is hindered. With regard to reacetylated CS, CS G210-R38,

which is the most reacetylated sample, was not effective as permeability enhancer at any of the test concentrations (1 and 5 mg/mL), whereas CS G210-R47 led to significantly increased permeabilities of all the subtances ($P < 0.05$) except FD40. Once again, the lowest concentration, in this case 1 mg/mL, provided the best results ($P < 0.05$). It has previously been reported that the ability of CS to improve transport of hydrophilic compounds across mucosal epithelia dependens on charge density. In this sense, Schipper et al. studied the effect of CS with DD ranging between 51% and 99% on permeability of ^{14}C-mannitol across Caco-2 cells. In agreement with our results, highly deacetylated CS resulted to be the most effective but also toxic, while CS with the lowest DD (51%), which could be comparable with our CS G210-R47 (DD 47%), provided significantly increased permeabilities at non-harmful and minimally harmful CS concentrations (0.050 and 0.25 mg/mL) (Schipper et al., 1996). On the part of CS NP, a significantly increased permeability was observed for ^{3}H-mannitol, FD4 and FD20 ($P < 0.05$), reaching similar values to those obtained with the highly deacetylated CS and also CS G210-R47 at the same concentration (1 mg/mL). In an overall view, the ability of the test enhancers to increase permeability could be ranked in the order CS G113≈CS G210 ≥ CS NP≈CS G210-R47 > CS G210-R38.

Table 5. Apparent permeability coefficients (P_{app}) of ^{3}H-mannitol, FD4, FD20, and FD40 measured in the apical to basolateral direction across the TR146 cell culture model in the absence or presence of chitosan of different deacetylation degree and also chitosan nanoparticles.

Formulation	Enhancer concentration (mg/mL)	$P_{app} \pm SD$ (x 10^{-7} cm s^{-1})			
		^{3}H-mannitol	FD4	FD20	FD40
Control	-	14.46 ± 8.63	2.53 ± 0.83	0.69 ± 0.10	0.21 ± 0.04
CS G113 UP	0.015	n.d	14.8 ± 3.55*	2.13 ± 0.21*	0.48 ± 0.09*
	1		10.7 ± 0.88*	1.31 ± 0.11*	0.57 ± 0.08*
CS G113 UP-NP	1	40.36 ± 8.76*	12.0 ± 2.19*	1.17 ± 0.13*	0.59 ± 0.29
CS G210	0.015	n.d	17.0 ± 8.51*	2.35 ± 0.51*	0.54 ± 0.17*
	1		11.9 ± 1.36*	1.58 ± 0.26*	0.66 ± 0.10*
CS G210-R47	1	n.d	9.65 ± 3.22*	1.89 ± 0.59*	0.57 ± 0.26
	5		6.82 ± 0.22*	1.13 ± 0.26*	0.68 ± 0.25
CS G210-R38	1	n.d	4.92 ± 2.68	0.93 ± 0.06	0.39 ± 0.11
	5		4.77 ± 3.63	0.83 ± 0.28	0.56 ± 0.17

* Denotes significant difference from control (P < 0.05). Values are means ± SD, n = 3. n.d = not determined.

The enhancement ratio (ER) values, as well as the corresponding cellular viabilities obtained for permeability of FD4, FD20 and FD40 across the TR146 cell culture model in presence of the different CS formulations, are represented in **Figure 2** and **Table 6**. It must be pointed out that the cellular viability remained over 80% in all cases, except for highly deacetylated CS (CS G113 and CS G210) in the 1 mg/mL concentration. However, the best ER values were found at a minimally harmful CS concentration (0.015 mg/mL, viability > 80%). It should be noted that a tendency of higher viability of the CS G113 UP was observed when formulated as NP.

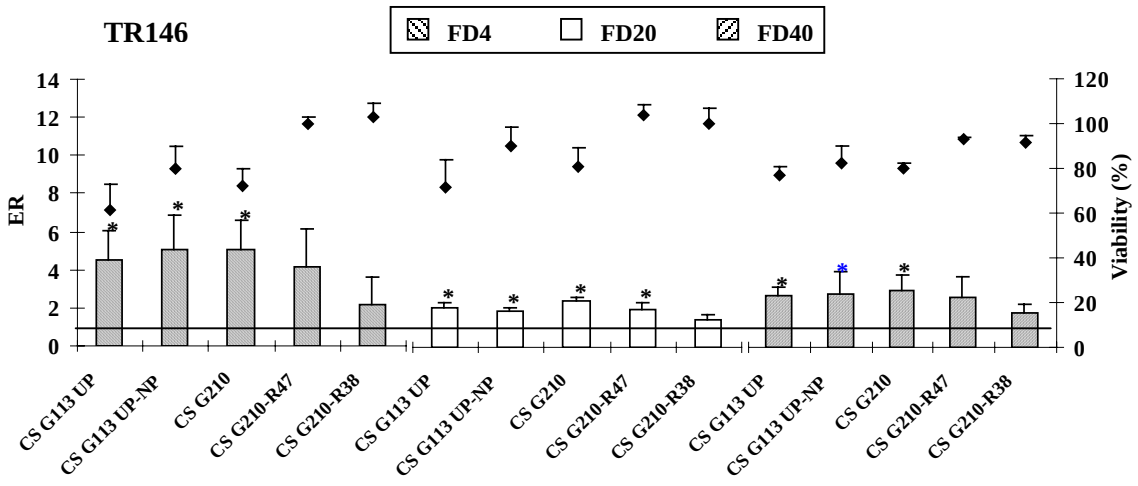

Figure 2. Enhacement ratio values (ER, bars) of FD4, FD20, and FD40 permeation across the TR146 cell culture model when applied together with different types of chitosan and chitosan nanoparticles (1 mg/mL) and cellular viability after the experiment (♦), relative to untreated cells (mean ± SD, n = 3). Enhacement ratio for untreated cells (ER = 1) is represented by the horizontal line.

Table 6. Enhancement ratio values (ER) of FD4, FD20, and FD40 permeation across the TR146 cell culture model treated with different types of chitosan (0.015 and 5 mg/mL) and cellular viability after the experiment, relative to untreated cells.

Formulation	Enhancer conc. (mg/mL)	FD4		FD20		FD40	
		ER	Viability (%)	ER	Viability (%)	ER	Viability (%)
CS G113 UP	0.015	5.97 ± 1.11*	84 ± 9	3.13 ± 0.44*	85 ± 1	2.32 ± 0.50	86 ± 3
CS G210	0.015	6.55 ± 1.52*	89 ± 2	3.41 ± 0.55*	86 ± 3	2.43 ± 1.04	83 ± 1
CS G210-R47	5	3.32 ± 0.23*	86 ± 8	1.80 ± 0.65	84 ± 9	3.20 ± 1.07*	90 ± 8
CS G210-R38	5	1.91 ± 0.70	82 ± 7	1.18 ± 0.24	80 ± 9	2.63 ± 0.34*	82 ± 5

* Denotes significant difference from control ($P < 0.05$). Values are means ± SD, n = 3.

All the observations made until now in the context of permeability enhancement presented a good correlation with measurements of TEER values. Measurement of TEER is believed to be a good indication of tightness of junctions between cells. In this sense, decrease in TEER was directly related with the ability of CS-based formulations to enhance the FD permeation across the TR146 cell culture model. Specifically, CS G210, CS G113 and CS NP, which were able to elicit the best ER, produced a drastical decrease in TEER to around 20% in comparisson with buffer-treated cells. The effect on the TEER values seemed to be saturable, since no major differences were found when increasing the CS concentration, as shown in **Figure 3**. This observation was previously reported for experiments in Caco-2 cell monolayers (Kotze et al., 1998; Artursson et al., 1994). It is also interesting to note that, as can be deduced from TEER and cytotoxicity experiments, the enhancing effect of CS on permeation across TR146 cells correlated with a marked decreased epithelial integrity but not necessarily with cellular damage, as found for the lowest CS concentrations.

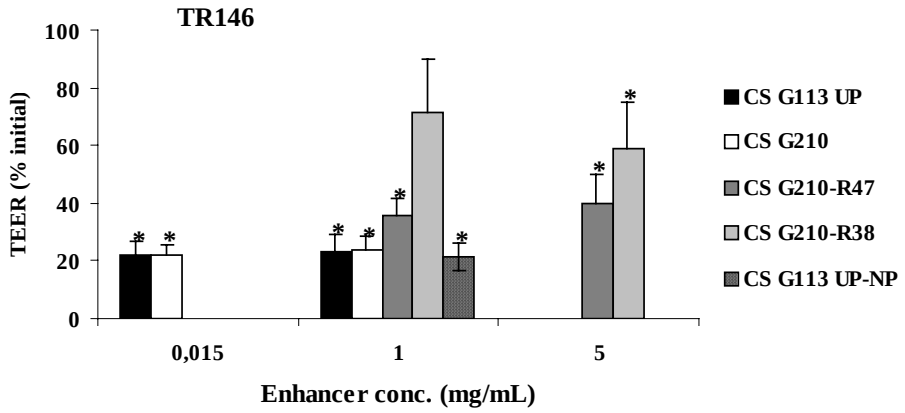

Figure 3. Reduction in transepithelial electrical resistance (TEER) of TR146 epithelium after permeability experiments with FITC-dextrans, expressed as percent of initial values (means ± SD, n = 6-9). * Denotes significant difference from untreated cell layers ($P < 0.05$).

In the buccal epithelium, it is believed that the main permeability barrier, responsible of epithelial cohesion in the superficial layers, is the result of intercellular

material derived from the membrane coating granules (MCGs). MCGs are spherical or oval organelles located in the intermediate cell layers of the epithelium that discharge their contents (lipids, glycolipids) into the intercellular space (Jasti et al., 2005). While the penetration enhancement properties of chitosan via mucosae (such as the intestinal and nasal) are mainly due to a transient widening of the tight junctions between cells, in buccal epithelium, which lack tight juntions, chitosan is suggested to act by adhesion and by disruption of the intercellular lipid material (Senel et al., 2000). Furthermore, the possible interaction of CS with the proteoglycan matrix by ionic interactions could led to a transient widening of the intercellular filaments, thus contributing to the permeation enhancement effect by the paracellular (intercellular) route (Portero et al., 2002) and also contributing to the decrease in TEER. However, a minor permeation enhancement effect of CS by the intracellular pathway could not be neglected, since perturbation of the plasma membrane and modifications of the intracellular milieu were found by Dodane et al. in Caco-2 cells exposed to CS (Dodane et al., 1999). Correspondingly, the present results indicate a (non-significant) tendency to slightly decreased enzymatic activity of the cells in the cell layers.

Permeability studies with the Calu-3 cell culture model

On day 21 after seeding, the apical surface of differentiated Calu-3 cell monolayer was covered with an uniform and abundant layer of mucus; the production of which is known to be more pronounced under air-liquid culture conditions (Florea et al., 2002). The mean TEER value, corrected for filter background, was 380 ± 48 $\Omega \times cm^2$ (n=100). This value is consistent with previously reported data for Calu-3 differentiated cells (Shen et al., 1994; Witschi and Mrsny, 1999; Borchard et al., 2002; Tréhin et al., 2004; Grainger et al., 2006) even though variations in Calu-3 cell culture methods (air-liquid or liquid-covered culture, filter coating, seeding density etc.) have resulted in substantial inter- and intra-laboratory variability in TEER and permeability values. In this sense, TEER values between 350 and 2300 Ω x cm^2 have been reported (Forbes and Ehrhardt, 2005), while the P_{app} values found for mannitol, a widely used integrity marker, varied from 1 to

22×10^{-7} cm/s (Sakagami, 2006). In the present work, permeability of ^{3}H-mannitol across the Calu-3 cells was 2.95×10^{-7} cm/s. As in the TR146 cells, in the absence of enhancers, the highest permeability value corresponded to ^{3}H-mannitol, followed by FD4, FD20, and FD40, which consecutively decreased from 0.86×10^{-7} to 0.14×10^{-7} cm/s. This inversely proportional relationship between permeability and FD Mw in Calu-3 cells has been previously reported (Mathias et al., 2002; Grainger et al., 2006). However, the P_{app} values found for the different FD by Mathias et al. were very low, in the range of $0.002\text{-}0.06\times10^{-7}$ cm/s, while those of Grainger et al. were in the range of $2\text{-}4\times10^{-7}$ cm/s. This increased permeability values could be attributted to the reported theoretical pore diameter of the cell monolayer (Grainger et al., 2006), almost twice as wide as that reported by Mathias and coworkers, and also to the TEER values, of 300 $\Omega \times cm^2$ opposite to >1000 $\Omega \times cm^2$, both factors contributting to a less restrictive barrier.

The permeability results obtained in the absence and presence of different concentrations of CS and NP across the Calu-3 cell culture are summarized in **Table 7**. With regard to the results obtained in the presence of enhancers, the highly deacetylated CS (G113 and G210), in a concentration of 1 mg/mL, showed a clear tendency to increase the permeability of all the model substances, being significant for FD20 and FD40 ($P < 0.05$). In contrast to the results found in TR146 cells, the low CS concentrations (0.015 mg/mL) as well as CS NP (1 mg/mL) were less effective as absorption enhancers, only significantly promoting the FD20 permeation ($P < 0.05$). Reacetylated CS (G210-R47 and G210-R38) were not able to increase permeability at any concentration, 1 mg/mL or 5 mg/mL.

Table 7. Apparent permeability coefficients (P_{app}) of ^{3}H-mannitol, FD4, FD20, and FD40 measured in the apical to basolateral direction across the Calu-3 cell culture model in the absence or presence of chitosan of different deacetylation degree and also chitosan nanoparticles.

Formulation	Enhancer concentration (mg/mL)	$P_{app} \pm SD$ (x 10^{-7} cm s^{-1})			
		^{3}H-mannitol	FD4	FD20	FD40
Control	-	2.95 ± 1.66	0.86 ± 0.11	0.22 ± 0.01	0.14 ± 0.03
CS G113 UP	0.015	n.d	0.94 ± 0.66	0.69 ± 0.01*	0.19 ± 0.13
	1		3.47 ± 1.75	1.70 ± 0.45*	1.69 ± 0.16*
CS G113 UP-NP	1	8.04 ± 6.11	0.95 ± 0.66	0.76 ± 0.09*	0.08 ± 0.02
CS G210	0.015	n.d	1.05 ± 0.85	0.76 ± 0.14*	0.26 ± 0.10
	1		3.09 ± 2.16	1.72 ± 0.19*	1.46 ± 0.16*
CS G210-R47	1	n.d	0.48 ± 0.21	0.06 ± 0.01	0.13 ± 0.04
	5		0.65 ± 0.23	0.11 ± 0.01	0.08 ± 0.02
CS G210-R38	1	n.d	0.48 ± 0.33	0.02 ± 0.01	0.10 ± 0.03
	5		0.46 ± 0.18	0.06 ± 0.01	0.18 ± 0.05

* Denotes significant difference from control ($P < 0.05$). Values are means ± SD, n = 3. n.d = not determined.

The ER values, as well as the corresponding cellular viabilities obtained for permeability of FD4, FD20 and FD40 across the Calu-3 cell culture model in presence of the different CS-based formulations, are represented in **Figure 4** and **Table 8**. The cellular viability remained over 80-90% in all cases, except for the highest concentration of highly deacetylated CS (CS G113 and CS G210, 1 mg/mL) enhancing the FD4 and FD20 permeation. Thus, the best ER values were associated with a slighty decrease in the cell viability to around 60-70 %. A similar decrease in Calu-3 cell viability was reported by Florea et al. for CS solutions, although in a higher concentration. The authors did not discard the possibility of loosing some cells during the washing steps due to the high bioadhesiveness of such highly deacetylated CS (Florea et al., 2006).

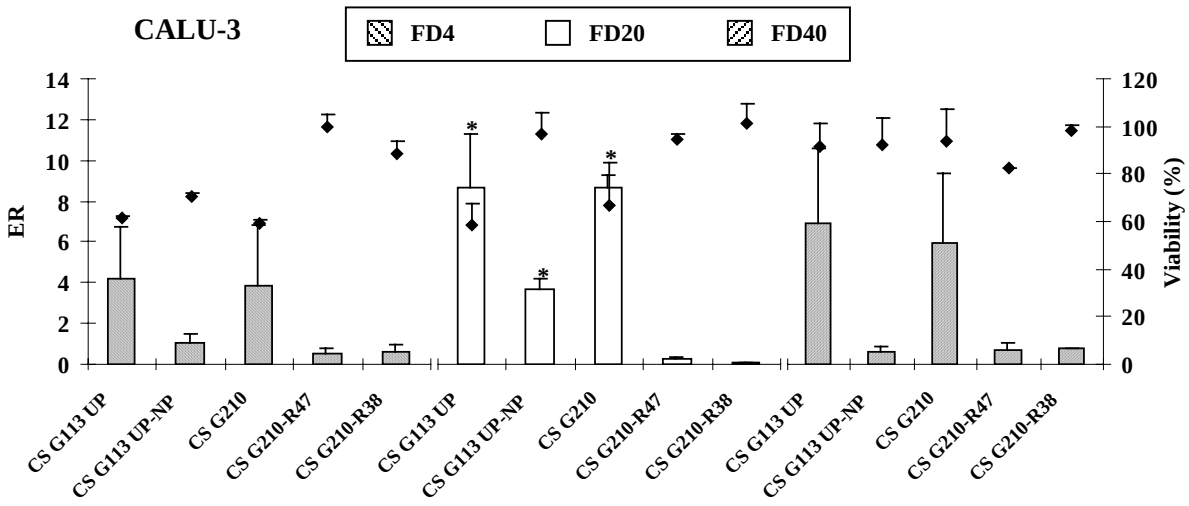

Figure 4. Enhacement ratio values (ER, bars) of FD4, FD20, and FD40 permeation across the Calu-3 cell culture model treated with different types of chitosan and chitosan nanoparticles (1 mg/mL) and cellular viability after the experiment (♦), relative to untreated cells (mean ± SD, n = 3). Enhacement ratio for untreated cells (ER = 1) is represented by the horizontal line.

Table 8. Enhancement ratio values (ER) of FD4, FD20, and FD40 permeation across the Calu-3 cell culture model treated with different types of chitosan (0.015 and 5 mg/mL) and cellular viability after the experiment, relative to untreated cells.

Formulation	Enhancer Conc. (mg/mL)	FD4		FD20		FD40	
		ER	Viability (%)	ER	Viability (%)	ER	Viability (%)
CS G113 UP	0.015	1.05 ± 0.59	84 ± 5	3.08 ± 0.14*	103 ± 3	0.90 ± 0.53	103 ± 2
CS G210	0.015	1.15 ± 0.79	80 ± 6	3.44 ± 0.75*	108 ± 14	1.45 ± 1.11	106 ± 5
CS G210-R47	5	0.83 ± 0.33	n.d	0.49 ± 0.01	n.d	0.65 ± 0.32	80 ± 12
CS G210-R38	5	0.54 ± 0.24	n.d	0.26 ± 0.07	n.d	1.00 ± 0.56	92 ± 10

* Denotes significant difference from control ($P < 0.05$). Values are means ± SD, n = 3. n.d = not determined.

The decrease in permeation-enhancing effectiveness of CS NP and reacetylated CS in Calu-3 as compared with other cell lines could be atributted to the presence of extracellular mucus on the apical surface. In this sense, highly deacetylated CS molecules, due to their great positive charge density, may strongly interact with mucus, reach the epithelial cell membrane, and finally disrupt tight junctions in a greater extent than CS NP and reacetylated CS, with a lower positive charge density. In fact, the mechanism for permeability enhancement by CS has been reported in Caco-2 cells to be related to the polymer binding to cell membranes through a charge-dependent mechanism (Schipper et al., 1997), which involves the translocation of tight junction proteins, such as ZO-1 and ocluddin, from the membrane to the cytoskeleton (Smith et al., 2004) and the redistribution of F-actin (Dodane et al., 1999). It must be mentioned that in our experiments, Calu-3 differentiated cells presented a very thick mucus layer, which was noticeable by simple macroscopical observation. Taking this into account, we decided to perform a permeability experiment in Calu-3 cells containing a lower amount of apical mucus. Therefore, the apical cell surface was carefully rinsed and the major part of diluted mucus removed, in order to somehow mimic physiological clearance mechanisms. After that, permeability of FD4 was assessed in presence of CS NP as absorption enhancer. Permeability values and the corresponding ER are depicted in **Figure 5** . As can be observed, CS NP were able to significantly increase the P_{app} and thus, enhance FD4 absorption around 2.5-fold. Interestingly, no cellular damage was produced since the viability remained over 80%.

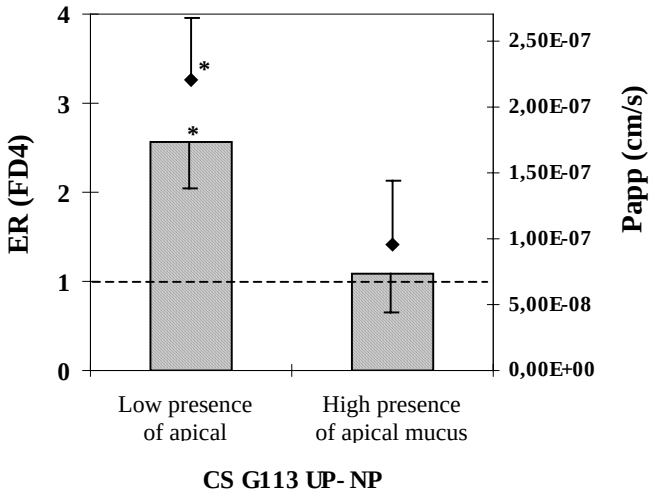

Figure 5. Enhacement ratio values (ER, bars) and apparent permeability coefficients (P_{app}, ♦) of FD4, in presence of chitosan nanoparticles (CS G113 UP- NP, 1 mg/mL), across the Calu-3 cell culture model with different apical mucus thickness (mean ± SD, n = 2-3). Enhacement ratio for untreated cells (ER = 1) is represented by the dashed line. * Denotes significant difference from untreated cells ($P < 0.05$).

A good correlation of permeability enhancing effects and the ability to decrease TEER was found. Thus, decrease in TEER was directly related with the ability of CS-based formulations to enhance the FD permeation across the Calu-3 cell culture model. Specifically, CS G210 and CS G113 (1 mg/mL), which were able to elicit the best ER, produced a drastical decrease in TEER to around 20% in comparisson with buffer-treated cells (Figure 6). A marked decrease in TEER has been also reported for experiments with CS solutions in Caco-2 cell monolayers (Kotze et al., 1998; Artursson et al., 1994; Smith et al., 2004) and 16HBE14o-cells (Lim et al., 2001). Specifically in Calu-3 cells, a strong but reversible decrease in TEER was observed, concluding no harmful effects on the cells as the TEER returned to 90-100% of the initial values alter a recovery period (Florea et al., 2006).

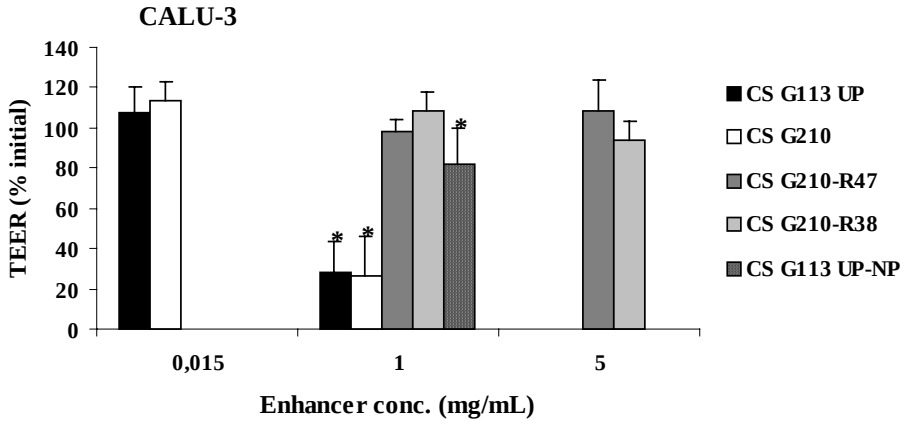

Figure 6. Reduction in transepithelial electrical resistance (TEER) of Calu-3 epithelium (high presence of apical mucus) after permeability experiments with FITC-dextrans, expressed as percent of initial values (means ± SD, n = 6-9). * Denotes significant difference from untreated cell layers ($P < 0.05$).

CONCLUSIONS

Sensitivity of TR146 and Calu-3 cells to CS-based formulations was increased with CS dose, deacetylation degree, solution relative to NP and with proliferating compared to differentiated cells. The ability of CS to enhance the transport of macromolecules across the TR146 and Calu-3 cell culture models was mainly related to polymer deacetylation degree (i.e. positive charge density), with the highest deacetylated CS being the most effective. Fortunately, it is possible to select CS formulations that, being minimally harmful, effectively enhance the absorption of macromolecules across the different epithelial barriers.

ACKNOWLEDGEMENTS

The authors thank B. Dinitzen and S. N. Sørensen from the Department of Pharmaceutics and Analytical Chemistry, Faculty of Pharmaceutical Sciences, University of Copenhagen, for technical assistance. This research has been supported by a Marie Curie Fellowship of the European Community program "Improving the Human Research Potential and the Socio-Economic Knowledge Base" under contract number HPMT-CT-2001-00403, the Spanish Government, CICYT (SAF 2002-03314), the Alfred Benzon Foundation (Denmark), and Drug Research Academy.

REFERENCES:

1. Artursson P., Lindmark T., Davis S.S., Illum L., Effect of chitosan on permeability of monolayers of intestinal epithelial cells (Caco-2), *Pharm. Res.*, 11 (1994) 1358-1361.
2. Borchard G., Cassara M.L., Roemele P.E., Florea B.I., Junginger H.E., Transport and local metabolism of budesonide and fluticasone propionate in a human bronchial epithelial cell line (Calu-3), *J. Pharm. Sci.*, 91 (2002) 1561-1567.
3. Calvo P., Remuñán-López C., Vila-Jato J.L., and Alonso M.J., Novel hydrophilic chitosan-polyethylene oxide nanoparticles as protein carriers, *J. Appl. Polym. Sci*., 63 (1997) 125-132.
4. Chang S.W., Westcott J.Y., Henson J.E., Voelkel N.F., Pulmonary vascular injury by polycations in perfused rat lungs, *J. Appl. Physiol.*, 62 (1987) 1932-1943.
5. De Campos A.M, Diebold Y., Carvalho E.L.S., Sánchez A., Alonso M.J., Chitosan nanoparticles as new ocular drug delivery systems: in vitro stability, in vivo fate, and cellular toxicity, *Pharm. Res.*, 21 (2004) 803-810.
6. Dodane V., Khan M.A., Merwin J.R., Effect of chitosan on epithelial permeability and structure, *Int. J. Pharm.*, 182 (1999) 21-32.
7. Domard A., pH and c.d. measurements on a fully deacetylated chitosan: application to Cu^{II}-polymer interactions, *Int. J. Biol. Macromol.*, 9 (1987) 98-104.
8. Ekrami H.M., Shen W.C., Carbamylation decreases the cytotoxicity but not the drug-carrier properties of polylysines, *J. Drug Target.*, 2 (1995) 469-475.

9. Fernández-Urrusuno R., Calvo P., Remuñán-López C., Vila-Jato J.L., Alonso M.J., Enhancement of nasal absorption of insulin using chitosan nanoparticles, *Pharm. Res.*, 16 (1999)1576-1581.

10. Florea B.I., Meaney C., Junginger H.E., Borchard G., Transfection efficiency and toxicity of polyethylenimine in differentiated Calu-3 and nondifferentiated COS-1 cell cultures, *AAPS PharmSci*, 4 (2002) article 12 (http://www.aapspharmsci.org).

11. Florea B.I., Thanou M., Junginger H.E., Borchard G., Enhancement of bronchial octreotide absorption by chitosan and N-trimethyl chitosan shows linear in vitro/in vivo correlation, *J. Control. Rel.*, 110 (2006) 353-361.

12. Forbes B., Ehrhardt C., Human respiratory epithelial cell culture for drug delivery applications, *Eur. J. Pharm. Biopharm.*, 60 (2005) 193-205.

13. Foster K.A., Avery M.L., Yazdanian M., Audus K.L., Characterization of the Calu-3 cell line as a tool to screen pulmonary drug delivery, *Int. J. Pharm.*, 208 (2000) 1-11.

14. Grainger C.I., Greenwell L.L., Lockley D.J., Martin G.P., Forbes B., Culture of Calu-3 cells at the air interface provides a representative model of the airway epithelial barrier, *Pharm. Res.*, 23 (2006) 1482-1490.

15. Hirai A., Odani H., Nakajima A., Determination of degree of deacetylation of chitosan by ^{1}H NMR spectroscopy, *Polym. Bull*., 26 (1991) 87-94.

16. Huang M., Khor E., Lim L.-Y., Uptake and cytotoxicity of chitosan molecules and nanoparticles: effects of molecular weight and degree of deacetylation, *Pharm. Res.*, 21 (2004) 344-353.

17. Jacobsen J., Pedersen M., Rassing M.R., TR146 cells as a model for human buccal epithelium. II. Optimization and use of a cellular sensitivity MTS/PMS assay, *Int. J. Pharm.,* 141 (1996) 217-225.

18. Jacobsen J., van Deurs B. Pederssen M., Rassing M.R., TR146 cells grown on filters as a model for human buccal epithelium. I. Morphology, growth, barrier properties and permeability, *Int. J. Pharm.* 125 (1995) 165-184.

19. Jasti B.R., Marasanapalle V., Li X., Modulation of oral transmucosal permeability: permeation enhancers, *Drugs and the Pharmaceutical Sciences*, 145 (2005) 67-87.

20. Junginger H.E., Hoogstraate J.A., Verhoef J.C., Recent advantages in buccal drug delivery and absorption – in vitro and in vivo studies, J. Control. Rel., 62 (1999) 149-159.

21. Kotze A.F., Lueβen H.L., De Boer A.G., Verhoef J.C., Junginger H.E., Chitosan for enhanced intestinal permeability: prospects for derivatives soluble in neutral and basic environments, *Eur. J. Pharm. Sci.*, 7 (1998) 145-151.

22. Lee V.H.L., Peptidase activities in absorptive mucosae, *Biochem. Soc. Trans*. 17 (1989) 937-940.

23. Lim S.T., Forbes B., Martin G.P., Brown M.B., In vivo and in vitro Characterization of novel microparticulates based on hyaluronan and chitosan hydroglutamate, *AAPS PharmsciTech*., 2 (2001) article 20 (http://www.pharmscitech.com).

24. Mathias N.R., Timoszyk J., Stetsko P.I., Megill J.R., Smith R.L., Wall D.A., Permeability characteristics of Calu-3 human bronchial epithelial cells: in vitro-in vivo correlation to predict lung absorption in rats, J. Drug Target., 10 (2002) 31-40.

25. Mima S., Miya M., Iwamoto R. and Yoshikawa S., Highly deacetylated chitosan and its properties, *J. Appl. Polym. Sci.,* 28 (1983) 1909-1917.

26. Nielsen H.M. and Rassing M.R., TR146 cells grown on filters as a model of human buccal epithelium. III. Permeability enhancement by different pH values, different osmolality values and bile salts, *Int. J. Pharm*., 185 (1999) 215-225.

27. Nielsen H.M., Verhoef J.C., Ponec M. and Rassing M.R., TR146 cells grown on filters as a model of human buccal epithelium: permeability of fluorescein isothiocyanate-labelled dextrans in the presence of sodium glycocholate, *J. Control. Rel,* 60 (1999) 223-233.

28. Portero A., Remuñán-López C., Nielsen H.M., The potential of chitosan in enhancing peptide absorption across the TR146 cell culture model-an in vitro model of the buccal mucosa, *Pharm. Res.*, 19 (2002) 169-174.

29. Rossi S., Sandri G., Ferrari F., Bonferoni M.C., Caramella C., Development of films and matrices based on chitosan and polyacrylic acid for vaginal delivery of acyclovir, *S.T.P. Pharma Sci.*, 13 (2003) 183-190.

30. Rupniak H.T., Rowlatt C., Lane E.B., Steele J.G., Trejdosiewicz L.K., Laskiewicz B., Povey S., Hill B.T., Characteristics of four new human cell lines derived from squamous cell carcinomas of the head and neck, *J. Natl. Cancer Inst*., 75 (1985) 621-634.

31. Sakagami M., In vivo, in vitro and ex vivo models to assess pulmonary absorption and disposition of inhaled therapeutics for systemic delivery, *Advanced Drug Delivery Reviews*, 58 (2006) 1030-1060.

32. Schipper N.G.M., Varum K.M., Artursson P., Chitosans as absorption enhancers for poorly water absorbable drugs. I. Influence of molecular weight and degree of acetylation on drug transport across human intestinal epithelial (Caco-2) cells, *Pharm. Res*., 13 (1996) 1686-1692.

33. Schipper N.G.M., Olson S., Hoogstraate J.A., De Boer A.G., Varum K.M., Artursson P., Chitosans as absorption enhancers for poorly absorbable drugs. II. Mechanism of absorption enhancement, *Pharm. Res.*, 14 (1997) 923-929.

34. Senel S., Kremer M.J., Kas S., Wertz P.W., Hincal A.A., Squier C.A., Enhancing effect of chitosan on peptide drug delivery across buccal mucosa, *Biomaterials*, 21 (2000) 2067-2071.

35. Shen B.Q., Finkbeiner W.E., Wine J.J., Mrsny R.J., Widdicombe J.H., Calu-3: a human airway epithelial cell line that shows cAMP-dependent Cl-secretion, *Am. J. Physiol. Cell Physiol.*, 266 (1994) 493-501.

36. Smith J., Wood E., Dornish M., Effect of chitosan on epithelial cell tight junctions, *Pharm. Res.*, 21 (2004) 43-49.

37. Teijeiro-Osorio D. and Remuñán-López C., *submitted*

38. Tomihata K., and Ikada Y., In vitro and in vivo degradation of films of chitin and its deacetylated derivatives, *Biomaterials*, 18 (1997) 567-575.

39. Tréhin R., Krauss U., Beck-Sickinger A.G., Merkle H.P. and Nielsen H.M., Cellular uptake but low permeation of human calcitonin-derived cell penetrating peptides and Tat(47-57) through well-differentiated epithelial models, *Pharm. Res.,* 21 (2004) 1248-1256.

40. Winton H.L., Wan H., Cannell M.B., Cell lines of pulmonary and non-pulmonary origin as tools to study the effects of house dust mite proteinases on the regulation of epithelial permeability, *Clin. Exp. Allergy*, 28 (1998) 1273-1285.

41. Witschi C., Mrsny R.J., *In vitro* evaluation of microparticles and polymer gels for use as nasal platforms for protein delivery, *Pharm. Res.*, 16 (1999) 382-390.

PARTE I: Discusión general

PARTE I

DISCUSIÓN GENERAL

Como se ha mencionado previamente, el objetivo general de la primera parte de esta memoria experimental ha sido el de desarrollar sistemas microparticulares destinados a la administración pulmonar de macromoléculas terapéuticas con fines sistémicos. Para ello, y teniendo en cuenta las interesantes propiedades descritas en la sección de Introducción, se seleccionaron dos polisacáridos hidrofílicos, quitosano (CS) y glucomanano (GM) y se prepararon sistemas simples (compuestos por un solo polímero) o mixtos (compuestos por ambos polímeros) mediante la técnica de atomización. Esta técnica, bien conocida y muy versátil, resulta adecuada para la preparación de micropartículas en un medio completamente acuoso, tanto a partir de soluciones como de suspensiones/dispersiones de polímeros y principios activos[1]. Las principales variables de formulación investigadas han sido el grado de desacetilación (DD) del CS (**Art. 1**) y el porcentaje de GM incorporado en el sistema microparticular (**Art. 2**). Así pues, se estudió el efecto de estas variables sobre las propiedades morfológicas y aerodinámicas de las microsferas, así como sobre su capacidad de asociar y liberar la macromolécula modelo (insulina). Adicionalmente, se estudió la influencia del DD del CS sobre sus propiedades como promotor de la absorción de macromoléculas de distinto peso molecular (FITC-dextranos de 4, 20 y 40 KDa) en cultivos celulares modelo de los epitelios bucal y traqueobronquial, donde también se evaluó su citotoxicidad, al igual que la del GM (**Art. 2** y **3**).

[1] **Agnihotri S.A., Mallikarjuna N.N., Aminabhavi T.M.**, Recent advances on chitosan-based micro- and nanoparticles in drug delivery, J. Control. Rel., 100 (2004) 5-28.

1. Reacetilación del quitosano

Para la obtención de microsferas de CS de distinto grado de desacetilación, el primer paso consistió en el proceso de reacetilación del CS comercial (DD = 83%) mediante la reacción del mismo con distintas cantidades de anhídrido acético (**Figura 1a**).

La determinación del DD resultante fue efectuada por ^{1}H-RMN, mediante la aplicación de la comúnmente utilizada expresión de Hirai y col.[2], obteniendo DDs del 47, 38, 26 y 23% (**Art. 1, Fig. 2** y **Tabla 1**). Como se puede observar en la **Figura 1b**, la cantidad de anhídrido acético empleada en la reacción y el DD finalmente obtenido no siguen una relación lineal, alcanzando casi un valor de DD constante para aquellas cantidades de reactivo superiores a los 5 μL/mg de CS.

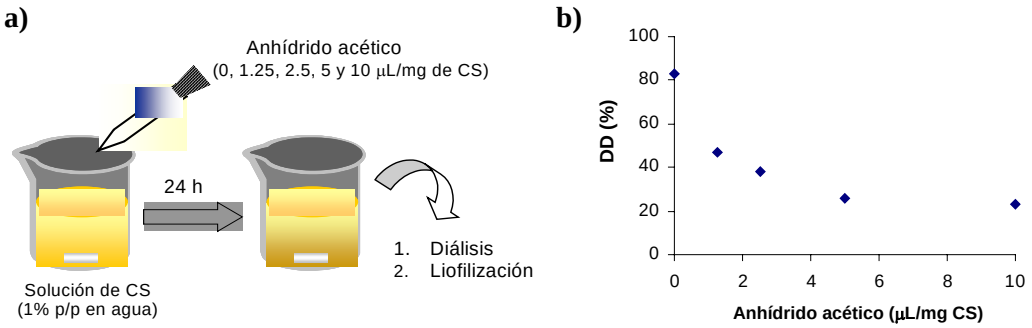

Figura 1. Esquema de preparación del CS reacetilado y grados de deacetilación obtenidos en función de la cantidad de anhídrido acético utilizada en la reacción.

[2] **Hirai A., Odani H., Nakajima A.**, Determination of degree of deacetylation of chitosan by ^{1}H NMR spectroscopy, Polym. Bull., 26 (1991) 87-94.

2. Preparación y caracterización de microsferas de quitosano y quitosano-glucomanano

Tras numerosas pruebas preliminares, en las que se fijaron las condiciones de atomización, se procedió a la preparación de las distintas formulaciones a partir, básicamente, de soluciones/dispersiones de: (a) CS de distinto DD (83, 47, 38, 26 y 23%); y (b) CS y GM en diferentes proporciones (100:0, 75:25, 50:50, 25:75 y 0:100).

Un primer paso en la caracterización de las microsferas se dirigió al estudio de su composición por espectroscopia de infrarrojos (IR). De este modo, en el caso de las microsferas preparadas con CS de distinto DD, la realización de los espectros de IR y su posterior análisis cuantitativo no hizo más que confirmar los datos de DD obtenidos previamente por RMN para las soluciones/dispersiones correspondientes (**Art. 1, Fig. 4** y **Tabla 3**). Para las microsferas compuestas por CS y GM, el análisis de IR determinó la existencia de interacciones entre ambos polímeros, principalmente por puentes de hidrógeno[3], lo que sugiere un grado de miscibilidad previo a la atomización que debiera derivar en una distribución homogénea de los mismos en la matriz polimérica de las microsferas (**Art. 2, Fig. 4**).

El estudio morfológico de las partículas, realizado por microscopía electrónica de barrido, reveló una gran influencia de la composición de las mismas sobre su forma y características superficiales (textura, rugosidad). Así, las microsferas compuestas en su totalidad por CS comercial (DD 83%) condujeron a la obtención de partículas perfectamente esféricas y con una superficie lisa. Sin embargo, tanto la inclusión de GM en su composición, como la utilización de CS reacetilado (menor DD), hizo que dicha morfología derivase hacia formas esferoidales irregulares, con superficies convolucionadas y rugosas, siendo este

[3] **Alonso-Sande M., Teijeiro-Osorio D., Remuñán-López C., Alonso M.J.**, Glucomannan, a promissing polysaccharide for biopharmaceutical purposes, (ANEXO II de la presente memoria)

hecho más notable a medida que la incorporación de GM en las microestructuras era mayor o, en su caso, que el DD del CS era menor. Esta evolución en las características morfológicas de las partículas puede verse claramente reflejada en las **Figuras 2** y **3**.

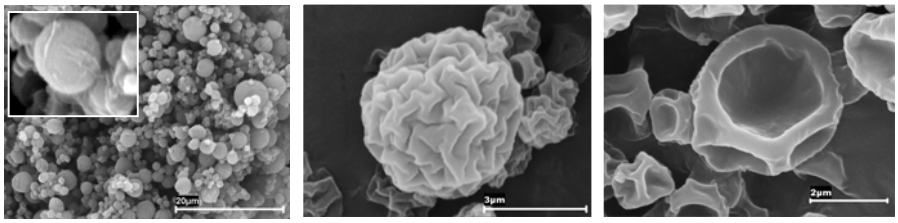

Figura 2. Fotografías de microscopía electrónica de barrido de microsferas obtenidas a partir de: (a) CS comercial (DD 83%); (b) CS DD 38%; y (c) CS DD 26%.

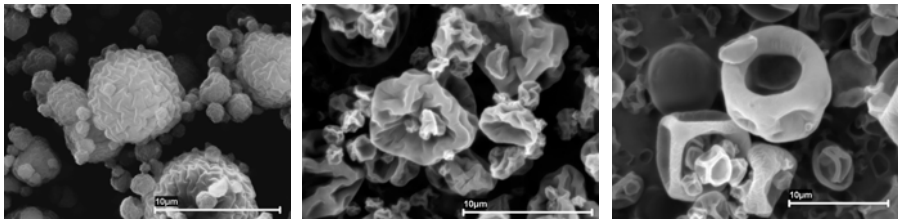

Figura 3. Fotografías de microscopía electrónica de barrido de microsferas obtenidas a partir de: (a) CS:GM (75:25) (b) CS:GM (25:75); y (c) CS:GM (0:100).

La obtención de morfologías irregulares podría estar condicionada por la consistencia de la matriz polimérica así como por la afinidad entre polímero y disolvente. Cuando durante el proceso de atomización las gotas de solución polimérica comienzan a secarse, es posible que primeramente se forme un film en la superficie que pueda dificultar la difusión del agua desde el interior al exterior, haciendo que la presión interna llegue a un punto crítico en el que la partícula se deforme o desintegre. Obviamente, esta dificultad de difusión del disolvente hacia el exterior estará condicionada por las características de ese hipotético film polimérico

superficial, tales como su flexibilidad y fuerza mecánica[4], que vienen dadas, a su vez, por su composición. Así pues, es sabido que existen materiales que tienden a formar estructuras microparticulares compactas, como ocurriría en el caso del CS, mientras otros forman partículas porosas o deformadas, tal y como acontece con el GM. Consecuentemente, las mezclas de ambos polímeros dieron lugar a estructuras con una morfología altamente dependiente del porcentaje de cada uno de sus componentes[5]. Del mismo modo, la mencionada dificultad de difusión del disolvente a través de la matriz polimérica también puede ser atribuida a una baja afinidad entre ambos[6,7]. Este hecho explicaría lo que ocurre con las microsferas preparadas con GM, dada la limitada solubilidad en agua de este polímero[8] y, asimismo, con el CS reacetilado, puesto que su solubilidad en agua disminuye a medida que lo hace su DD[9].

Interesantemente, estas características morfológicas podrían contribuir a mejorar la dispersabilidad de las partículas, dado que la rugosidad superficial hace más difícil el contacto entre las mismas y el establecimiento de fuerzas de van der Waals que favorecerían su aglomeración[10].

Teniendo en cuenta que el objetivo central de este trabajo era el de conseguir microsferas con propiedades adecuadas para su administración

[4] **Ameri M., Maa Y.–F.**, Spray drying of biopharmaceuticals: stability and process considerations, Drying Technology, 24 (2006) 763-768.

[5] **Huang Y. -C., Yeh M. -K., Chiang C. -H.**, Formulation factors in preparing BTM-chitosan microspheres by spray drying method, Int. J. Pharm., 242 (2002) 239-242.

[6] **Zhang Z.Y., Ping Q.N., Xiao B**., Microencapsulation and characterization of tramadol-resin complexes, J. Control. Rel., 66 (2000) 107-113.

[7] **Fu Y.J., Mi F.L., Wong T.B., Shyu S.S.**, Characteristics and controlled release of anticancer drug loaded poly (D,L-lactide) microparticles prepared by spray-drying technique, J. Microencapsul., 18 (2001) 733-747.

[8] **Alonso-Sande M., Teijeiro-Osorio D., Remuñán-López C., Alonso M.J.**, Glucomannan, a promissing polysaccharide for pharmaceutical and biomedical purposes, (ANEXO II de la presente memoria)

[9] **Remuñán-López C., Portero A., Lemos M., Vila-Jato J.L., Núñez M.J., Riveiro P., López J.M., Piso M., Alonso M.J.**, Chitosan microspheres for the specfic delivery of amoxycillin to the gastric cavity, S.T.P. Pharma. Sci., 10 (2000) 69-76.

[10] **Tarara T. E, Hartman M. S., Gill H., Kennedy A. A., and Weers J. G.**, Characterization of suspension-based metered dose inhaler formulations composed of spray-dried budesonide microcrystals dispersed in HFA-134a, Pharm. Res., 21 (2004) 1607-1614.

pulmonar y depósito a nivel alveolar, se investigaron las propiedades aerodinámicas de los sistemas obtenidos. Así, se determinaron importantes parámetros como el tamaño de partícula, la densidad y el diámetro aerodinámico, los cuales se recogen en las **Tablas 1** y **2** para algunas de las formulaciones más representativas.

Tabla 1. Características aerodinámicas de las microsferas obtenidas a partir de quitosanos de distinto grado de desacetilación (media ± D.E., *n* = 3-6).

Formulación	Diámetro de Feret (μm)	Densidad real (g/cm^3)	Densidad aparente (g/cm^3)	Diámetro aerodinámico (μm)
MS DD 83%	2.04 ± 0.93	1.48 ± 0.09	0.48 ± 0.01	1.96 ± 1.53
MS DD 38%	1.93 ± 1.37	1.43 ± 0.09	0.42 ± 0.02	1.56 ± 1.49
MS DD 26%	1.85 ± 0.65	1.37 ± 0.04	0.40 ± 0.01	1.56 ± 1.45
MS DD 23%	1.79 ± 1.16	1.36 ± 0.04	0.38 ± 0.03	1.46 ± 1.45

MS: microsferas; DD: grado de desacetilación

Tabla 2. Características aerodinámicas de las microsferas obtenidas a partir de diferentes proporciones de quitosano y glucomanano (media ± D.E., *n* = 3-6).

Formulación (CS:GM)	Diámetro de Feret (μm)	Densidad real (g/cm^3)	Densidad aparente (g/cm^3)	Diámetro aerodinámico (μm)
100:0	2.15 ± 1.05	1.49 ± 0.21	0.48 ± 0.02	1.35 ± 1.44
50:50	2.21 ± 1.04	1.42 ± 0.08	0.46 ± 0.04	1.56 ± 1.50
25:75	2.69 ± 1.10	1.20 ± 0.08	0.30 ± 0.02	1.64 ± 1.46
0:100	3.19 ± 1.52	0.97 ± 0.09	0.20 ± 0.02	1.61 ± 1.54

CS: quitosano; GM: glucomanano RX-L (baja viscosidad)

En general, los tamaños de partícula obtenidos se situaron entre las 2 y 4 μm. En el caso de las microsferas compuestas por CS y GM, se registró una tendencia al incremento de tamaño a medida que la cantidad de GM en la formulación era mayor, encontrándose este hecho directamente relacionado con el

incremento en la viscosidad de la dispersión polimérica, el cual afecta el tamaño de gotícula durante la atomización[11].

Del mismo modo, las densidades (reales y aparentes) determinadas para las distintas microsferas también se hallaron altamente influenciadas por el contenido en GM de las mismas, siendo menores cuanto mayor es la cantidad de GM presente en la formulación. Este hecho podría ser explicado por los aspectos morfológicos antes mencionados, sin embargo, dado que en el caso de las microsferas de CS de diferentes DD, las mismas características morfológicas dan lugar a una disminución de la densidad de partícula menos notable, ha de existir alguna razón adicional. En este sentido, la tendencia del GM a la formación de matrices más porosas y menos compactas sería un factor añadido y determinante en la obtención de estructuras tan ligeras o poco densas[12]. Interesantemente, se ha descrito que las microsferas de baja densidad poseen una menor tendencia a la agregación que las partículas compactas[13].

En cuanto al diámetro aerodinámico, determinado mediante la utilización de un equipo Aerosizer®-Aerodisperser®, todas las formulaciones presentaron valores en el rango 1.5 - 2 μm. En base a que el diámetro aerodinámico apropiado para alcanzar las regiones más profundas del pulmón se encuentra entre 1-5 μm[14], las microsferas obtenidas pueden ser consideradas adecuadas para este propósito. Asimismo, sus previamente mencionados tamaños de partícula o diámetros de

[11] **He P., Davis S. S., Illum L.**, In vitro evaluation of the mucoadhesive properties of chitosan microspheres, Int. J. Pharm., 166 (1998) 75-68.

[12] **Wang K., He Z**., Alginate-konjac glucomannan-chitosan vedas as controlled release matrix, Int. J. Pharm., 244 (2002) 117-126.

[13] **Edwards D.A., Ben-Jebria A., Langer R**., Recent advances in pulmonary drug delivery using large, porous inhaled particles, J. Applied Physiol., 85 (1998) 379-385.

[14] **Vanbever R., Ben-Jebria A., Mintzes J. D., Langer R., Edwards D. A**., Sustained release of insulin from insoluble inhaled particles, Drug Deliv. Research, 48 (1999) 178-185.

Feret, generalmente ≥ 2 μm, harían menos factible, o cuando menos retrasarían, su captación y eliminación por los macrófagos[15].

Aunque, paralelamente, se estudiaron numerosas variables de formulación, tales como las concentraciones poliméricas de partida y diferentes tipos de GM de distinta viscosidad, de la caracterización de las microsferas resultantes no se extrajeron diferencias significativas ni, *a priori*, ventajas añadidas que pudiesen justificar seguir investigando en esa línea.

3. Asociación y liberación *in vitro* de macromoléculas terapéuticas (insulina)

El siguiente paso consistió en investigar la capacidad de las microsferas como vehículos de macromoléculas terapéuticas. Para ello se seleccionaron las formulaciones más representativas de cada estrategia (reacetilación del CS e inclusión de GM) y se atomizaron sus correspondientes soluciones poliméricas (CS:GM = 100:0, 50:50, 25:75, 0:100 y CS de DD = 83, 38 y 23%) mezcladas con una solución de la proteína terapéutica modelo (insulina en HCl, 15% p/p referido al total de polímeros). Las partículas cargadas no presentaron cambios morfológicos ni de tamaño significativos, manteniendo así su idoneidad para ser administradas por vía pulmonar.

La determinación de la asociación de la insulina a las microsferas fue realizada a 22ºC para evitar la tendencia del péptido a formar agregados a temperaturas superiores[16] y, de esta manera, poder evaluar el contenido total de insulina. En general, las eficacias de encapsulación (EE) de insulina obtenidas fueron elevadas, aproximadamente de entre el 80 y el 98%, para las microsferas compuestas por CS y GM, solo GM, o por CS reacetilado (DD 38% y DD 23%). Sin embargo, la cuantificación de insulina fue significativamente menor para aquellas formulaciones compuestas únicamente por CS de alto DD, concretamente de en

[15] **Roser M., Fisher D., Kissel T**., Surface modified biodegradable albumin nano- and microspheres. II: effect of surface charges on in vitro phagocytosis and biodistribution in rats, Eur. J. Pharm. Biopharm., 4 (1998) 255-263.

[16] **Reithmeier H., Herrman J., Göpferich A.**, Lipid microparticles as a parenteral controlled release device for peptides, 73 (2001) 339-350.

torno al 60-70%, lo que sugiere la existencia de interacciones entre el CS y la insulina que impidieron la determinación de la misma. Además, el hecho de que las EE obtenidas sean menores cuanto mayor es la proporción de CS en la composición microparticular y cuanto mayor es el DD del CS, sugiere que estas interacciones CS-insulina puedan estar mediadas principalmente por interacciones iónicas con los grupos amino libres del CS, aunque puedan coexistir otro tipo de interacciones, previamente descritas para ambas especies, tales como uniones por puentes de hidrógeno o interacciones hidrofóbicas[17].

La liberación *in vitro* de insulina a partir de las microsferas se realizó a 37ºC para mimetizar la temperatura fisiológica. Los perfiles de liberación obtenidos para las microsferas de CS-GM y para las microsferas formadas por CS de diferente DD durante la primera hora de ensayo se representan en las **Figuras 4** y **5**, respectivamente. La liberación de insulina a partir de microsferas compuestas únicamente por GM fue muy rápida, con un 82% liberado en tan solo 15 minutos. Sin embargo, las formulaciones que combinan ambos polímeros, CS y GM, experimentaron una notable ralentización en la liberación del péptido, dando lugar a valores de aproximadamente un 37% de insulina liberada a los 15 minutos y hacia el 40% a los 30 minutos.

[17] **Fernández-Urrusuno R., Calvo P., Remuñán-López C., Vila-Jato J.L., Alonso M.J.**, Enhancement of nasal absorption of insulin using chitosan nanoparticles, Pharm. Res., 16 (1999) 1576-1581.

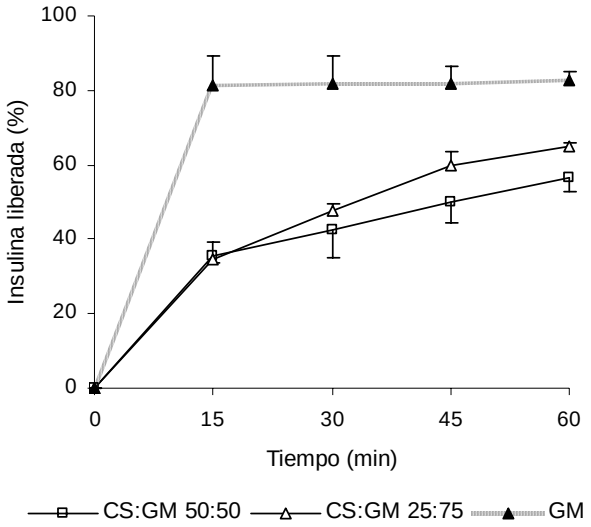

Figura 4. Perfil de liberación de insulina *in vitro* en PBS pH 7.4 a partir de microsferas de quitosano y glucomanano (*n* = 3).

La casi inmediata liberación a partir de las microsferas de GM podría venir dada por la característica morfología de las mismas, cuyas marcadas convoluciones y oquedades determinan una elevada superficie específica en contacto con el medio de liberación. Además, su estructura interna, que a juzgar por los valores de densidad obtenidos es poco compacta o porosa, también contribuiría a la rápida liberación del péptido. Sin embargo, para las microsferas compuestas por CS y GM (50:50 y 25:75), cuya morfología y valores de densidad resultaron ser bastante diferentes entre sí (ver **Figura 3** y **Tabla 2**), se obtuvieron perfiles de liberación muy similares, de manera que ha de ser la interacción entre ambos polímeros, previamente demostrada por IR, la responsable de este fenómeno.

En cuanto a las partículas compuestas por CS de distinto DD, la tendencia observada fue la de una liberación algo más rápida cuanto menor era el DD del CS. Concretamente, a los 15 minutos se liberó en torno a un 45% de insulina para las microsferas de CS DD 83%, un 50% para las de DD 38% y un 60% para las de DD

23%. Las diferencias a los 15 minutos resultaron ser significativas solamente en este último caso, aunque a los 30 y 45 minutos lo fueron para ambos CS reacetilados.

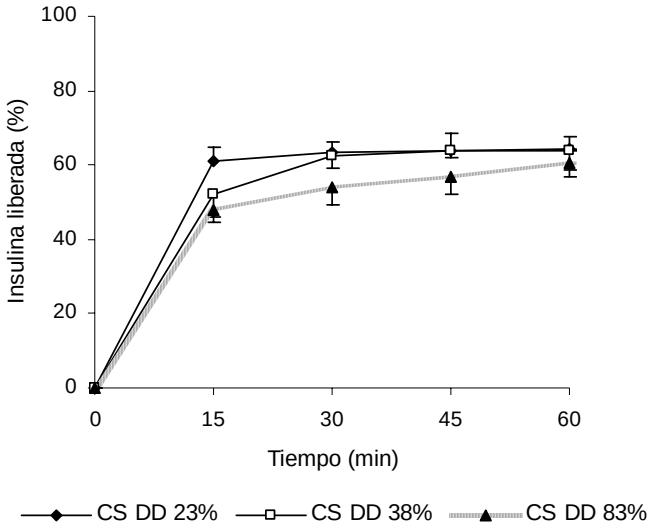

Figura 5. Perfil de liberación de insulina *in vitro* en PBS pH 7.4 a partir de microsferas de quitosano de distintos grados de deacetilación (*n* = 3-6).

Este hecho, una vez más, podría ser explicado por una morfología más irregular y, por tanto, con valores de superficie específica en contacto con el medio más elevados, así como con valores de densidad algo menores a medida que disminuye el grado de desacetilación (ver **Figura 2** y **Tabla 1**). Así, el hecho de que el CS reacetilado sea menos soluble es contrarrestado por la influencia de la morfología de las partículas.

Sin embargo, en general, cabría esperar un comportamiento diferente de las partículas una vez administradas en forma de polvo seco por vía pulmonar, donde el fluido existente en el pulmón (obviamente más escaso que el medio de liberación *in vitro*) simplemente humectaría las microsferas, favoreciendo una liberación del péptido más lenta.

4. Estudios de mucoadhesión

Es sabido que la acetilación de los grupos amino libres del CS reduce la carga positiva del polímero y afecta, de este modo, a características como la mucoadhesión[18,19], la cual está mediada principalmente por la interacción electrostática con los grupos cargados negativamente presentes en el mucus. Por otro lado, la incorporación de GM, un polisacárido para el que no se han descrito propiedades mucoadhesivas, también podría *a priori* repercutir en las características de las microsferas resultantes.

Así pues, se llevó a cabo un primer estudio que consistió en medir el grado de interacción de las soluciones poliméricas y la mucina mediante turbidimetría[20]. En dichos ensayos se confirmó, como era esperado, que el GM no posee capacidad mucoadhesiva alguna. Sin embargo, curiosa e interesantemente, las mezclas poliméricas de CS y GM vieron potenciado el grado de mucoadhesión observado para el CS solo, pudiendo concluir la existencia de un efecto sinérgico entre CS y GM (**Art. 2, Fig. 3**). En relación a los resultados obtenidos con el CS de diferentes DD en líneas generales, y como era de esperar, la interacción del CS con la mucina se vio disminuida a medida que el grado de acetilación de los grupos amino del CS era mayor, pero manteniéndose en un rango de valores de mucoadhesión positivos (**Art. 1, Fig. 3**).

Además, mediante la breve incubación de las microsferas de CS y CS:GM con una solución de mucina y la observación de las mismas, completamente recubiertas de mucina, por microscopía electrónica de barrido, pudo nuevamente comprobarse de un modo cualitativo el alto grado de mucoadhesión de las partículas[21] (**Figura 5**).

---

[18] **Tomihata K., Ikada Y**., In vitro and in vivo degradation of films of chitin and its deacetylated derivatives, Biomaterials, 18 (1997) 567-575.

[19] **Mima S., Miya M., Iwamoto R. and Yoshikawa S.**, Highly deacetylated chitosan and its properties, J. Appl. Polym. Sci., 28 (1983) 1909-1917.

[20] **He P., Davis S.S., Illum L.**, In vitro evaluation of the mucoadhesive properties of microspheres, Int. J. Pharm., 166 (1998) 75-68.

[21] **Genta I., Pavanetto F., Conti B., Giunchedi P., Conte U**., Improvement of dexamethasone dissolution rate from spray-dried chitosan microspheres, S. T. P. Pharma Sci., 5 (1995) 202-207.

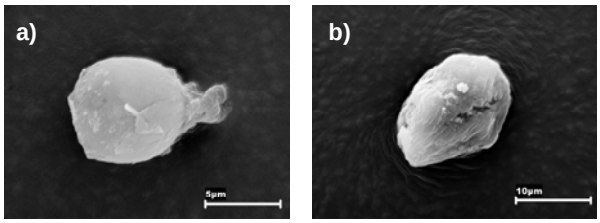

Figura 5. Imágenes de microscopía electrónica de barrido de microsferas de: (a) CS y (b) CS:GM (50:50) recubiertas de mucina.

5. Estudios en cultivos celulares

Puesto que las microsferas desarrolladas, al no estar reticuladas, no se mantienen en suspensión, no fue posible la realización de diluciones seriadas que permitiesen trabajar con pequeñas concentraciones, como las comúnmente empleadas en estudios en cultivos celulares. Asimismo, los dispositivos de administración de polvo seco tampoco permiten la emisión de dosis tan reducidas de una manera reproducible y homogénea. Obviamente, este hecho limitó el número de estudios que se pudieron hacer con las microsferas como tales, reduciéndose a ensayos de carácter cualitativo. Así pues, los estudios en células fueron llevados a cabo, principalmente, utilizando las soluciones poliméricas correspondientes a la composición de los sistemas, intentando extrapolar y extraer conclusiones, en la medida de lo posible, a partir estos resultados. Adicionalmente, en el **Artículo 3**, además de soluciones poliméricas también se evaluaron, a modo comparativo, nanopartículas de CS. Sin embargo, dado que se trata de un experimento añadido en el que no se debe centrar el interés de la presente discusión, será obviado y referido, si procede, en la segunda parte de la memoria experimental, dedicada específicamente a la investigación de sistemas de tipo nanoparticular.

Para los estudios en células se utilizaron dos líneas diferentes, una de ellas modelo del epitelio bucal (células TR146) y la otra del epitelio respiratorio (células Calu-3). Ambos modelos difieren, fundamentalmente, en que las células TR146 crecen formando una estructura pseudoestratificada y no presentan uniones "tight" intercelulares ni mucus[22], mientras la Calu-3 forman una monocapa con presencia de uniones intercelulares íntimas y mucus en su parte apical[23] (**Art. 3, Tabla 1**). Los estudios de citotoxicidad se realizaron en células en proliferación, dado que este estado de crecimiento exponencial de las células permite el ensayo de una batería de concentraciones y formulaciones más amplia. Sin embargo, para el resto de estudios se utilizaron células completamente diferenciadas, puesto que es en este estado cuando constituyen una verdadera barrera biológica modelo.

5.1. Citotoxicidad

Sin duda, un importante aspecto a tener en cuenta es el relativo a la toxicidad de los polímeros utilizados en la preparación de las microsferas, GM y CS. Por ello, se evaluó la toxicidad del GM y el CS de diferente DD en los dos cultivos celulares previamente mencionados (**Art. 2** y **Art. 3**). Los resultados obtenidos en ambas líneas celulares fueron similares por lo que, de modo representativo, se muestran en la **Figura 6** aquellos relativos a algunas de las concentraciones de CS y GM ensayadas en las células Calu-3.

La viabilidad celular obtenida tras la incubación de las células con el GM se mantuvo en torno a un 90-100% incluso para la concentración de 1 mg/mL, la cual se correspondería con una dosis de polímero de 303 $\mu g/cm^2$. Pero incluso para concentraciones 2 veces mayores, la viabilidad resultó ser muy alta, concretamente de un 82% (**Art. 2, Fig. 2**). Cabe decir que, aunque el GM se ha considerado como un polisacárido no tóxico debido a su utilización como complemento dietético en los países asiáticos, y existen estudios de toxicidad aguda, sub-aguda y sub-crónica

[22] **Jacobsen J., van Deurs B., Pederssen M., Rassing M.R.**, TR146 cells grown on filters as a model for human buccal epithelium. I. Morphology, growth, barrier properties and permeability, Int. J. Pharm., 125 (1995) 165-184.

[23] **Foster K.A., Avery M.L., Yazdanian M., Audus K.L.**, Characterization of the Calu-3 cell line as a tool to screen pulmonary drug delivery, Int. J. Pharm., 208 (2000) 1-11.

que corroboran su inocuidad por vía oral[24], su efecto a nivel de otras superficies mucosas del organismo no habían sido hasta ahora investigados.

Con respecto al CS, es especialmente destacable la gran influencia del DD sobre su perfil de toxicidad. Así, una concentración de polímero de 1 mg/mL (303 $\mu g/cm^2$) dio lugar a una viabilidad celular de tan solo el 20% cuando se trató de CS comercial (DD = 83%) y de entre un 90 y un 100% cuando se trató de polímero reacetilado (DD = 38 y 47%). Además, al igual que con el GM, una dosis de polímero reacetilado incluso dos veces mayor (606 $\mu g/cm^2$) mantuvo la viabilidad celular en un porcentaje superior al 90%. En este sentido, diversos estudios han dejado patente la gran influencia de la densidad de carga positiva del CS sobre su perfil de toxicidad y biodegradabilidad[25,26,27]. Esta relación directa entre carga positiva y toxicidad ha sido también descrita para otros polímeros de naturaleza catiónica, tales como la poli-L-lisina, la poli-L-arginina y la protamina[28,29].

[24] **Alonso-Sande M., Teijeiro-Osorio D., Remuñán-López C., Alonso M.J.**, Glucomannan, a promissing polysaccharide for pharmaceutical and biomedical purposes, (ANEXO II de la presente memoria)

[25] **Schipper N.G.M., Varum K.M., Artursson P.**, Chitosans as absorption enhancers for poorly water absorbable drugs. I. Influence of molecular weight and degree of acetylation on drug transport across human intestinal epithelial (Caco-2) cells, Pharm. Res., 13 (1996) 1686-1692.

[26] **Tomihata K., Ikada Y.**, In vitro and in vivo degradation of films of chitin and its deacetylated derivatives, Biomaterials, 18 (1997) 567-575.

[27] **Zhang H., Neau S.H.**, In vitro degradation of chitosan by a commercial enzyme preparation: effect of molecular weight and degree of deacetylation, Biomaterials, 22 (2001) 1653-1658.

[28] **Chang S.W., Westcott J.Y., Henson J.E., Voelkel N.F.**, Pulmonary vascular injury by polycations in perfused rat lungs, J. Appl. Physiol., 62 (1987) 1932-1943.

[29] **Ekrami H.M., Shen W.C.**, Carbamylation decreases the cytotoxicity but not the drug-carrier properties of polylysines, J. Drug Target., 2 (1995) 469-475.

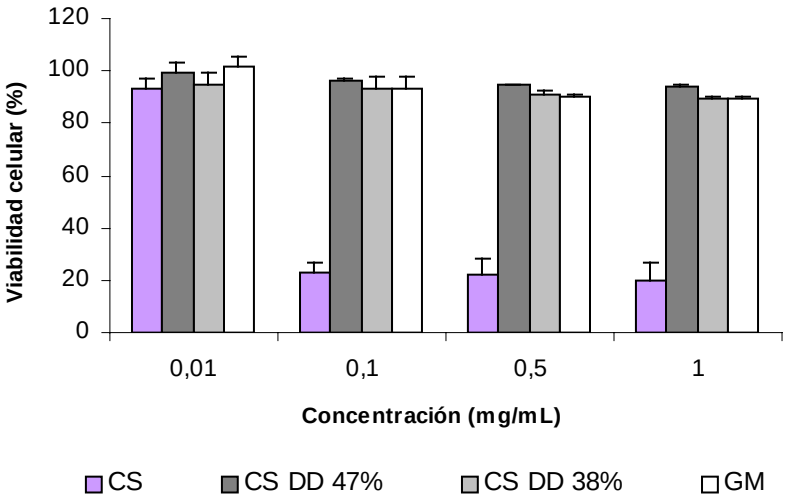

Figura 6. Viabilidad celular obtenida en células Calu-3 para diferentes concentraciones de quitosano de distintos grados de desacetilación y glucomanano (*n* = 3-4).

Así pues, cabe esperar que los sistemas microparticulares compuestos por CS reacetilado o, al menos parcialmente, por GM, presenten un muy buen perfil de biocompatibilidad y no toxicidad.

5.2. Efecto promotor de la absorción de macromoléculas

Como ya se señaló en la Introducción, son numerosos los trabajos que demuestran la capacidad del CS para promover la absorción de macromoléculas a través de distintos epitelios[30,31,32,33], principalmente mediante la apertura reversible

[30] **Portero A., Remuñán-López C., Nielsen H.M.,** The potential of chitosan in enhancing peptide and protein absorption across the TR146 cell culture model- an in vitro model of buccal epithelium, Pharm. Res., 19 (2002) 169-174.

[31]**Aspden T.J., Illum L., Skaugrud, O.,** Chitosan as a nasal delivery system: evaluation of the absorption enhancement and effect on nasal membrane integrity using rats models, Eur. J. Pharm. Sci., 22 (1996) 23-31.

[32]**Artursson P., Lindmark T., Davis S.S., Illum L.**, Effect of chitosan on permeability of monolayers of intestinal epithelial cells (Caco-2), Pharm. Res., 11 (1994) 1358-1361.

[33] **Florea B.I., Thanou M., Junginger H.E., Borchard G.**, Enhancement of bronchial octreotide absorption by chitosan and N-trimethyl chitosan shows linear in vitro/in vivo correlation, J. Control. Rel., 110 (2006) 353-361.

de las uniones "tight" intercelulares[34,35]. En esta línea, el objetivo de este estudio ha sido evaluar la capacidad del CS de potenciar la permeabilidad de las mucosa bucal y traqueobronquial frente a macromoléculas hidrofílicas de diferente peso molecular y relacionar, asimismo, dicha capacidad con el DD del CS y con efectos que puedan estar asociados, tales como el descenso de la resistencia transepitelial (TEER) y la viabilidad celular. Para ello se utilizaron dextranos marcados con isotiocianato de fluoresceína (FD) de distintos pesos moleculares (4, 20 y 40 KDa), como modelos de macromoléculas hidrofílicas, y ^{3}H-manitol, como marcador de bajo peso molecular del paso paracelular o, lo que es lo mismo, como marcador de la integridad de membrana (**Art. 2**).

En líneas generales, el CS de alto DD (83%) fue capaz de promover la absorción de todos las FD a través de ambos modelos epiteliales, bucal y traqueobronquial. Curiosamente, y en consonancia con estudios previos[31], la concentración de CS más efectiva en las células TR146 fue la más baja de las ensayadas (0.015 mg/mL). No así en las células Calu-3, donde se obtuvieron mejores resultados con la dosis más alta (1 mg/mL) (**Art. 3, Tablas 5, 6 y 7**).

Por otro lado, el CS de DD 47% consiguió aumentar significativamente la permeabilidad de los FD de hasta 20 KDa a través de las células TR146 pero no en las Calu-3; mientras el CS de DD 38% solo produjo pequeños incrementos que no resultaron ser significativos en ninguno de los epitelios.

Así pues, una primera observación ha de dirigirse a las diferencias obtenidas entre ambas líneas celulares, TR146 y Calu-3. Obviamente, la existencia de uniones "tight" entre las células Calu-3 ya supone, de por sí, una mayor barrera a la absorción, hecho que se refleja en la magnitud de las permeabilidades obtenidas, en ausencia de promotores de la absorción, para el ^{3}H-manitol, marcador de la

[34] **Dodane V., Khan M.A., Merwin J.R.**, Effect of chitosan on epithelial permeability and structure, Int. J. Pharm., 182 (1999) 21-32.

[35] **Smith J., Wood E., Dornish M.,** Effect of chitosan on epithelial cell tight junctions, Pharm. Res., 21 (2004) 43-49.

integridad celular. Pero además, cabe resaltar que la presencia de abundante mucus en la parte apical de las células Calu-3 supone una importante barrera adicional. En este sentido, las Calu-3 utilizadas en el presente trabajo presentaron una secreción de mucus particularmente abundante, evidenciada por la simple observación macroscópica del epitelio. La influencia de este "exceso" de mucus fue demostrada mediante la realización de un experimento control, en el que se retiró cuidadosamente parte del mismo antes de la incubación con las muestras, las cuales, de este modo, sí resultaron ser eficaces en la promoción de la absorción de la molécula modelo y, además, a dosis no tóxicas (**Art. 3, Fig. 5**).

En general, el aumento significativo de la permeabilidad de las macromoléculas modelo como consecuencia del tratamiento con las soluciones de CS se reflejó en un fuerte descenso de la TEER en ambas líneas celulares, lo que puede indicar la apertura de uniones "tight" en las células Calu-3 y una posible relajación de la adhesión célula-célula en el caso de las TR146 (**Art. 3, Figs. 3 y 6**). Sin embargo, este marcado descenso en la TEER no estuvo necesariamente asociado con la producción de daño celular. Así, por ejemplo, la concentración de polímero que resultó ser más efectiva en las células TR146 se relacionó con una elevada viabilidad celular (>83%). No así en las células Calu-3, en donde, debido al exceso de mucosidad ya mencionado, para conseguir un efecto promotor significativo hizo falta una mayor concentración de polímero de elevado DD que sí ocasionó una disminución de la viabilidad celular.

Así pues, como cabía esperar en base a la bibliografía[36], la capacidad del CS de aumentar el paso celular de las macromoléculas de distinto peso molecular a través de los epitelios modelo estuvo altamente influenciada por su densidad de carga positiva, al igual que ocurre con sus propiedades mucoadhesivas y su perfil de toxicidad. De este modo, queda patente la importancia de alcanzar un

[36] **Schipper N.G.M., Varum K.M., Artursson P.**, Chitosans as absorption enhancers for poorly water absorbable drugs. I. Influence of molecular weight and degree of acetylation on drug transport across human intestinal epithelial (Caco-2) cells, *Pharm. Res*., 13 (1996) 1686-1692.

compromiso entre los distintos parámetros de mucoadhesión, efecto promotor y toxicidad-biodegradabilidad, a través de la selección del DD adecuado.

5.3. Interacción/bioadhesión

Por último, se utilizaron células Calu-3 diferenciadas para estudiar la capacidad de las microsferas de CS y CS-GM de interaccionar con el mucus y permanecer adheridas al epitelio. Para ello se prepararon microsferas conteniendo albúmina bovina marcada con isotiocianato de fluoresceína (FITC-BSA). Las partículas fueron administradas sobre el epitelio mediante la conveniente adaptación de un dispositivo insuflador de polvo seco (PennCentury™ DP-4), comúnmente utilizado para la administración pulmonar a animales de experimentación[37,38]. La emisión de las microsferas desde el dispositivo resultó ser muy satisfactoria y el polvo se dispersó fácilmente para depositarse sobre las células. Tras la incubación y lavado del epitelio, las microsferas permanecieron adheridas sobre la superficie sin ser, como era esperado, internalizadas, tal y como se muestra en la **Figura 7**. Es en la superficie celular donde se espera que los sistemas desarrollados se adhieran y liberen la macromolécula terapéutica asociada, promoviendo, a su vez, su absorción.

[37] **Surendrakumar K., Martín G.P., Hodgers E.C.M., Jansen M., Blair J.A.**, Sustained release of insulin from sodium hyaluronate based dry powder formulations after pulmonary delivery to beagle dogs, J. Control. Rel., 91 (2003).

[38] **Grainger C.I., Alcock R., Gard T.G., Quirk A.V., van Amerongen G., de Swart R.L., Hardy J.G.**, Administration of an insulin powder to the lungs of cynomolgus monkeys using a Penn Cantury insufflator, Int. J. Pharm., 269 (2004) 523-527.

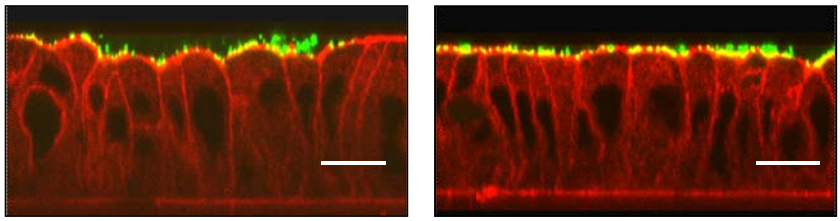

Figura 7. Imágenes de microscopía confocal de la monocapa de células Calu-3 tras la incubación con microsferas de: (a) CS (b) CS:GM (50:50) conteniendo FITC-BSA. La escala se corresponde con un valor de 20μm.

PARTE II: Antecedentes, hipótesis y objetivos

PARTE II

ANTECEDENTES

1. Las nanopartículas de quitosano presentan una gran versatilidad como vehículos de macromoléculas terapéuticas, permitiendo una eficaz encapsulación y liberación de las mismas en su forma activa[1].

2. Tras su administración por vía nasal, las nanopartículas de quitosano han permitido mejorar significativamente la absorción sistémica de insulina[2] y, además, bien sea a través de la encapsulación de proteínas antigénicas[3] o ADN plasmídico codificador de las mismas[4], han permitido generar respuestas inmunes adecuadas.

3. Algunas ciclodextrinas han demostrado una gran eficacia como promotoras de la absorción de macromoléculas, tales como la insulina o la calcitonina, a través de distintos epitelios como el nasal[5,6] y el pulmonar[7,8], e incluso se ha descrito su capacidad para desactivar ciertos enzimas proteolíticos[9].

---

[1] **Janes K.A., Calvo P., Alonso M.J.**, Polysaccharide colloidal particles as delivery systems for macromolecules, Adv. Drug Deliv. Rev., 47 (2001) 83-97.

[2] **Fernández-Urrusuno R., Calvo P., Remuñán-López C., Vila-Jato J.L., Alonso M.J.**, Enhancement of nasal absorption of insulin using chitosan nanoparticles, Pharm. Res., 16 (1999) 1576-1581.

[3] **Vila A., Sánchez A., Janes K., Behrens I., Kissel T., Vila-Jato J.L., Alonso M.J.**, Low molecular weight chitosan nanoparticles as new carriers for nasal vaccine delivery in mice, Eur. J. Pharm. Biopharm., 57 (2004) 123-131.

[4] **Csaba N., Koping-Hoggard M., Fernández-Megía E., Novoa-Carballal R., Riguera R., Alonso M.J.**, Ionically Crosslinked chitosan nanoparticles as gene delivery systems: effect of PEGylation on in vitro and in vivo gene transfer, *submitted*

[5] **Merkus F.W., Verhoef J.C., Marttin E., Romeijn S.G., van der Kuy P.H.M., Hermens W.A.J.J., Schipper N.G.M.**, Cyclodextrins in nasal drug delivery, Adv. Drug Deliv. Rev., 36 (1999) 41-57.

[6] **Yu S., Zhao Y., Wu F., Zhang X., Lü W., Zhang H., Zhang Q.**, Nasal insulin delivery in the chitosan solution : in vitro and in vivo studies, Int. J. Pharm., 281 (2004) 11-23.

[7] **Kobayashi S., Kondo S., Juni K.**, Pulmonary delivery of salmon calcitonin dry powders containing absoption enhancers in rats, Pharm. Res., 13 (1996) 80-83.

4. Recientemente, se ha propuesto un nuevo sistema nanoparticular compuesto por quitosano y ciclodextrinas que resulta adecuado tanto para la encapsulación y liberación de principios activos hidrofóbicos[10] como de macromoléculas hidrofílicas[11], no habiendo sido hasta el momento investigado su potencial *in vivo*.

HIPÓTESIS

1. Dada la capacidad las ciclodextrinas de incrementar la permeabilidad epitelial, bien mediante la apertura de uniones "tight" o bien por acción directa sobre las membranas celulares, las nanopartículas de quitosano y ciclodextrina podrán, al igual que aquéllas compuestas únicamente por quitosano, promover la absorción de macromoléculas (péptidos, proteínas, ADN) y actuar como eficientes vehículos de las mismas.

2. Las interesantes propiedades de las ciclodextrinas acompañadas de su bien conocido perfil de seguridad contribuirán a la obtención de sistemas que, presentando una significativamente menor toxicidad, no vean sin embargo disminuida su eficacia.

[8] **Hussain A., Yang T., Zaghloul A.A., Ahsan F.**, Pulmonary absorption of insulin mediated by tetradecyl-beta-maltoside and dimethyl-beta-cyclodextrin, Pharm. Res., 20 (2003) 1551-1557.

[9] **Matsubara M., Ando Y., Irie T., Uekama K.**, Protection afforded by maltosyl-β-cyclodextrin against α-chymotrypsin-catalyzed hydrolysis of a luteinizing-releasing hormone agonist, bserelin acetate, Pharm. Res., 14 (1997) 1401-1405.

[10] **Maestrelli F., García-Fuentes M., Mura P., Alonso M.J.**, A new drug nanocarrier consisting of chitosan and hydroxypropylcyclodextrin, Eur. J. Pharm. Biopharm., 63 (2006) 79-86.

[11] **Krauland A.H., Alonso M.J**., Chitosan/cyclodextrin nanoparticles as macromolecular drug delivery system, Int. J. Pharm., *in press.*

OBJETIVOS

Teniendo en cuenta los antecedentes e hipótesis expuestos, el objetivo de la segunda parte de esta memoria experimental se ha dirigido al desarrollo de sistemas nanoparticulares, compuestos por quitosano y distintos derivados de ciclodextrina, destinados a la administración nasal de macromoléculas, tales como proteínas y ADN plasmídico. Desde un punto de vista práctico, el trabajo experimental llevado a cabo para alcanzar este objetivo se ha recogido en los apartados que se detallan a continuación:

1. Preparación y caracterización de nanopartículas de quitosano y ciclodextrina. Evaluación de su capacidad promotora de la absorción de insulina a través del epitelio nasal: estudios *in vitro* e *in vivo*.

   Los resultados han sido recogidos en el **Artículo 4**: ""A new generation of hybrid polysaccharide nanoparticles as carriers for the nasal delivery of macromolecules".

2. Asociación de ADN plasmídico a nanopartículas de quitosano y ciclodextrina. Evaluación de su capacidad transportadora de material genético *in vitro* (cultivo celular modelo del epitelio nasal/traqueobronquial).

   Los resultados han sido recogidos en el **Artículo 5**: "Chitosan/cyclodextrin nanoparticles can efficiently transfect the airway epithelium".

PARTE II: Trabajo experimental

ARTÍCULO 4

A New Generation of Hybrid Polysaccharide Nanoparticles as Carriers for the Nasal Delivery of Macromolecules

---

Desirée Teijeiro-Osorio, Carmen Remuñán-López y María José Alonso

Abstract

We have recently reported a new generation of polysaccharide nanoparticles consisting of chitosan (CS) and cyclodextrin (CD) derivatives, which exhibit a number of advantages as compared to the classical CS nanoparticles. In the present work our goal was to explore the potential of these hybrid CS/CD nanoparticles as carriers for the nasal delivery of macromolecules. First, we evaluated the effect of the amount and type of CD (sulfobutylether-β-CD or carboximethyl-β-CD), on the physicochemical properties of the nanocarriers. Second, we investigated the interaction of CS/CD nanoparticles with the nasal epithelium by studying their ability to modulate the tight junctions between epithelial cells (Calu-3 cell model) as well as their capacity to overcome mucosal barriers (nasal epithelium of rats). Finally, we loaded some selected nanocarriers with insulin and studied their potential for enhancing the nasal transport of insulin in rabbits. The results showed that CS/CD nanoparticles caused a reversible reduction in the transepithelial resistance of the cell monolayer, thus increasing the membrane permeability. Moreover, the results obtained following the in vivo administration of fluorescent CS/CD nanoparticles to rats, evidenced their capability to overcome the nasal mucosal barrier. Finally, the in vivo evaluation in concious rabbits revealed that insulin-loaded nanoparticles (association efficiencies >88%) were able to significantly decrease plasma glucose levels (more than 35% reduction). Overall, these results suggest that these new nanoparticles work as nasal carriers and, therefore, have a potential for enhancing the transport of complex molecules across the nasal barrier.

Key words: absorption enhancement, chitosan, cyclodextrins, insulin, nanoparticles, nasal delivery.

1. INTRODUCTION

Recent advances in biotechnology have resulted in the availability of a large number of newly designed therapeutic and antigenic molecules (peptides, proteins, plasmid DNA), which are generally characterized by a low permeability through biological membranes and an insufficient stability in the biological environment. Over the last decades, significant efforts have been dedicated to extensively explore new routes, alternative to the parenteral, for the administration of these macromolecules (Kopping-Hoggard et al., 2001; Prego et al., 2005; Csaba et al., 2006). Among them, the nasal mucosa is an attractive site for drug delivery, because it is easily accessible, extensively vascularised and avoids hepatic first pass metabolism (Arora et al., 2002). However, despite these advantages, there are still major barriers which limit the nasal absorption of macromolecules i.e. the poor permeability of the nasal mucosa and the mucociliary clearance mechanism. Among the approaches aimed to overcome these barriers, the use of bioadhesive nanoparticulate carriers represents a challenging but promising strategy, since they are able to: (1) increase the residence time of the formulation in the nasal cavity, (2) facilitate the transport of the associated drug through the mucosal epithelium, and (3) provide protection to the encapsulated molecules against degradation. Particular interest for generation of these nanocarriers has received the polysaccharide chitosan (CS), which, besides of excellent biological properties (mucoadhesion, biodegradability and low toxicity), has demonstrated to enhance the absorption of peptides and proteins across mucosal barriers (van der Lubben, 2001). These penetration-enhancing properties were initially attributed to the transient widening of the junctions between epithelial cells (Artursson et al., 1994; Schipper et al., 1997) and, subsequently, were also related to reversible effects on the intracellular pathways (Dodane et al., 1999).

The ability of CS nanoparticles to facilitate the nasal transport of macromolecules has been clearly shown using insulin as peptide model. More specifically, the plasma glucose levels following intranasal instillation of insulin-loaded CS nanoparticles to rabbits were significantly lower than those corresponding to the same dose of CS solutions (Fernández-Urrusuno et al., 1999a,b). A step forward on

the evidence of the potential of CS nanoparticles as nasal carriers for macromolecules was done using tetanus toxoid as a model antigen. CS nanoparticles were able to elicit high and long-lasting mucosal and humoral immune responses following nasal administration to conscious mice (Vila et al., 2004).

Among many others absorption promoters investigated to overcome the above mentioned mucosal barriers, cyclodextrins (CDs) are especially attractive since they present well-researched pharmaceutical and toxicological profiles. CDs are cyclic oligosaccharides with lipophilic inner cavities and hydrophilic outer surfaces containing six (α), seven (β) or eight (γ) D-(+) glucopyranose units attached by α-(1, 4) glucosidic bonds (Challa et al., 2005). As a result of their molecular structure and shape, CDs possess a unique ability to act as molecular containers by entrapping guest molecules in their internal cavity. The resulting inclusion complexes offer several potential advantages in pharmaceutical formulations, such as protection of drugs from physical, chemical and enzymatic degradation, increase of drug solubility, minimization of irritation effects and modulation of drug release (Loftsson and Brewster, 1996; Uekama et al., 1998). Although macromolecular drugs are usually too hydrophilic and bulky to be wholly included in the CD cavity, they can partially be complexed by CDs by interaction with their hydrophobic side chains (Irie and Uekama, 1999). Even if only partially included, the stability of macromolecular drugs can be significantly improved (Dotsikas and Loukas, 2002). Additionally, CDs are known to enhance the nasal absorption of different peptides and proteins, such as calcitonin and insulin (Merkus et al., 1999; Yu et al., 2004), as well as deactivate certain proteolytic enzymes (Matsubara et al., 1997).

Here we propose a new generation of polysaccharide hybrid nanocarriers for the nasal delivery of macromolecules. This new generation, whose principle of formation was recently reported by our group (Maestrelli et al., 2006; Krauland and Alonso, 2007), combines the favourable properties of CDs together with the advantages of CS nanoparticles in a unique drug delivery system.

Bearing all this in mind, in the present work, we first studied the effect of type and amount of CD (sulfobutylether-β-CD and carboximethyl-β-CD) on the

physicochemical properties of the resulting nanoparticles. Secondly, we investigated the interaction of CS/CD nanoparticles with the nasal epithelium in terms of their ability to modulate the tight junctions between epithelial cells and also their capacity to enter the nasal epithelium. Finally, as a conclusive proof-of-concept, we evaluated the efficacy of these nanocarriers for the transport of complex molecules, i.e. insulin, in rabbits.

2. MATERIALS AND METHODS

2.1. Materials

Ultrapure chitosan (CS) hydrochloride salt (Protasan UP CL 113, having a molecular weight of 110 KDa and deacetylation degree = 86%) was purchased from FMC Biopolymers (Norway). Cyclodextrin (CD) anionic derivatives, sulfobutylether-β-CD (SBE-β-CD or Captisol, substitution degree = 7.0) and carboximethyl-β-CD (CM-β-CD, substitution degree = 3.0-3.5) were purchased from Cydex Inc. (USA) and Fluka Biochem. (France), respectively. Eagle´s Minimum Essential Medium (MEM) was purchased from ATCC (USA). Foetal Bovine Serum (FBS), penicillin/streptomycin (100 µg/mL), fluorescein sodium salt, phosphotungstic acid, insulin (from bovine pancreas), trifluoroacetic acid (HPLC grade) and pentasodium tripolyphosphate (TPP) were all obtained from Sigma Chemical Co. (USA). Acetonitril of HPLC grade was purchased from J.T. Baker. Phosphate-buffered saline (PBS), Hanks' balanced salt solution (HBSS) 1x and 10x were purchased from Gibco™ (UK). 12-well tissue culture plates with cell culture inserts (0.9 cm^2, 0.4μm pore size, Becton Dickinson Labware, USA). Ultrapure water (MilliQ Plus, Millipore Iberica, Spain) was used throughout. All other solvents and chemicals were of the highest grade commercially available.

Male Sprague-Dawley rats (225-250 g) and Male New Zealand albino rabbits (2-3 kg) were used in the *in vivo* studies. The animals were allowed access to food and water *ad libitum* (rabbits fasted 16 h before the experiments).

2.2. Fluorescein labelling of chitosan (Fl-CS)

CS was labelled with fluorescein, following a slightly modified method described by De Campos et al. (De Campos et al., 2004). The covalent attachment of fluorescein to CS was achieved by the formation of amide bonds between primary amino groups of the polymer and the carboxylic acid groups of fluorescein. Briefly, 250 mg of CS were dissolved in 25 mL of water and an amount of 10 mg of fluorescein was dissolved in 1 mL of ethanol. Thereafter, both solutions were mixed together and, to catalyse the formation of amide bonds, EDAC (1-ethyl-3-(3-dimethylaminopropyl) carbodiimide hydrochloride) was added in a final concentration of 0.05 M. The reaction mixture was incubated under permanent magnetic stirring for 12 h in the dark at room temperature. The resulting conjugate was isolated by exhaustive dialysis (cellulose dialysis tubing, pore size 12,400 Da; Sigma-Aldrich, Spain) against demineralised water and then freeze-dried.

2.3. Preparation of chitosan/cyclodextrin nanoparticles

Nanoparticles were spontaneously obtained by ionotropic gelification using a previously developed method (Calvo et al., 1997) which was slightly modified to allow the incorporation of CD (Krauland and Alonso, 2007). Two aqueous phases consisting of: 1) the CS solution (CS or Fl-CS), and 2) the cyclodextrin solution (SBE-β-CD or CM-β-CD) with/without the crosslinker TPP, were mixed under magnetic stirring and maintained under agitation for 10 minutes to be sure about the complete formation of the nanosystem. The CS, and Fl-CS solutions were prepared at a concentration of 2 mg/mL, and the volume employed was fixed at 3 mL. On the other hand, in order to modulate the mass ratio of the components that constituted the nanoparticles (CS/CD/TPP), the corresponding volumes of the CD aqueous solution (SBE-β-CD or CM-β-CD, 6-12 mg/mL) and TPP solution (1.5 mg/mL) were

mixed at a final volume of 1 mL. For the association of insulin to the selected nanoparticle systems, insulin was directly dissolved in the CD/TPP phase in a concentration of 2.4 mg/mL.

Nanoparticles were isolated by centrifugation on a glycerol bed (16000 g, 30 min; Beckman Avanti™ 30, USA) and afterwards resuspended in water. For nanoparticles containing insulin, supernatants were collected before resuspension of the pellet for determination of the amount of unbound insulin.

The production yield of the nanoparticles was obtained by centrifuging fixed volumes of the nanoparticle suspensions (16000 x *g*, 30 min, Beckman Avanti™ 30, USA) without glycerol bed. The supernatants were discarded and the pellets freeze-dried (Labconco Freeze Dry System, USA). The production yield was calculated comparing the actual weight with the theoretical weight of the nanoparticles.

2.4. Characterization of nanoparticles

2.4.1. Size, zeta potential and morphology

The mean particle size and the size distribution of the nanoparticles were determined by Photon Correlation Spectroscopy (PCS). The zeta potential values of the nanoparticles were obtained by Laser Doppler Anemometry (LDA), measuring the mean electrophoretic mobility. The PCS and LDA analysis were performed with a Zetasizer® 3000 HS (Malvern Instruments, UK). Each batch was analysed in triplicate.

The morphological examination of the nanoparticles was performed by transmission electron microscopy (TEM) (CM12 Philips, Eindhoven, Netherlands). The samples were stained with 2% w/v phosphotungstic acid, immobilised on copper grids with Formvar® and dried overnight for viewing by TEM.

2.4.2. Elemental analysis

For Elemental analysis nanoparticles were prepared as described above, but omitting glycerol during centrifugation, and finally freeze-dried (Labconco Freeze Dry System, USA). Samples of pure CS, pure CD (SBE-β-CD and CM-β-CD) and freeze-dried nanoparticles were analysed by Elemental Analyzer Fisons (model EA 1108, Thermo Finnigan, Italy) for their content of carbon (C), hydrogen (H), nitrogen (N) and sulfur (S) (S only for SBE-β-CD and nanoparticles containing SBE-β-CD). The CS content of the sample was analysed by the N content of the sample in comparison with that of pure CS. For CD content determination, the C content of the samples arising from CS was calculated and subtracted from the observed value. In the case of those nanoparticles containing SBE-β-CD, the S content was also used for CD determination. The composition values obtained by both methods were in close agreement and, thus, the data reported here represent an average of the two. The remaining fraction of the nanoparticles composition was attributed to counterions (i.e. TPP).

2.4.3. Insulin association efficiency

The association efficiency of the nanoparticles was determined after isolation of nanoparticles by centrifugation as described in section 2.3. The amount of unbound insulin was determined in the supernatant by HPLC analyses (Agilent 1100 Series, CA, USA) (Krauland and Alonso, 2007). Briefly, 20 µL of the supernatant was injected into HPLC. Insulin and/or degradation products were separated on a protein and peptide C18 column (Grace Vydac, W.R. Grace & Co., MD, USA) at room temperature. Gradient elution was performed as follows: flow rate 1.0 mL/min, 0–10 min; linear gradient from 70%A / 30%B to 39%A / 61%B (eluent A: 0.1% trifluoroacetic acid in water; eluent B: acetonitrile). Insulin and/or degradation products were detected by absorbance at 220 nm with a diode array absorbance detector. Concentrations of insulin were quantified from integrated peak areas and calculated by interpolation from an according standard curve.

The loading efficiency and the association efficiency of insulin were calculated as indicated below:

$$\text{Loading efficiency (\%)} = \frac{\text{Total amount of insulin} - \text{Amount of unbound drug}}{\text{Nanoparticles weight}} \text{ X } 100$$

$$\text{Association efficiency (\%)} = \frac{\text{Total amount of insulin} - \text{Amount of unbound drug}}{\text{Total amount of insulin}} \text{ X } 100$$

2.5. Interaction of nanoparticles with the nasal epithelium

2.5.1. Effect of nanoparticles on epithelial cell tight junctions : TEER studies

Calu-3 cells were purchased from American Type Culture Collection ATCC (Rockville, USA) and grown in MEM (supplemented with 10% FBS and 100 µg/mL penicillin/streptomycin) at 37ºC in a 5% CO_2 humidified atmosphere. Cells were detached from culturing flasks by trypsin-EDTA and subcultivated. To obtain a differentiated epithelium, cells were cultured on inserts with a density of 2 x 10^5 cells/cm^2 (0.9 cm^2/insert). Post seeding onto the filter, the Calu-3 cells attached to the filter overnight and the medium was then removed from the apical compartment to allow the cells to form a monolayer at an air-liquid interface. The differentiation stage during cultivation was followed by monitoring the transepithelial electric resistance (TEER) of cells. TEER was measured with a Millicell®-ERS system connected to a pair of chopstick electrodes (Millipore Corp., USA). After 15-16 days the differentiated cells (passage numbers 27 to 29), with TEER values within 1000-1200 Ω x cm^2, were used for the TEER experiments.

One hour prior to the TEER studies, the cell culture medium was removed and Calu-3 cells were equilibrated in 1.5 mL HBSS pH 7.4 in the basolateral chamber and 0.5 mL HBSS, pH 6.4 or 7.4, in the apical compartment. At *t* = 0, the apical medium was

replaced by 0.5 mL nanoparticle suspensions (CS/SBE-β-CD/TPP and CS/CM-β-CD/TPP) in HBSS (final pH = 6.4) or by 0.5 mL HBSS, pH 6.4 or 7.4, used as controls. The TEER was measured before administration (*t* = -30 min) and *t* = 30, 60, 90 and 120 min after administration. Between every measurement, the cells were kept in the incubator at 37ºC in an atmosphere of 95% air and 5% CO_2. At the end of the experiments, the samples were carefully removed and the cells were washed 3 times with HBSS and returned to culture medium. Finally, the cells were kept in the incubator to determine the recovery of the monolayer integrity.

The TEER value for every monolayer at t =0 min was normalised to 100% to exclude inter-group differences caused by differences in initial TEER value between monolayers. Each data point shows the mean ± S.D. of five experiments with duplicate determination of TEER.

2.5.2. Interaction of nanoparticles with the nasal epithelial cells by confocal laser scanning microscopy (CLSM)

CS/SBE-β-CD (4/4) and CS/CM-β-CD (4/6) nanoparticles, which were prepared using Fl-CS, were intranasally administered to fully awake rats by following the method of Vila et al. with slight modifications (Vila et al., 2004). Two doses of nanoparticles suspended in 20 μL of trehalose (5% w/v) (10 μL/nostril), which corresponded to 200 μg of Fl-CS/dose, were administered in 5 minutes time interval to each group of animals (n = 3). Another group received only the trehalose solution (non treated, control group). Rats were killed by cervical dislocation 5 min after the last administration and 40 μL of 4% paraformaldehyde solution was introduced in each nostril. The whole nasal mucosa was excised, fixed again in paraformaldehyde and directly observed by CLSM (Leica TCS-SP2, Leica GmbH, Germany) at 488 nm excitation wavelength (Ar laser).

2.6. In vivo studies in rabbits

In vivo studies were performed as previously reported for CS nanoparticles (Fernández-Urrusuno et al.,1999a, b). Thus, Male New Zealand albino rabbits (2 to

3 Kg) were provided with laboratory diet *ad libitum* and fasted 16 h before experiments. In order to avoid any influence of the anaesthesia in glucose levels and insulin absorption the animals were kept conscious during the experiments. The following preparations were administered at pH 4.3: (1) Control insulin solution, (2) Insulin-loaded CS/SBE-β-CD/TPP (4/3/0.25) nanoparticles, and (3) Insulin-loaded CS/CM-β-CD/TPP (4/4/0.25) nanoparticles.

The required dose of insulin (5 IU/Kg) was administered in a volume range of 130 to 150 μL to rabbits (65 to 75 μL/nostril), depending on the insulin loading of the nanoparticles and the animal weight. The amounts of CS/SBE-β-CD/TPP and CS/CM-β-CD/TPP nanoparticles instilled were 74.8 mg/Kg and 37.3 mg/Kg, respectively. Formulations were intranasally administered using a polyethylene tubing inserted about 3 cm into the nostril.

Blood samples were collected from the ear vein 30 min prior the nasal administration (t = -30 min), in order to establish the baseline glucose levels, and at different times after dosing (t = 0, 15, 30, 45, 60, 90, 120, 180, 240, and 300 min). Glycaemia was determined in plasma samples by the glucose-oxidase method (Glucose-TR, Spinreact S.A, Spain). Results are shown as the mean values of plasma glucose levels (% of initial level ± SEM) of 6 animals.

2.7. Statistical analysis

Statistical differences were investigated by using one-way ANOVA followed by the Student-Newman-Keuls method for multiple comparisons. All analysis were run using the SigmaStat statistical program (version 3.1) and differences between groups were judged significant at $P < 0.05$.

3. RESULTS AND DISCUSSION

3.1. Preparation and physicochemical characterization of nanoparticles

We have recently described the mechanisms of formation of new nanocarriers combining different oligo and polysaccharides such as CD and CS (Maestrelli et al., 2006; Krauland and Alonso, 2007). The mechanism and the amount of CD incorporated into the nanocarrier varied depending on the structure and charge of the CD. For example, the association of an anionic CD such as CM-β-CD led to the formation of nanocarriers with a great content in CD (more than 50% of their weight) (Krauland and Alonso, 2007). This was obviously due to the important abililty of the anionic CD to interact with the positively charged CS molecules.

In this work, we prepared nanoparticles combining CS and two different anionic CD and studied the effect of the CD derivatives on nanoparticle characteristics and their biological behavior. SBE-β-CD was selected on account of its negative charge, high aqueous solubility and minimal toxicity. In fact, this CD has been widely investigated for parenteral use, and two different formulations containing SBE-β-CD are already available in the market for IV and intramuscular administration (Challa et al., 2005). In addition, CM-β-CD had been shown to be more efficient in increasing the stability of proteins compared with other CD (Sigurjónsdóttir et al., 1999).

First, experiments were conducted in order to select the suitable CS/CD and CS/CD/TPP mass ratios for the production of nanoparticles containing both types of CD. In general, for very low CD amounts no nanoparticles were formed, whereas an excess of CD in the medium led to the formation of imperfect nanoparticles, which were not resuspendable after isolation, or even to the precipitation of the system. As expected, for a fixed quantity of CS, the amount of CD that could be used for the nanoparticles formation varied as function as the CD type and also by the presence of TPP. This fact was related with the different degree of substitution (D.S.) of the CDs, which is higher in SBE-β-CD (D.S. = 6.4-7) than in CM-β-CD (D.S. = 3.0-3.5), as well as for the presence of TPP anions able to compete with CD for the positively charged amino groups of CS.

Table 1 shows the size, polydispersity index, zeta potetial and production yield of the nanoparticles containing either SBE-β-CD or CM-β-CD. It can be noted that all selected compositions are in the nanometric size range. However, nanoparticles containing SBE-β-CD have a smaller size (200-300 nm) than those prepared with CM-β-CD (300-400 nm). This could be related to the more important negative charge of SBE-β-CD, as compared to CM-β-CD, and, hence, its stronger ability to interact with CS, leading to the formation of more compacted and smaller nanoestructures. All the nanoparticles showed a positive zeta potential, ranging from +17 to +32 mV.

Table 1. Physicochemical properties of selected CS/SBE-β-CD/TPP and CS/CM-β-CD/TPP nanoparticles (means ± S.D., n = 3).

CD type	Ratio CS/CD/TPP	Size (nm)	P.I [a]	Zeta potential (mV)	Yield (%)
SBE-β-CD	4/2/0.5	299 ± 25	0.36-0.46	+32 ± 0.3	46.7 ± 2.0
	4/3/0.25	264 ± 18	0.23-0.37	+27 ± 0.6	49.8 ± 5.4
	4/3/0	200 ± 13	0.11-0.16	+ 26 ± 1.4	18.7 ± 1.5
	4/4/0	238 ± 16	0.08-0.10	+ 27 ± 2.4	47.8 ± 0.3
CM-β-CD	4/3/0.5	392 ± 36	0.27-0.44	+28 ± 2.3	35.5 ± 4.9
	4/4/0.25	358 ± 13	0.43-0.46	+17 ± 2.2	30.1 ± 2.6
	4/5/0	346 ± 10	0.60-0.68	+28 ± 3.7	19.3 ± 4.2
	4/6/0	359 ± 37	0.52-0.59	+29 ± 4.5	38.5 ± 2.9

[a] P.I = Polydispersity index

The morphological appearance of the nanoparticles was examined by TEM. As shown in **Figure 1**, homogeneus populations of spherical shaped nanoparticles were obtained, irrespectively of their composition. This morphology is consistent with that previously observed for nanoparticles prepared by the same technique but composed of CS/TPP or CS and other polysaccharides, such as glucomannan (Calvo et al., 1997; Alonso-Sande et al., 2006). Interestingly, the morphology of the nanoparticles was not affected by the presence or absence of TPP.

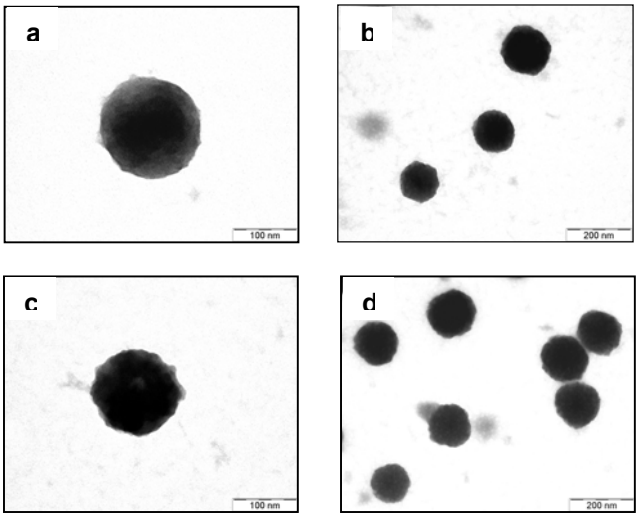

Figure 1. Electron transmission microphotographs of CS/CD/TPP nanoparticles with compositions: (a) CS/SBE-β-CD/TPP (4/3/0), (b) CS/SBE-β-CD/TPP (4/3/0.25), (c) CS/CM-β-CD/TPP (4/5/0), and (d) CS/CM-β-CD/TPP (4/4/0.25).

In addition, elemental analysis of the nanoparticles was carried out in order to determine the actual composition of the different systems. As depicted in **Figure 2**, both CDs, SBE-β-CD (a) and CM-β-CD (b) could be very efficiently entrapped into the nanostructures, representing more than 50% of the total weight. This high incorporation of CD is explained by the already mentioned ionic interaction between the positively charged CS and the negatively charged CD. This high CD incorporation could benefit the nanoparticle properties, specially in terms of toxicity, protection of drug molecules and enhancing permeability.

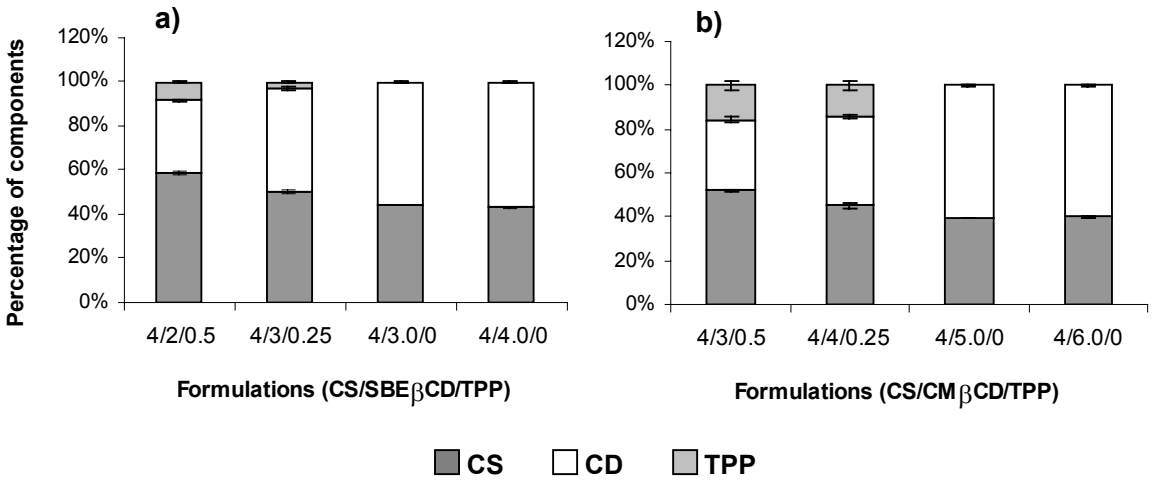

Figure 2. Elemental analysis data of nanoparticle composition (means ± S.D., n = 3).

3.2. Interaction of nanoparticles with the nasal epithelium

3.2.1. Effect of nanoparticles on epithelial cell tight junctions: TEER studies

The Calu-3 monolayer has been considered as an appropriate model of the nasal and bronchotracheal airway epithelia because of some special features, which are also present in normal human tissues, such as tight junctions (expressing the tight

junction associated protein ZO-1 and the adherin protein E-catherin), high TEER values and mucous excretions (Witchi and Mrsny, 1999; Florea et al., 2002). Therefore, we selected this model for the evaluation of the effect of CS/CD nanoparticles on the tightness of junctions between epithelial cells.

Consequently, we measured the TEER values at different time points following exposure of the cells to different doses of CS/SBE-β-CD/TPP and CS/CM-β-CD/TPP nanoparticles and to the controls (HBSS pH 7.4 and HBSS pH 6.4) (**Figure 3, Table 3**). The results showed that incubation with both nanoparticle formulations led to a significant decrease in the TEER of the cell monolayers, thus evidencing their ability to open the tight junctions between the epithelial cells. The effect on the TEER values was dose-dependent and saturable, since no major differences were found when increasing the nanoparticle dose from 75 to 150 $\mu g/cm^2$ (**Table 3**). Interestingly, for all the doses assayed, a complete reversibility of the TEER effect was observed following removal of the nanoparticles, thus indicating that cells remained functionally intact.

These results, which are in agreement with those previously reported for CS nanoparticles on TEER of Calu-3 cell monolayers (Teijeiro-Osorio et al., 2005) indicate that nanostructured CS maintains the intrinsic permeabilizing properties of CS polymer solutions. In this sense, it is well-known that CS solutions have the ability to open the tight junctions between epithelial cells, such as Caco-2 cell monolayers (Artursson et al., 1994; Kotze et al., 1998; Smith et al., 2004) and 16HBE14o- cells (Lim et al., 2001). This effect has been mainly attributted to a reorganization of the actin rings (Artursson et al., 1994) and a translocation of the ZO-1 and ocluddin tight junction proteins from the membrane to the cytoskeleton (Smith et al., 2004).

On the other hand, CDs are also believed to open the tight junctions between epithelial cells (Marttin et al., 1995; 1998). This phenomenon has been traditionally related with the ability of CDs to solubilize membrane components, e.g., cholesterol (Shao et al., 1992; Marttin et al., 1995). More recently, immunohystochemistry studies performed by Yang et al. in confluent 16HBE14o$^-$ cells, suggested that the

effects of dimethyl-β-CD on decreasing TEER was also caused by forcing a reorganization of ZO-1 protein in cell-cell contact sites (Yang et al., 2004).
Consequently, based on this information, it could be argued that both components of the nanoparticles, CS and CD, might be responsible for the permeabilizing properties of the nanoparticles.

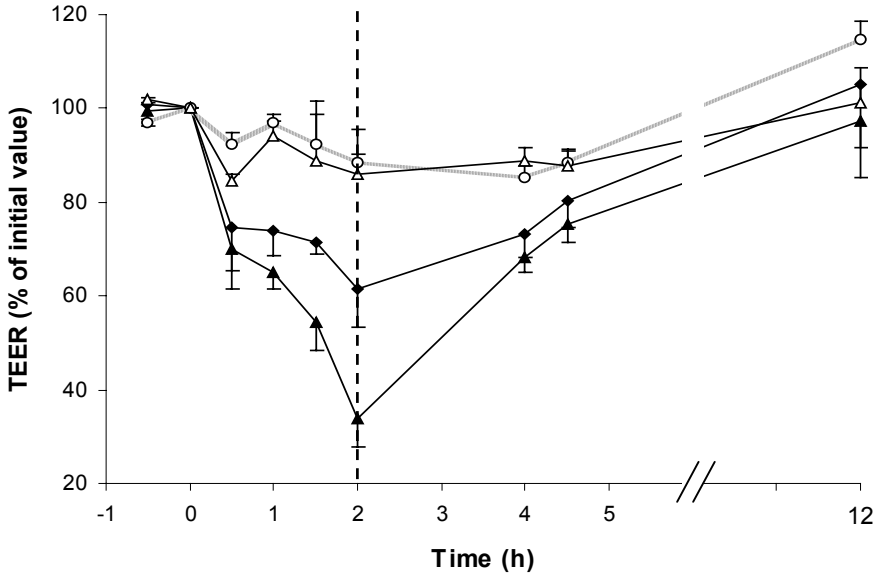

Figure 3. Effect of CS/CD nanoparticles (40 μg/cm^2) on the TEER of Calu-3 cell monolayers at pH 6.4. Each point represents the mean ± S.D. (n = 5). Keys: (o) control HBSS pH 7.4, (Δ) control HBSS pH 6.4, (▲) CS/SBE-β-CD/TPP (4/3/0.25) nanoparticles, (♦) CS/CM-β-CD/TPP (4/4/0.25) nanoparticles, dotted line (----) represents start of reversibility experiment.

Table 3. Reduction in TEER of Calu-3 cell monolayers 2 h after incubation with different doses of CS/CD nanoparticles (expressed as μg of nanoparticles per cm^2) at pH 6.4. (Mean ± S.D., n = 5). The monolayer integrity was completely recovered after 12 h in all cases.

Formulation	TEER (% of initial value)		
	40 μg/cm^2	75 μg/cm^2	150 μg/cm^2
CS/SBE-β-CD/TPP	33.82 ± 5.98	32.49 ± 4.45	22.38 ± 1.81
CS/CM-β-CD/TPP	61.40 ± 8.24	31.80 ± 3.25	22.25 ± 2.11

3.2.2. Interaction of nanoparticles with the nasal epithelial cells

The transport of particles through mucosal surfaces has been extensively investigated in the last coupe of decades (Florence et al., 1997). The overall conclusion is that the size and surface composition of the particles are the main factors affecting their interaction and transport across mucosal surfaces. In general, particles smaller than 1 μm are more efficient in penetrating through mucosal barriers (Jung et al., 2000). In order to elucidate whether CS/SBE-β-CD and CS/CM-β-CD nanoparticles are simply able to adhere to the nasal mucosa or further able to enter the epithelium, formulations of selected nanoparticles were prepared using a fluorescent CS derivative (Fl-CS) and administered intranasally to rats. As can be deduced from comparisson of results in **Tables 1** and **4**, the use of Fl-CS did not affect the characteristics of the resulting labelled nanoparticles.

Table 4. Physicochemical properties of selected CS/SBE-β-CD/TPP and CS/CM-β-CD/TPP prepared with a fluorescein-labelled CS (Fl-CS) (means ± S.D., n = 3).

CD type	Ratio Fl-CS/CD/TPP	Size (nm)	P.I [a]	Zeta potential (mV)
SBE-β-CD	4/4/0	241 ± 4	0.07 - 0.21	+ 25 ± 0.4
CM-β-CD	4/6/0	338 ± 25	0.35 - 0.46	+ 27 ± 0.9

[a] P.I = Polydispersity index

Figure 4 displays the CLSM images of different optical cross sections of the rat nasal mucosa, which are fully representative of all animals receiving the same treatment. The micrographs show an important fluorescence intensity in the case of the mucosas treated with the fluorescent nanoparticles (**Figures 4b** and **4c**), whereas no signal was observed in the mucosa control (**Figure 4a**). Moreover, it can be noted that the fluorescence is maintained, although its intensity is slightly reduced, as we go 10 microns down into the mucosa, thus evidencing the ability of the nanoparticles to enter the nasal epithelium.

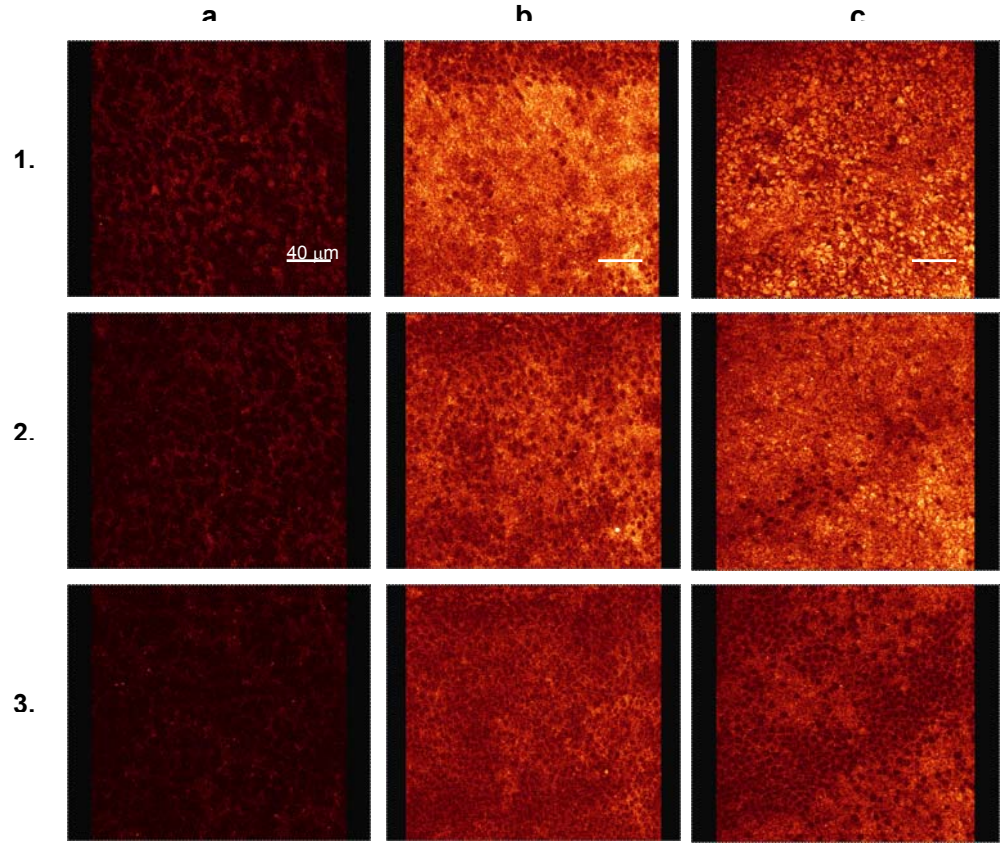

Figure 4. Confocal laser scanning micrographs of the rat nasal tissue excised following: (a) non treatment (control), (b) treatment with Fl-CS/SBE-β-CD nanoparticles, (c) treatment with Fl-CS/CM-β-CD nanoparticles. (1) Mucosal surface, (2) cross section of 5 μm, (3) cross section of 10 μm, scale bar corresponds to 40 μm.

A closer view of the epithelium (**Figure 5**) permitted us to visualize the intracellular localization of the nanoparticles and, thus, the transcellular mechanism of transport. These results agree with those previously reported for the transport of different nanoparticulate compositions, such as CS nanoparticles (Vila et al., 2004) and PLGA:poloxamer and PLGA:poloxamine nanoparticles (Csaba et al., 2006) across the nasal epithelium. However, more detailed studies need to be performed in order to further elucidate the mechanism of interaction and internalization of the nanoparticles within the nasal epithelial cells.

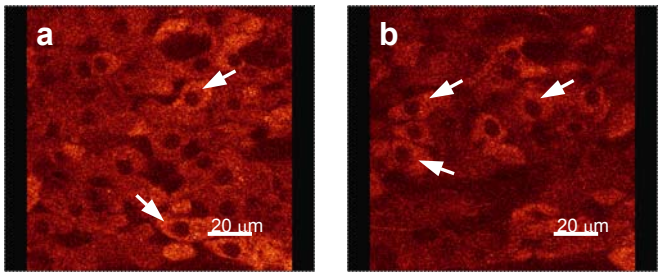

Figure 5. Confocal laser scanning micrographs of the rat nasal tissue excised following treatment with FI-CS/SBE-β-CD nanoparticles. (a) cross section at 5 μm, (b) cross section at 10 μm. The white arrows show the intracellular localization of the particles.

3.3. In vivo studies

Following the observed ability of this new generation of nanoparticles to overcome the nasal barrier, we decided to explore their potential as carriers for improving the nasal absorption of complex molecules such as insulin.

For the incorporation of insulin into the nanocarriers and the subsequent in vivo studies, we selected two formulations: CS/SBE-β-CD/TPP (4/3/0.25) and CS/CM-β-CD/TPP (4/4/0.25). As shown in **Table 5**, and in agreement with a previous work (Krauland and Alonso, 2007), the resulting insulin-loaded nanoparticles have a size in the range of 327-436 nm, a positive zeta potential (+23 - +32 mV) and very high insulin loading (47%).

Table 5. Characteristics of selected insulin loaded CS/SBE-β-CD/TPP and CS/CM-β-CD/TPP nanoparticles (means ± S.D., n = 3).

Formulation	Ratio CS/CD/TPP	Size (nm)	P.I [a]	Zeta potential (mV)	Association efficiency [b] (%)	Loading efficiency (%)	Yield (%)
SBE-β-CD	4/3/0.25	327 ± 27	0.21-0.42	+ 32 ± 0.1	94.9 ± 0.1	23.3 ± 1.9	74 ± 6
CM-β-CD	4/4/0.25	436 ± 34	0.10-0.23	+ 23 ± 0.4	88.6 ± 0.8	46.7 ± 0.8	28 ± 2

[a] P.I = Polydispersity index
[b] Concentration of insulin in the SBE-β-CD/TPP or CM-β-CD/TPP phase: 2.4 mg/mL

As indicated in the methodology section, insulin-loaded CS/SBE-β-CD/TPP and CS/CM-β-CD/TPP nanoparticles, as well as a control insulin solution, were administered in acetate buffer pH 4.3. In previous studies performed by our group it was observed that the manipulation of the conscious animals did not cause any alteration in their blood glucose levels (Fernández-Urrusuno et al., 1999a).

The blood glucose levels attained in rabbits following their treatment with the formulations indicated above are displayed in **Figure 6**. The intranasal administration of 5 IU/Kg insulin solution was found to elicit only a maximum 14% decrease of blood glucose levels at 30 min post-administration. Interestingly, a significantly higher response was achieved after the administration of the same dose of insulin associated to the CS/CD/TPP nanoparticles ($p< 0.05$). In fact, the blood glucose levels decreased to about 35% respective to their baseline levels at 1 h post-administration (maximum glucose decrease). Despite of their different composition and insulin loading capacities (23 and 47%) (**Table 5**), CS/SBE-β-CD/TPP (4/3/0.25) and CS/CM-β-CD/TPP (4/4/0.25) nanoparticles led to similar hypoglycaemic effects. Consequently, these results indicate that the intensity of the hypoglycaemic response is not related with the amount of the nanocarrier components (CS and CD). The same type of conclusion was extracted from the previous work reporting the ability of CS/TPP nanoparticles to enhance the nasal

insulin absorption (Fernández-Urrusuno et al., 1999a). However, a critical difference is that the amount of CS required to achieve a similar effect was much lower in the present study (0.096 mg/Kg) than in the previous one (0.16 mg/Kg).

The mechanisms by which CS and CDs enhance the nasal absorption of macromolecules have been not fully elucidated until now. As previously mentioned, CS penetration-enhancing properties have been attributed to the transient widening of the tight junctions between cells (Artursson et al.,1994; Schipper et al., 1997), as well as to reversible effects on the intracellular pathways (Dodane et al., 1999). On the other hand, CDs are believed to enhance nasal absorption of peptides and proteins by inhibiting their enzymatic degradation, disrupting the epithelial membrane by extraction of phospholipids and proteins, and/or opening tight junctions (Marttin et al., 1995; 1997; Merkus et al., 1999). Nevertheless, a series of studies have led us to accept that the mechanism of action of nanoparticles may be different as compared to that of the corresponding polymer solutions. In this sense, we have previously shown that, under the same experimental conditions used in the present study, insulin loaded-CS nanoparticles were able to decrease plasma glucose levels in a greater extension than the corresponding insulin dose administered in CS solutions to rabbits (Fernández-Urrusuno et al., 1999a,b).

The ability of CS/CD nanoparticles to enhance the absorption of macromolecules (e.g. insulin) could be explained by two different mechanisms. One could be related to the adhesion of the nanoparticles to the mucus layer, where the systems, thank to their components (CS and CD), act as penetration enhancers by opening the tight junctions, and, simultaneously, deliver the associated insulin. This hypothesis could be supported by the demonstrated effect of CS/CD nanoparticles on decreasing the TEER of epithelial cells.

On the other hand, there is also the possibility that CS/CD nanoparticles cross the nasal mucosa, thereby acting as real macromolecule carriers. This interpretation agrees with the ability of these particles to be internalized by nasal epithelial cells in vivo, as shown in the CLSM cross sections.

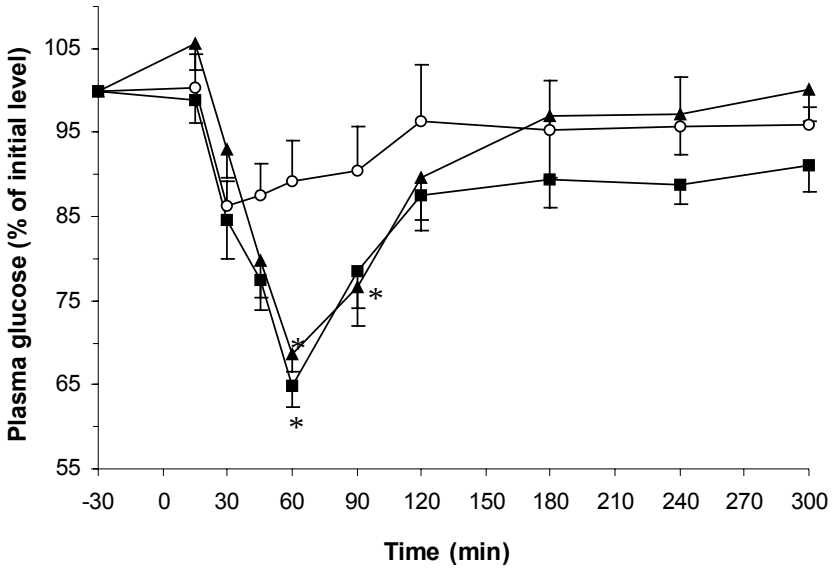

Figure 6. Plasma glucose levels achieved in rabbits following nasal administration (at pH 4.3, acetate buffer) of: (o) insulin solution, (■) CS/SBE-β-CD/TPP nanoparticles, (▲) CS/CM-β-CD/TPP nanoparticles. (Mean ± SEM, n = 6). * Statistically significant differences from control insulin solution ($p < 0.05$).

CONCLUSIONS

In this report we present a novel type of nanoparticles consisting on CS and two different anionic CDs, SBE-β-CD and CM-β-CD, which exhibit a number of features that make them a promising nanocarrier for nasal (mucosal) delivery of macromolecules, namely: (i) the nanoparticles are prepared by a very mild technique (ii) they exhibit permeation-enhancing properties (iii) they are able to penetrate in the nasal mucosa; and, finally, (iv) they are able to transport insulin across the nasal barrier, leading to a significant decrease in the plasma glucose levels.

ACKNOWLEDGEMENTS

This work has been supported by the European Commission within the 6th Framework programme – NanoBiosaccharides – Contract nr. 013882. Desirée Teijeiro-Osorio acknowledges the pre-doctoral fellowship granted by this Program. The authors thank to Rafael Romero for his help with the in vivo studies.

REFERENCES

1. Alonso-Sande M., Cuña M., Remuñán-López C., Teijeiro-Osorio D., Alonso-Lebrero J.L., Alonso, M.J., Formation of new glucomannan-chitosan nanoparticles and study of their ability to associate and deliver proteins, Macromolecules, 39 (2006) 4152-4158.
2. Arora P., Sharma S., Garg S., Permeability issues in nasal drug delivery, DDT, 7 (2002) 967-975.
3. Artursson P., Lindmark T., Davis S.S., Illum L., Effect of chitosan on permeability of monolayers of intestinal epithelial cells (Caco-2), Pharm. Res., 11 (1994) 1358-1361.
4. Calvo P., Remuñán-López C., Vila-Jato J.L., Alonso M.J., Novel hydrophilic chitosan-polyethylene oxide nanoparticles as protein carriers, J. Appl. Pol. Sci., 63 (1997) 125-132.
5. Challa R., Ahuja A., Ali J., Khar R.K., Cyclodextrins in drug delivery: an updated review, AAPS PharmSciTech, 6 (2005) E329-E357. (http://www.aapspharmscitech.org).
6. Cryan S.-A., Holohan A., Donohue R., Darcy R., O´Driscoll C.M., Cell transfection with polycationic cyclodextrin vectors, Eur. J. Pharm. Sci., 21 (2004) 625-633.
7. Csaba N., Sánchez A., Alonso M.J., PLGA:Poloxamer and PLGA:Poloxamine blen nanostructures as carriers for nasal gene delivery, J. Control. Rel., 113 (2006) 164-172.
8. De Campos A.M, Diebold Y., Carvalho E.L.S., Sánchez A., Alonso M.J., Chitosan nanoparticles as new ocular drug delivery systems: in vitro stability, in vivo fate, and cellular toxicity, Pharm. Res., 21 (2004) 803-810.
9. Dodane V., Khan M.A., Merwin J.R., Effect of chitosan on epithelial permeability and structure, Int. J. Pharm., 182 (1999) 21-32.

10. Dotsikas Y., Loukas Y.L., Kinetic degradation study of insulin complexed with methyl-beta cyclodextrin. Conformation of complexation with electrospray mass spectroscopy and ^{1}H NMR, J. Pharm. Biomed. Anal., 29 (2002) 487-494.

11. Fernández-Urrusuno R., Calvo P., Remuñán-López C., Vila-Jato J.L., Alonso M.J., Enhancement of nasal absorption of insulin using chitosan nanoparticles, Pharm. Res., 16 (1999b) 1576-1581.

12. Fernández-Urrusuno R., Romani D., Calvo P., Vila-Jato J.L., Alonso M.J., Development of a freeze-dried formulation of insulin-loaded chitosan nanoparticles intended for nasal administration, S.T.P. Pharma Sci., 9 (1999a) 429-436.

13. Florea B.I., Meaney C., Junginger H.E., Borchard G., Transfection efficiency and toxicity of polyethylenimine in differentiated Calu-3 and nondifferentiated COS-1 cell cultures, AAPS PharmSci, 4 (2002) E12 (http://www.aapspharmsci.org).

14. Florence A.T., The oral absorption of micro- and nanoparticulates: neither exceptional nor unusual, Pharm. Res., 14 (1997) 259-266.

15. Irie T., Uekama K., Cyclodextrins in peptide and protein delivery, Adv. Drug Deliv. Rev., 36 (1999) 101-123.

16. Jung T., Kamm W., Breitenbach A., Kaiserling E., Xiao J.X., Kissel T., Biodegradable nanoparticles for oral delivery of peptides : is there a role for polymers to affect mucosal uptake?, Eur. J. Pharm. Biopharm., 50 (2000) 147-160.

17. Kopping-Hoggard M., Tubulekas I., Guan H., Edwards K., Nilsson M., Varum K.M., Chitosan as a non viral gene delivery system. Structure-property relationships and characteristics compared with polyethylenimine in vitro and after lung administration in vivo, Gene Ther., 8 (2001) 1108-1121.

18. Kotze A.F., Lueβen H.L., De Boer A.G., Verhoef J.C., Junginger H.E., Chitosan for enhanced intestinal permeability: prospects for derivatives soluble in neutral and basic environments, Eur. J. Pharm. Sci., 7 (1998) 145-151.

19. Krauland A.H., Alonso M.J., Chitosan/cyclodextrin nanoparticles as macromolecular drug delivery system, Int. J. Pharm., 339 (2007).

20. Lim S.T., Forbes B., Martin G.P., Brown M.B., In vivo and in vitro Characterization of novel microparticulates based on hyaluronan and chitosan hydroglutamate, AAPS PharmSciTech., 2 (2001) article 20 (http://www.pharmscitech.com).

21. Loftsson T., Brewster M.E., Pharmaceutical applications of cyclodextrins. 1. Drug solubilization and stabilization, J. Pharm. Sci., 85 (1996) 1017-1025.

22. Maestrelli F., García-Fuentes M., Mura P., Alonso M.J., A new drug nanocarrier consisting of chitosan and hydroxypropylcyclodextrin, Eur. J. Pharm. Biopharm., 63 (2006) 79-86.

23. Marttin E., Verhoef J.C., Merkus F.W.H.M., Efficacy, safety and mechanism of cyclodextrins as absorption enhancers in nasal delivery of peptide and protein drugs, J. Drug Target., 6 (1998) 17-36.

24. Marttin E., Verhoef J.C., Romeijn S.G., Merkus F.W.H.M., Effects of absorption enhancers on rat nasal epithelium in vivo: release of marker compounds in the nasal cavity, Pharm. Res., 12 (1995) 1151-1157.

25. Matsubara M., Ando Y., Irie T., Uekama K., Protection afforded by maltosyl-β-cyclodextrin against α-chymotrypsin-catalyzed hydrolysis of a luteinizing-releasing hormone agonist, bserelin acetate, Pharm. Res., 14 (1997) 1401-1405.

26. Merkus F.W., Verhoef J.C., Marttin E., Romeijn S.G., van der Kuy P.H.M., Hermens W.A.J.J., Schipper N.G.M., Cyclodextrins in nasal drug delivery, Adv. Drug Deliv. Rev., 36 (1999) 41-57.

27. Prego C., García M., Torres D., Alonso M.J., Transmucosal macromolecular drug delivery, J. Control. Rel., 101 (2005) 151-162.

28. Schipper N.G.M., Olson S., Hoogstraate J.A., De Boer A.G., Varum K.M., Artursson P., Chitosans as absorption enhancers for poorly absorbable drugs. II. Mechanism of absorption enhancement, Pharm. Res., 14 (1997) 923-929.

29. Shao Z., Krishnamoorthy R., Mitra A.K., Cyclodextrins as nasal absorption promoters of insulin: mechanistic evaluations, Pharm. Res., 9 (1992) 1157-1163.

30. Sigurjónsdóttir J.F., Loftsson T., Másson M., Influence of cyclodextrins on the stability of the peptide salmon calcitonin in aqueous solution, Int. J. Pharm., 186 (1999) 205-213.

31. Smith J., Wood E., Dornish M., Effect of chitosan on epithelial cell tight junctions, *Pharm. Res.*, 21 (2004) 43-49.

32. Teijeiro-Osorio D., Remuñán-López C., Nielsen H.M., Comparative studies of chitosan nanoparticles and molecules in Calu-3 and TR146 cells, 32nd Ann. Meet. Exp. Control. Rel. Soc., (2005) 378.

33. Uekama K., Hirayama F., Irie T., Cyclodextrin drug carrier systems, Chem. Rev., 98 (1998) 2045-2076.

34. van der Lubben I.M., Verhoef J.C., Borchard G., Junginger H.E., Chitosan and its derivatives in mucosal drug and vaccine delivery, Eur. J. Pharm. Sci., 14 (2001) 201-207.

35. Vila A., Sánchez A., Janes K.A., Behrens I., Kissel T., Vila-Jato J.L., Alonso M.J., Low molecular weight nanoparticles as new carriers for nasal vaccine delivery in mice, Eur. J. Pharm. Biopharm., 57 (2004) 123-131.

36. Witchi C., Mrsny R. J., In vitro evaluation of microparticles and polymer gels for use as nasal platforms for protein delivery, Pharm. Res., 16 (1999) 382-390.

37. Yang T., Hussain A., Paulson J., Abbruscato T.J., Ahsan F., Cyclodextrins in nasal delivery of low-molecular-weight heparins : in vivo and in vitro studies, Pharm. Res., 21 (2004) 1127-1136.

38. Yu S., Zhao Y., Wu F., Zhang X., Lü W., Zhang H., Zhang Q., Nasal insulin delivery in the chitosan solution : in vitro and in vivo studies, Int. J. Pharm., 281 (2004) 11-23.

ARTÍCULO 5

Chitosan/Cyclodextrin Nanoparticles Can Efficiently Transfect the Airway Epithelium

---

Desirée Teijeiro-Osorio, Carmen Remuñán-López y María José Alonso

Abstract

The main goal of the present study was to investigate the potential of a new generation of hybrid polysaccharide nanocarriers, composed by chitosan (CS) and anionic cyclodextrins (CD), for gene delivery to the airway epithelium. More specifically, these nanocarriers were investigated with regard to their ability to enter epithelial cells and promote gene expression in the Calu-3 cell culture model.

In the search for the most suitable nanocarrier composition for gene delivery, the effect of CS molecular weight (Mw) on the nanocarriers characteristics and their ability to transfect cells was investigated. Thus, hybrid CS/CD nanoparticles were prepared with two different CS Mw, medium (110 kDa) and low (10 kDa), and loaded with pSEAP (plasmid DNA model that encodes the expression of secreted alkaline phosphatase). The resulting nanoparticles presented an adequate size range (100-200 nm, depending on CS Mw), a positive surface charge (+22-+35 mV) and very high DNA association efficiency values (>90%). Cellular uptake studies showed that the nanoparticles were effectively internalized by the cells, providing a good indication of their potential as gene carriers. The transfection efficiency of the different formulations, measured by the concentration of secreted gene product (SEAP), indicated that all the nanoparticles were able to elicit a significantly higher response than the naked DNA (control), being the transfection efficiency more important for low Mw CS nanoparticles than for those composed of medium Mw CS. Overall, this report is the first evidence of the potential of a new generation of safe polysaccharide nanocarriers for gene delivery to the airway epithelium.

Key words: Calu-3 cells, chitosan, cyclodextrin, nanoparticles, nanocarriers, gene/DNA delivery.

Introduction

Over the last years, there has been an increasing interest in the delivery of genes to the airway epithelium, either for therapeutic (e.g. cystic fibrosis, α1-antitripsin deficiency) or vaccination purposes (Graham and Launspach, 1997; Brigham et al., 2000; Griesenbach, 2001). In spite of the advances made in facilitating the delivery of drugs to the nasal/bronchial epithelium there are still important barriers to overcome before achieving a successful gene transfer in these respiratory regions. Probably, the most critical barriers are represented by the mucus-gel layer involved in the mucociliary clearance mechanisms and the low rate of endocytosis taking place on the apical side of airway epithelial cells (Pickles et al., 1998; Lemoine et al., 2005).

Currently, the transport of exogenous DNA to cells can be accomplished by using viral and non-viral vectors. Although both gene delivery systems are under investigation, virus-based gene therapy is limited by concerns about endogenous virus recombinations, oncogenic effects and immunological reactions (Lee et al., 2007). Alternatively, the non-viral gene delivery agents offer several advantages, including easiness of production and low cost, safety, and lack of immunogenicity. However, their use has been limited by their relatively low transfection efficiency in vivo (Lollo et al., 2000; Gautam et al., 2002).

Most commonly, the non-viral systems consist of ionic complexes formed by the condensation of DNA through electrostatic interactions with cationic polymers (polyplexes) or lipids (lipoplexes). Among cationic polymers, chitosan (CS), which is a natural linear polysaccharide obtained by partial deacetylation of chitin, exhibits several favorable biological properties, such as biodegradability, low toxicity, biocompatibility and mucoadhesiveness (Felt et al., 1998). Although CS polyplexes are promissing for mucosal gene delivery, they still suffer from several limitations, such as undefined physical shapes, dissociation of the complexes in presence of anions and a limited capacity to co-associate other functional molecules that could help to achieve efficient gene transfer and expression. As an alternative, our research group and others have recently reported the preparation of CS

nanoparticles formed by ionic gelation with tripolyphosphate (TPP) as delivery systems for DNA (Koping-Hoggard et al.,*submitted*; Csaba et al., *submitted*) and siRNA (Katas and Alpar, 2006). These nanoparticles consisting of CS were able to associate high amounts of genetic material and provided high gene expression levels both *in vitro* and *in vivo*.

Recently, we reported a new generation of polysaccharide nanocarriers consisting of the polysaccharide CS and cyclic oligosaccharides named cyclodextrins (CD) (Maestrelli et al., 2006; Krauland and Alonso, 2007). The rational behind the design of these new nanocarriers was to combine the promising behaviour of CS nanoparticles with the excellent biopharmaceutical properties of CD. Indeed, CD are very well-known in the pharmaceutical field because of their ability to protect drugs from physical, chemical and enzymatic degradation, and to enhance membrane permeability (Cryan et al., 2004). Currently, there are several kinds of neutral, amphiphilic and cationic CD, which can be used for the design of novel gene delivery systems. For example, CDs have been also conjugated with polycationic polymers, such as polyamidine and polyethylenimine, and dendrimers, to form polyplexes, which were found to elicit an increased transfection efficiency and stability against enzymatic degradation with low in vitro and in vivo toxicity (Hwang et al., 2001; Arima et al., 2001; Forrest et al., 2005; Challa et al., 2005).

Bearing all this information in mind, we hypothesized that the incorporation of CDs to the already effective CS-based gene delivery nanocarriers could positively contribute to: (a) offer further DNA protection from degradation, (b) promote cellular-uptake, and (c) decrease the cytotoxicity of the systems.

The aim of the present work was to investigate the potential of CS/CD nanoparticles as gene delivery systems to the airway epithelium. For this purpose, different nanoparticulate compositions of CS and CD (different CS Mw and different anionic CD derivatives) were prepared and characterized. The nanoparticle cytotoxicity and ability to enter and transfect cells in vitro was evaluated in the human mucus-producing cell line Calu-3, a model for the nasal and bronchotracheal airway

epithelium, recently proposed as an adequate model for gene delivery (Florea et al., 2002).

2. Materials and methods

2.1. Materials

Ultrapure chitosan (CS) hydrochloride salt (Protasan UP CL 113, having a molecular weight of around 110 KDa and deacetylation degree = 86%) was purchased from FMC Biopolymers (Norway). Cyclodextrin (CD) anionic derivatives, sulfobutylether-β-CD (SBE-β-CD, substitution degree ≈ 7) and carboximethyl-β-CD (CM-β-CD, substitution degree = 3.0-3.5) were purchased from Cydex Inc. (USA) and Fluka Biochem. (France), respectively. Plasmid DNA (pDNA) encoding secreted alkaline phosphatase (pSEAP) based on the gWiz™ high-expression vector system, was pursached from Aldevron (USA). Eagle´s Minimum Essential Medium (MEM) was purchased from ATCC (BMG Lab., Spain). Foetal Bovine Serum (FBS), penicillin/streptomycin (100 µg/mL), MTT ((3-4,5-Dimethylthiazol-2-yl)-2,5-diphenyltetrazolium bromide), fluorescein sodium salt, and pentasodium tripolyphosphate (TPP) were all obtained from Sigma-Aldrich (Spain). Phosphate-buffered saline (PBS), Hanks' balanced salt solution (HBSS) 1x and 10x were purchased from Gibco™ (UK). One KBp DNA ladder was obtained from Life Technologies (Spain). Triton® X-100 and DMSO was acquired from Fluka Biochem. (Spain). 12-well tissue culture plates with cell culture inserts (0.9 cm^2, 0.4µm pore size) and flatbottomed 96-well plates were obtained from Falcon™ (Becton Dickinson Labware, USA). Ultrapure water (MilliQ Plus, Millipore Iberica, Spain) was used throughout. All other solvents and chemicals were of the highest grade commercially available.

2.2. Preparation of fluorescein labelled chitosan (Fl-CS)

CS was labelled with fluorescein, following a slighty modified method described by De Campos et al. (De Campos et al., 2004). The covalent attachment of fluorescein

to CS was achieved by the formation of amide bonds between primary amino groups of the polymer and the carboxylic acid groups of fluorescein. Briefly, 250 mg of CS were dissolved in 25 mL of water and an amount of 10 mg of fluorescein was dissolved in 1 mL of ethanol. Thereafter, both solutions were mixed together and, to catalyse the formation of amide bonds, EDAC (1-ethyl-3-(3-dimethylaminopropyl) carbodiimide hydrochloride) was added in a final concentration of 0.05 M. The reaction mixture was incubated under permanent magnetic stirring for 12 h in the dark at room temperature. The resulting conjugate (Fl-CS) was isolated by exhaustive dialysis (cellulose dialysis tubing, pore size 12,400 Da; Sigma-Aldrich, Spain) against demineralised water and then freeze-dried.

2.3. Depolymerization of chitosan

Low molecular weight CS (LMwCS) was obtained from Protasan UP CL 113 by sodium nitrite degradation as previously described (Janes and Alonso, 2003). Briefly, 200 µL of 0.1M $NaNO_2$ were added to 4 mL of the CS solution (10 mg/mL) at room temperature under magnetic stirring. The reaction was left overnight to assure completion of the degradation, and fragments with an approximate Mw of 10 KDa were recovered by freeze-drying. The molecular size of the LMwCS was verified by size exclusion chromatography (SEC).

2.4. Nanoparticle preparation

Nanoparticles were spontaneously obtained by ionotropic gelification (Calvo et al., 1997). Two aqueous phases containing: 1) the CS solution (CS, Fl-CS or LMwCS), and 2) the cyclodextrin solution (SBE-β-CD or CM-β-CD) with the crosslinker TPP, were mixed under magnetic stirring and maintained under agitation for 10 minutes to allow the complete formation of the system. The CS, Fl-CS or LMwCS solutions were prepared at a concentration of 2 mg/mL, and the volume employed was fixed at 3 mL. On the other hand, in order to modulate the mass ratio of the components that constituted the nanoparticles (CS/CD/TPP), the corresponding volumes of the

CD aqueous solution (SBE-β-CD or CM-β-CD, 6-12 mg/mL) and TPP solution (1.5 mg/mL) were mixed at a final volume of 1 mL.

For nanoparticles encapsulating a pDNA model, the required amount of the plasmid encoding secreted alkalin phosphatase (gWiz^{TM}pSEAP) was incorporated directly in the CD/TPP phase. The theoretical loadings were fixed at 5% (w/w).
As a control, nanoparticles composed solely by CS and TPP were prepared by the same method and loaded by including the corresponding amount of pDNA model in the TPP solution.

2.5. Nanoparticle characterization

The mean particle size and the size distribution of the nanoparticles were determined by Photon Correlation Spectroscopy (PCS). The zeta potential values of the nanoparticles were obtained by Laser Doppler Anemometry (LDA), measuring the mean electrophoretic mobility. The PCS and LDA analysis were performed with a Zetasizer® 3000 HS (Malvern Instruments, UK).
Eventually, nanoparticles were concentrated by centrifugation (Beckman Avanti TM 30, Beckman, Spain) on a glycerol bed. In order to resuspend the nanoparticles at the required concentration, the amount of nanoparticles in the sediment was calculated by weight upon their freeze-drying.
The association of pDNA to the nanoparticles was studied by a conventional agarose gel electrophoresis assay. Samples of the nanoparticles were placed in 1% agarose gel containing ethidium bromide, and ran for 90min at 60V in TAE buffer (Sub-Cell GT 96/192, Bio-Rad Laboratories Ltd., England).

2.6. Cell culture

Calu-3 cells were purchased from American Type Culture Collection ATCC (Rockville, USA) and grown in MEM (supplemented with 10% FBS and 100 µg/mL penicillin/streptomycin) at 37ºC in a 5% CO_2 humidified atmosphere. Cells were detached from culturing flasks by trypsin-EDTA and subcultivated for studies with

proliferating cells or a well-differentiated epithelium. For cytotoxicity studies with proliferating cells the cells were seeded in flat-bottomed 96-well culture plates in a density of 6 x 10^4 cell/well and cultured for 72 h. To obtain a differentiated epithelium, cells were cultured on inserts with a density of 2 x 10^5 cells/cm^2 (0.9 cm^2/insert). Post seeding onto the filter, the Calu-3 cells attached to the filter overnight and the medium was then removed from the apical compartment to allow the cells to form a monolayer at an air-liquid interface. The differentiation stage during cultivation was followed by measuring the transepithelial electric resistance (TEER) (Millicell®-ERS, Millipore Corp., USA). After 15-18 days the differentiated cells, with mean TEER values around 1100-1200 Ω x cm^2, were used in cellular uptake studies and transfection experiments with pSEAP. Pass numbers 28 to 40 were used for the following experiments.

2.7. Cytotoxicity studies

The effect of different nanoparticle compositions and concentrations on cellular viability of proliferating Calu-3 cells was determined by MTT colorimetric assay, which was conveniently optimized. MTT is a yellow tetrazolium salt that is reduced only in living, metabolically active cell mitochondria. Cells grown in 96-well culture plates were washed twice with 100 μL of HBSS and the test nanoparticle suspensions (100 μL, in HBSS pH 6.4) were added in concentrations ranging from 0.0125 to 2.5 mg/mL to the wells. At the end of the incubation time (2 h, 37ºC) and according to extensive pretests, samples were discarded and replaced by 25 μL of MTT solution (5 mg/mL) and 100 μL of HBSS pH 7.4. The plates were further incubated for 4 h at 37ºC (protected from light) and the MTT solution was removed. The blue crystals formed in each well were dissolved with 100 μL of DMSO. Positive (Triton® X solution, 2% w/v) and negative (HBSS) control wells were treated similarly as above. Absorbance values were measured at 570 nm using a microplate reader. Cell viability, as a percent of the negative control, was calculated from the absorbance values. The IC_{50} was defined as the sample concentration inhibiting

50% cell viability. Analysis of four replicates was conducted in two different passages of cells (*n* = 8).

2.8. Uptake studies

Nanoparticles were prepared with a fluorescein-labelled CS (Fl-CS) according to the procedure described before, suspended in trehalose (5% w/v) and then added to the Calu-3 differentiated cells. After 1h incubation at 37ºC, samples were removed and cells were rinsed three times with HBSS. Samples were fixed with 4% paraformaldehyde, permeabilised with 0.1% Triton®-X and the cell nuclei were stained with propidium iodide according to manufacturers instructions, including the ribonuclease A pre-treatment. Thereafter, the filters were cut and examined under Confocal Laser Scanning Microscopy (CLSM) (Leica TCS SP2, Leica GmbH, Germany), that allowed the simultaneous visualization of the two different fluorescent markers. Excitation wavelengths were 488 nm for fluorescein and 633 nm for propidium iodide.

2.9. Transfection studies

Transfection studies were performed with nanoparticles loaded with 5% (w/w) gWiz™pSEAP and naked pDNA (control) (2 µg/insert), placed on the apical compartment and incubated for 4 h. The yield of gene expression was non-invasively evaluated by monitoring concentrations of secreted alkaline phosphatase (SEAP) in the basolateral compartment at different time points. The first samples were taken inmediatly after incubation of cells with the formulations, transferred to 1.5 mL eppendorf tubes and stored at –20ºC. Remaining medium from the basolateral compartment and solutions from the apical compartment were removed. Both sides were washed with PBS and fresh culture medium was applied on the basolateral side. Thereafter, samples were taken in the same manner during 6 days (*t* = 1, 2, 4 and 6 days). Finally, the samples were analyzed for SEAP quantification with a fluorescence assay using the Great EscAPe™ SEAP Reporter System Kit

protocol (BD Biosciences Clontech, USA) and Fluorimeter (LS 50B Luminescence Spectrometer, Perkin-Elmer, USA).

2.10. Statistical Analysis

Statistical differences were investigated by using one-way ANOVA followed by the Student-Newman-Keuls method for multiple comparissons. All analysis were run using the SigmaStat statistical program (version 3.1) and differences between groups were judged significant at $P < 0.05$.

3. Results and discussion

As indicated in the introduction, the overall goal of this work was to asses the potential of a new nanocarrier based on biodegradable and non toxic poly and oligosaccharides as a vehicle for the delivery of genes to the airway epithelia. To reach this goal several stages need to be taken into consideration:

(i) the ability to associate genes to the proposed nanocarrier without altering the inherent properties of the gene and also of the carrier
(ii) the interaction of the nanocarrier with the selected target cells (Calu-3 cells)
(iii) the capacity of the gene-loaded nanocarrier to achieve cell transfection
These three stages will be analized in detail in this specific section.

3.1. Definition of nanocarriers formation conditions and their ability to associate pDNA

CS and CS/CD nanoparticles were prepared by ionic gelation in the presence of TPP, as described in the methodology section. The mechanism of formation of the nanosystems combines the electrostatic interaction between CS and CDs, which are oppositely charged, with the ability of CS to undergo a liquid-gel transition due to its ionic interaction with TPP. As we postulated that the incorporation of CD would benefit the system properties, preliminar experiments were aimed at finding the

maximum CD/CS mass ratio in which nanoparticles formed can be conveniently isolated, resuspended and characterized. This maximum ratio was found to be 3/4 (w/w) for SBE-β-CD/CS and 4/4 for CM-β-CD/CS. This great and different incorporation capacity of CD could be determined by their degree of substitution (D.S.) which is higher in SBE-β-CD (D.S. = 6.4-7) than in CM-β-CD (D.S. = 3.0-3.5). As shown in **Table 1**, all particles were in the nanometric range (234 – 358 nm) and exhibited a positive zeta potential (+35-+17 mV), however these properties were dependent on the composition. The smallest size was observed for SBE-β-CD/CS nanoparticles. This could be due to the fact that SBE-β-CD is more substituted than CM-β-CD and consequently led to the formation of more compacted and, thus, smaller nanoestructures. As expected, a decrease in the surface charge was found in nanoparticles containing CD as compared to those made solely by CS. The lowest value was observed for nanoparticles containing CM-β-CD, thus indicating the presence of an important amount of CD on the surface of the nanoparticles.

Table 1. Physicochemical characteristics of nanoparticles composed solely by CS or CS and two different CD derivatives (SBE-β-CD, CM-β-CD) (means ± S.D., *n* = 3).

CD type	CS/CD/TPP mass ratio	Size (nm)	P.I	Zeta Potential (mV)
SBE-β-CD	4/3/0.25	264 ± 18	0.2 - 0.3	+27 ± 0.6
CM-β-CD	4/4/0.25	358 ± 13	0.4 - 0.5	+17 ± 2.2
-	4/0/1	335 ± 18	0.3 - 0.4	+35 ± 0.9

P.I = Polydispersity index

Once we defined the appropriate conditions for the formation of the nanoparticles, we studied the possibility to efficiently associate pSEAP, a pDNA model that encodes the expression of secreted alkaline phosphatase. With this idea in mind, we explored the influence of CS Mw on the characteristics of the nanoparticles and, afterwards, on their ability to transfect cells. More specifically, we chose CS, ≈110 KDa (Protasan UP CL 113) and low molecular weight CS (LMwCS, ≈10 KDa), obtained by partial depolymerization of the previous one. On the other hand, we fixed the theoretical pDNA loading at 5% (w/w, based on weight of all nanoparticle components: CS or LMwCS, CD and TPP) and we used nanoparticles made of solely CS as a control, given their reported efficacy for gene delivery (Koping-Hoggard et al., *submitted*; Csaba et al., *submitted*).

As shown in **Tables 2** and **3,** all the formulations were in the desired nanometric range, presenting low polydispersity and positive zeta potential values. It can also be noted that nanoparticles made of LMwCS presented a lower positive zeta potential and a smaller size than those made of regular CS. This fact agrees with previous results on CS nanoparticles prepared by ionic gelation (Janes and Alonso, 2003; Katas and Alpar, 2006; Koping-Hoggard et al., *submitted*). The effect of CS Mw on the nanoparticle size could be related to the greater ability of lower Mw CS molecules to organize forming smaller structures. Moreover, the smaller size and higher solubility of LMwCS could led to a more efficient interaction with the pDNA, thus resulting in the formation of smaller particles (Katas and Alpar, 2006; Koping-Hoggard et al., *submitted*).

Table 2. Physicochemical characterization of 5% gWiz™pSEAP-loaded nanoparticles consisting of CS (110 kD) and two different CD derivatives (SBE-β-CD, CM-β-CD) (means ± S.D., *n* = 3).

CD type	CS/CD/TPP mass ratio	Size (nm)	P.I	Zeta Potential (mV)
SBE-β-CD	4/3/0.25	180 ± 2	0.1 - 0.2	+ 35 ± 6
CM-β-CD	4/4/0.25	234 ± 15	0.1 - 0.2	+ 25 ± 5
-	4/0/1	192 ± 25	0.2 - 0.3	+ 34 ± 5

P.I = Polydispersity index

Table 3. Physicochemical characterization of 5% gWiz™pSEAP-loaded nanoparticles consisting of CS with a low Mw (10 kD) and two different CD derivatives (SBE-β-CD, CM-β-CD) (means ± S.D., *n* = 3).

CD type	LMwCS/CD/TPP mass ratio	Size (nm)	P.I	Zeta Potential (mV)
SBE-β-CD	4/1.5/0.25	143 ± 2	0.0 - 0.1	+ 24 ± 4
CM-β-CD	4/3/0.25	140 ± 8	0.0 - 0.1	+ 22 ± 6

P.I = Polydispersity index

The ability of the polysaccharide nanoparticles to entrap pDNA was studied using agarose electrophoresis technique. From the photograph of the obtained agarose gel, depicted in **Figure 1**, it could be stated that most of the DNA was associated to the nanoparticles, since no migration of free DNA was observed. This fact is in agreement with previous results obtained for other CS-based nanometric systems and it can be easily explained by the high affinity of CS for the DNA (Csaba et al., *submitted;* De la Fuente et al., *submitted a*). Indeed, it is known the strong

electrostatic interaction existing between the phosphate groups of DNA and the amino groups of CS, as well as hydrophobic and hydrogen bonds (Li et al., 2003).

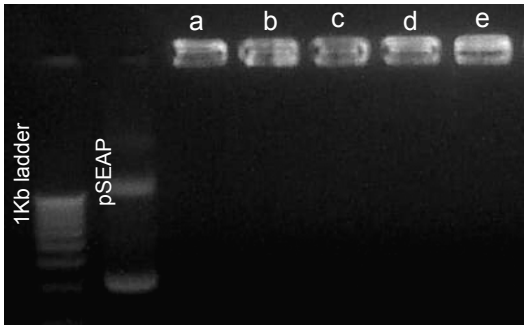

Figure 1. Agarose gel electrophoresis of the different nanoparticles encapsulating plasmid DNA: (a) CS/SBE-β-CD/TPP; (b) CS/CM-β-CD/TPP; (c) CS/TPP; (d) LMwCS/SBE-β-CD/TPP; (e) LMwCS/CM-β-CD/TPP. 1kb DNA ladder and untreated gWiz™pSEAP were used as control.

Consequently, overall these data show the possibility to obtain different compositions of these novel nanocarriers containing a great amount of CD; all of them with adequate physicochemical properties in terms of size, polydispersity and zeta potential, and a very high association capacity of pDNA.

3.2. Study of the toxicity of the nanocarrier and its interaction with the selected target cells (Calu-3 cells)

A critical step towards the design of a new pDNA carrier is the information about its ability to enter the target cells. However, since this ability is often connected with cytotoxicity, we found it important to evaluate first the toxicity of these new nanocarriers in the Calu-3 cell line model (proliferating cells). We chose cells in the

proliferating stage due to their greater sensitivity against toxic materials than the well differentiated cells (Teijeiro-Osorio et al., 2005).

The percentage of cell viability as a function of the administered nanoparticle dose ($\mu g/cm^2$) is depicted in **Figure 2**. It can be noted that CD/CS nanoparticles exhibit a significantly lower cytotoxicity than those composed of solely CS. More specifically, the estimated IC_{50} values, which are the nanoparticle doses causing a reduction of 50% cell viability, were 3-fold higher for CD-containing nanoparticles than for the CS control nanoparticles. This very good viability profile exhibited by this new generation of polysaccharide nanoparticles could be easily explained by the good safety record of CD (Challa et al., 2005). Moreover, when comparing both types of CD-containing nanoparticles, we observed a significantly lower toxicity for those containing CM-β-CD than those containing SB-β-CD.

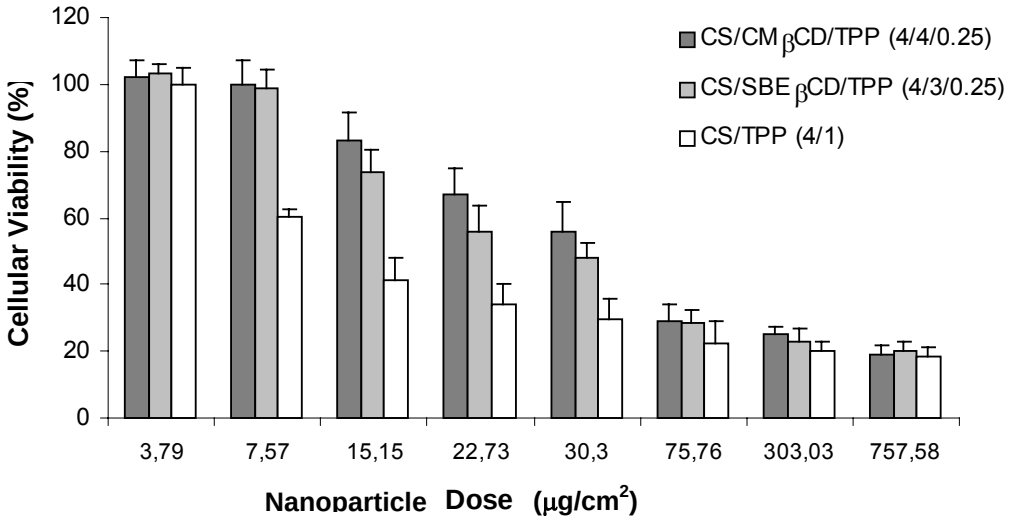

Figure 2. Sensitivity of Calu-3 proliferating cells toward various doses of different nanoparticle formulations (CS/SBE-β-CD/TPP, CS/CM-β-CD/TPP, CS/TPP) determined by the MTT assay (means ± SD, *n* = 8). * Denotes significant differences (*P* < *0.05*).

In a second stage, once we knew about the cytotoxicity of the nanocarriers, we studied the interaction of nanoparticles with the Calu-3 cells. For this specific type of study we selected differentiated rather than proliferating cells. The Calu-3 differentiated cells are considered as an appropriate model for the nasal and bronchotracheal airway epithelia because of its features typically observed in the normal human tissues, such as tight junctions, high TEER values and mucous excretions (Witschi and Mrsny, 1999; Florea et al., 2002). Additionally, as previously mentioned in the methodology section, Calu-3 differentiated cells were cultured at an air-liquid interfase (removal of apical culture medium one day after seeding), in order to better reproduce the physiological situation (Borchard, 2002; Grainger et al., 2006).

The study of the interaction of the nanocarriers with the cells was performed by confocal fluorescence microscopy. Therefore, for the purpose of this study we also developed fluorescent nanoparticles from a fluorescent CS derivative (Fl-CS). The results showed that the labelling procedure did not alter the physicochemical properties of the nanoparticles.

The Calu-3 monolayer was then exposed to the fluorescent nanoparticles and the cell nuclei were stained with propidium iodide in order to facilitate the localization of the particles in the cells. As noted by the localization of the green signal corresponding to the nanoparticles, the CLSM images depicted in **Figure 3A** (x-y sections) indicate that, irrespective of their composition, the nanoparticles were effectively internalized by the cells. The localization of the nanoparticles can be better visualized in the x-z cross sections of the cells, in which the green fluorescence derived from the nanoparticles can be localized around the cell nuclei (red emission) (example shown on **Figure 3B**). These results are in accordance with previous studies reported by our group for CS nanoparticles (Koping-Hoggard et al., *submitted*) and CS/hyaluronic acid nanoparticles (De la Fuente et al., *submitted a*), and provides a good indication of their potential as gene carriers. The mechanism of this transcellular penetration is thought to occur predominantly by adsortive

endocytosis iniciated by nonspecific interactions between nanoparticles and cell membranes (Huang et al., 2002).

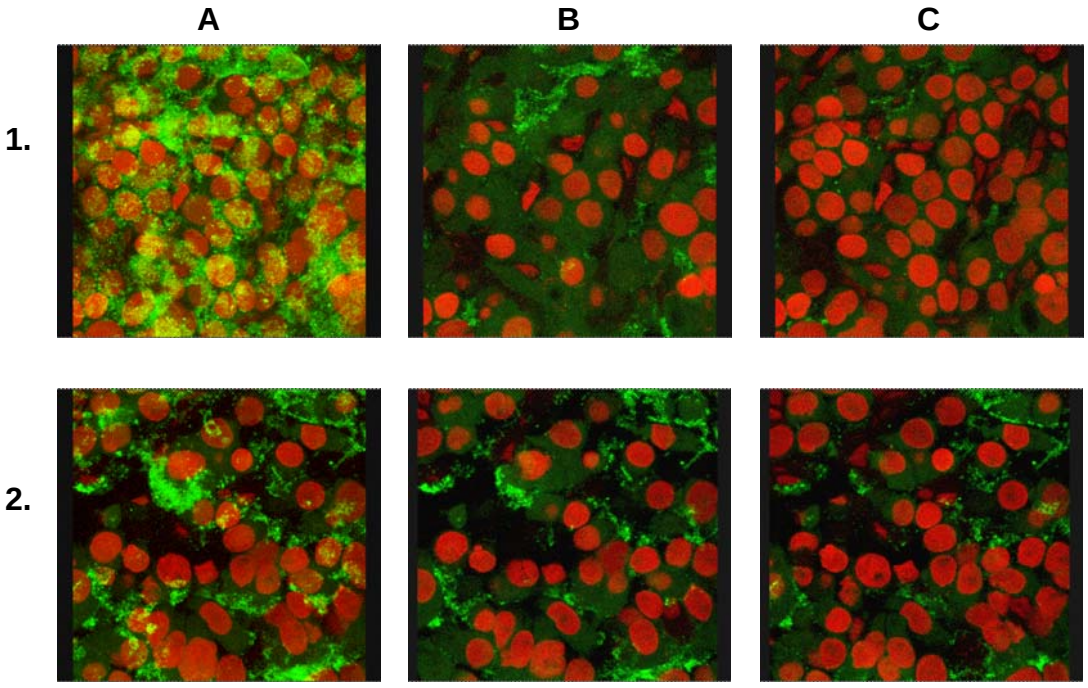

Figure 3A. Confocal laser scanning microphotograps of Calu-3 cells incubated with (1) CS/CM-β-CD/TPP and (2) CS/SBE-β-CD/TPP nanoparticles prepared with fluorescein-labelled chitosan (Fl-CS, green channel), x-y cross sections: A) epithelium surface, B) 5 μm, and C) 10 μm. Cell nuclei are stained with propidium iodide (red channel).

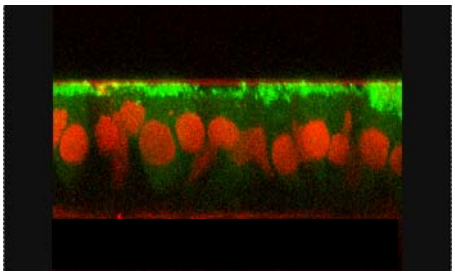

Figure 3B. Confocal laser scanning microphotograps of Calu-3 cells incubated with CS/CM-β-CD/TPP nanoparticles prepared with fluorescein-labelled chitosan (Fl-CS, green channel), x-z section. Cell nuclei are stained with propidium iodide (red channel).

3.3. Study of the capacity of the gene-loaded nanocarrier to achieve cell transfection

Following the observation of the capacity of the nanocarriers to enter the cells, and with the final goal of exploring their potential in gene therapy, we studied their ability to transfect the cell monolayer. It should be pointed out that the *in vitro* transfection studies are commonly carried out in proliferating and fast-growing cells, which are relatively easy to transfect. In contrast, the well-differentiated cells, which represent a most adequate model of the in vivo situation, are difficult to transfect since they are not prepared to easily accept a foreign pDNA (Florea et al., 2002). For this reason, we selected these Calu-3 differentiated cells as an useful tool for predicting their further real possibilities in gene therapy.

For this study we used a non-invasive method previously reported for epidermal (REK cells) and corneal (HCE cells) cell culture models (Paasonen et al., 2006; De la Fuente et al., *submitted b*). More specifically, the nanoparticles containing pSEAP were added to the monolayer and the amount of alkaline phosphatase produced by the cells and, then, secreted to the culture medium was determined for up to 6 days. The nanoparticle dose selected for this study was of 45 μg/cm^2, which resulted in a cellular viability within 90-100% in differentiated Calu-3 cells (data not shown).

As shown in **Figures 4** and **5**, transfection with naked pDNA produced very low gene expression, whereas all the nanoparticle formulations were able to elicit a significantly higher response. This fact can also be clearly noted in **Table 4,** which depicts the pharmacokinetic parameters of SEAP secretion by the monolayer. The maximum transfection levels were observed at 2 days post-incubation in all cases. The comparison of the efficiency of the nanocarrier prototypes (**Figure 4**), led us to the conclusion that the nanocarriers composed by CS and CM-β-CD are the most promising, since they elicit values which are closed to those of positive control (CS nanoparticles). The lower efficacy of SBE-β-CD/CS nanoparticles could be related to the strong electrostatic interaction between CS and SBE-β-CD, which may prevent the intracellular DNA release. Interestingly, this reduced efficacy was not observed for the nanoparticles made of LMwCS (**Figure 5**), in which case both prototypes containing either SBE-β-CD or CM-β-CD elicited a similar and high expression level.

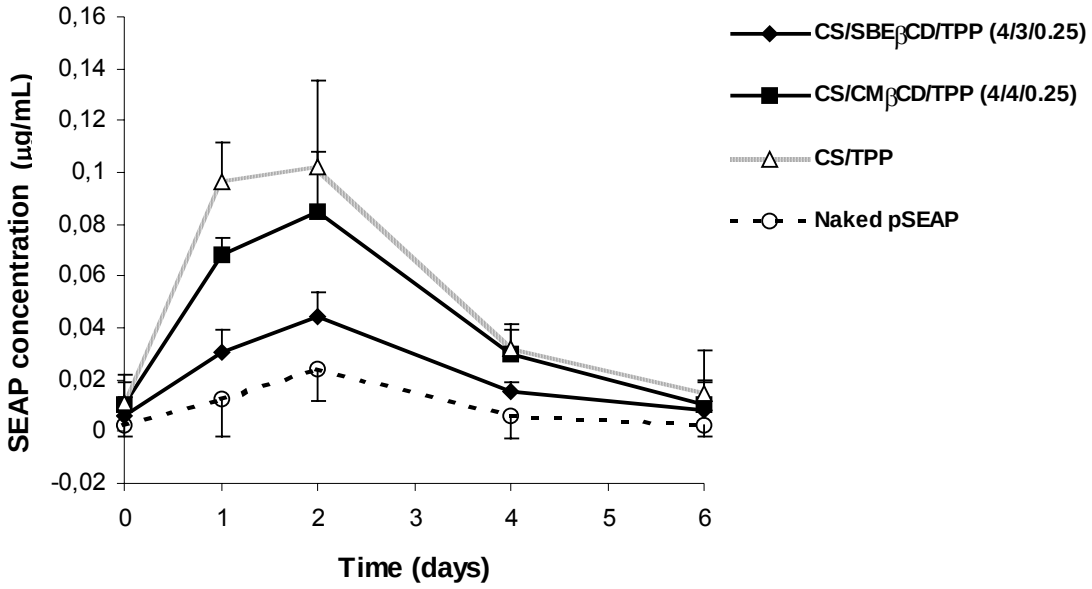

Figure 4. Secreted alkaline phosphatase (SEAP) concentration in the Calu-3 cell culture model after transfection with naked pDNA and three different nanoparticle formulations (CS/SBE-β-CD/TPP; CS/CM-β-CD/TPP; and CS/TPP) encapsulating pDNA (means ± S.D., *n* = 5).

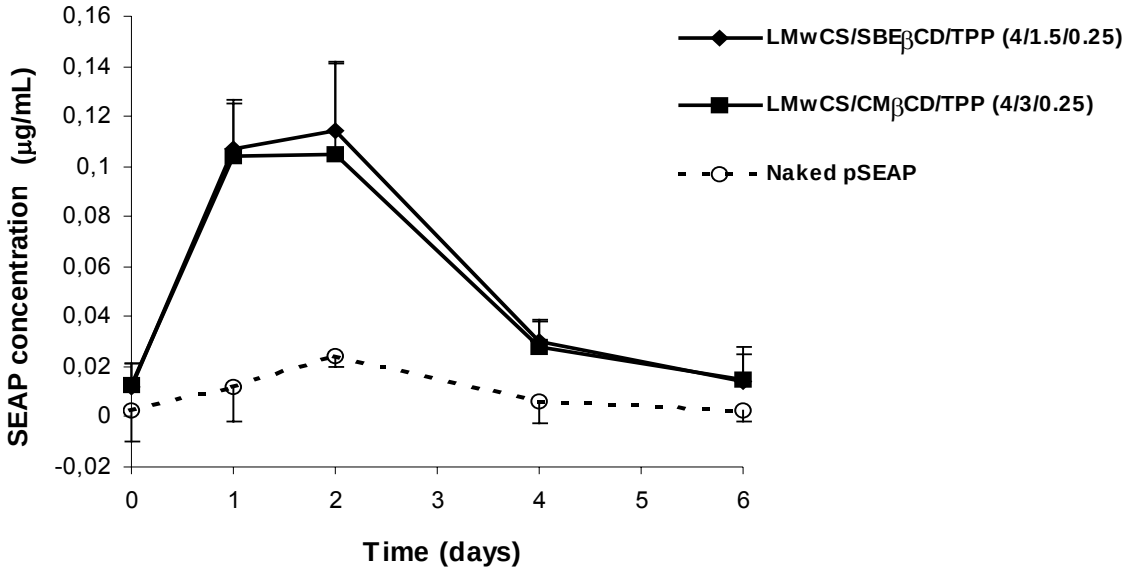

Figure 5. Secreted alkaline phosphatase (SEAP) concentration in the Calu-3 cell culture model after transfection with naked pDNA and two different nanoparticle formulations (LMwCS/SBE-β-CD/TPP; LMwCS/CM-β-CD/TPP) encapsulating pDNA (means ± S.D., *n* = 5).

Moreover, this response was significantly higher than the one obtained with the original CS (Mw 100 KDa) (**Figure 4; Table 4**). These results agree with those reported by other authors, who related the higher efficacy of nanoparticles and polyplexes composed of low Mw CS with the easier intracellular release of the pDNA (Koping-Hogard et al., 2004; Koping-Hogard et al., *submitted*). A similar finding was described by De la Fuente et al. for the nanoparticles composed of hyaluronic acid and different CS Mw (De la Fuente el al., *submitted b*).

To summarize, this final step of the work represents a clear evidence of the ability of this new generation of polysaccharide nanocarriers to transfect complex and structured cell monolayers such as the Calu-3 monolayer.

Table 4. Pharmacokinetic parameters of the SEAP expression by the Calu-3 cell culture model after transfection with naked DNA (gWiz™pSEAP) and several nanoparticle formulations (means ± S.D, *n* = 5).

Formulation	C_{max} (μg/mL)	Cumulative SEAP secretion* (μg)	AUC (μg h/mL)
gWiz™pSEAP	0.024 ± 0.01	0.045 ± 0.01	2.33 ± 0.41
CS/SBE-β-CD/TPP	0.044 ± 0.01	0.101 ± 0.03	4.39 ± 1.76
CS/CM-β-CD/TPP	0.084 ± 0.02	0.202 ± 0.02	10.16 ± 0.93
CS/TPP	0.102 ± 0.03	0.255 ± 0.05	12.50 ± 2.33
LMwCS/SBE-β-CD/TPP	0.113 ± 0.03	0.276 ± 0.04	13.45 ± 1.61
LMwCS/CM-β-CD/TPP	0.105 ± 0.04	0.264 ± 0.04	12.72 ± 1.60

* after 6 days

Conclusions

In this work we present a new generation of polysaccharide nanocarriers consisting of CD and CS as a nonviral gene delivery system. Besides their great pDNA association capacity, these nanoparticles exhibit a low citotoxicity and the ability to enter the cells, deliver the associated DNA and elicit high levels of protein expression. Consequently, these nanocarriers represent a promising approach for gene therapy at the level of mucosal surfaces and, in particular the respiratory mucosa.

Acknowledgments

This work has been supported by the European Commission within the 6th Framework programme – NanoBiosaccharides – Contract nr. 013882. The first author acknowledges the pre-doctoral fellowship granted by this Program.

References

1. Arima H., Kihara F., Hirayama F., Uekema K., Enhancement of gene expression by polyamidoamine dendrimer conjugates with α-, β-, and γ-cyclodextrins, Bioconjugate Chem., 12 (2001) 476-484.
2. Borchard G., Calu-3 cells, a valid model for the airway epithelium?, S.T.P. Pharm. Sci., 12 (2002) 205-211.
3. Brigham K.L.,. Lane K.B, Meyrick B., Stecenko A.A. , Strack S., Cannon D.R., Caudill M., Canonico A.E., Transfection of nasal mucosa with a normal alpha$_1$-antitrypsin gene in alpha$_1$-antitrypsin-deficient subjects: comparison with protein therapy, Human Gene Therapy, 11 (2000) 1023-1032.
4. Calvo P., Remuñán-López C., Vila-Jato J.L., Alonso M.J., Novel hydrophilic chitosan-polyethylene oxide nanoparticles as protein carriers, J. Appl. Pol. Sci., 63 (1997) 125-132.
5. Challa R., Ahuja A., Ali J., Khar R.K., Cyclodextrins in drug delivery: an updated review, AAPS PharmSciTech, 6 (2005) E329-E357 (http://www.aapspharmscitech.org).
6. Cryan S.-A., Holohan A., Donohue R., Darcy R., O´Driscoll C.M., Cell transfection with polycationic cyclodextrin vectors, Eur. J. Pharm. Sci., 21 (2004) 625-633.
7. Csaba N., Sánchez A., Fernández-Mejía E., Novoa-Carballal R., Alonso M.J., Chitosan nanoparticles for the delivery of plasmid DNA. Preparation and characterization, *submitted*
8. De Campos A.M, Diebold Y., Carvalho E.L.S., Sánchez A., Alonso M.J., Chitosan nanoparticles as new ocular drug delivery systems: in vitro stability, in vivo fate, and cellular toxicity, Pharm. Res., 21 (2004) 803-810.

9. De la Fuente M., Seijo B., Alonso M.J., A novel bioactive nanocarrier for ocular gene delivery: hyaluronan-chitosan nanoparticles, *submitted (a).*

10. De la Fuente M., Seijo B., Alonso M.J., New hyaluronic acid-chitosan nanoparticles as ocular gene carriers: studies in human corneal and conjunctival epithelial cell lines, *submitted (b).*

11. Felt O., Buri P., Gurny R., Chitosan: a unique polysaccharide for drug delivery, Drug Dev. Ind. Pharm., 24 (1998) 979-993.

12. Florea B.I., Meaney C., Junginger H.E., Borchard G., Transfection efficiency and toxicity of polyethylenimine in differentiated Calu-3 and nondifferentiated COS-1 cell cultures, AAPS PharmSci, 4 (2002) E12 (http://www.aapspharmsci.org).

13. Forrest M.L., Gabrielson N., Pack D.W., Cyclodextrin-Polyethylenimine conjugates for targeted in vitro gene delivery, 89 (2005) 416-423.

14. Gautam A., Waldrep C.J., Densmore C.L., Delivery systems for pulmonary gene therapy, Am. J. Respir. Med., 1 (2002) 35-46.

15. Graham S.M., Launspach J.L., Utility of the nasal model in gene transfer studies in cystic fibrosis, Rhinol., 35 (1997) 149-153.

16. Grainger C.I., Greenwell L.L., Lockley D.J., Martin G.P., Forbes B., Culture of Calu-3 cells at the air interface provides a representative model of the airway epithelial barrier, Pharm. Res., 23 (2006) 1482-1490.

17. Griesenbach U., Cassady R.L., Ferrari S., Fukumura M., Müller C., Schmitt E., Zhu J., Jeffery P.K., Nagai Y., Geddes D.M., Hasegawa M., Alton E.W.F.W., Molecular Therapy, 5 (2001) 98-103.

18. Guang Liu W., De Yao K., Chitosan and its derivatives-a promissing non-viral vector for gene transfection, J. Control. Rel., 83 (2002) 1-11.

19. Huang M., Ma Z., Khor E., Lim L.-Y., Uptake of FITC-Chitosan nanoparticles by A549 cells, Pharm. Res., 19 (2002) 1488-1494.

20. Hwang S.J., Bellocq N.C., Davis M.E., Effects of structure of β-cyclodextrin-containing polymers on gene delivery, Bioconjugate Chem., 12 (2001) 280-290.

21. Janes K.A., Alonso M.J., Depolymerized chitosan nanoparticles for protein delivery: preparation and characterization, J. Appl. Polym. Sci., 88 (2003) 2769-2776.

22. Katas H., Alpar H.O., Development and characterisation of chitosan nanoparticles for siRNA delivery, J. Control. Rel., 115 (2006) 216-225.

23. Koping-Hoggard M., Csaba N., Alonso M.J., Chitosan nanoparticles as gene delivery systems: effect of chitosan molecular weight and protein-coencapsulation, *submitted.*

24. Koping-Hoggard M., Varum K.M, Issa M., Danielsen S., Christensen B.E., Stokke B.T., Artursson P., Improved chitosan-mediated gene delivery based on easily dissociated chitosan polyplexes of highly defined chitosan oligomers, Gene Therapy, 11 (2004) 1441-1452.

25. Krauland A.H., Alonso M.J., Chitosan/cyclodextrin nanoparticles as macromolecular drug delivery system, Int. J. Pharm., 339 (2007).

26. Lee D., Zhang W., Shirley S.A., Kong X., Hellermann G.R., Lockey R.F., Mohapatra S.S., Thiolated chitosan/DNA nanocomplexes exhibit enhanced and sustained gene delivery, Pharm. Res., 24 (2007) 157-167.

27. Li X.W., Lee D.K.L., Chan A.S.C., Alpar H.O., Sustained expression in mammalian cells with DNA complexes and chitosan nanoparticles, Biochim. Biophys. Acta, 1630 (2003) 7-18.

28. Lollo C.P., Banaszczyk M.G., Chiou H.C., Obstacles and advances in non-viral gene delivery, Curr. Opin. Mol. Ther., 2 (2000) 136-142.

29. Maestrelli F., García-Fuentes M., Mura P., Alonso M.J., A new drug nanocarrier consisting of chitosan and hydroxypropylcyclodextrin, Eur. J. Pharm. Biopharm., 63 (2006) 79-86.

30. Paasonen L., Korhonen M., Yliperttula M., Urtti A., Epidermal cell culture model with tight stratum corneum as a tool for dermal gene delivery studies, Int. J. Pharm., 307 (2006) 188-193.

31. Teijeiro-Osorio D., Remuñán-López C., Nielsen H.M., Comparative studies of chitosan nanoparticles and molecules in Calu-3 and TR146 cells, 32nd Ann. Meet. Exp. Control. Rel. Soc., (2005) 378.

32. Witchi C., Mrsny R. J., In vitro evaluation of microparticles and polymer gels for use as nasal platforms for protein delivery, Pharm. Res., 16 (1999) 382-390.

PARTE II: Discusión general

PARTE II

DISCUSIÓN GENERAL

Recientemente, nuestro grupo de investigación ha diseñado un nuevo sistema nanoparticular compuesto por quitosano (CS) y ciclodextrina (CD) para la administración, a través de mucosas, de principios activos de carácter lipofílico[1] y macromoléculas hidrofílicas[2].

Teniendo en cuenta la versatilidad de este sistema, y tomando como referencia los interesantes resultados que en nuestro laboratorio se han obtenido con nanopartículas de quitosano[3,4,5], el principal objetivo del presente trabajo experimental ha sido el de investigar el potencial de las nanopartículas de CS y CD como vehículos para la administración de macromoléculas terapéuticas a través de mucosas, y más específicamente, a través de la mucosa nasal.

Para los estudios en cultivos celulares se ha seleccionado la línea Calu-3, ampliamente descrita en la bibliografía como un modelo que simula adecuadamente las características del epitelio respiratorio (nasal y tráqueobronquial)[6,7].

---

[1] **Maestrelli F., García-Fuentes M., Mura P., Alonso M.J.**, A new drug nanocarrier consisting of chitosan and hydroxypropylcyclodextrin, Eur. J. Pharm. Biopharm., 63 (2006) 79-86.

[2] **Krauland A.H., Alonso M.J.**, Chitosan/cyclodextrin nanoparticles as macromolecular drug delivery system, Int. J. Pharm., *in press.*

[3] **Janes K.A., Calvo P., Alonso M.J.,** Polysaccharide colloidal particles as delivery systems for macromolecules, Avd. Drug Del. Rev., 47 (2001) 83-97.

[4] **Vila A., Sánchez A., Janes K., Behrens I., Kissel T., Vila-Jato J.L., Alonso M.J.**, Low molecular weight chitosan nanoparticles as new carriers for nasal vaccine delivery in mice, Eur. J. Pharm. Biopharm., 57 (2004) 123-131.

[5] **Alonso M.J., Sánchez A.**, The potential of chitosan in ocular drug delivery, J. Pharm. Pharmacol., 55 (2003) 1451-1463.

[6] **Witchi C., Mrsny R. J.**, In vitro evaluation of microparticles and polymer gels for use as nasal platforms for protein delivery, Pharm. Res., 16 (1999) 382-390.

[7] **Florea B.I., Meaney C., Junginger H.E., Borchard G.**, Transfection efficiency and toxicity of polyethylenimine in differentiated Calu-3 and nondifferentiated COS-1 cell cultures, AAPS PharmSci, 4 (2002) E12 (http://www.aapspharmsci.org).

1. Preparación y caracterización de nanopartículas de quitosano y ciclodextrina

La técnica empleada para la producción de las nanopartículas es la de gelificación iónica, previamente puesta a punto en nuestro laboratorio para la preparación de nanopartículas de CS[8], y ligeramente modificada para la incorporación de CD[9]. Esta técnica es extremadamente suave y, por tanto, adecuada para la encapsulación de macromoléculas terapéuticas.

Para la preparación de los sistemas se utilizaron dos CDs aniónicas diferentes, la carboximetil-β-CD (CM-β-CD) y la sulfobutileter-β-CD (SBE-β-CD) y, opcionalmente, se incluyó tripolifosfato (TPP) como agente reticulante. La selección de derivados de CD de carácter aniónico se basó en que, gracias a su carga negativa, poseen una mayor capacidad de incorporación a las nanoestructuras de CS cargadas positivamente. Estos derivados aniónicos de CD poseen, además, una elevada solubilidad en agua y una toxicidad mínima. De hecho, existen dos formulaciones que contienen SBE-β-CD ya comercializadas para su administración por vía parenteral[10,11].

En primer lugar se seleccionaron los ratios CS/CD y CS/CD/TPP óptimos para cada una de las CDs, SBE-β-CD y CM-β-CD, en términos de obtención de nanopartículas con rendimientos de producción aceptables y que pudiesen ser convenientemente aisladas y resuspendidas.

[8] **Calvo P., Remuñán-López C., Vila-Jato J.L., Alonso M.J.**, Novel hydrophilic chitosan-polyethylene oxide nanoparticles as protein carriers, J. Appl. Pol. Sci., 63 (1997) 125-132.

[9] **Krauland A.H., Alonso M.J.**, Chitosan/cyclodextrin nanoparticles as macromolecular drug delivery system, Int. J. Pharm., *in press.*

[10] **Challa R., Ahuja A., Ali J., Khar R.K.**, Cyclodextrins in drug delivery: an updated review, AAPS PharmSciTech, 6 (2005) E329-E357. (http://www.aapspharmscitech.org).

[11] **Cydex Inc. website**, disponible en: http://www.cydexinc.com, Consultada el 04/05/07.

1.1. Caracterización físico-química y morfológica de las nanopartículas

En la **Tabla 1** se muestran los valores de tamaño, índice de polidispersión, y potencial zeta de los sistemas obtenidos. Todas las formulaciones preparadas presentaron un tamaño nanométrico, variando ligeramente en función de la composición. Concretamente, las nanopartículas compuestas por SBE-β-CD resultaron ser más pequeñas (200-300 nm) que aquéllas preparadas con CM-β-CD (300-400 nm). Esto puede ser debido a una interacción más fuerte entre el CS y la SBE-β-CD (puesto que la SBE-β-CD posee un mayor grado de sustitución que le confiere una más alta densidad de carga negativa), que conduciría a la obtención de nanoestructuras con un mayor grado de compactación y, por tanto, de menor tamaño. Por otra parte, la carga superficial o potencial zeta de las partículas presentó valores positivos en todos los casos, entre +17 y +32 mV.

Tabla 1. Características físico-químicas de nanopartículas de CS/SBE-β-CD y CS/CM-β-CD con o sin TPP.

Tipo de CD	CS/CD/TPP[a]	Tamaño (nm)	I.P [b]	Potencial Zeta (mV)
SBE-β-CD	4/2/0.5	299 ± 25	0.36-0.46	+32 ± 0.3
	4/3/0.25	264 ± 18	0.23-0.37	+27 ± 0.6
	4/3/0	200 ± 13	0.11-0.16	+ 26 ± 1.4
	4/4/0	238 ± 16	0.08-0.10	+ 27 ± 2.4
CM-β-CD	4/3/0.5	392 ± 36	0.27-0.44	+28 ± 2.3
	4/4/0.25	358 ± 13	0.43-0.46	+17 ± 2.2
	4/5/0	346 ± 10	0.60-0.68	+28 ± 3.7
	4/6/0	359 ± 37	0.52-0.59	+29 ± 4.5

[a] Relación en masa; [b] Índice de polidispersión

El estudio morfológico de las nanopartículas (**Figura 1**) reveló que presentan una forma completamente esférica y que además son poblaciones muy homogéneas, independientemente de su composición y presencia de TPP (**Art. 4, Fig. 1**).

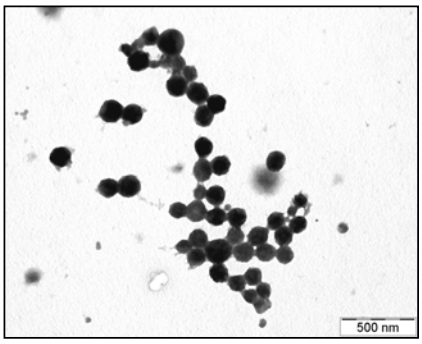

Figura 1. Fotografía obtenida por microscopía electrónica de transmisión de nanopartículas de CS/SBE-β-CD (4/3).

Mediante análisis elemental de las diferentes nanopartículas, se determinaron los porcentajes reales de cada componente (CS, CD y TPP) presente en las mismas (**Art. 4, Fig. 2**). La eficacia de incorporación de las CDs fue muy elevada, detectándose una cantidad de CD incluso superior al 50% de la composición total de las nanopartículas. Esto es especialmente importante dadas las interesantes propiedades de las CDs[12,13], mencionadas con anterioridad.

[12] **Loftsson T., Brewster M.E.**, Pharmaceutical applications of cyclodextrins. 1. Drug solubilization and stabilization, J. Pharm. Sci., 85 (1996) 1017-1025.

[13] **Uekama K., Hirayama F., Irie T.**, Cyclodextrin drug carrier systems, Chem. Rev., 98 (1998) 2045-2076.

1.2. Estudios de citotoxicidad

Un importante parámetro a la hora de valorar el potencial de un nuevo vehículo de liberación de fármacos es su toxicidad celular. Teniendo esto en cuenta, la toxicidad de las nanopartículas de CS/SBE-β-CD y CS/CM-β-CD fue evaluada incubando dosis crecientes de las mismas sobre células Calu-3 en proliferación. Del mismo modo, y con la intención de determinar el efecto de la incorporación de CDs sobre la citotoxicidad de los sistemas, se ensayaron como control nanopartículas compuestas únicamente por CS.

Como se muestra claramente en la **Figura 2**, las nanopartículas que contienen CD en su composición resultaron ser menos tóxicas en un amplio rango de dosis, lo que puede ser atribuido al excelente perfil de biocompatibilidad de las CDs[14]. Concretamente, los valores de IC_{50} fueron aproximadamente 3 veces mayores que para la formulación de CS sin CD.

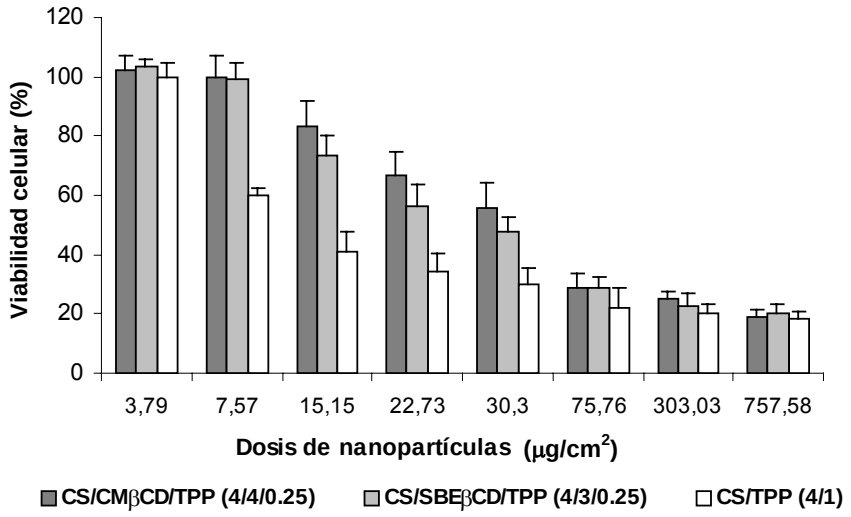

Figura 2. Estudio de viabilidad celular tras la incubación de células Calu-3 con distintas formulaciones y dosis de nanopartículas durante 2 h.

[14] **Challa R., Ahuja A., Ali J., Khar R.K.**, Cyclodextrins in drug delivery: an updated review, AAPS PharmSciTech, 6 (2005) E329-E357. (http://www.aapspharmscitech.org).

Por otro lado, las pequeñas diferencias encontradas entre los sistemas compuestos por una u otra CD podrían deberse a sus diferentes cargas superficiales (ver **Tabla 1**), dada la bien establecida relación entre citotoxicidad y densidad de carga positiva[15].

2. Aplicación de las nanopartículas a la administración nasal de péptidos y proteínas

2.1. Interacción de las nanopartículas con el epitelio nasal

Para evaluar el potencial de nanopartículas de CS y CD como vehículos de transporte de macromoléculas a través del epitelio nasal, se consideró de gran interés el estudio de su interacción con el mismo. Este objetivo se abordó de dos formas diferentes; una de ellas dirigida a evaluar el efecto de los sistemas en términos de modulación de la barrera intercelular, lo que se midió mediante la monitorización de los cambios en la resistencia transepitelial (TEER); y la otra vertiente del estudio dirigida a la visualización del proceso de interacción de las nanopartículas con el epitelio, mediante microscopía confocal (CLSM).

- Efecto sobre las uniones "tight" intercelulares: estudios de TEER

El efecto de nanopartículas de CS/CD (CS/SBE-β-CD y CS/CM-β-CD) sobre las uniones "tight" intercelulares o, lo que es lo mismo, sobre el grado de unión de las células epiteliales, se llevó a cabo en células Calu-3 diferenciadas, que como ya se mencionó con anterioridad, representan un modelo adecuado del epitelio nasal. Puesto que el CS, en solución[16,17] o en forma nanoparticular[18,19], y algunas CDs[20]

[15] **Forrest M.L., Gabrielson N., Pack D.W.**, Cyclodextrin-Polyethylenimine conjugates for targeted in vitro gene delivery, 89 (2005) 416-423.

[16] **Smith J., Wood E., Dornish M.**, Effect of chitosan on epithelial cell tight junctions, *Pharm. Res.*, 21 (2004) 43-49.

[17] **Dodane V., Khan M.A., Merwin J.R.**, Effect of chitosan on epithelial permeability and structure, Int. J. Pharm., 182 (1999) 21-32.

han demostrado actuar sobre la permeabilidad de diferentes epitelios mediante la disminución de la TEER, cabía esperar que las nanopartículas de CS/CD fuesen capaces de mediar un efecto al menos similar. Para comprobarlo, las células fueron expuestas a diferentes dosis de nanopartículas de CS/CD, midiendo los valores de TEER a distintos tiempos hasta las 2 h y, una vez retiradas las muestras, hasta las 12 h (para comprobar la reversibilidad del efecto, si lo hubiese). Mientras los controles (HBSS pH 6.4 y HBSS pH 7.4) no produjeron cambios, las nanopartículas de CS/CD redujeron la TEER de una manera significativa incluso a la menor de las dosis ensayadas (40 $\mu g/cm^2$) (**Art. 4, Fig. 3**). Para las dosis de nanopartículas mayores (75 y 150 $\mu g/cm^2$) el descenso de la TEER fue más acusado y tendió a igualarse entre las dos formulaciones (CS/ SBE-β-CD y CS/ CM-β-CD). En líneas generales, se puede hablar de un efecto dosis-dependiente y saturable (**Art. 4, Tabla 3**), como se ha descrito anteriormente para el CS en solución[21,22].

Este descenso de la TEER, que suele atribuirse principalmente a la apertura de uniones "tight" intercelulares supone, en cualquier caso, un aumento de la permeabilidad del epitelio al paso de moléculas por vía paracelular, lo que demuestra el potencial de estos sistemas como promotores de la absorción de fármacos. Interesantemente, se registró una completa reversibilidad del efecto, lo que indicaría que las células se encuentran funcionalmente intactas tras el experimento.

---

[18] **Teijeiro-Osorio D., Remuñán-López C., Nielsen H.M.**, Comparative studies of chitosan nanoparticles and molecules in Calu-3 and TR146 cells, 32nd Ann. Meet. Exp. Control. Rel. Soc., (2005) 378.

[19] **Prego C., García M., Torres D., Alonso M.J.**, Transmucosal macromolecular drug delivery, J. Control. Rel., 101 (2005) 151-162.

[20] **Marttin E., Verhoef J.C., Merkus F.W.H.M.**, Efficacy, safety and mechanism of cyclodextrins as absorption enhancers in nasal delivery of peptide and protein drugs, J. Drug Target., 6 (1998) 17-36.

[21] **Artursson P., Lindmark T., Davis S.S., Illum L.**, Effect of chitosan on permeability of monolayers of intestinal epithelial cells (Caco-2), Pharm. Res., 11 (1994) 1358-1361.

[22] **Kotze A.F., Lueβen H.L., De Boer A.G., Verhoef J.C., Junginger H.E.**, Chitosan for enhanced intestinal permeability: prospects for derivatives soluble in neutral and basic environments, Eur. J. Pharm. Sci., 7 (1998) 145-151.

- Transporte de las nanopartículas a través del epitelio nasal: estudios de CLSM tras su administración "in vivo"

La efectividad de cualquier formulación administrada por vía nasal va a estar altamente influenciada por el rápido aclaramiento mucociliar que tiene lugar en la cavidad nasal, una de las principales limitaciones de esta vía. Así pues, en el caso concreto de las nanopartículas, la interacción de las mismas con el epitelio va a condicionar en gran parte el éxito de la terapia a la que estén dirigidas. Para el estudio de la capacidad de las nanopartículas de CS/CD de adherirse y/o atravesar el epitelio nasal, se utilizó CS marcado con fluoresceína (Fl-CS), el cual no modificó las características de las formulaciones resultantes (**Art. 4, Tabla 4**) y permitió su visualización. Tras la administración por vía intranasal a ratas de la suspensión de nanopartículas marcadas, los animales fueron sacrificados y la mucosa nasal extraída y fijada para su observación directa por CLSM. La presencia de nanopartículas se identificó con facilidad mediante la simple comparación de la mucosa tratada con las mismas frente al tejido control (mucosa no tratada). En la **Figura 3** se presenta una serie imágenes que corresponden a secciones transversales de la mucosa, tratada con nanopartículas de Fl-CS/CD (Fl-CS/SBE-β-CD) y no tratada, desde la superficie de la misma hasta una profundidad de 15 μm. Dichas fotografías ponen en evidencia la capacidad de las nanopartículas de CS/CD para atravesar superficies mucosas, mostrando así su capacidad para actuar como verdaderos vehículos de moléculas activas. Este hecho coincide con lo descrito para otros sistemas coloidales[23,24] evaluados bajo condiciones experimentales similares.

[23] **Vila A., Sánchez A., Janes K.A., Behrens I., Kissel T., Vila-Jato J.L., Alonso M.J.**, Low molecular weight nanoparticles as new carriers for nasal vaccine delivery in mice, Eur. J. Pharm. Biopharm., 57 (2004) 123-131.

[24] **Csaba N., Sánchez A., Alonso M.J.**, PLGA:Poloxamer and PLGA:Poloxamine blen nanostructures as carriers for nasal gene delivery, J. Control. Rel., 113 (2006) 164-172.

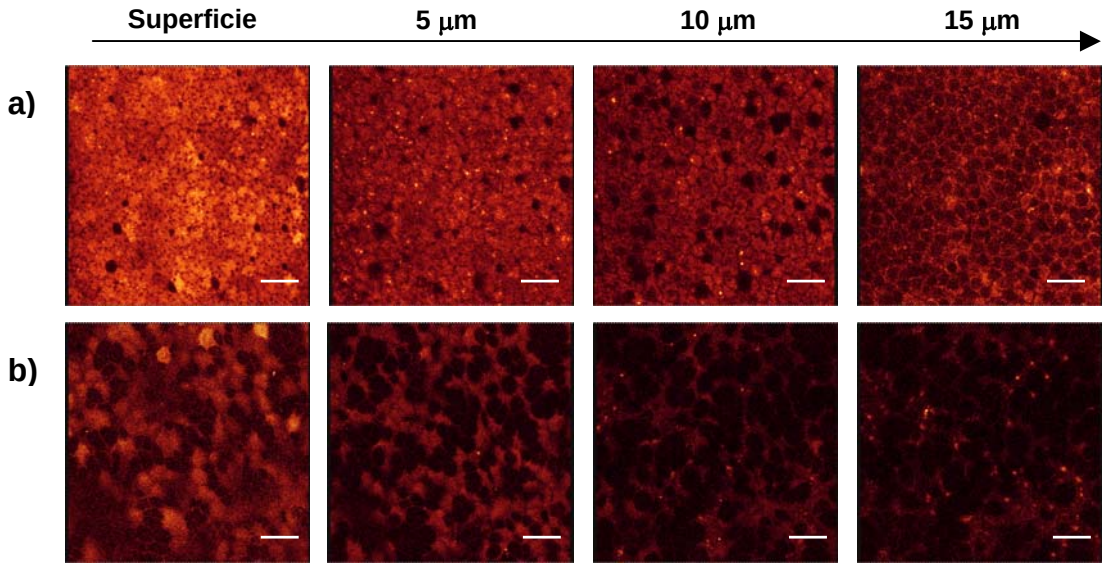

Figura 3. Imágenes de microscopía confocal de mucosa nasal: (a) tras la administración de nanopartículas de FI-CS/SBE-β-CD (4/4) y (b) sin tratamiento. Imagen de superficie y cortes a distintas profundidades (5, 10 y 15 μm). Escala = 20 μm.

Al menos de un modo cualitativo, no se registraron diferencias entre las formulaciones preparadas con una u otra CD, SBE-β-CD o CM-β-CD (**Art. 4, Figura 4**).

2.2. Estudios *in vivo*

Teniendo en cuenta la aplicación final de estos sistemas nanoparticulares de CS y CD, se investigó su potencial como vehículos de macromoléculas *in vivo*. Para ello se encapsuló insulina como molécula modelo, dada la facilidad de medir los niveles de glucemia y, de este modo, la eficacia de las formulaciones.

En la **Tabla 2** se representan las características físico-químicas de las formulaciones de CS/SBE-β-CD y CS/CM-β-CD cargadas con insulina. Las nanopartículas presentaron un adecuado tamaño (≈300-400 nm), carga superficial positiva y una elevada eficiencia de asociación de insulina (> 88%). Esta elevada

asociación del péptido, que condujo a valores de capacidad de carga de las nanopartículas de hasta casi un 47%, podría explicarse principalmente por la interacción electrostática entre la insulina, que al pH básico de la fase de CD y TPP se encuentra cargada negativamente, y los grupos amino del CS, cargados positivamente[25].

Tabla 2. Características de nanopartículas de CS/SBE-β-CD/TPP y CS/CM-β-CD/TPP cargadas con insulina.

Tipo de CD	CS/CD/TPP[a]	Tamaño (nm)	I.P [b]	Potencial Zeta (mV)	Eficiencia de asociación[c] (%)	Capacidad de carga (%)
SBE-β-CD	4/3/0.25	327 ± 27	0.21-0.42	+ 32 ± 0.1	94.9 ± 0.1	23.3 ± 1.9
CM-β-CD	4/4/0.25	436 ± 34	0.10-0.23	+ 23 ± 0.4	88.6 ± 0.8	46.7 ± 0.8

[a] Relación en masa; [b] Índice de polidispersión
[c] Concentración de insulina en la fase SBE-β-CD/TPP o CM-β-CD/TPP: 2.4 mg/mL

Los estudios *in vivo* consistieron en la administración nasal a conejos de ambas formulaciones de nanopartículas de CS/CD conteniendo insulina, así como de un control constituido por el péptido en solución. Los resultados obtenidos mostraron que las nanopartículas produjeron un descenso máximo de los niveles de glucosa plasmática en torno a un 35% con respecto al nivel basal, frente a sólo un 14% producido por la administración de la misma dosis de insulina en solución (5 UI/Kg) (**Figura 4**). A pesar de la diferente composición de los sistemas (CS/SBE-β-CD y CS/CM-β-CD) y la diferente capacidad de carga de insulina de los mismos (23 y 47%, respectivamente), el efecto hipoglucémico obtenido fue muy similar. El hecho de que las nanopartículas de CS/CM-β-CD presenten una capacidad de carga 2 veces mayor que la de las de CS/SBE-β-CD, y consigan igualar la respuesta hipoglucémica de éstas implica que la efectividad no se vio influenciada

[25] **Krauland A.H., Alonso M.J.**, Chitosan/cyclodextrin nanoparticles as macromolecular drug delivery system, Int. J. Pharm., 2007

por la cantidad de CS y CD presente en la formulación, lo cual había sido previamente demostrado por nuestro grupo con nanopartículas compuestas únicamente por CS[26], siendo 0.160 mg/Kg la menor dosis de polímero utilizada en el estudio. En el presente trabajo, gracias a la presencia de CD en la composición de los sistemas, la dosis de CS utilizada fue aún más reducida, concretamente de 0.096 mg/Kg, hecho que, sin afectar a la eficacia de los sistemas, sin duda contribuirá a minimizar aún más la toxicidad de los mismos.

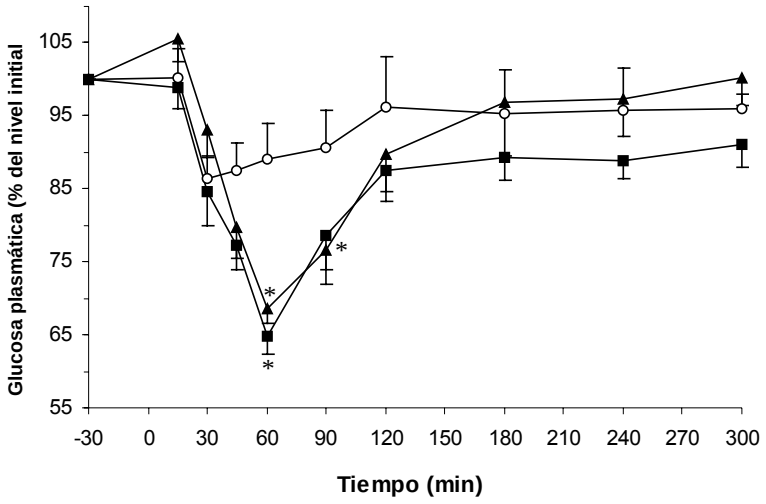

Figura 4. Niveles de glucemia obtenidos en conejos tras la administración nasal a pH 4.3 de: (o) insulina en solución, (■) nanopartículas de CS/SBE-β-CD/TPP, y (▲) nanopartículas de CS/CM-β-CD/TPP (Media ± SEM, n = 6). * Denota diferencias significativas con respecto a la solución de insulina ($p < 0.05$).

[26] **Fernández-Urrusuno R., Calvo P., Remuñán-López C., Vila-Jato J.L., Alonso M.J.**, Enhancement of nasal absorption of insulin using chitosan nanoparticles, Pharm. Res., 16 (1999) 1576-1581.

En base a los resultados de interacción de las nanopartículas de CS/CD con el epitelio reflejados en el **Apartado 2.1** y estudios previos realizados por nuestro grupo de investigación[27,28,29] con diferentes sistemas nanoparticulares, se pueden sugerir dos principales mecanismos por los que las nanopartículas son capaces de incrementar la absorción sistémica de insulina. Por una parte, las nanopartículas se adhieren al epitelio nasal donde, gracias a sus componentes (CS y CD), actúan como promotores de la absorción mediante la apertura de las uniones "tight" intercelulares y, simultáneamente, liberan la insulina. De este modo, el péptido vería facilitado el paso por vía paracelular. Por otro lado, de un modo minoritario, las nanopartículas pueden ser internalizadas y atravesar el epitelio nasal por vía transcelular, actuando como verdaderos vehículos de macromoléculas.

[27] **Fernández-Urrusuno R., Calvo P., Remuñán-López C., Vila-Jato J.L., Alonso M.J.**, Enhancement of nasal absorption of insulin using chitosan nanoparticles, Pharm. Res., 16 (1999) 1576-1581.

[28] **Fernández-Urrusuno R., Romani D., Calvo P., Vila-Jato J.L., Alonso M.J.**, Development of a freeze-dried formulation of insulin-loaded chitosan nanoparticles intended for nasal administration, S.T.P. Pharma Sci., 9 (1999) 429-436.

[29] **Alonso-Sande M., des Rieux A., Schneider Y.J., Remuñán-López C., Alonso M.J., Préat V.**, Pharm. Res., *sometida a evaluación*.

3. Aplicación de las nanopartículas a la administración nasal de material genético

3.1. Internalización celular de las nanopartículas

Para el estudio del potencial de las nanopartículas de CS/CD como vehículos sintéticos de ADN se evaluó su interacción con células diferenciadas en cultivo mediante microscopía confocal. Para ello se utilizaron nanopartículas preparadas con CS marcado con fluoresceína (emisión en verde) (**Tabla 3**), mientras que para la precisa localización de los sistemas se consideró la utilización de un segundo marcador, el yoduro de propidio (emisión en rojo), como marcador del núcleo celular[30]. Las imágenes mostraron que las nanopartículas penetran de forma eficiente en las células y se distribuyen de forma homogénea en el medio intracelular (**Figura 5b) (Art. 5, Figs. 3a y 3b**), independientemente de su composición (CS/SBE-β-CD o CS/CM-β-CD), tras su incubación con las células. Estos resultados concuerdan con lo observado en el caso de nanopartículas compuestas solo por CS[31] o CS/hialurónico[32] en donde, además, se demostró la muy limitada capacidad de internalización celular del ADN plasmídico en forma libre. Así pues, se puede deducir que el ADN, una vez encapsulado en las nanopartículas de CS/CD, podrá penetrar de manera eficiente al interior de las células.

Adicionalmente, y dada la dificultad que entrañó la realización de un eficiente triple marcaje, se utilizó Bodipy® Phalloidin para la tinción de las membranas celulares sin tratar con las nanopartículas, únicamente como control para observar la correcta formación de la monocapa de células y la morfología de las mismas (**Figura 5a**).

[30] **Csaba N., Sánchez A., Alonso M.J**., PLGA:poloxamer and PLGA:poloxamine blend nanostructures as carriers for nasal gene delivery, J. Control. Rel., 113 (2006) 164-172.

[31] **Csaba N., Sánchez A., Fernández-Mejía E., Novoa-Carballal R., Alonso M.J.**, Chitosan nanoparticles for the delivery of plasmid DNA. Preparation and characterization, *sometida a evaluación.*

[32] **De la Fuente M., Seijo B., Alonso M.J**., New hyaluronic acid-chitosan nanoparticles as ocular gene carriers: studies in human corneal and conjunctival epithelial cell lines, *sometida a evaluación.*

Tabla 3. Características físico-químicas de nanopartículas preparadas con CS marcado con fluoresceína (Fl-CS) y ciclodextrinas.

Tipo de CD	CS/CD/TPP	Tamaño (nm)	I.P [a]	Potencial Zeta (mV)
SBE-β-CD	4/3/0.25	253 ± 13	0.2 - 0.3	+25 ± 1.1
CM-β-CD	4/4/0.25	364 ± 32	0.3 - 0.4	+16 ± 0.8
-	4/0/1	312 ± 11	0.3 - 0.4	+32 ± 1.4

[a] Índice de polidispersión

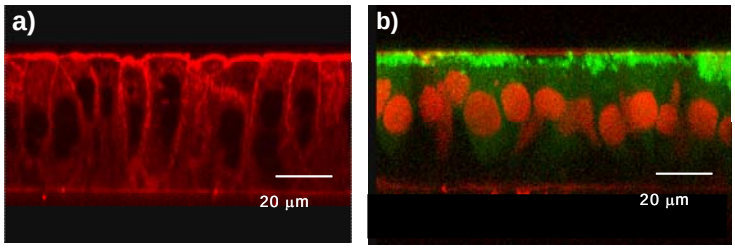

Figura 5. Imágenes de microscopía confocal de: (a) membrana celular no tratada (tinción con Bodipy® Palloidin), y (b) localización de las nanopartículas de Fl-CS/CM-β-CD (fluoresceína, canal verde) tras el estudio de internalización celular (tinción de núcleos con ioduro de propidio, canal rojo).

3.2. Optimización de los sistemas de quitosano y ciclodextrina para su utilización en terapia génica. Asociación de ADN plasmídico.

Así pues, la encapsulación de material genético fue el siguiente objetivo a abordar. Las condiciones de formación de las nanopartículas fueron ligeramente adaptadas, ajustando tanto las concentraciones como los volúmenes de las soluciones de CS, CD y TPP para la preparación de lotes más reducidos, pero sin modificar las relaciones en masa de los componentes. El ADN plasmídico fue

añadido en la fase de CD/TPP previamente a la formación de las nanopartículas, siendo la carga teórica del 5% (p/p). En esta etapa del trabajo se desarrollaron, además, nuevas formulaciones preparadas con CS de bajo peso molecular (≈10 KDa) obtenido por depolimerización del polisacárido comercial (≈110 KDa). Para ello, y en base a mantener fija la carga teórica de ADN en un 5%, fue necesario disminuir la cantidad de CD, debido al elevado número de cargas negativas presentes durante la constitución del nanosistema en relación a las positivas.

Como control, dados los buenos resultados obtenidos recientemente en experimentos de transfección *in vitro* e *in vivo*[33], se prepararon nanopartículas compuestas únicamente por CS y TPP.

Como modelo de ADN plasmídico se utilizó el plásmido SEAP (pSEAP), el cual codifica la expresión de la fosfatasa alcalina. Las características de los diferentes sistemas preparados se muestran en la **Tabla 4**. Se obtuvieron nanopartículas de pequeño tamaño (140-234 nm), reducidos índices de polidispersión y carga superficial positiva (+22-35 mV). En cuanto a la eficacia de encapsulación, los valores fueron muy elevados (>90%), independientemente de la composición de las nanopartículas (**Art. 5, Fig. 1**). Valores similares han sido obtenidos para otros sistemas nanoparticulares que presentan, como denominador común, CS en su composición[34,35]. En este sentido, se ha descrito una fuerte interacción electrostática entre los grupos fosfato del ADN y los grupos amino del CS, además de otras interacciones de tipo hidrofóbico y por puentes de hidrógeno[36].

[33] **Csaba N., Koping-Hoggard M., Alonso M.J.**, Chitosan nanoparticles as gene delivery systems: effect of chitosan molecular weight and protein-coencapsulation, *sometida a evaluación.*

[34] **Csaba N., Sánchez A., Fernández-Mejía E., Novoa-Carballal R., Alonso M.J.**, Chitosan nanoparticles for the delivery of plasmid DNA. Preparation and characterization, *sometida a evaluación.*

[35] **De la Fuente M., Seijo B., Alonso M.J**., New hyaluronic acid-chitosan nanoparticles as ocular gene carriers: studies in human corneal and conjunctival epithelial cell lines, *sometida a evaluación.*

[36] **Li X.W., Lee D.K.L., Chan A.S.C., Alpar H.O.**, Sustained expression in mammalian cells with DNA complexes and chitosan nanoparticles, Biochim. Biophys. Acta, 1630 (2003) 7-18.

Tabla 4. Características físico-químicas de nanopartículas preparadas con CS de peso molecular medio (CS comercial, 110 KDa) y bajo (10 KDa) y CD (SBE-β-CD, CM-β-CD) y cargadas con gWiz™pSEAP al 5%.

CS	CD	CS/CD/TPP [a]	Tamaño (nm)	I.P [b]	Potencial zeta (mV)
Peso molecular medio	SBE-β-CD	4/3/0.25	180 ± 2	0.1 - 0.2	+ 35 ± 6
	CM-β-CD	4/4/0.25	234 ± 15	0.1 - 0.2	+ 25 ± 5
	-	4/0/1	192 ± 25	0.2 - 0.3	+ 34 ± 5
Peso molecular bajo	SBE-β-CD	4/1.5/0.25	143 ± 2	0.0 - 0.1	+ 24 ± 4
	CM-β-CD	4/3/0.25	140 ± 8	0.0 - 0.1	+ 22 ± 6

[a] Relación en masa; [b] Índice de polidispersión

3.3. Estudios de transfección *in vitro*

La utilidad de células Calu-3 diferenciadas como modelo del epitelio respiratorio (nasal, traqueobronquial) ha sido propuesta como método alternativo a los ensayos *in vivo* para la evaluación de la eficiencia de transfección de vehículos de liberación de ADN[37]. Por ello, se ha utilizado en este trabajo para estudiar la capacidad de transfección de las nanopartículas desarrolladas. La selección del pSEAP, que codifica la expresión de fosfatasa alcalina, como plásmido modelo se realizó en base a la posibilidad de cuantificar la proteína secretada al medio de cultivo mediante una técnica no destructiva[38,39] (ver **Figura 7**).

[37] **Florea B.I., Meaney C., Junginger H.E., Borchard G.**, Transfection efficiency and toxicity of polyethylenimine in differentiated Calu-3 and nondifferentiated COS-1 cell cultures, AAPS PharmSci, 4 (2002) E12 (http://www.aapspharmsci.org).

[38] **Paasonen L., Korhonen M., Yliperttula M., Urtti A.**, Epidermal cell culture model with tight stratum corneum as a tool for dermal gene delivery studies, Int. J. Pharm., 307 (2006) 188-193.

[39] **De la Fuente M., Seijo B., Alonso M.J.**, A novel bioactive nanocarrier for ocular gene delivery: hyaluronan-chitosan nanoparticles, *sometida a evaluación.*

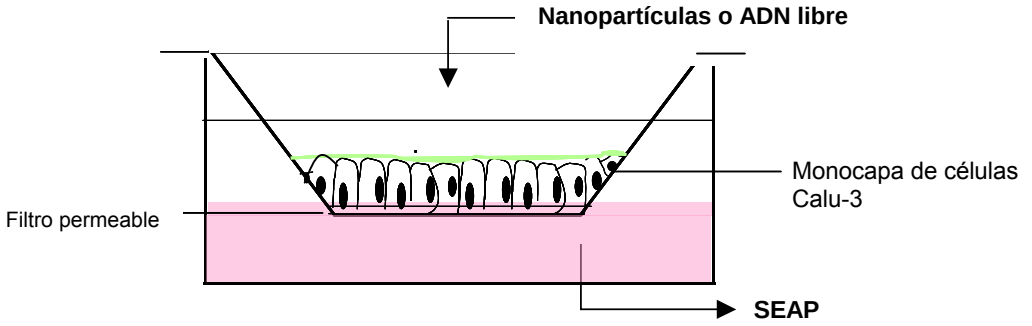

Figura 7. Dibujo esquemático del experimento de transfección en células diferenciadas.

Las formulaciones ensayadas fueron las representadas en la **Tabla 4**. Tras la incubación de las nanopartículas sobre las células, la expresión de proteína secretada al medio de cultivo (compartimiento basolateral) fue cuantificada durante 6 días. En la **Figura 8** se muestran las cantidades acumuladas de proteína expresada correspondientes a las diversas formulaciones y, como se puede apreciar, existen diferencias notables entre los resultados obtenidos para cada una de ellas. Todas las formulaciones ensayadas dieron lugar a un mayor nivel de expresión que el plásmido libre. Si se comparan los resultados obtenidos con las nanopartículas de CS de peso molecular medio (**Figura 8a**), se observa que las de CS/CM-β-CD produjeron los mayores niveles de expresión, alcanzando niveles similares a los obtenidos con las nanopartículas utilizadas como control positivo (CS/TPP). Sin embargo, y aunque no era esperable, la formulación compuesta por CS/SBE-β-CD no dio lugar a niveles de expresión significativamente superiores a los alcanzados con el plásmido libre. Posiblemente, el mayor grado de sustitución de la SBE-β-CD, que le confiere más carga negativa, sería responsable de una interacción más fuerte entre CS y CD que dificultaría la liberación del plásmido.

Por otra parte, las nanopartículas preparadas con CS de bajo peso molecular mediaron niveles de expresión prácticamente idénticos y elevados,

independientemente del tipo de CD (**Figura 8b**), resultando ser mayores que aquellos obtenidos para los sistemas compuestos por CS de peso molecular medio. Estos resultados concuerdan con los obtenidos en diversos estudios realizados con nanopartículas de CS y CS/hialurónico y complejos de CS-ADN plasmídico, en los cuales las mayores eficacias de transfección encontradas con la utilización de CS de bajo peso molecular se atribuyeron a una más fácil y rápida liberación intracelular del plásmido mientras, en el caso de las nanopartículas, se preserva igualmente la capacidad de proteger el ADN de la degradación[40,41,42] . Asimismo, esta más débil asociación del CS y el ADN plasmídico podría explicar los elevados niveles de transfección obtenidos con las nanopartículas de CS de bajo peso molecular y SBE-β-CD, en comparación con los descritos para la formulación equivalente preparada con CS de peso molecular medio.

[40] **Koping-Hoggard M., Varum K.M, Issa M., Danielsen S., Christensen B.E., Stokke B.T., Artursson P.**, Improved chitosan-mediated gene delivery based on easily dissociated chitosan polyplexes of highly defined chitosan oligomers, Gene Therapy, 11 (2004) 1441-1452.

[41] **Csaba N., Koping-Hoggard M., Alonso M.J.**, Chitosan nanoparticles as gene delivery systems: effect of chitosan molecular weight and protein-coencapsulation, *sometida a evaluación.*

[42] **De la Fuente M., Seijo B., Alonso M.J.**, New hyaluronic acid-chitosan nanoparticles as ocular gene carriers: studies in human corneal and conjunctival epithelial cell lines, *sometida a evaluación.*

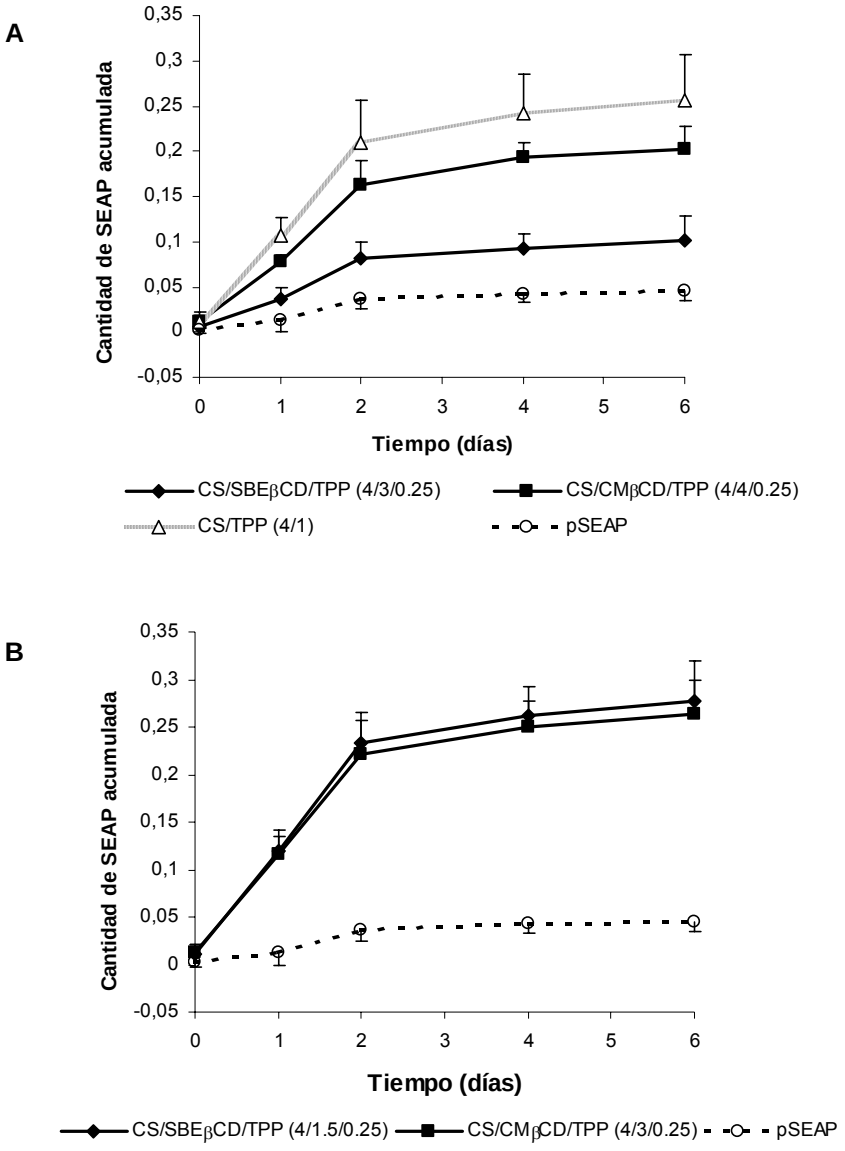

Figura 8. Cantidad acumulada (μg) de fosfatasa alcalina (SEAP) secretada en células diferenciadas Calu-3 tras la transfección con: (A) nanopartículas de CS/CD y CS sólo preparadas con CS de peso molecular medio y (B) nanopartículas de CS/CD preparadas con CS de peso molecular bajo. Control = pSEAP libre.

Conclusiones

CONCLUSIONES

El trabajo experimental que se recoge en la presente memoria se ha dirigido al diseño de sistemas micro- y nanoparticulares constituidos por polisacáridos y destinados a la administración de macromoléculas por las vías mucosas pulmonar y nasal, respectivamente. De un modo más específico, los resultados obtenidos nos han permitido extraer las siguientes conclusiones:

Parte I. Desarrollo de microsferas de polisacáridos para la administración pulmonar de macromoléculas terapéuticas

1. Se han preparado microsferas compuestas por los polisacáridos quitosano y/o glucomanano con características morfológicas y aerodinámicas adecuadas (diámetros aerodinámicos entre 1 y 5 μm) para administración por vía pulmonar, utilizando una técnica de atomización. La morfología y densidad de las microsferas se encuentran altamente influenciados por el grado de desacetilación del quitosano empleado en su preparación, así como por el contenido en glucomanano. Estas microsferas presentan una excelente capacidad de asociar y liberar insulina, utilizada como péptido modelo en este estudio.

2. Los estudios llevados a cabo en cultivos celulares revelaron que el glucomanano posee un excelente perfil de biocompatibilidad, no pudiendo alcanzarse el parámetro IC_{50} a ninguna de las concentraciones ensayadas. En cuanto al quitosano, su citotoxicidad depende básicamente de la dosis de polímero y grado de desacetilación, siendo el de menor grado de desacetilación el menos citotóxico. Por otra parte, la capacidad del quitosano de favorecer el paso de macromoléculas a través de epitelios, aumenta a medida que se incrementa el grado de desacetilación. No

obstante, este aumento de la permeabilidad celular no se encuentra necesariamente asociado a la producción de daño celular. Todo esto denota la importancia de alcanzar un compromiso entre dosis de polímero, grado desacetilación y efectividad como promotor de la absorción.

Estudios de interacción de las microsferas, realizados *in vitro* en células epiteliales procedentes del epitelio respiratorio humano, evidenciaron el carácter mucoadhesivo de los sistemas.

Parte II. Desarrollo de nanopartículas de polisacáridos para la administración nasal de macromoléculas terapéuticas

1. Se han preparado nanopartículas compuestas por quitosano y diferentes derivados aniónicos de ciclodextrina mediante la técnica de gelificación iónica. Esta técnica ha permitido encapsular macromoléculas, tales como la insulina y el ADN plasmídico, en condiciones extremadamente suaves dando lugar a la obtención de nanoestructuras con tamaños dentro del rango nanométrico, carga superficial positiva y forma esférica.

2. El análisis estructural de los nanosistemas desarrollados ha permitido comprobar la eficaz incorporación de las ciclodextrinas en la matriz polimérica de los mismos, alcanzándose una cantidad superior al 50% de la composición total de las nanopartículas, lo que se traduce, según se ha demostrado en estudios celulares *in vitro*, en una significativa reducción de la citotoxicidad de los sistemas.

3. Asimismo, estas nanopartículas muestran una excelente capacidad de atravesar barreras celulares y mucosas, así como de incrementar la permeabilidad del epitelio al paso de moléculas por vía paracelular mediante la apertura reversible de las uniones íntimas intercelulares.

4. Tras ser administradas *in vivo* por vía nasal, las nanopartículas de quitosano/ciclodextrina conteniendo insulina han dado lugar a una respuesta hipoglucémica muy satisfactoria, poniendo de manifiesto su potencial para la administración de macromoléculas terapéuticas a través de vías mucosas.
5. Por último, en estudios de expresión genética *in vitro*, en los que se utilizó un modelo de epitelio nasal/bronquial, se ha demostrado la capacidad de estas nanopartículas de dar lugar a elevados niveles de transfección. Asimismo, se observó que la composición de las nanopartículas determina en gran medida la eficacia de las mismas para promover la transfección genética. En este sentido, las formulaciones preparadas a partir de quitosano de bajo peso molecular han resultado ser significativamente más efectivas.

Bibliografía

BIBLIOGRAFÍA

1. Agnihotri S.A., Mallikarjuna N.N., Aminabhavi T.M., Recent advances on chitosan-based micro- and nanoparticles in drug delivery, J. Control. Rel., 100 (2004) 5-28.

2. Aguiar M.M.G., Rodríguez J.M., Silva C.A., Encapsulation of insulin-cyclodextrin complex in PLGA microspheres: a new approach for prolonged pulmonary insulin delivery, J. Microencapsul., 21 (2004) 553-564.

3. Ahsan F., Rivas I.P., Khan M.A., Torres-Suárez A.I., Targeting to macrophages: role of physicochemical properties of particulate carriers-liposomes and microspheres- on the phagocytosis by macrophages, J. Control. Rel., 79 (2002) 29-40.

4. Almeida A.J., Alpar H.O., Brown M.R.W., Immune response to nasal delivery of antigenically intact tetanus toxoid associated with poly(L-lactic acid) microspheres in rats, rabbits and guinea pigs, J. Pharm. Pharmacol., 45 (1993) 198-203.

5. Alonso M.J., Nanomedicines for overcoming biological barriers, Biomedicine and Pharmacotherapy, 58 (2004) 168-172.

6. Alonso M.J., Sánchez A., The potential of chitosan in ocular drug delivery, J. Pharm. Pharmacol., 55 (2003) 1451-1463.

7. Alonso-Sande M., des Rieux A., Schneider Y.J., Remuñán-López C., Alonso M.J., Préat V., Proc. 33rd Meeting of the Controlled Release Society, Vienna 2006.

8. Alonso-Sande M., Remuñán-López C., Alonso-Lebrero J.L., Alonso M.J, Proc. 32nd Meeting of the Controlled Release Society, Miami 2005.

9. Alonso-Sande M., Teijeiro-Osorio D., Remuñán-López C., Alonso M.J., Glucomannan, a promissing polysaccharide for pharmaceutical and biomedical purposes, (ANEXO II de la presente memoria)

10. Alpar H.O., Almeida A.J., Identification of some of the physico-chemical characteristics of microspheres which influence the induction of the immune response following mucosal delivery, Eur. J. Pharm. Biopharm., 40 (1994) 198-202.

11. Altiere R.J., Thompson D.C., Physiology and Pharmacology of the airways. En: Hickey A.J. (Ed.), Inhalation aerosols: physical and biological basis for therapy, Marcel Dekker, New York, (1996) pp. 85-138.

12. Ameri M., Maa Y.–F., Spray drying of biopharmaceuticals: stability and process considerations, Drying Technology, 24 (2006) 763-768.

13. Amidi M., Romeijn S.G., Verhoef J.C., Junginger H.E., Bungener L., Huckriede A., Crommelin D.J.A., Jiskoot W., N-Trymethyl chitosan (TMC) nanoparticles loaded with influenza subunit antigen for intranasal vaccination: biological properties and immunogenicity in a mouse model, Vaccine, 25 (2007) 144-153.

14. Anal A.K., Stevens W.F., Remuñán-López C., Ionotropic cross-linked chitosan microspheres for controlled release of ampicillin, Int. J. Pharm, 2006

15. Arora P., Sharma S., Garg S., Permeability issues in nasal drug delivery, DDT, 7 (2002) 967-975.

16. Arora P., Sharma S., Garg S., Permeability issues in nasal drug delivery, DDT, 7 (2002) 967-975.

17. Artursson P., Lindmark T., Davis S.S., Illum L., Effect of chitosan on permeability of monolayers of intestinal epithelial cells (Caco-2), Pharm. Res., 11 (1994) 1358-1361.

18. Artursson P., Lindmark T., Davis S.S., Illum L., Effect of chitosan on permeability of monolayers of intestinal epithelial cells (Caco-2), Pharm. Res., 11 (1994) 1358-1361.

19. Aspden T.J., Illum L., Skaugrud Ø., Chitosan as nasal delivery system: evaluation of insulin absorption enhancement and effect on nasal membrane integrity using rat models, Eur. J. Pharm. Sci., 4 (1996) 23-31.

20. Aspden T.J., Illum L., Skaugrud, O., Chitosan as a nasal delivery system: evaluation of the absorption enhancement and effect on nasal membrane integrity using rats models, Eur. J. Pharm. Sci., 22 (1996) 23-31.

21. Avrill A. y Bodin L., Effect of short-term ingestion of konjac glucomannan on serum cholesterol in healthy men, Am. J. Clin. Nutr., 61 (1995) 585-589.

22. Behrens I., Vila A., Alonso M.J., Kissel T., Comparative uptake studies of bioadhesive nanoparticles in human intestinal cell lines and rats: The effect of mucus on particle adsorption and transport, Pharm. Res., 19 (2002) 1185-1193.

23. Brooking J., Davis S.S., Illum L., Transport of nanoparticles across the rat nasal mucosa, J. Drug Target., 9 (2001) 267-279.

24. Calvo P., Remuñán-López C., Vila-Jato J.L., Alonso M.J., Novel hydrophilic chitosanpolyehtylene-oxide nanoparticles as protein carriers, J. Appl. Polym. Sci., 63 (1997) 125-132.

25. Carrión-Recio D., Taboada-Montero C., Vila-Jato J.L., Remuñán-López C., Enhancement of protein lung absorption using chitosan microspheres, *(sometida a evaluación)*

26. Challa R., Ahuja A., Ali J., Khar R.K., Cyclodextrins in drug delivery: an updated review, AAPS PharmSciTech, 6 (2005) E329-E357. (http://www.aapspharmscitech.org).

27. Chang S.W., Westcott J.Y., Henson J.E., Voelkel N.F., Pulmonary vascular injury by polycations in perfused rat lungs, J. Appl. Physiol., 62 (1987) 1932-1943.

28. Cryan S.-A., Carrier-based strategies for targeting protein and peptide drugs to the lungs, The AAPS J., 7 (2005) E20-E41 (http://www.aapsj.org)

29. Csaba N., García-Fuentes M., Alonso M.J., The performance of nanocarriers for transmucosal drug delivery, Expert Opin. Drug Deliv., 3 (2006) 463-478.

30. Csaba N., Koping-Hoggard M., Alonso M.J., Chitosan nanoparticles as gene delivery systems: effect of chitosan molecular weight and protein-coencapsulation, *sometida a evaluación.*

31. Csaba N., Sánchez A., Alonso M.J., PLGA:Poloxamer and PLGA:Poloxamine blen nanostructures as carriers for nasal gene delivery, J. Control. Rel., 113 (2006) 164-172.

32. Csaba N., Sánchez A., Fernández-Mejía E., Novoa-Carballal R., Alonso M.J., Chitosan nanoparticles for the delivery of plasmid DNA. Preparation and characterization, *sometida a evaluación.*

33. Cui, Z., Hsu, C.H. y Mumper, R.J., Physical characterization and macrophage cell uptake of mannan-coated nanoparticles, *Drug Develop. Ind. Pharm.* 29, 689-700 (2003).

34. Cyclodextrins for pharmaceutical applications [International Specialty Products, Technical Brochure] (2000), Disponible en: http://www.ispcorp.com/products/pharma/content/forwhatsnew/cyclodex/cyclodex.pdf. (consultada el 25/08/06).

35. Cydex Inc. website, disponible en: http://www.cydexinc.com, Consultada el 04/05/07.

36. Davis S.S., Delivery of peptide and non-peptide drugs through the respiratory tract, PSTT, 2 (1999) 450-456.

37. De la Fuente M., Seijo B., Alonso M.J., A novel bioactive nanocarrier for ocular gene delivery: hyaluronan-chitosan nanoparticles, *sometida a evaluación.*

38. De la Fuente M., Seijo B., Alonso M.J., New hyaluronic acid-chitosan nanoparticles as ocular gene carriers: studies in human corneal and conjunctival epithelial cell lines, *sometida a evaluación.*

39. Debin A., Kravtzoff R., Santiago J.V., Cazales L., Sperandio S., Melber K., Janowicz Z., Betbeder D., Moynier M., Intranasal immunization with recombinant antigens associated with new cationic particles induces strong mucosal as well as systemic antibody and CTL responses, Vaccine, 20 (2002) 2752-2763.

40. Desai, P-M., Labhasetwar, V., Walter, E., Levy, R.J. y Amidon, G.L., The mechanism of uptake of biodegradable microparticles in Caco-2 cells is size dependent, Pharm. Res., 14 (1997) 1568-1573.

41. Dodane V., Khan M.A., Merwin J.R., Effect of chitosan on epithelial permeability and structure, Int. J. Pharm., 182 (1999) 21-32.

42. Dondeti P., Zia H., Needham T.E., Bioadhesive and formulation parameters affecting nasal absorption, Int. J. Pharm., 127 (1996) 115-133.

43. Dotsikas Y., Loukas Y.L., Kinetic degradation study of insulin complexed with methyl-beta cyclodextrin. Conformation of complexation with electrospray mass spectroscopy and ^{1}H NMR, J. Pharm. Biomed. Anal., 29 (2002) 487-494.

44. Edwards D.A., Ben-Jebria A., Langer R., Recent advances in pulmonary drug delivery using large, porous inhaled particles, J. Applied Physiol., 85 (1998) 379-385.

45. Edwards D.A., Hanes J., Caponetti G., Hikach J., Ben-Jebria A., Eskew M.L., Mintzes J., Deaver D., Lotan N., Langer R., Large porous particles for pulmonary drug delivery, Science, 276 (1997) 1868-1871.

46. Ekrami H.M., Shen W.C., Carbamylation decreases the cytotoxicity but not the drug-carrier properties of polylysines, J. Drug Target., 2 (1995) 469-475.

47. Farraj N.F., Johansen B.R., Davis S.S., Illum L., Nasal administration of insulin using bioadhesive microspheres as a delivery system, J. Control. Rel., 13 (1990) 253-261.

48. Fernández-Urrusuno R., Calvo P., Remuñán-López C., Vila-Jato J.L., Alonso M.J., Enhancement of nasal absorption of insulin using chitosan nanoparticles, Pharm. Res., 16 (1999) 1576-1581.

49. Fernández-Urrusuno R., Romani D., Calvo P., Vila-Jato J.L., Alonso M.J., Development of a freeze-dried formulation of insulin-loaded chitosan nanoparticles intended for nasal administration, S.T.P. Pharma Sci., 9 (1999) 429-436.

50. Florea B.I., Meaney C., Junginger H.E., Borchard G., Transfection efficiency and toxicity of polyethylenimine in differentiated Calu-3 and nondifferentiated COS-1 cell cultures, AAPS PharmSci, 4 (2002) E12 (http://www.aapspharmsci.org).

51. Florea B.I., Thanou M., Junginger H.E., Borchard G., Enhancement of bronchial octreotide absorption by chitosan and N-trimethyl chitosan shows linear in vitro/in vivo correlation, J. Control. Rel., 110 (2006) 353-361.

52. Florence A.T., The oral absorption of micro- and nanoparticulates: neither exceptional nor unusual, Pharm. Res., 14 (1997) 259-266.

53. Forrest M.L., Gabrielson N., Pack D.W., Cyclodextrin-Polyethylenimine conjugates for targeted in vitro gene delivery, 89 (2005) 416-423.

54. Foster K.A., Avery M.L., Yazdanian M., Audus K.L., Characterization of the Calu-3 cell line as a tool to screen pulmonary drug delivery, Int. J. Pharm., 208 (2000) 1-11.

55. Friede M., Aguado M.T., Need for new vaccine formulations and potential of particulate antigen and DNA delivery systems, Adv. Drug Deliv. Rev., 57 (2005) 325-331.

56. Fu Y.J., Mi F.L., Wong T.B., Shyu S.S., Characteristics and controlled release of anticancer drug loaded poly (D,L-lactide) microparticles prepared by spray-drying technique, J. Microencapsul., 18 (2001) 733-747.

57. García-Contreras L., Morcol T., Bell S.J., Hickey A.J., Evaluation of novel particles as pulmonary delivery systems for insulin in rats, AAPS Pharm. Sci., (2003) 1-11 (http://www.aapsj.org)

58. García-Fuentes M., Prego C., Torres D., Alonso M.J., A comparative study of the potential of solid triglyceride nanostructures coated with chitosan or poly(ethylene glycol) as carriers for oral calcitonin delivery. Eur. J. Pharm. Sci., 25 (2005) 133-143.

59. Gizurarson S., Animal models for intranasal drug delivery studies, Acta. Pharm. Nord., 2 (1990) 105-122.

60. Gizurarson S., Animal models for intranasal drug delivery studies, Acta. Pharm. Nord., 2 (1990) 105-122.

61. Gordon G.S., Moses A.C., Silver R.D., Flier J.S., Carey M.C., Nasal absorption of insulin: enhancement by hydrophobic bile salts, Proc. Natl. Acad. Sci. USA, 82 (1985) 7419-7423.

62. Grainger C.I., Alcock R., Gard T.G., Quirk A.V., van Amerongen G., de Swart R.L., Hardy J.G., Administration of an insulin powder to the lungs of cynomolgus monkeys using a Penn Cantury insufflator, Int. J. Pharm., 269 (2004) 523-527.

63. Grenha A., Carrión-Recio D., Teijeiro-Osorio D., Seijo B., Remuñán-López C., 2007 (ver Anexo I de la presente memoria)

64. Hanes J., Dawson M., Har-el Y., Suh J., Fiegel J., Gene delivery to the lung. En: Hickey A.J. (Ed.), Pharmaceutical inhalation aerosol technology, Marcel Dekker, New York, (2004) pp. 489-539.

65. He P., Davis S.S., Illum L., In vitro evaluation of the mucoadhesive properties of microspheres, Int. J. Pharm., 166 (1998) 75-68.

66. Hirai A., Odani H., Nakajima A., Determination of degree of deacetylation of chitosan by ^{1}H NMR spectroscopy, Polym. Bull., 26 (1991) 87-94.

67. Hirai S., Yashiki T., Mima H., Effect of surfactants on the nasal absorption of insulin in rats, Int. J. Pharm., 9 (1981) 165-172.

68. Huang Y. -C., Yeh M. -K., Chiang C. -H., Formulation factors in preparing BTM-chitosan microspheres by spray drying method, Int. J. Pharm., 242 (2002) 239-242.

69. Hussain A., Yang T., Zaghloul A.A., Ahsan F., Pulmonary absorption of insulin mediated by tetradecyl-beta-maltoside and dimethyl-beta-cyclodextrin, Pharm. Res., 20 (2003) 1551-1557.

70. Illum L., Nanoparticulate systems for nasal delivery of drugs : a real improvement over simple systems ?, J. Pharm. Sci., 96 (2007) 473-483.

71. Irie T., Uekama K., Cyclodextrins in peptide and protein delivery, Adv. Drug Deliv. Rev., 36 (1999) 101-123.

72. Jacobsen J., van Deurs B., Pederssen M., Rassing M.R., TR146 cells grown on filters as a model for human buccal epithelium. I. Morphology, growth, barrier properties and permeability, Int. J. Pharm., 125 (1995) 165-184.

73. Janes K.A., Calvo P., Alonso M.J., Polysaccharide colloidal particles as delivery systems for macromolecules, Avd. Drug Del. Rev., 47 (2001) 83-97.

74. Jung T., Kamm W., Breitenbach A., Hungerer K.D., Hundt E., Kissel T., Tetanus toxoid loaded nanoparticles from sulfobutylated poly(vinilalcohol)-graf-

poly(lactide-co-glycolide): evaluation of antibody response after oral and nasal application in mice, Pharm. Res., 18 (2001) 352-360.

75. Jung T., Kamm W., Breitenbach A., Kaiserling E., Xiao J.X., Kissel T., Biodegradable nanoparticles for oral delivery of peptides: is there a role for polymers to affect mucosal uptake?, Eur. J. Pharm. Biopharm., 50 (2000) 147-160.

76. Kawashima Y., Yamamoto H., Takeuchi H., Fujioka S., Hino T., Pulmonary delivery of insulin with nebulized DL-lactide/glycolide copolymer (PLGA) nanospheres to prolong hypoglycemic effect, J. Control. Rel., 62 (1999) 279-287.

77. Kobayashi S., Kondo S., Juni K., Pulmonary delivery of salmon calcitonin dry powders containing absoption enhancers in rats, Pharm. Res., 13 (1996) 80-83.

78. Koping-Hoggard M., Varum K.M, Issa M., Danielsen S., Christensen B.E., Stokke B.T., Artursson P., Improved chitosan-mediated gene delivery based on easily dissociated chitosan polyplexes of highly defined chitosan oligomers, Gene Therapy, 11 (2004) 1441-1452.

79. Kotze A.F., Lueβen H.L., De Boer A.G., Verhoef J.C., Junginger H.E., Chitosan for enhanced intestinal permeability: prospects for derivatives soluble in neutral and basic environments, Eur. J. Pharm. Sci., 7 (1998) 145-151.

80. Krauland A.H., Alonso M.J., Chitosan/cyclodextrin nanoparticles as macromolecular drug delivery system, Int. J. Pharm., 2007.

81. Le Buanec H., Vetu C., Lachgar A., Benoit M.A., Gillard J., Paturance S., Aucouturier J., Gane V., Zagury D., Bizzini B., Induction in mice of anti-Tat mucosal immunity by the intranasal and oral routes, Biomed. Pharmacother., 55 (2001) 316-320.

82. Lehr C.M., Bowstra J.A., Schacht E.H., Junginger H.E., In vitro evaluation of mucoadhesive properties of chitosan and some other natural polymers, Int. J. Pharm.. 78 (1992) 43-48.

83. Li W.-I., Perlz M., Heyder J., Langer R., Brain J.D., Englmeier K.-H., Niven R.W., Edwards D.A., Aerodynamics and aerosol particle deaggregation phenomena in model oral-pharyngeal cavities, J. Aerosol Sci., 27 (1996) 1269-1286.

84. Loftsson T., Brewster M.E., Pharmaceutical applications of cyclodextrins. 1. Drug solubilization and stabilization, J. Pharm. Sci., 85 (1996) 1017-1025.

85. Lowrie D.B., DNA vaccination exploits normal biology, Nature Med., 4 (1998) 147-148.

86. Maeda M., Shimahara H., Sugiyama N., Detailed examination of the branched Structure of konjac glucomannan, Agric. Biol. Chem., 44 (1980) 245-252.

87. Maestrelli F., García-Fuentes M., Mura P., Alonso M.J., A new drug nanocarrier consisting of chitosan and hydroxypropylcyclodextrin, Eur. J. Pharm. Biopharm., 63 (2006) 79-86.

88. Martín E., Schipper N.G.M., Verhoef J.C., Merkus W.H.M., Nasal mucociliary clearance as factor in nasal drug delivery, Adv. Drug Del. Rev., 29 (1998) 13-38.

89. Marttin E., Verhoef J.C., Merkus F.W.H.M., Efficacy, safety and mechanism of cyclodextrins as absorption enhancers in nasal delivery of peptide and protein drugs, J. Drug Target., 6 (1998) 17-36.

90. Matsubara M., Ando Y., Irie T., Uekama K., Protection afforded by maltosyl-β-cyclodextrin against α-chymotrypsin-catalyzed hydrolysis of a luteinizing-releasing hormone agonist, bserelin acetate, Pharm. Res., 14 (1997) 1401-1405.

91. McCarty M.F., Glucomannan minimizes the postprandial insulin surge: a potential adjuvant for hepatothermic therapy, Medical hipotheses, 58 (2002) 487-490.

92. Merkus F.W., Verhoef J.C., Marttin E., Romeijn S.G., van der Kuy P.H.M., Hermens W.A.J.J., Schipper N.G.M., Cyclodextrins in nasal drug delivery, Adv. Drug Deliv. Rev., 36 (1999) 41-57.

93. Mima S., Miya M., Iwamoto R. and Yoshikawa S., Highly deacetylated chitosan and its properties, J. Appl. Polym. Sci., 28 (1983) 1909-1917.

94. Mygind N., Dahl R., Anatomy, physiology and function of the nasal cavities in health and disease, Adv. Drug Del. Rev., 29 (1998) 3-12.

95. Nagamoto T., Hattori Y., Takayama K., Maitani Y., Novel chitosan particles and chitosan-coated emulsions inducing immune response via intranasal vaccine delivery, Pharm. Res., 21 (2004) 671-674.

96. Nishinari K., Konjac Glucomannan, En Doxastakis G. y Kiosseoglou V. (Eds.), Novel Macromolecules in Food Systems, Elsevier Science (2000).

97. Paasonen L., Korhonen M., Yliperttula M., Urtti A., Epidermal cell culture model with tight stratum corneum as a tool for dermal gene delivery studies, Int. J. Pharm., 307 (2006) 188-193.

98. Partidos C.D., Intranasal vaccines: fothcoming challenges, PSTT, 3 (2000) 273-280.

99. Patton J.S., Mechanisms of macromolecule absorption by the lungs, Adv. Drug Del. Rev., 19 (1996) 3-36.

100. Patton J.S., Platz R.M., Routes of delivery: case studies. 2. Pulmonary delivery of peptides and proteins for systemic action, Adv. Drug. Del. Rev., 8 (1992) 179-196.

101. Paul W., Sharma C., Chitosan, a durg carrier for the 21th century, STP Pharma Sci., 10 (2000) 5-22.

102. Pereswetoff-Morath L., Bjurstrom S., Khan R., Dhalin M., Edman P., Toxicological aspects of the use of dextran microspheres and thermogelling ethyl (hysroxyethyl) cellulose (EHEC) as nasal drug delivery systems, Int. J. Pharm., 128 (1996) 9-21.

103. Pfutzner A., Mann A.E., Steiner S., Technosphere™/insulin- a new approach for effective delivery of human insulin via the pulmonary route, Diabetes Tech. Ther., 4 (2002) 589-594.

104. Pillion D.J., Ahsan F., Arnold J., Balasubramaniam B.M, Piraner O., Meezan E., Synthetic long chain alkyl maltosides and alkyl sucrose esters as enhancers of nasal insulin absorption, J. Pharm. Sci., 91 (2002) 1456-1462.

105. Portero A., Remuñán-López C., Nielsen H.M., The potential of chitosan in enhancing peptide and protein absorption across the TR146 cell culture model-an in vitro model of buccal epithelium, Pharm. Res., 19 (2002) 169-174.

106. Prego C., García M., Torres D., Alonso M.J., Transmucosal macromolecular drug delivery, J. Control. Rel., 101 (2005) 151-162.

107. Rajewski R., Stella V.J., Pharmaceutical applications of cyclodextrins. 2. In vivo drug delivery, J. Pharm. Sci., 85 (1996) 1142-1169.

108. Reithmeier H., Herrman J., Göpferich A., Lipid microparticles as a parenteral controlled release device for peptides, 73 (2001) 339-350.

109. Remuñán-López C., Portero A., Lemos M., Vila-Jato J.L., Núñez M.J., Riveiro P., López J.M., Piso M., Alonso M.J., Chitosan microspheres for the specfic delivery of amoxycillin to the gastric cavity, S.T.P. Pharma. Sci., 10 (2000) 69-76.

110. Roser M., Fisher D., Kissel T., Surface modified biodegradable albumin nano- and microspheres. II: effect of surface charges on in vitro phagocytosis and biodistribution in rats, Eur. J. Pharm. Biopharm., 4 (1998) 255-263.

111. Schipper N.G.M., Varum K.M., Artursson P., Chitosans as absorption enhancers for poorly water absorbable drugs. I. Influence of molecular weight and degree of acetylation on drug transport across human intestinal epithelial (Caco-2) cells, Pharm. Res., 13 (1996) 1686-1692.

112. Schipper N.G.M., Varum K.M., Artursson P., Chitosans as absorption enhancers for poorly water absorbable drugs. I. Influence of molecular weight and degree of acetylation on drug transport across human intestinal epithelial (Caco-2) cells, *Pharm. Res*., 13 (1996) 1686-1692.

113. Sharma P., Chaudhari P., Kolsure P., Ajab A., Varia N., Recent trends in nasal drug delivery - an overview, http://www.pharmainfo.net (consultada el 21/03/07).

114. Singh J., Pandit S., Bramwell V.W., Alpar H.O., Diphteria toxoid loaded poly-(ε-caprolactone) nanoparticles as mucosal vaccine delivery systems, Methods, 38 (2006) 96-105.

115. Sinha V.R., Singla A.K., Wadhawan S., Kaushik R., Kumria R., Bansal K., Dhawan S., Chitosan microspheres as a potential carrier for drugs, Int. J. Pharm., 274 (2004) 1-33.

116. Smith J., Wood E., Dornish M., Effect of chitosan on epithelial cell tight junctions, Pharm. Res., 21 (2004) 43-49.

117. Somavarapu S., Alpar H.O., Song C.Y.S., Biodegradable nanoparticles in nasal vaccine delivery: effect of particle size and loading, Proceed. Inter. Symp. Control. Rel. Bioact. Mater., 25 (1998) 451-452.

118. Stanley A.C., Buxton D., Innes E.A., Huntley J.F., Intranasal immunization with Toxoplasma gondii tachyzoite antigen encapsulated into PLG microspheres induces humoral and cell-mediated immunity in sheep, Vaccine, 22 (2004) 3929-3941.

119. Steiner S., Pfutzner A., Harzer O., Heineman L., Rave K., Technosphere™/insulin- Proof of concept study with a new insulin formulation for pulmonary delivery, Exp. Clin. Endocrinol. Diabetes, 110 (2002) 17-21.

120. Stieneker F., Kreuter J., Löwer J., High antibody titres in mice with polymethylmethacrylate nanoparticles as adjvants for HIV vaccines, AIDS, 5 (1991) 431-435.

121. Surendrakumar K., Martín G.P., Hodgers E.C.M., Jansen M., Blair J.A., Sustained release of insulin from sodium hyaluronate based dry powder formulations after pulmonary delivery to beagle dogs, J. Control. Rel., 91 (2003) 385-394.

122. Takeuchi H., Yamamoto H., Niwa T., Hino T., Kawashima Y., Enteral absorption of insulin in rats from mucoadhesive chitosan coated liposomes, Pharm. Res., 13 (1996) 896-901.

123. Tarara T. E, Hartman M. S., Gill H., Kennedy A. A., and Weers J. G., Characterization of suspension-based metered dose inhaler formulations composed of spray-dried budesonide microcrystals dispersed in HFA-134a, Pharm. Res., 21 (2004) 1607-1614.

124. Teijeiro-Osorio D., Remuñán-López C., Nielsen H.M., Comparative studies of chitosan nanoparticles and molecules in Calu-3 and TR146 cells, 32nd Ann. Meet. Exp. Control. Rel. Soc., (2005) 378.

125. Tobío M., Gref R., Sánchez A., Langer R., Alonso M.J., Stealth PLA-PEG nanoparticles as nasal protein delivery systems, Pharm. Res., 15 (1998) 274-279.

126. Tomihata K., Ikada Y., In vitro and in vivo degradation of films of chitin and its deacetylated derivatives, Biomaterials, 18 (1997) 567-575.

127. Türker S., Onur E., Özer Y., Nasal route and drug delivery systems, Pharm. World Sci., 26 (2004) 137-142.

128. Uekama K., Hirayama F., Irie T., Cyclodextrin drug carrier systems, Chem. Rev., 98 (1998) 2045-2076.

129. Vanbever R., Ben-Jebria A., Mintzes J. D., Langer R., Edwards D. A., Sustained release of insulin from insoluble inhaled particles, Drug Deliv. Research, 48 (1999) 178-185.

130. Varhosaz J., Sadrai H., Heidari A., Nasal delivery of insulin using bioadhesive chitosan gels, Drug Delivery, 13 (2006) 31-38.

131. Vila A., Sánchez A., Évora C., Soriano I., Vila-Jato J.L., Alonso M.J., PEG-PLA nanoparticles as carriers for nasal vaccine delivery, Journal of Aerosol Medicine, 17 (2004) 174-185.

132. Vila A., Sánchez A., Janes K., Behrens I., Kissel T., Vila-Jato J.L., Alonso M.J., Low molecular weight chitosan nanoparticles as new carriers for nasal vaccine delivery in mice, Eur. J. Pharm. Biopharm., 57 (2004) 123-131.

133. Vila A., Sánchez A., Pérez C., Alonso M.J., PLA-PEG nanospheres: new carriers for transmucosal delivery of proteins and plasmid DNA, Polym. Adv. Technol.,13 (2002) 851-858.

134. Vila A., Sánchez A., Tobío M., Calvo P., Alonso M. J., Design of biodegradable particles for protein delivery, J. Control. Rel. 78 (2002) 15-24.

135. Wang K., He Z., Alginate-konjac glucomannan-chitosan vedas as controlled release matrix, Int. J. Pharm., 244 (2002) 117-126.

136. Win, K. Y. y Feng, S.S., Effects of the particle size and surface coating on the cellular uptake of polymeric nanoparticles for oral delivery of anticancer drugs, Biomaterials, 26 (2005) 2713-2722.

137. Witchi C., Mrsny R. J., In vitro evaluation of microparticles and polymer gels for use as nasal platforms for protein delivery, Pharm. Res., 16 (1999) 382-390.

138. Yu S., Zhao Y., Wu F., Zhang X., Lü W., Zhang H., Zhang Q., Nasal insulin delivery in the chitosan solution : in vitro and in vivo studies, Int. J. Pharm., 281 (2004) 11-23.

139. Zhang H., Neau S.H., In vitro degradation of chitosan by a commercial enzyme preparation: effect of molecular weight and degree of deacetylation, Biomaterials, 22 (2001) 1653-1658.

140. Zhang Z.Y., Ping Q.N., Xiao B., Microencapsulation and characterization of tramadol-resin complexes, J. Control. Rel., 66 (2000) 107-113.

Anexos

Anexo I

Nano- and Microparticulate Carriers for Pulmonary Drug Delivery

A. Grenha, D. Carrión-Recio, D. Teijeiro-Osorio, B. Seijo,
C. Remuñán-López

CHAPTER 9

Nano- and Microparticulate Carriers for Pulmonary Drug Delivery

Ana Grenha, Dayamí Carrión-Recio, Desirée Teijeiro-Osorio, Begoña Seijo, Carmen Remuñán-López

Department of Pharmacy and Pharmaceutical Technology, University of Santiago de Compostela, Campus Sur, 15782 Santiago de Compostela, Spain

CONTENTS

1. INTRODUCTION

Progress made in the field of drug delivery has accelerated enormously over the past two decades in parallel with major discoveries of new low molecular weight active molecules, and, primarily, the introduction of the therapeutic products from biotechnology such as proteins and peptides, which pose particular physicochemical and biopharmaceutical challenges. Their usual bioavailability problems presented when administered by the oral route, always the first to consider due to its convenience [1], led to their administration by intravenous injection and to investigations to identify noninvasive alternative mucosal routes such as nasal, buccal, and pulmonary routes, among others. Mucosal routes for systemic drug administration present a great advantage in comparison to parenteral routes because they are noninvasive. Thus, development of suitable noninjectable delivery systems for mucosal drug administration could significantly enhance patient compliance, thereby leading to increased therapeutic benefits [2]. However, major barriers limit drug delivery via these unconventional routes; these include poor permeability across epithelial barriers, enzymatic degradation at the site of administration, immune reactions at the delivery site, and limitations in the available surface area for absorption [3]. Therefore, their application for drug administration, and, in the end, the successful

ISBN: 1-58883-079-9

Handbook of Particulate Drug Delivery
Edited by M. N. V. Ravi Kumar
Pages: 1–28

exploitation of a new generation of peptides and proteins as therapeutic agents, clearly depends on simultaneous progress in the development of new carriers for specific active molecules. These carriers should allow the molecules to remain stable in their specific biological environment, and, ideally, enable them to cross mucosal barriers to reach their specific sites of action. Aside from this, the materials and technologies used to prepare these vehicles also seem to be relevant issues, the selection of which depends on the final goal of the administration [4].

Among the mucosal routes, lung drug delivery has attracted remarkable scientific and biomedical interest in recent years for the treatment of systemic diseases such as diabetes mellitus. In fact, lung mucosa has proven particularly attractive for systemic administration due to the large alveolar area exposed for drug absorption (approximately 100 m^2) and the thin alveolar-vascular epithelium (0.1–0.2 μm) that permits rapid absorption, low proteolytic activity compared to other mucosal routes, and the possibility of avoiding the first-pass effect [5–7].

The development of an inhaled therapy that is efficacious and safe depends on a well-designed administration device and a drug carrier with appropriate particle size and density distribution to ensure optimal dose deposition in the desired region of the lung.

The main purpose of this chapter is to provide an overview of the advances in nano- and microparticulate carriers aimed at improving the delivery of drugs, mainly peptides and proteins, to the lung. The most representative carriers are classified according to their particle size (microparticles and nanoparticles) and the nature of the materials used for obtaining them. Special emphasis will be placed on the application of the new technologies developed for their preparation. In addition, delivery systems proposed for local and systemic effects as well as those intended for gene delivery will be discussed. *In vivo* and clinical studies as well as marketed products will also be addressed. Over the last few years, our group has taken on the challenge of designing different types of nano- and microparticles mainly based on the polysaccharide chitosan. We have investigated their aerodynamic properties, their ability to associate peptides and proteins, and their biocompatibility with lung cells. Furthermore, we have administered them to rats and demonstrated their potential as insulin lung carriers. Therefore, the present chapter is also aimed at reviewing the characteristics and potential of these particles as protein carriers for lung delivery.

2. FACTORS AFFECTING DRUG DELIVERY TO THE LUNG

The lung performs complex functions at a metabolic and endocrine level, but it also provides structural and immunologic protection against inhaled pathogens, preventing unwanted airborne particles from entering the body. Airway geometry, humidity, and other drug-clearance mechanisms contribute to this filtration process.

Comprised of a well-organized structure, the lung can be divided in two main regions: the tracheobronchial region (from the larynx to the terminal bronchioles) and the alveolar region (the respiratory bronchioles and alveoli in a number of 200–600 million). The former region is mainly formed by ciliated and goblet cells and presents mucous, which is a complex mixture of proteins, glycoproteins, and lipids. This substance, together with the ciliated cells, forms a self-cleaning mechanism known as the mucociliary escalator or mucociliary clearance, which consists of propelling the mucous blanket with all the entrapped materials by the coordinated movement of cilia. In contrast, the alveolar region is devoid of mucous, and its epithelium is much thinner (0.1–0.5 μm) in order to permit efficacious gas exchange [7–9]. The alveoli include a dense capilar net supported by collagen and elastic fibers and covered by a thin epithelial layer composed of two different cell types: Type I pneumocytes and Type II pneumocytes [10]. Type I cells represent approximately 95% of the whole alveolar surface and form tight unions between them to prevent the passage of extracellular liquid to the alveolar lumen, thus maintaining the cellular structure and functional polarity [11]. Except for certain ions and very small solutes, these tight junctions are impermeable to hydrosoluble molecules. These Type I cells are large, flat, and unable to divide. When damaged, they are replaced by Type II cells that differentiate into Type I cells [12–13]. Type II pneumocytes are small cells, interposed between Type I cells, with the ability to synthesize and secrete a tensio-active fluid usually referred to as the pulmonary surfactant. This substance, which remains stored in the cell inside lamellar bodies, covers the alveolar epithelial cells at the air-tissue interface, forming a 10–20 nm thick layer [2, 7, 11–12]. This surfactant has the important function of preventing the natural tendency of the lung to collapse and reducing the surface tension in the air-liquid interface. Surfactant is composed of a complex mixture of lipids and proteins consisting of 80–90% lipids (mainly phosphatidylcholine and phosphatidylglycerol) and 5–10% proteins [10–13]. Released by exocytosis, its continuous secretion creates a surface gradient that favors the flux from the alveoli to the bronchioles until reaching the mucociliary escalator, thus playing a role in the elimination of exogenous substances such as drug-loaded nano- and microparticles reaching the alveoli [10]. The surfactant is eliminated by phagocytic mechanisms by macrophages and is recycled by Type II secretary cells [10–11]. Both types of cells constitute enzymatic and transport barriers to drug delivery systems that might reach this area, although Type I cells present lower proteolytic activity than Type II cells [14].

Macrophages are the mononuclear phagocytes of the lung, representing its main defense mechanism. Derived from blood-circulating monocytes, they differentiate in alveolar macrophages when they arrive at the lung [10–11]. These cells are not part of the alveolar wall. They form a suspension over the surface, therefore, they move freely, and, by phagocytosis, eliminate inhaled particles that manage to arrive at the alveolar surface after escaping mucociliary clearance [10, 15]. Macrophages range from 15 to 40 μm in size, contain many lysosomes rich in hydrolytic enzymes (acid phosphatase, glucuronidase, and lysozyme), and have a lifetime of months or even years [10, 16]. After phagocytosis, they usually migrate from the alveoli to the bronchial surface, where they integrate into the mucociliary

escalator by being transported to the pharynx and swallowed. Macrophages are continuously eliminated and replaced, and it is estimated that approximately 100 million macrophages migrate to the bronchioles daily. Moreover, those that are not eliminated migrate to the lymphatics [10–11, 13, 17].

Before reaching the deep lung, inhaled particles must overcome obstacles and lung defense mechanisms, essentially the effect of the airways' structure and the mucus layer, which protect the epithelium in the tracheobronchial region. Particles targeted to the deep lung should be small enough to pass through the mouth, throat, and conducting airways and reach the deep lung, but not so small that they fail to deposit and are breathed out again. Even so, a certain number of particles will be transported away from the lung by mucociliary clearance [6–7, 18–19]. Once in the deep lung, particles will have to face at least two other defense mechanisms: alveolar macrophages and enzymatic activity. Therefore, the challenge in developing therapeutic aerosols is to produce an aerosol that eludes the lung's mechanisms of defense.

Table 1 depicts the most relevant advantages and limitations of the pulmonary drug delivery route. From the above mentioned comments and considering referred characteristics such as large surface area, low thickness of the alveolar epithelium, and high vascularization (which could lead to rapid absorption), it is clear that drug administration through this route represents an alternative, very promising opportunity for some new macromolecules as well as for some other drugs that did not gather good results through other routes. In spite of these advantages of pulmonary systemic administration, many challenges will have to be faced from now on, and drugs will only be successfully administered by the pulmonary route when formulations have properties that enable them to overcome the distinct barriers opposing drug absorption such as difficult accessibility, mucociliary clearance, and safety concerns.

The specific characteristics of the lungs and the inherent issues to access the desired area influence the achievement of satisfactory formulations into an appropriate aerosol device. Therefore, designing adequate carriers for local or systemic effects has been a major concern for researchers in this area. This has resulted in the appearance of novel liposome and nano- and microparticulate systems that are gaining popularity due to their specific morphological and aerodynamic properties. In addition, using these recently developed systems, a more sustained release could be achieved, thus prolonging the therapeutic effect of the administered drugs and leading both to a reduction of dosage frequency and to increased patient compliance [5, 7, 9]. The great limitation, however, will be tailoring these systems to reach the desired site of action.

Pulmonary delivery of pharmaceutics can be performed using three different types of devices: nebulizers, pressurized metered dose inhalers (pMDI), and dry powder inhalers (DPI). While they all generate an aerosol of particles/droplets, they differ in the technology used for aerosol production. Nebulizers presented a disadvantage by not being portable, a limitation overcome by both pMDIs and DPIs as well as by the recent introduction of new types of compact, portable devices. Following the ratification of the Montreal Protocol, the production of clorofluorocarbonates (CFCs) has been banned, except for specific exemptions [20]. This has forced the introduction of non-ozone-depleting substitutes such as hydrofluoroalkanes (HFAs) and the reformulation of pMDI-delivered formulations to suit the new propellants. In addition, the phasing out of CFCs has encouraged the development of alternative pulmonary drug delivery systems such as DPIs. The greatest difference between pMDIs and DPIs is that in the former the drug is dispersed in a liquid propellant under pressure, while DPIs contain dry powders. Therefore, the latter avoids the stability problems usually presented by suspensions, and, additionally, presents the advantage of avoiding the need for coordination between inhalation and device actuation required by pMDIs. Furthermore, recent advances in MDI technology such as the use of breath-actuated instruments have solved the main limitation related to DPIs—the necessity of a high inspiration capability—and have generated increased interest in these devices [21]. Extensive reviews on inhalation devices are available elsewhere [9, 22], and it is recognized that the technology of aerosol-producing devices plays a very important role in the efficacy of treatment because they can influence aerosol distribution in the lung.

The success of inhaled aerosol particles for either a local or systemic effect depends on their aerodynamic properties. Particles intended to provide a local effect should have an aerodynamic diameter (diameter of a spherical particle with unit density that settles at the same rate as the particle in question) adequate to reach the specific site of action, usually the bronchial region (for local respiratory diseases such as asthma or cystic fibrosis, among others). This means that

Table 1. Potential advantages and disadvantages of pulmonary systemic drug administration.

Advantages	Disadvantages
Non-invasive route	Airway structure acts as a filter
Large alveolar surface area suitable for drug absorption (100 m^2)	Mucociliary clearance
Extensive vascularization	Alveolar macrophages
Low thickness epithelial barrier	Particles can be exhaled
Low proteolytic activity compared to other routes	Absorption affected by pathological conditions
Avoidance of first-pass metabolism and gastrointestinal degradation	Lungs are not readily accessible without design of adequate formulations
Rapid absorption and onset of action	Requires complex devices and particles with specific aerodynamic properties
Reduced systemic side effects	Difficulties associated with handling of inhalation device
Possibility of administering lower doses	Many factors affecting reproducibility

they should be small enough to pass the oropharyngeal region, but not too small that they pass the target region and reach the alveoli. On the contrary, particles aimed at systemic absorption should be small enough to pass through the mouth, throat, and conducting airways into the alveoli, but not so small that they fail to deposit and are breathed out again [5–6, 23]. Any particle arriving at the lungs will deposit, and, depending on its size and density, different deposition mechanisms may occur. Three different mechanisms are known: impact, sedimentation, and diffusion. Particles with an aerodynamic diameter larger than 6 μm and traveling at a high speed will deposit by impact. This mechanism is more prone to occur in the extrathoracic and tracheobronchial area, where particle velocity is usually high. Sedimentation occurs in the smallest airways as well as in the alveolar region, and it is particularly significant for particles of approximately 4–6 μm, although it has been observed with particles as small as 0.5 μm. Deposition by diffusion, occurring mainly in the alveolar region, is due to Brownian movements, and, therefore, is more significant for particles smaller than 0.5 μm [24–25]. In this manner, it has been reported that particles intended for a local effect should possess an aerodynamic diameter between 5 and 10 μm, while particles intended to reach the deep lung for systemic action should be in the range of 1–5 μm, with maximum effect achieved for particles of 2–3 μm [7, 26]. For a broad review on the factors affecting the pulmonary delivery of drugs, the publications of Courrier et al., Labiris and Dolovich, and Taylor and Kellaway [7, 9, 27] can be consulted.

3. THERAPEUTIC APPLICATIONS

As previously mentioned, pulmonary drug delivery offers the possibility of both local drug targeting for the treatment of specific respiratory diseases and systemic absorption of therapeutic molecules and macromolecules. So far, the most common drugs administered by the pulmonary route are anti-inflammatories and mucolytics intended to treat specific respiratory disorders such as asthma, bronchitis, chronic obstructive pulmonary disease, pulmonary emphysema, and cystic fibrosis. This restriction was principally due to inefficiency of available inhalation devices that deposited only 10–15% of the emitted dose in the lungs; while this is appropriate for local therapies, it is not enough for systemic drugs [27].

Table 2 displays some relevant new molecules currently under study for a local effect [28–30]. From these molecules, we can rebound macromolecules such as the protein B, the base of the pulmonary surfactant Surfaxin®, and rDNase (Pulmozyme®), which is a unique enzyme marketed for a local pulmonary effect in the treatment of cystic fibrosis. Several other molecules referred to in the table are presently in clinical trials such as cyclosporin A as an immunosuppressive for lung transplants (submitted for FDA approval), alpha-1-antitrypsin for the treatment of emphysema (phase II), interferon-γ for the treatment of cystic fibrosis (phase II), and interferon-β for the treatment of asthma (phase I), among others.

The unique features of the pulmonary route are opening a way toward systemic delivery. Recent advances in aerosol and formulation technologies have led to the development of more efficient delivery systems that produce small particle aerosols, allowing higher drug doses to be deposited in the alveolar region of the lungs, where they are available for systemic absorption [27]. In fact, there are already a few drugs on the market for systemic delivery through the lungs (e.g., halothane, an anaesthetic, and ergotamine, available as an inhaler for the treatment of migraines). Furthermore, many peptides and proteins—growth factors, hormones, monoclonal antibodies, cytokines, and antiinfection agents—are undergoing clinical investigation for a range of medical conditions.

It has been assumed that the lungs represent an ideal site for absorption of therapeutic macromolecules such as peptides, proteins, plasmids, DNA, and oligonucleotides, among others. The principal limitation presented by the majority of these molecules is their lack of activity when administered orally, a direct consequence of the intense degradation suffered in the gastrointestinal tract, their high molecular weight, and hydrophilic character, which all contribute to poor permeation across the intestinal epithelium. Consequently, these macromolecules are usually parenterally administered, resulting in inconvenience for the patient and limits on their applications. Recently, great interest has arisen in administering these macromolecules via the lung with the intention of achieving a systemic effect. This interest is based on the already mentioned high permeability of the alveolar epithelium [31] and its low enzymatic activity in comparison with other routes of administration such as oral and nasal routes [14, 32].

It has been reported that macromolecules with a molecular weight (Mw) less than 40 kDa and a diameter smaller

Table 2. Examples of active molecules currently under investigation for local effect by inhalation.

Active molecule	Therapeutic indication
Surfactant proteins (approved)	Adult Respiratory Distress Syndrome
rDNase (approved), Interferon-γ	Cystic Fibrosis
Succinyl peptide chloromethylketone, Alpha-1-antitrypsin	Emphysema
Cyclosporin A	Lung transplant
Alpha1 proteinase inhibitor	Alpha-1-antitrypsin deficiency
Interferon-γ, Interleukin-2	Cancer
IL-1R, Anti-IgE Mab, Isoprenaline, Salbutamol sulfate, Albuterol sulfate, Beclometasone, Interferon-β	Asthma
Muramyl dipeptide, Rifampicin, Isoniazid	Antituberculosis vaccine
Catalase, Superoxide dismutase	Oxidative stress

than 5–6 nm such as insulin (5.7 kDa, 2.2 nm) rapidly appear in the blood following inhalation into the airways. Macromolecules of Mw with diameters larger than 40 kDa and 5–6 nm, respectively, such as inhaled albumin (68 kDa) and α_1-antitrypsin (45–51 kDa), are slowly absorbed over many hours [27]. Although the mechanism of absorption is unknown, it has been hypothesized that macromolecules either pass through cells via absorptive transcytosis (absorptive or receptor mediated), paracellular transport between junctions, or large transitory pores in the epithelium caused by cell injury or apoptosis [8, 33]. Thus, the high bioavailability of macromolecules deposited in the lung is likely due to its enormous surface area, very thin diffusion layer, slow surface clearance, and antiprotease defense system [8].

Table 3 shows some of the active molecules currently under investigation for systemic administration via the lung [28–30]. Most of these molecules are peptides and proteins, including insulin, which has been exhaustively investigated by many labratories and is already approved for commercialization in Europe and the United States in a formulation from Pfizer, Nektar and Aventis called *Exubera®*. Furthermore, some of the molecules are currently in clinical trials, including parathyroid hormone, which is in phase I for osteoporosis therapy, and human growth hormone, which is in phase I for the treatment of growth deficiency.

Attention should be paid to the fact that some of the molecules included in both Tables 2 and 3, although already available for pulmonary delivery, are currently under investigation for their incorporation into micro- or nanoparticulate carriers aimed to improve their aerosolization, lung deposition, and therapeutic efficacy, as is the case for insulin, salbutamol, beclometasone, and gentamicin, among others.

The application of the lung for gene therapy has been gaining interest in the last few years, especially concerning therapy for specific lung disorders. Therefore, attention has been growing concerning its value for many acute and chronic diseases including cancer, asthma, cystic fibrosis, alpha-1-antitrypsin deficiency, and respiratory distress syndrome, among others. A variety of administration routes and delivery systems, viral and nonviral, have been investigated for this purpose. Administration routes include systemic administration, in which the gene carrier may become trapped in the capillary network of the lung, and intratracheal instillation of a gene suspension or even inhalation of aerosolized material carrying the therapeutic gene either as droplets or dry powders (see Hanes et al., 2004) [25]. Once in the lung, however, a gene transfer carrier can encounter highly effective defenses that have evolved to protect the airways from particles of all sizes, including allergens, viruses, and bacteria [34].

4. DRUG CARRIER SYSTEMS FOR PULMONARY DELIVERY

The therapeutic efficiency of numerous drugs, mainly peptides and proteins, is limited by their lack of specificity toward a given target, and, as a result, a major portion of the dose remains unavailable for the intended therapeutic effect, increasing the occurrence of side effects. Therefore, a carrier system designed with a specific size, density, or surface properties for drug delivery to the lung can play a key role in increasing the drug therapeutic index by the following mechanisms: (a) improving lung deposition and the amount of protein that reaches the site of action (either extracellular or intracellular), and, as a consequence, decreasing adverse effects due to nonspecific drug delivery to non-target tissues; (b) protecting the protein and improving its *in vivo* stability; and (c) reducing clearance and prolonging the drug residence time at its site of action. Furthermore, it can be employed to provide passive or active targeting. Topical delivery to the airways is itself a (passive) targeting approach for specific lung diseases, whereas active targeting refers more specifically to the use of a homing device such as antibodies attached to the carrier to target specific tissues, cells, or organelles. The choice of appropriate carrier depends on several factors including the nature of the drug to be delivered, the delivery device, the type of disease and site of action, and the nature and safety of the carrier.

Together with the development of new technologies for drug delivery capable of rendering efficacious administration of a selected drug, an investment in the improvement of the materials applied to the design of the systems has become a significant issue. The safety of the adjuvant used to develop lung carriers for protein delivery has to be determined, and issues regarding local irritancy and toxicity,

Table 3. Examples of active molecules currently under investigation for systemic effect by inhalation.

Active molecules	Therapeutic indication
Calcitonin, Parathyroid hormone	Osteoporosis
Human growth hormone	Growth deficiency
Estradiol	Hormone replacement therapy
Interferon-β	Multiple sclerosis
Insulin (approved)	Diabetes
LH-RH analogs	Cancer
Ribavirin, Interferon-α	Viral infections
Gentamicin sulfate	Pneumonia
rhG-CSF	Neutropenia
Erythropoetin	Anemia
Heparin	Anticoagulation
dDAVP (1-diaminocystein-8-D-arginine vasopressin)	Diabetes insipidus

long-term accumulation and immunogenicity will all have to be addressed using suitable models [35]. While the safety of some carriers (e.g., conventional liposomes) has been examined [36], that of many others has not. For example, concerns have been raised about the use of excipients such as absorption enhancers and enzyme inhibitors [37–38].

Several different materials have been utilized in the production of nano- and microparticulate carriers such as polysaccharides, polyester derivatives, acrylates, and lipids, among others. Concerning mucosal administration, and, specifically, pulmonary delivery, one of the most promising strategies is the incorporation of polymers that prolong the residency time of drug carriers at the absorption sites, thus facilitating an increased uptake of the loaded molecule and resulting in higher absorption [4, 39]. These types of approaches include the use of polymers that have mucoadhesive properties such as cellulose derivatives or polysaccharides such as chitosan, either alone, in combination with a preformed particulate carrier, or incorporated into the structure of the carrier itself [39–41].

Moreover, research has been focusing on the development of surface-modified carriers with the aim of improving their targeting properties, preventing uptake by the mononuclear phagocytic system (MPS), or favoring their interaction with specific epithelial cells, thereby overcoming their biological barriers [42]. For these purposes, strategies such as the application of wheat germ agglutinin (WGA), which is known to interact with specific WGA receptors on cell membranes, or the inclusion of lipids in the formulations, which are known to reduce alveolar phagocytic activity [43–44], have been gaining popularity.

The bioavailability of macromolecular drugs by the pulmonary route is still poor when compared to parenteral routes due to enzymatic degradation and clearance processes [7]. In an attempt to overcome these problems, the use of enzyme inhibitors and absorption enhancers has been proposed to improve pulmonary drug absorption. Many reports have been published on the enhancement of pulmonary absorption of peptides and proteins, including reports on the introduction of bile acids, surfactants, phospholipids, and enzyme inhibitors [23, 45]. Although the addition of absorption enhancers is a promising method to increase the systemic bioavailability of inhaled macromolecules, long-term safety is an important issue that should be extensively examined. Therefore, the major challenge that remains is to find those enhancers that will reversibly increase membrane permeability without causing toxicity during long-term use. Actually, only a few studies have been performed on the local toxicity of these agents following administration, and it was recently demonstrated that some of them, although efficient pulmonary absorption enhancers (i.e., *n*-lauryl β-*D*-maltopyranoside, laureth-9, and sodium glycocholate), induce lung damage [37, 46], indicating that these substances should be used very cautiously. The absorption enhancement effect can be dependent on the administered formulation because some studies report a positive effect of the polymers in solution and an absence of effect when assayed as particulates [47]. An absorption enhancer of particular interest, given the absence of toxicity already demonstrated by several mucosal routes, is the mucoadhesive polymer chitosan. Our group demonstrated its absorption enhancement effect both as a solution and in particulate form in TR146 and Caco-2 cells, representative of buccal and intestinal mucosa, respectively [48–50]. The inclusion of enzyme inhibitors, and, more specifically, protease inhibitors in formulations, has also been reported. These substances enable the absorption enhancement of proteins and peptides by reducing the proteolytic activity of various enzymes responsible for degrading peptides and proteins. The degree of absorption enhancement will rely on the enzyme to be inhibited. Investigated enzyme inhibitors include bacitracin, trypsin inhibitor, chymostatin, potato carboxypeptidase inhibitor, nafamostat mesilate, phosphoramidon, leupeptin, aprotonin, and amastatin, among others [45, 51]. For an extensive review on pulmonary absorption enhancers, consult Hussain et al. [45].

Phosphatidylcholine is the only excipient currently approved by the FDA for lung delivery; therefore, there is a long regulatory road ahead before the more sophisticated polymeric and targeted carriers may be used in clinics. This is an extremely important feature to have in consideration of the nano- and microparticulate carriers discussed below. Lactose is also approved as a carrier in dry powder products for pulmonary administration, but it is not intended to enter the lungs; rather, its particle size limits deposition to the oropharynx.

In the following sections, we will discuss the most representative nano- and microparticulate lung drug carriers. It should be noted that most of them are not yet licensed for use in humans, and many are only in the early stages of development. The limited number of products on the market based on polymeric nano- and microparticles can be justified by two main reasons: the polymers' cytotoxicity and the lack of a suitable large-scale production method. Indeed, polymers accepted for use in other forms such as implants are not necessarily well tolerated in their particulate form. Presenting a size in the range of nano- or micrometers, the polymer can be internalized by macrophages, which can lead to cytotoxic effects.

5. MICROPARTICULATE LUNG DRUG DELIVERY CARRIERS

The majority of the inhalation systems currently available use the active drug in a micronized form by itself or together with an excipient such as lactose (as was mentioned before, lactose is not inhaled in the case of dry powders and is acting only as a vehicle to facilitate drug administration) or suspended or dissolved in a liquid propellant (as is the case with pressurized metered dose inhalers).

Recently, research work in this field has focused on the design and formulation of microspheres as an alternative system that can be tailored with the desired morphologic (shape and porosity) and aerodynamic (size and density) characteristics by simply modifying the composition and variables of the production process. The development of a microparticulate system, which enables the whole dose of loaded drug to reach the desired area, thus exhibiting a controlled release profile, will permit a decrease in the number of needed doses to achieve a determined effect while reducing undesirable side effects and increasing

therapeutic efficacy. In this manner, microspheres have been proposed as carriers for pulmonary administration, using a wide range of naturally occurring or synthetic polymers and materials because they can offer efficient and controlled delivery as well as protection of the encapsulated molecules.

Until the mid-1990's, particles with a 1 to 3 μm geometric diameter and density around 1 g/cm^3 were thought to be the most suitable for lung delivery because significant loss due to impact (large particles) and exhalation (small particles) would be avoided [29]. Unfortunately, however, this range of size and density were responsible for aggregation and rapid phagocytosis by alveolar macrophages [5, 52]. In an attempt to overcome these inconveniences, Edwards et al. introduced a new and promising concept based on the design of large porous particles [53]. These particles are lighter and larger than the typical dry powder particles with a mass density of approximately 0.1 g/cm^3 and geometric diameter of >5 μm. By virtue of their hollow and porous characteristics, they give rise to an aerodynamic diameter smaller (<5 μm) than their geometric diameter. Because of these features, particles can be aerosolized more efficiently (less aggregation) than smaller, nonporous particles, resulting in higher respirable fractions of the formulation. In addition, they can evade alveolar phagocytosis. Since the introduction of this new concept, a significant amount of research has addressed the development of new technologies to produce similar systems, achieving promising results that will be commented on later [54–57]. Interesting approaches in particle engineering technologies such as hollow and porous microspheres include the already registered PulmoSpheres™ (Alliance Pharmaceutical), made of phosphatidylcholine, the primary component of human lung surfactant, and AIR™ Microspheres (Alkermes), prepared with PLGA, which were proposed to deliver hIgG and insulin to the lung, respectively [53, 58–60]. Technospheres™ (Pharmaceutical Discovery Corporation), based on diketopiperazine derivatives, which captures and stabilizes peptides in small particles [61–62], have also been registered as a new drug delivery system for pulmonary administration. Special mention of the Trojan particles is required. Prepared from different materials such as polystyrene, upon spray drying, the Trojan particles assemble into microparticles with low density (<0.1 g/cm^3), which are easily aerosolized from a dry powder inhaler, and they redisperse into nanoparticles once in solution. They are called Trojan particles because of their ability to escape both phagocytic and mucociliary clearance within the airways [63].

The fate of microspheres entering the lungs is dependent on the manufactured material and technique, the latter selected according to the drug and polymer physicochemical properties and on the delivery device.

The synthetic polymers polylactic acid (PLA) and polylactic-co-glycolic acid (PLGA) acid (PLGA) [53, 64–71] comprise an important type of microspheres developed for pulmonary delivery. Other options include the use of natural polymers such as albumin, gelatine, chitosan, dextran, oligosaccharide derivatives, or sodium hyaluronate, among others [72–78]. Recently, a good deal of work has been presented on microspheres containing lipids such as dipalmitoylphosphatidylcholine (DPPC) [54–56, 58, 60, 79–80] because it was reported that their presence avoids the adsorption of opsonic proteins, thereby reducing macrophagic phagocytosis in the alveoli [43, 81]. Additionally, the biocompatibility of some lipids was demonstrated upon pulmonary administration of lipid particles, which did not induce any inflammatory response [82]. Lung-targeted microparticles based on these polymers can be elaborated using techniques such as spray drying [40, 54–56, 67–68, 74–75, 79–80, 83–86]; spray congealing [87]; emulsion solvent evaporation [53, 65, 67–70, 83] or solvent extraction/evaporation [66]; supercritical fluid technology [71]; and interfacial cross-linking [88]. When encapsulating labile molecules such as peptides/proteins, the effect of solvents, heat, moisture, pH, oxygen, and mechanical stresses must be assessed. Spray drying is a very simple technique that consists of spraying a polymer drug solution, suspension, or emulsion into a drying air stream at a temperature that allows the instantaneous evaporation of the solvent, leading to the formation of dried particulates of variable size [89]. Spray congealing is a similar technique in which the solution, suspension, or emulsion is sprayed into a cryogenic medium such as liquid nitrogen. The frozen material is subsequently lyophilized, and microparticles are obtained at the end of this process [90–91]. In the technique of emulsion solvent evaporation, an organic phase containing the drug and the polymer is generally incorporated in another aqueous phase containing a surfactant by means of sonication or homogenization. The solvent diffuses to the external phase and evaporates from the surface, leading to precipitation of the polymer and resulting in the formation of particles [42]. In the so-called emulsion solvent extraction/evaporation method, a solvent soluble in the polymer solvent is added to accelerate its evaporation. In supercritical fluid technology, a solution of the drug material is fed with a stream of supercritical fluids (e.g., CO_2) through a specially designed nozzle under controlled temperature and pressure. The supercritical fluid disperses, mixes with, and rapidly extracts the solvent from the drug solution, leading to the formation of particles, which are retained in a particle formation vessel. Manipulation of the operating conditions enables accurate control of particle size, shape, and morphology, which renders the process particularly attractive for use in pulmonary delivery [92–94]. Later in this section, we will present an overview of the most recent studies aimed at developing microparticulate systems for pulmonary drug administration. Table 4 displays a summary of the polymers and materials used to produce the referred microparticulates. Tables 5 and 6, respectively, summarize aspects of the *in vitro* and *in vivo* research works described herein, indicating polymers, methods, and major findings of the respective studies.

5.1. Microparticles Made of Synthetic Hydrophobic Materials

5.1.1. Microparticles of Polyester Derivatives

Much attention has been given to the biodegradable and biocompatible polymers polylactic acid (PLA) (used in medical applications such as sutures, orthopedic implants, and medical dressings) and polylactic-co-glycolic acid (PLGA) for the

Table 4. Main excipients used to produce microparticulate lung drug delivery carriers.

Synthetic hydrophobic excipients	
Polyester derivatives	Polylactic-co-glycolic acid (PLGA), polylactic acid (PLA), poly-ε-caprolactone (PCL)
Lipids	Egg phosphatidylcholine (EPC), dipalmitoylphosphatidylcholine (DPPC)
Natural hydrophilic excipients	
Proteins	Albumin, gelatin
Cellulose derivatives	Hydroxypropylcellulose (HPC)
Polysaccharides	Chitosan (CS), Hyaluronic acid (HA)
Others	
Sugars	Mannitol, oligosaccharide ester derivatives (OED)

production of lung-targeted microparticles, given their recognized safety by the parenteral route, which led to their FDA approval for this application [95]. Nevertheless, despite the knowledge of their safety by the parenteral route, it could not be dismissed that the slow rate of PLGA degradation in the lung periphery, possibly due to the small area of contact between the polymer and lung fluid, could induce lung toxicity [96]. Therefore, concerns about this led to the development of some new polymers derived from PLGA such as polyvinyl alcohol (PVA) grafted PLGA (PVA-g-PLGA) or this same polymer grafted with diethylamino-propylamine (DEAPA) (DEAPA-PVA-g-PLGA), which are degraded in a shorter time [96–97]. Furthermore, oligolactic acid, an oligomer of lactic acid, has a shorter biological half-life than PLA, and, therefore, may be better suited for pulmonary drug delivery [98].

Most of the microspheres prepared with these polymers are intended to target antitubercular drugs such as isoniazid and rifampicin to lung macrophages, which are mainly found in the alveolar space [66, 70–71, 83, 86], although the administration of proteins such as insulin [53] or corticosteroids such as budesonide and beclomethasone has also been proposed [65, 69].

Beclomethasone-loaded PLA microspheres prepared by solvent evaporation evidenced a respirable fraction of 42% and a controlled release of the drug over six days [65]. Studies on the effect of PLA microspheres prepared by the emulsion solvent extraction/evaporation and supercritical fluids techniques [66, 71] containing a combination of these two drugs (to reduce drug resistance) or a prodrug of isoniazid (tetraheptylammonium isoniazid methanesulfonate) in macrophage cell lines (J774A.1 and NR8383) demonstrated a higher macrophagic concentration of the drugs upon incubation of cells with microspheres in comparison to the unformulated drugs [66, 71]. Rifampicin-loaded PLGA microspheres were also proposed for the treatment of tuberculosis and prepared using both spray drying [83, 86] and emulsion solvent evaporation [70, 83], rendering particles adequate for pulmonary delivery with mean diameters between 2 and 5 μm. Encapsulation efficiencies were around 100%, and drug release was faster (77% at 24 hours) for particles obtained by spray drying in comparison to those obtained by solvent evaporation. This was attributed to a predominant accumulation of the drug near the microspheres' surface when they were obtained by spray drying, which did not occur when the technique of solvent evaporation was used [83]. Moreover, in a study performed by Tomoda et al., rifampicin release was found to be pH dependent, with microspheres delivering the drug in macrophages rather than in alveolar lining fluid [86]. Pandit et al. further proposed the formulation of microspheres containing a mixture of PLGA and poly-ε-caprolactone (PCL) and coated by chitosan to encapsulate rifampicin. The presence of chitosan was found to increase drug encapsulation, which reached 40%, and microspheres exhibited a controlled-release profile over 21 days [70]. Budesonide was also encapsulated in PLGA microspheres as a tool to reduce the expression of the vascular endothelial growth factor, which plays a key role in the angiogenesis in tumors, including lung cancer. This drug was successfully encapsulated with 70% efficacy, and microspheres were shown to provide a sustained release (53%) over three weeks [69]. Finally, we should mention the work from Edwards et al., who, as was previously indicated, was first to introduce the concept of large porous particles [53]. These PLGA particles, produced by solvent evaporation, exhibit a large diameter (>5 μm) and low density (0.1 g/cm^3), and, hence, aerodynamic properties optimal for deep lung deposition resulting in respirable fractions as high as 50%.

In addition to their *in vitro* characterization, several *in vivo* studies have been performed with microspheres based on PLA and PLGA in which they were administered intratracheally or by inhalation to guinea pigs, rats, or mice. Except for two cases, in which the encapsulated drug was budesonide [69] or insulin [53], all of the studies assay microspheres containing antitubercular drugs such as rifampicin and isoniazid [66–68, 71]. All these works reported a higher efficiency of drugs encapsulated in microspheres compared with the intratracheal or intravascular administration of the unformulated drug as either an increased drug concentration in macrophages [66, 71] or a reduction in the number of *Mycobacterium tuberculosis* in the lung [67–68]. Furthermore, nebulization has proven to be more efficient than intratracheal insufflation as a means of delivering the drug to the macrophages, and, therefore, it reduces the number of viable microorganisms more effectively [68]. Among the above-mentioned studies, three of them will be discussed.

The study described by Zhou et al. using a prodrug of isoniazid (THA-INHMS, tetraheptylammonium-isoniazid) reports the most significant results among the works performed with polyester-based microspheres containing antitubercular drugs. In this study, microparticles prepared using supercritical fluids technology were evaluated for

Table 5. Description of *in vitro* studies performed with microparticulate systems developed for lung drug delivery.

Main excipient	Associated molecule	Preparation method	Performed studies	Major findings	Ref.
PLA	Beclomethasone	Solvent evaporation	Aerosolization with a DPI, drug release	Particle size: approximately 1 μm, respirable fraction: 42%, sustained drug release during 6 days	[65]
PLA	Isoniazid + Rifampicin	Solvent extraction and evaporation	Cell culture (J774A.1)	Higher macrophage concentration of drug upon cellular incubation with microspheres when compared to free drug	[66]
PLA	THA-INHMS	Supercritical fluids	Drug release Cell culture (NR8383)	Initial burst effect (40%) and sustained release (60%) for 10 days. Higher macrophage concentrations of isoniazid upon incubation with microspheres when compared to free drug	[71]
PLGA	Rifampicin	Solvent evaporation Spray-drying	Drug release	Smaller particle size (VMD <3 μm), higher encapsulation efficiency (100%) and faster release (77% at 24 h) for particles obtained by spray-drying compared to those prepared by solvent evaporation	[83]
PLGA	Rifampicin	Spray-drying	Drug release	Pulmonary surfactants do not affect rifampicin release, which is pH dependent. Microspheres deliver rifampicin to macrophages rather than in alveolar lining liquid, given the pH influence	[86]
PLGA	Budesonide	Solvent evaporation	Drug release	Particle size: approximately 1 μm, encapsulation efficiency: 70%, controlled drug release (53%) during 3 weeks	[69]
PLGA	Insulin	Solvent evaporation	Aerosolization with a DPI	Large and porous particles with large diameter: >5 μm, low density: <0.1 g/cm^3, respirable fraction: 50%	[53]
PLGA-PCL (CS)	Rifampicin	Solvent evaporation	Drug release	VMD: approximately 2 μm, encapsulation efficiency: 30–40%, sustained drug release (40–50%) during 21 days	[70]
EPC	Salbutamol	Spray-drying	Aerosolization with a DPI	Very low density (0.02 g/cm^3), respirable fraction: 20–60%	[80]
EPC	Cromolyn sodium, albuterol, formoterol	Spray-drying	Aerosolization with a pMDI	Hollow porous particles with VMD: 2–4 μm, tap density: 0.06–0.12 g/cm^3, respirable fraction: 70%. Particles are stable in HFA propellant	[59]
DPPC-albumin	Insulin Albuterol	Spray-drying	Aerosolization with a DPI	MMAD: 2–5 μm, respirable fraction: 50–92%. Albumin is responsible for sponge-like shape of microparticles	[55–56, 79]
CS-gelatin	Betamethasone	Spray-drying	Drug release	Particle size: 1–5 μm, low density: <0.4 g/cm^3, encapsulation efficiency: up to 95%, sustained release for 12 h	[76, 118]
OED	Leuprolide	Spray-drying	Drug release Stability	Controlled release dependent on choice of OED or on combination of several OEDs in different ratios. Microparticles are stable for 3 months in 4–40°C and 60–75% relative humidity	[74]

CS: chitosan; DPI: dry powder inhaler; EPC: egg phosphatidylcholine; DPPC: dipalmitoylphosphatidylcholine; HFA: hydrofluoroalkane; OED: oligosaccharide ester derivatives; MMAD: mass mean aerodynamic diameter; PCL: poly-ε-caprolactone; PLA: polylactic acid; PLGA: polylactic-co-glycolic acid; pMDI: pressurized metered dose inhaler; THA-INHMS: tetraheptylammonium-isoniazid methanesulfonate; VMD: volume median diameter

Table 6. Description of *in vivo* studies performed with microparticulate systems developed for lung drug delivery.

Main excipient	Associated molecule	Preparation method	Animal	Delivery method	Major findings	Ref.
PLA	THA-INHMS	Supercritical fluids	Rat	Intratracheal instillation	Microspheres induce higher isoniazid macrophage levels compared to free drug and reduced blood levels of potential toxic metabolite	[71]
PLA	Isoniazid + Rifampicin	Solvent extraction and evaporation	Rat	Inhalation	Inhalation gives higher intracellular drug concentrations, compared to oral delivery of free drug	[66]
PLGA	Rifampicin	Spray-drying	Guinea pig	Intratracheal insufflation	Intratracheal administration of rifampicin microspheres significantly reduces number of bacteria in the lung, compared to free drug	[67]
PLGA	Rifampicin	Solvent evaporation	Guinea pig	Intratracheal insufflation or nebulization	Microspheres nebulization is more efficient at reducing the number of viable microorganisms compared to insufflation. Microspheres are more efficient compared to free drug	[68]
PLGA	Budesonide	Solvent evaporation	Mouse	Intratracheal instillation	Intratracheal administration of microspheres provides higher lung drug levels after 1 week relative to intramuscular administration	[69]
PLGA	Insulin	Solvent evaporation	Rat	Intratracheal powder aerosol ventilation	Large porous microspheres induce low glucose levels (30% of initial value) for 96 h. Insulin bioavailability is 88% relative to sc, whereas nonporous particles yield 12% bioavailability	[53]
DPPC-albumin	Insulin	Spray-drying	Rat	Intratracheal powder aerosol ventilation	Microspheres induce sustained insulin plasma levels for 12 h (similar to subcutaneous administration) and bioavailability of 81% relative to subcutaneous administration	[55]
DPPC-albumin	Albuterol	Spray-drying	Guinea pig	Intratracheal powder aerosol ventilation	Large porous microspheres provide an albuterol effect for 15 h, compared to a 5 h effect achieved with small nonporous particles	[54]
DPPC	Parathyroid hormone (1–34)	Spray-drying	Rat	Intratracheal powder aerosol insufflation	Intratracheal administration of parathyroid hormone microspheres gives 34% absolute bioavailability compared to 18% achieved with subcutaneous administration of free drug. Administration with insufflator achieved better results than with ventilator	[85, 99]
EPC	IgG	Spray-drying	Rat	Intratracheal instillation	Microspheres instillation resulted in 27% relative bioavailability compared to intravenous administration of free drug and generated high titers of specific IgG antibodies in serum	[58]
HPC	Fluorescein	Spray-drying	Guinea pig	Intratracheal powder aerosol ventilation	Microspheres enhance fluorescein bioavailability 2-fold as compared to fluorescein control solution	[40]
HPC	Beclometasone	Spray-drying	Asthmatic Guinea pig	Intratracheal powder aerosol ventilation	Microspheres induce prolonged drug retention in the lung compared to free drug	[84]
HA	Insulin	Spray-drying	Beagle dog	Intratracheal powder aerosol insufflation	Microspheres extended insulin mean residence time (MRT) and terminal half-life compared to spray dried pure insulin. Zn^{2+} and HPC improved MRT (7–9 fold), AUC/dose (2.5–5 fold) and T_{max} (3 fold)	[75]
OED	Leuprolide	Spray-drying	Rat	Intratracheal powder aerosol insufflation	Leuprolide was detected in plasma up to 25 h post-administration, compared to the 150 min. provided by i.v. administration	[74]
Mannitol	Insulin	Spray-drying	Rat	Intratracheal powder aerosol insufflation	Microspheres induced stronger hypoglycemic response (15% decrease of glucose level) compared to intratracheal insulin solution (5% decrease of glucose level).	[121]

AUC: area under the curve; DPPC: dipalmitoylphosphatidylcholine; EPC: egg phosphatidylcholine; HA: hyaluronic acid; HPC: hydroxypropylcellulose; IgG: Immunoglobulin G; OED: oligosaccharide ester derivatives; PLA: polylactic acid; PLGA: polylactic-co-glycolic acid; THA-INHMS: Tetraheptylammonium-isoniazid methanesulfonate

their potential in targeting the ionizable prodrug of isoniazid THA-INHMS. The charged prodrug was ion-paired with two different hydrophobic cations (terapentylammonium and tetraheptylammonium bromide) and loaded separately into PLA microparticles. A high level of isoniazid was detected in a rat alveolar macrophage cell line (NR8383) following exposure of these cells to drug-loaded microparticles. To confirm that microparticles can target alveolar macrophages *in vivo,* the INH levels in lavaged bronchoalveolar macrophages were compared after the rats were administered INHMS in PLA microparticles by intratracheal instillation. Indeed, as shown in Figure 1, delivering a solution of isoniazid intratracheally led to a peak of the drug in the macrophages at 30 minutes, corresponding to approximately 140 ng/mL, after which the drug was no longer detected. On the contrary, when PLA microspheres containing the prodrug were intratracheally administered, the first peak in the macrophages was detected after approximately 1 hour and remained above 2800 ng/mL for 48 hours [71].

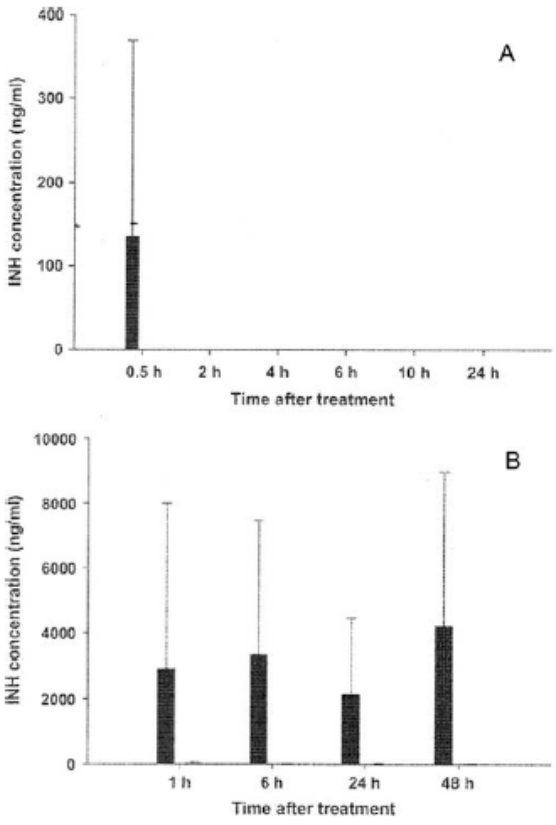

Figure 1. Concentration of INH in rat plasma and bronchiolavaged AMs after (A) IT instillation of INH solution and (B) IT instillation of THA-INHMS-loaded PLA microparticles. Data are means ± S.D. ($n = 3$, time-dependent concentration of INH in rat plasma in panel A was below the limit of quantification of the LC-MS/MS assay). Reprinted with permission from [71], H. Zhou et al., *J. Control. Release*, 107, 288 (2005). © 2005, Elsevier Science.

Insulin-loaded porous PLGA microspheres enabled increased systemic absorption of the peptide, inducing low glucose levels (30% of initial value) for as long as 96 hours upon intratracheal administration with a ventilator, which was not observed for small nonporous microspheres. Moreover, for large porous particles, insulin bioavailability was 88% relative to subcutaneous injection, whereas small nonporous particles yielded 12% bioavailability [53].

The work from Bandi et al. should also be mentioned in detail because it is the only report of the application of polyester-based microparticles in the field of lung cancer. The purpose of this study was to determine whether intratracheally instilled polymeric budesonide PLGA microparticles could sustain lung budesonide levels for one week and inhibit early biochemical changes associated with benzo(a)pyrene feeding in a mouse model for lung tumors. Microparticles of budesonide-PLGA, prepared using a solvent evaporation technique, were intratracheally administered to benzo(a)pyrene fed mice, and the results from intratracheal administration were compared to those obtained by intramuscular administration at one week post-administration by comparing drug levels in the lung tissue and bronchoalveolar lavage. Budesonide-PLGA microparticles (1–2 μm, budesonide loading efficiency of 69–94%) sustained *in vitro* budesonide release over 21 days and resulted in higher budesonide levels in the bronchoalveolar lavage and lung tissue compared with the intramuscular route. They reduced malondialdehyde accumulation, glutathione depletion, vascular leakage, and endothelial growth factor and c-myc expression in benzo(a)pyrene-fed mice, indicating the potential of locally delivered sustained-release particles to inhibit angiogenic factors in lung cancer. In fact, as seen in Table 7, intratracheal administration of microparticles led to much higher budesonide levels in both lung tissue and bronchoalveolar lavage (approximately 225 $ng \cdot (mg\ tissue)^{-1} \cdot (mg\ dose)^{-1}$ and 61 $ng \cdot mL^{-1}$, respectively), when compared to intramuscular administration of microparticles (approximately 16 $ng \cdot (mg\ tissue)^{-1} \cdot (mg\ dose)^{-1}$, and 23 $ng \cdot mL^{-1}$, respectively). A suspension of the drug was further administered by the intramuscular route, resulting in drug levels lower than any of those reported by the microparticles, which is consistent with the capability of the microparticles to sustain drug release, as mentioned before when describing the *in vitro* studies [69]. As was previously shown, Zhou et al. showed that PLA microparticles were able to target alveolar macrophages *in vivo*. Concerning toxicity, it is known that isoniazid induces liver toxicity, which is caused by acetylhydrazine formed by hydrolysis of acetylisoniazid, the major metabolite of isoniazid. In this respect, Zhou et al. reported that the pulmonary administration of isoniazid-loaded PLA microspheres bypassed hepatic first-pass metabolism, reducing the blood levels of acetylisoniazid [71].

5.1.2. Lipidic Microparticles

The incorporation of lipids in particulate formulations has been gaining popularity since it was reported that the addition of extra lipids enhances airway permeability due to

Table 7. Budesonide levels in the lung tissue and BAL following single-dose administration of budesonide-PLGA 50:50 (intrinsic viscosity: 0.17 $dL \cdot g^{-1}$) microparticles or budesonide suspension to bezo(a)pyrene mice. Drug levels were quantified at the end of one week following drug administration. Reprinted with permission from [69], N. Bandi et al., *J. Pharm. Pharmacol.* 57, 851 (2005). © 2005, Ingenta.

Drug levels	Intramuscular suspension	Intramuscular microparticles	Intratracheal microparticles
Lung tissue ng (mg tissue)$^{-1}$(mg dose)$^{-1}$)	6.14 ± 0.94	15.76 ± 4.30	224.93 ± 21.65*
Bronchoalveolar lavage ($ng \cdot mL^{-1}$)	n.d.	22.91 ± 20.15	60.65 ± 20.85*

Budesonide was administered at a dose of 150, 500, and 500 μg for intratracheal microparticle, intramuscular suspension, and intramuscular microparticle groups, respectively. *$P < 0.05$, significance between intratracheal and intramuscular groups. Data are expressed as mean ± s.d. for n = 5 for lung tissue, n = 3 for bronchoalveolar lavage with intramuscular suspension, n = 4 for bronchoalveolar lavage with intratracheal and intramuscular microparticles. n.d. indicates drug levels were below detection limits in the intramuscular suspension group.

transient alterations to local lipids' concentration and/or surfactant organization, although the mechanism of this process is not known so far [99]. Moreover, enhanced drug absorption induced by the lipids was also reported. The mechanism of absorption enhancement was attributed to the presence of surfactant on the alveolar surface and the addition of extra phospholipids hastened the surfactant recycling process, leading to increased uptake of the protein into the systemic circulation [45, 100–101]. Furthermore, the presence of lipids was already described to reduce phagocytic uptake upon interaction of microparticles with alveolar macrophages in culture [43].

As previously mentioned in this chapter, because aggregation lowers the respirable fraction of an inhalation aerosol, an active goal of the pharmaceutical industry has been the design of dry powders engineered as large and porous particles that have been recently demonstrated to be a promising approach to increase deposition as well as to obtain sustained release of the carried drug in the alveoli [5, 53]. Large (>5 μm) and porous (<0.4 g/cm^3) aerosol particles yielding aerodynamic diameters (1–5 μm) suitable for deep lung deposition can be successfully inspired into the lungs. These powders can be prepared using combinations of generally recognized as safe (GRAS) excipients, and, particularly, applying soluble excipients approved for inhalation such as lactose as well as materials that are endogenous to the lungs such as phospholipids, e.g., dipalmitoylphosphatidylcholine (DPPC). The production of particulates containing these last referred materials, mostly achieving large porous particles, will be addressed. In all cases, the preparation procedure was a spray-drying technique, and efforts were focused on exploring the dependence of the dry powder physical characteristics, i.e., particle size, tap density, and morphology, on the formulation and spray-drying parameters [54–56, 79–80, 85].

Steckel and Brandes proposed the production of low-density drug particles using a modified spray-drying technique that consists of spray drying an oil-in-water emulsion, leading to particles with a network-like morphology and irregular shape. The oil-in-water emulsion consisting of an aqueous phase containing the dissolved model drug (salbutamol sulfate), suitable surfactants such as poloxamer or phosphatidylcholine, an optional bulking agent such as lactose or cyclodextrin derivative, and a lipid-phase that is essentially a liquefied propellant were spray dried from a pressurized canister. The main excipient utilized for the particle formation was hydrated egg phosphatidylcholine, which is endogenous to the lung. Through this process, particles of very low density (0.02 g/cm^3) and a drug load of 40% were obtained. These particles exhibited a porous to hollow structure and irregular shape depending on the composition of the aqueous phase [80]. The particles' properties resulted in good powder flowability, making the powders ideally suited for use in carrier-free dry powder inhalers.

Vanbever et al. widely exploited another approach, demonstrating that the powder composition and solution properties greatly affected particle characteristics. In particular, they verified the important role of lipid content in the formation of large and porous particles. They prepared dry powders of water-soluble excipients (e.g., lactose, albumin) combined with water-insoluble material (e.g., lung surfactant) using a standard single-step, spray-drying process. They found that by properly choosing an excipient concentration and varying the spray-drying parameters, a high degree of control was achieved over the physical properties of the produced microspheres. Mean geometric diameters ranged between 3 and 15 μm and tap densities between 0.04 and 0.6 g/cm^3. It was further observed that the particle size was maximized (8 μm) and density reached the minimum value (0.1 g/cm^3), therefore obtaining ideal particles when particles contained 60% DPPC. Particles possessing high porosity and large size, with theoretical estimates of mean aerodynamic diameter between 1–3 μm, exhibited emitted doses as high as 96% and respirable fractions ranging up to 49% or 92% depending on the measurement technique. The incorporation of albumin was also reported, and it seems that it is responsible for the sponge-like shape of the particles. This suggests that the combination of these two excipients in the powder formulation facilitates the formation of porous particles and/or induces long particle life [56]. Moreover, this combination of albumin/DPPC could be an optimal candidate to be part of an inhalation system as both excipients are present in abundant concentration in the lungs [102], so their use in aerosols should not lead to significant accumulation of these endogenous materials in the lung following chronic daily administration. Additionally, Bosquillon and coworkers studied the influence of the powder composition and spray-drying parameters on aerosolization properties measured in terms of the respirable fraction of the emitted dose. Among all the tested compositions, the albumin/lactose/DPPC (30/10/60) powder demonstrated particularly efficient aerosolization performance, reaching respirable fraction values as high as 50% using a

first-generation inhaler device [79]. Following this exhaustive characterization, these dry powders were evaluated to determine their capacity to provide sustained insulin plasma levels. After verification of the integrity of insulin in dried particles *in vitro*, it was demonstrated that inhaled powders provide sustained plasma levels with a similar pharmacokinetic profile and bioavailability to those of the subcutaneous injected form. Thus, the bioavailability was 49% relative to subcutaneous (SC) injection of the soluble form of insulin and 81% relative to SC injection of the same formulation used for inhalation [55].

A similar dry powder, though one that included albuterol (β_2-specific-adrenergic amine and short-acting bronchodilator agonist) as active drug, demonstrated the ability to produce sustained local protection from carbachol-induced bronchoconstriction for at least 15 hours, whereas inhalation of small nonporous albuterol particles protected against bronchoconstriction for up 5 hours. The change in airway resistance in response to the carbachol challenge was almost identical at the three doses (10, 100, and 200 μg) of inhaled albuterol, corresponding to a significant inhibition (50–60%) of carbachol-induced bronchoconstriction. These results indicate that a dose as low as 10 μg of albuterol encapsulated in inhaled large porous particles offered statistically significant protection of animal airways from the carbachol challenge for at least 15 hours. While it was difficult to specify the contribution of the deep lung fraction of deposited particles to bronchodilation (given that β-receptors are widespread in the respiratory tract), it is possible that the long-lasting protection from bronchoconstriction by the inhaled porous albuterol particles is at least partially due to the more slowly cleared deep-lung particles because the large particle size enables escape from phagocytosis. The absence of substantial side effects was verified over a period of 24 hours by evaluating cardiorespiratory parameters as well as pulmonary inflammation. An important finding of this study is that sustained release of a hydrophilic substance (albuterol) can be achieved from large and porous particles by combining the drug with a high percentage of DPPC, which is an endogenous lung excipient and remains insoluble in water for long periods. As a whole, these results indicated that inhalation of porous albuterol dry powder might be clinically beneficial to patients with chronic asthma and other lung diseases by effectively preventing bronchoconstriction for long periods of time, diminishing the frequency of drug use, and minimizing side effects [54].

Another practical application of these particles in which DPPC content was shown to be crucial to guarantee the above mentioned characteristics is their application to systemically deliver parathyroid hormone (PTH, 1–34) (an endogenous polypeptide of 84 amino acids synthesized in the chief cells of the parathyroid glands and regulates calcium homeostasis and bone turnover) after intratracheal administration in rats.

Initially, the absolute PTH bioavailability was 21% for the powder form of PTH/albumin/lactose/DPPC and 18% after subcutaneous injection in rats. The powder had an average particle diameter between 3.9 and 5.9 μm, a tap density of 0.06 g/cm^3, an MMAD (mass mean aerodynamic diameter) between 3.9 and 5.9 μm, and reached up to 98% emitted dose and up to 61% fine particle fraction in the multistage liquid impinger using a Spinhaler® inhaler device. After checking the binding of PTH to albumin (78%), the withdrawal of the latter from the powder led to increased absolute bioavailability after inhalation from 21 to 34%, compared to 18% of PTH SC injection in the absence of albumin. No acute inflammation appeared in the lung up to 48 hours after a single inhalation. According to the authors, the main novelty of this study consisted of the demonstration of unexpected physical interactions between the drug and excipients that caused a significant decrease in systemic absorption [85]. Subsequently, the same research group tried to optimize the absorption of PTH in the lung by determining factors favoring its transport from the air spaces into the bloodstream. For this purpose, they simultaneously conducted pharmacokinetic and regional lung deposition studies *in vivo* in rats, following intratracheal administration of PTH in solution or the dry powder form with the powder being administered using a ventilator and an insufflator. Inhalation of the PTH powder using the insufflator resulted in high systemic bioavailability, despite deposition of most of the formulation in the upper airways. In this study, it was demonstrated that the increased absorption was related to the DPPC content, which revealed permeation enhancer properties even though it was abundantly present locally in pulmonary surfactant [99].

Finally, a new formulation technology of engineered lipid-based, drug-loaded hollow porous microspheres (PulmoSpheres™) produced by spray drying is mentioned because their main excipient is also a phosphatidylcholine derivative. They are prepared in a two-step process. In the first step, an oil-in-water emulsion is prepared using oils such as perflubron or perfluoroctyl ethane [58], which serve as the blowing agent during the spray-drying second step, retarding shrinkage of droplets while simultaneously creating pores in the particle surface. These particles, encapsulating cromolyn sodium, albuterol sulfate, and formoterol fumarate, have been shown to stabilize drug suspensions in hydrofluoralkane propellants with improved physical stability and aerosolization efficiency. They are lighter and larger than the typical dry powder particles, displaying a mass density of approximately 0.4 g/cm^3 and geometric diameter of >5 μm, exhibiting hollow and porous characteristics. Accordingly, these particles can be more efficiently aerosolized than smaller nonporous particles, leading to higher respirable fractions of the formulation. The hollow porous morphology of the particles allows the propellant to permeate freely within them, creating a novel form of suspension termed a homodispersion™, in which the dispersed and continuous phases are identical and are separated by an insoluble, interfacial layer of drug and excipient. Homodispersion formation improves suspension stability by minimizing the difference in density between the particles and the medium and by reducing attractive forces between particles, thus leading to improved dose uniformity. Excellent aerosolization efficiencies are also observed with fine particle fractions of about 70%. When IgG-loaded microparticles were intratracheally administered to rats, 27% relative bioavailability of IgG was achieved compared to intravenous administration of free drug and high titers of specific IgG

antibodies were detected in serum. In conclusion, the production of particles with such characteristics provides a new formulation technology for stabilizing suspensions of drugs in hydrofluoroalkane propellants with improved content uniformity and aerosolization efficiency [58–59]. Moreover, they serve as a platform to deliver a wide variety of compounds including peptides, proteins, vaccines, and, in particular, immunoglobulins, to the respiratory mucosa [58, 60, 103].

Large and porous particles are currently one of the most promising approaches in the field of pulmonary delivery. The possibility of particles' endowment with a large geometric size enables avoidance or delay of macrophagic capture, given the knowledge that phagocytosis is maximized for particles in the size range of 1–2 μm [15, 104]. On the other hand, their low density renders them aerodynamic diameters that are adequate for lung delivery, thus making these particles the objective of many research groups worldwide.

5.2. Microparticles Made of Natural Hydrophilic Mucoadhesive Materials

5.2.1. Cellulose-based Microparticles

Hydroxypropylcellulose (HPC) is a water-soluble and mucoadhesive polymer with a long tradition in several pharmaceutical formulations as a mucoadhesive and/or sustained release excipient. For example, it has been used in nasal administration to decrease the mucociliary clearance rate in the nasal cavity [105]. The application of such HPC powder systems was extended to inhalation formulations through preparation by spray-drying microspheres, incorporating a poorly soluble drug model drug, fluorescein (acid form, aqueous solubility 13.5 μg/mL), and a variety of HPC polymers in different fluorescein-HPC ratios. The drug was incorporated in the microspheres in either the crystalline or amorphous form, and, therefore, in addition to mucoadhesion, the microspheres potentially provide sustained-release or enhanced-dissolution characteristics.

Respirable-sized HPC microparticles were produced from a variety of HPC grades using a spray-drying technique. These particles, encapsulating either crystalline or amorphous fluorescein or beclometasone, displayed aerodynamic diameters (MMAD) between 1 and 3 μm, and, hence, were adequate for pulmonary delivery. They were assayed *in vivo* in guinea pigs by intratracheal administration of powder aerosols. The results indicated that the pulmonary absorption of poorly soluble fluorescein was enhanced when formulating the molecule in HPC microspheres. The spray drying of ethanol solutions, dissolving both fluorescein and HPC, altered fluorescein's crystallinity in the amorphous form, which enhanced dissolution when compared to the crystalline counterpart. More importantly, these microspheres were successful in retarding mucociliary clearance when highly viscous HPCs were employed. Consequently, amorphous fluorescein-HPC high viscosity microspheres showed rapid absorption with T_{max} = 0 minutes, and, hence, achieved 88% bioavailability, a value 1.9-fold higher that that obtained for the crystalline compound (control 45.6%). This was only achieved by virtue of both increased dissolution of amorphous fluorescein and retarded mucociliary clearance in the lung. The formulation may be successful in reducing the therapeutic dose of poorly soluble inhalation drugs such as beclometasone, thus reducing the risks of undesired side effects associated with extra-lung and/or systemic absorption of the drug. When the appropriate HPC polymer was selected, microspheres achieved a bioavailability of 88% (relative to intravenous profile) relative to 46% of unformulated fluorescein. This effect was attributed to the HPC mucoadhesive properties [40]. On the other hand, inhaled HPC microspheres encapsulating beclometasone dipropionate had the potential of prolonging the drug therapeutic effect by prolonging the inhibition of eosinophil infiltration into the airways of asthmatic guinea pigs for up to 24 hours, compared to 6 hours with the unformulated drug. Furthermore, increasing the drug dose was not necessary for this benefit, thereby reducing the risks of undesired side effects associated with extra-lung and/or systemic absorption of the drug [84].

5.2.2. Polysaccharide Microparticles

Chitosan (CS) is a polysaccharide with well-documented favorable biological properties such as biocompatibility, low toxicity, and biodegradability [106–107]. Furthermore, it is mucoadhesive [108]. (Its mucoadhesive properties are mediated by an electrostatic interaction between the positively charged CS amino groups and the negatively charged sialic acid residues of the mucus.) It also has the capability of promoting macromolecule permeation through well-organized epithelia (nasal, intestinal, ocular, buccal, pulmonary) [48, 109–114]. Obtained from the deacetylation of chitin, CS is formed from D-glucosamine and *N*-acetylglucosamine units [115], whose β-(1–4) glycosidic bonds between glucosamine units can be destroyed, namely by pulmonary lysozyme [116]. Based on these excellent properties, our group has been investigating the use of CS to develop mucoadhesive delivery systems specifically adapted for administration of drugs and therapeutic macromolecules by the different mucosal routes. CS has been proposed elsewhere to be a polymeric component of pulmonary drug delivery systems [72, 76–78, 117]. At present, we are evaluating CS nano- and microparticles as potential protein lung carriers. In this section, we will comment on our work on CS microparticles, and later we will refer to the recently proposed CS nanoparticles microencapsulated within mannitol microspheres.

Microspheres are produced by spray drying polymer solutions or dispersions of different types (salts, molecular weights, deacetylation degrees) of CS alone or with extra ingredients such as polysaccharide glucomannan (GM). Furthermore, CS microspheres are prepared by a double-emulsion/solvent evaporation method, which consists of adding a certain volume of an organic solvent in a CS aqueous solution by sonication to form the first simple emulsion, O_1/W, which is then added to cottonseed oil containing surfactant, obtaining the $O_1/W/O_2$ emulsion. The system is then stirred to allow the inner phase solvent to diffuse and evaporate from the CS phase, leading to polymer precipitation. The preparation procedures are being conveniently adapted to obtain particles with different morphological

characteristics and adequate aerodynamic properties to reach and deposit in the alveolar region, where the protein is intended to be delivered and absorbed. Our hypothesis was that once in the absorption site, CS would improve pulmonary protein absorption by interacting with the epithelial cells as had been previously reported for CS nanoparticles [111, 114]. Results show that the morphology and surface appearance of the CS microspheres (see Figures 2 and 3), as well as their densities and aerodynamic diameters, are highly dependent on their composition (presence of glucomannan), CS deacetylation degree, preparation method, and, for microspheres obtained from an emulsion, the type of inner organic solvent (Table 8). Microspheres prepared by spray drying a CS solution were spherical and had a small size of around 2.2 μm. It is quite noteworthy that there was an evolution from the spherical shape of CS microspheres prepared using CS with a deacetylation degree (DD) of 83% to the very characteristic convoluted surface corresponding to the most reacetylated CS (DD = 23%) particles and to those containing glucomannan in their composition. Their tap densities were as low as 0.23 ±

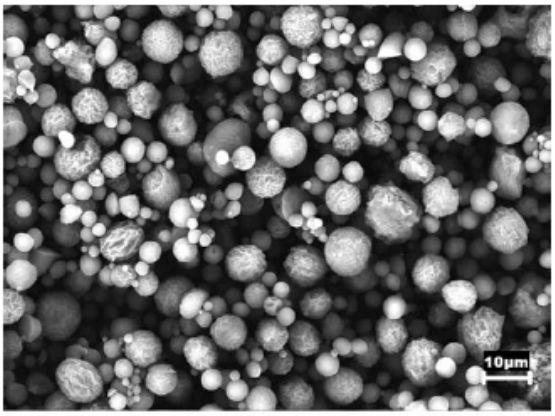

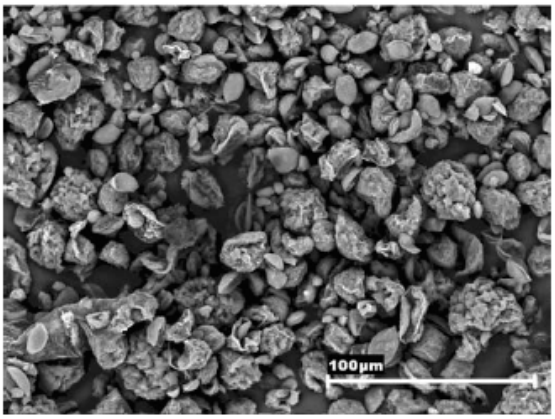

Figure 2. SEM microphotographs of CS microspheres produced by emulsification/solvent evaporation method using (a) dichloromethane and (b) ethylene acetate as inner oil phase.

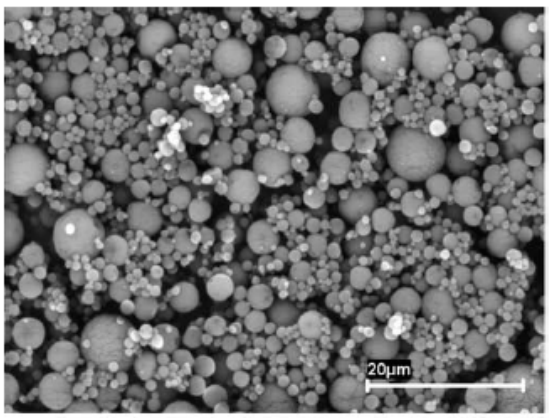

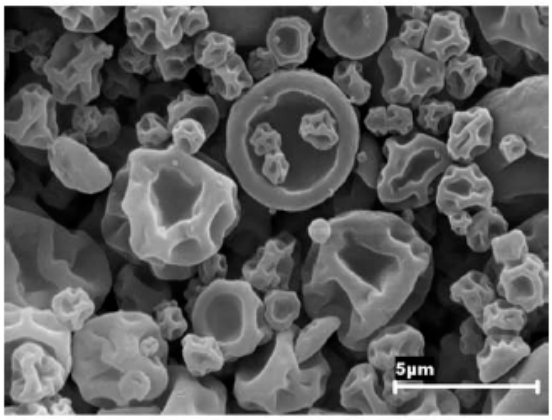

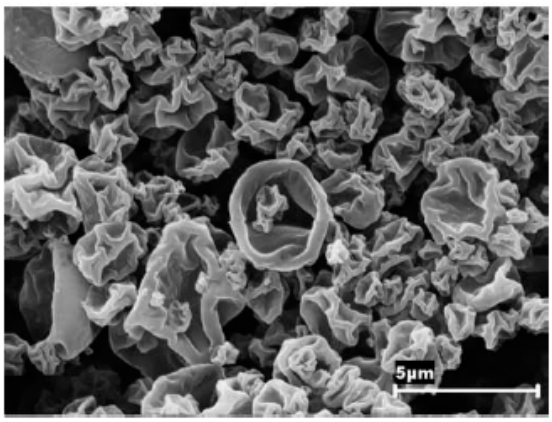

Figure 3. SEM microphotographs of CS microspheres produced by spray drying: (a) CS (deacetylation degree >85%) solution, (b) CS (deacetylation degree 23%) dispersion, and (c) CS-glucomannan (25:75) solution.

Table 8. Densities and aerodynamic diameters of chitosan microspheres obtained by spray-drying and double emulsification ($O_1/W/O_2$)/evaporation techniques (n = 3).

Preparation method	Polymer	Feret's diameter (μm)	ρr (g/cm^3)	ρa (g/cm^3)	Daer (μm)
Spray-drying	CS (DD > 80%)	2.04 ± 0.93	1.48 ± 0.09	0.48 ± 0.01	1.96 ± 1.53
Spray-drying	CS (DD = 23%)	1.79 ± 1.16	1.36 ± 0.04	0.38 ± 0.03	1.46 ± 1.45
Spray-drying	CS:GM (25:75) CS (DD > 80%)	2.69 ± 1.1	1.20 ± 0.08	0.30 ± 0.02	1.64 ± 1.46
Spray-drying[1]	CS:GM (25:75) CS (DD < 80%)	2.20 ± 1.08	1.42 ± 0.03	0.23 ± 0.02	1.07 ± 1.35
Emulsion ($O_1/W/O_2$) solvent evaporation[2]	CS (DD > 80%)	2.64 ± 1.10	1.46 ± 0.03	0.50 ± 0.01	3.52 ± 1.77

ρr: real density; ρa: apparent density; daer mean count (number) aerodynamic diameter determined using an Aerosiser® analyzer and real density values; Feret's diameter was determined by optical microscopy; CS: chitosan; GM: glucomanann; DD: deacetylation degree

[1] the spray-dried polymer dispersion has a concentration of 0.1% w/w; [2] dicloromethane was used as inner phase organic solvent.

0.02 g/cm^3 and their aerodynamic diameters were less than 5 μm, thus demonstrating the adequacy of these small microspheres to be delivered to the deep lung. Furthermore, the modification of these properties may have a significant impact on the agglomeration properties of the dispersed particles. Microspheres obtained by emulsion solvent evaporation had a geometric particle size of approximately 3 μm, apparent density of 0.5 g/cm^3, and aerodynamic diameter of less than 5 μm, thus being suitable for pulmonary drug delivery. The application of these microspheres as lung protein carriers was investigated using insulin and fluorescein isothiocyanate-labeled bovine serum albumin (FITC-BSA) as model compounds. High protein association efficiencies up to 90%–100% were obtained with microspheres prepared by both techniques. We are currently evaluating the *in vivo* behavior of the insulin-loaded microspheres. More specifically, the extent of hypoglycemic responses following intratracheal administration of powder insulin-loaded formulations to rats is being compared to that corresponding to insulin solution. Preliminary results are very encouraging, demonstrating that microspheres induce a prolonged reduction of glucose levels (time to reach the minimum plasma glucose level increases from 180 to 240 minutes for emulsion evaporation microspheres, while the minimum % of glucose level reached at this time increases approximately 1.6 times for both types of particles) (data not shown). Interestingly, CS microspheres, whose physicochemical properties were modified through the use of different cross-linking agents, have been shown to be compatible with the hydrofluoralkane propellant P134a, and, therefore, are good candidates for lung delivery via pressurized metered dose inhalers (pMDI) [72].

Huang et al. produced betamethasone-loaded CS microspheres by spray drying with encapsulation efficiency up to 95%, using CS as raw material and type-A gelatin and ethylene oxide-propylene oxide block copolymer (Pluronic F68) as modifiers. Microspheres are spherical and smooth and have a size distribution of 1–5 μm and a density of <0.4 g/cm^3, with all of these properties compatible with use for therapy via the lungs [76, 118]. Furthermore, by properly choosing excipient type and concentration, a high degree of control was achieved over the physical and release properties of microparticles. Although CS has been described in the literature as biocompatible, biodegradable, and nontoxic, few studies have focused on this subject. Therefore, these authors decided to examine biological effects related to inflammation of rat lung upon contact with the produced particles. They demonstrated that CS could induce proinflammatory responses in rat lung tissues in a dose-dependent manner, and these responses were probably related to its cationic polyelectrolyte properties (high positive surface charge of +45 mV), although the effects were mild relative to lipopolysaccharides. The lower doses tested were within the upper range of levels previously used in some therapeutic applications in which CS was used for pulmonary DNA delivery in mice [119]; but relatively higher doses of CS may be needed for delivery of other non-DNA therapeutic agents. Therefore, the main conclusion of this study was that these effects need to be considered in the context of therapeutic application via pulmonary delivery, especially if relatively high concentrations of CS are used. Furthermore, the type of CS chosen is crucial because the factors referred to that greatly influence CS toxicity are the type of salt, molecular weight, and deacetylation degree. In this respect, a higher degree of deacetylation of CS, which represents a higher positive zeta potential of the particles, was related to a higher *in vitro* cytotoxicity [120]. Accordingly, in this context, the use of less deacetylated CS could be desirable. With this idea in mind, we have recently tested the Calu-3 cells' sensitivity to chitosans of different deacetylation degree (>80%, 47%, and 38%) in both proliferating and well-differentiated cells, observing significant differences. As an example, for a chitosan concentration of 1mg/mL, cell viability in proliferating cells remained around 100% with respect to buffer control after four hours incubation for both less deacetylated chitosans, whereas it was only 20% for the high deacetylated polymer. It must be mentioned, however, that this marked difference was less pronounced in differentiated cells.

Hyaluronic acid (HA) is a naturally occurring hydrogel based on a linear polysaccharide comprised of repeating units of D-glucuronic acid and *N*-acetyl-D-glucosamine linked by β-1,4 and β-1,3 glycosidic bonds. It is a hygroscopic, amorphous material that slowly dissolves in water to form highly viscous solutions. Applications using HA for pulmonary controlled drug delivery are reported in the literature [75]. Inhalable dry powders (mass mean aerodynamic diameter, MMAD = 1–4 μm), which were produced by co-spray drying HA and insulin, induced modifications in insulin pharmacokinetics (the mean residence time

(MRT) and terminal half-life were extended when compared to spray-dried pure insulin) following administration to conscious dogs. Furthermore, the addition of Zn^{2+} or hydroxipropylcellulose to the microspheres improved MRT (more than 9 and 7 fold, respectively), AUC/dose (2.5 and 5 fold, respectively), and T_{max} (by a factor of 3 in both cases) [75].

5.3. Others

Materials such as mannitol and oligosaccharide ester derivatives (OED) have also been applied to produce microparticles for delivery through the pulmonary route using a spray-drying technique [74, 121]. OEDs are low molecular weight, lipophilic sugar-based compounds intended to address some technical problems (poor physical stability, erosion prior to drug release) presented by other polymers frequently used to obtain microspheres. Mannitol is one of the excipients most used in lung delivery, given its innocuous properties and low hygroscopicity.

Using ester derivatives from lactose and trehalose, Alcock et al. produced microspheres encapsulating leuprolide. These microspheres displayed a controlled release of the drug, which was dependent on the selected OED or combination of several OEDs and demonstrated to be stable for three months in 4–40°C and 60–75% humidity. Moreover, upon intratracheal administration of the microspheres to rats, leuprolide was detected in plasma for up to 25 hours, while the drug was detected for only 150 minutes after i.v. administration [74]. Okamoto et al. produced mannitol-insulin microparticles, which induced a stronger hypoglycemic response (glucose level decreased 15%) compared to an insulin solution (glucose diminished 5%), both administered intratracheally [121].

More recently, papers have reported the combination of some of the previously mentioned delivery systems to form a single one. For example, nanoparticles have been encapsulated inside microspheres in an attempt to integrate their advantages while avoiding their particular limitations, thus leading to more efficient delivery systems [63, 77, 122–123]. Delivery systems developed on this basis and intended for pulmonary administration of drugs will be addressed in a specific section in this chapter.

6. NANOPARTICULATE LUNG DRUG DELIVERY CARRIERS

Among the previously mentioned novel carrier systems, nanoparticulate-based technologies have proven successful, and their application has been introduced as an exciting alternative for drug administration through several routes [1, 42, 124–126]. This development has occurred mainly because it was demonstrated that particle size plays a key role in their ability to cross epithelia, with transport more favorable for nanoparticles (particles in the nanometric range) than for microparticles [1, 127–128]. Furthermore, it has been demonstrated that transport is more favorable for some hydrophilic polymers. These colloidal carriers have recently been proposed as vehicles for drug transport to the lung epithelium as we will review in this section using a wide range of materials such as polyesters, polysaccharides, and polyacrylates [7, 29]. Moreover, they have shown several important advantages, including improvement of drug stability, and, in some cases, the ability to control the drug release profile. Furthermore, an experiment with latex nanoparticles revealed that, given their small size, they are able to avoid mucociliary clearance and phagocytic activity [104, 129], while nanoparticles made of diverse polymers were efficiently taken up by alveolar epithelial cells [44, 96, 130]. There is no consensus concerning the ideal size range to avoid or delay macrophage-mediated phagocytosis. However, it has been reported that this phagocytic activity is maximum for particles of 1–2 μm, decreasing for both smaller and larger particles out of this range [15, 104, 131]. Generally, there is agreement that for particles in the micrometer range, the smaller the particle size, the higher the probability of being captured [15, 132].

In general, nanoparticles can be formulated and administered either in aqueous or dry powder form [133–134], the latter representing a possibility of overcoming frequent stability problems. The challenge of developing adequate particulate delivery systems is truly succeeding, and appreciable amounts of new carriers are appearing. In fact, the combination of various delivery systems to form a single complex system, such as the production of dry powders containing colloidal systems to solve aerodynamic and stability limitations, was recently proposed by several authors [63, 77, 133, 135–137].

In this section, we will present selected research works reporting the design and application of some new nanoparticulate technologies for pulmonary administration. Table 9 shows a summary of the polymers and materials used to produce the referred nanoparticulates. Special mention will be made of the application of nanoparticles in gene therapy. Studies reporting *in vitro* characterization of the systems as well as those containing studies on pulmonary cell lines and *in vivo* studies will be described. Furthermore, Tables 10 and 11 summarize, respectively, the most relevant nanoparticulate systems developed for lung delivery as well as the most interesting aspects of the *in vitro* and *in vivo* studies performed with them, indicating polymers, preparation methods, type of studies, and major results.

Table 9. Main excipients used to produce nanoparticulate lung drug delivery carriers.

Synthetic hydrophobic excipients	
Polyester derivatives	Polylactic-co-glycolic acid (PLGA), polylactic acid (PLA),
Acrylic polymers	Polybutylcyanoacrylate (PBCA), polyhexylcyanoacrylate (PHCA)
Lipids	Lecithin, gliceryl behenate
Natural hydrophilic excipients	
Proteins	Gelatin, albumin
Polysaccharides	Chitosan (CS)

Table 10. Description of *in vitro* studies performed with nanoparticulate systems developed for lung drug delivery.

Main excipient	Associated molecule	Preparation method	Performed studies	Major findings	Ref.
PLGA-PVA	Rifampicin Isoniazid Pyrazinamide	Solvent evaporation	Aerosol nebulization behaviour	96% of aerosol particles are in the respirable fraction size range (<6 μm). Aerosol droplets have MMAD of 1.9 μm. Optimum nebulization is achieved with jet and ultrasonic nebulizers	[138]
PVA-g-PLGA	Coumarin-6	Nanoprecipitation	Aerosol nebulization behaviour	Presence of nanoparticles does not negatively affect aerosol droplets size, which have an MMAD of approximately 4 μm	[97]
DEAPA-PVA-g-PLGA (CMC)	—	Nanoprecipitation	Nebulization Cell culture (A549)	Nanoparticles' zeta potential is controlled by CMC content. Presence of CMC has a positive effect on nanoparticle stabilization and internalization by lung cells	[96]
PLGA-WGA	—	Solvent evaporation	Cell culture (A549). Confocal microscopy of fluorescent nanoparticles	Nanoparticles are taken up and internalized by cells via a specific interaction with WGA-receptors	[44]
PLGA-WGA-IPM	Paclitaxel	Solvent evaporation	Cell culture (A549)	IPM increases nanoparticles' porosity. Higher antiproliferation activity compared to conventional paclitaxel formulation, which is attributed to more efficient cellular uptake via WGA-receptor mediated endocytosis.	[139]
CS-PLGA	Elcatonin	Nanoprecipitation	Aerosol nebulization behaviour	51% of nanoparticle suspension is in the respirable fraction size range. Aerosol droplets have a geometrical diameter of 6.5 μm	[114]
PBCA PHCA	—	Emulsion polymerization	Cell culture (16HBE14o- and primary airway epithelium)	PBCA and PHCA nanoparticles are highly toxic to pulmonary cell lines	[144]
PBCA	Insulin	Emulsion polymerization	Insulin release	Nanoparticles show a biphasic release profile with initial burst effect (50%) followed by slower release	[145]
Lecithin	Salbutamol	Microemulsion freeze-drying	Aerosolization with a pMDI	Nanoparticles are efficiently dispersed in HFA propellant. 58–65% of particles are in the respirable fraction size range, with a MMAD of 1.2–1.5 μm	[149]
Gelatin Albumin	—	Desolvation	Cell culture (16HBE14o- and primary airway epithelium)	Gelatin and albumin nanoparticles show little or no cytotoxicity	[144]
CS-TPP	Fluorescein isothyocyanate	Ionic gelation	Cell culture (A549)	Higher uptake of nanoparticles by A549 cells, compared to CS solutions. Nanoparticle internalization by the cells occurs predominantly by adsorptive endocytosis initiated by non-specific interaction between nanoparticles and cell membranes and partially mediated by clathrin-mediated processes	[130]

CMC: carboxymethylcellulose; CS: chitosan; DEAPA: diethylamino-propylamine; HFA: hydrofluoroalkane; IPM: isopropyl myristate; MMAD: mass mean aerodynamic diameter; PBCA: polybutylcyanoacrylate; PHCA: polyhexylcyanoacrylate; PLGA: polylactic-co-glycolic acid; pMDI: pressurized metered dose inhaler; PVA: polyvinyl alcohol; PVA-g-PLGA: polyvinyl alcohol–grafted–polylactic-co-glycolic acid; TPP: tripolyphosphate; WGA: wheat germ agglutinin

Table 11. Description of *in vivo* studies performed with nanoparticulate systems developed for lung drug delivery.

Main excipient	Associated molecule	Preparation method	Animal	Administration method	Major findings	Ref.
PVA-PLGA	Rifampicin Isoniazid Pyrazinamide	Solvent evaporation	Guinea pigs	Nebulization	Nanoparticles give significantly higher plasmatic levels of drug from 6 h up to 192 h compared to free drug	[138]
CS-PLGA	Elcatonin	Nanoprecipitation	Guinea pigs	Nebulization	CS modified nanoparticles give a prolonged pharmacological action and are eliminated slower than unmodified particles	[114]
PBCA	Insulin	Emulsion polymerization	Rats	Intratracheal instillation	Nanoparticles give more prolonged hypoglycaemia than insulin solutions	[145]
Gliceryl behenate	^{99m}Tc	Melted homogenization	Rats	Nebulization	Solid lipid nanoparticles are significantly taken up by the lymphatics. They are suitable for imaging or lung cancer therapy	[148]

CS: chitosan; PBCA: polybutylcyanoacrylate; PLGA: polylactic-co-glycolic acid; PVA: polyvinyl alcohol; ^{99m}Tc: radiolabeled Tecnetium

6.1. Nanoparticles Made of Synthetic Hydrophobic Materials

6.1.1. Nanoparticles of Polyester Derivatives

As was previously discussed, biodegradable and biocompatible derivatives of lactic acid, PLA and PLGA are excellent materials to prepare particulate lung carriers given their documented safety. The preparation of nanoparticles based on these polyester derivatives has been performed using techniques such as emulsion solvent evaporation [44, 138–139] and solvent displacement [96–97, 114]. Solvent displacement, also called nanoprecipitation, involves the use of an organic phase completely soluble in the external aqueous phase. The organic phase diffuses instantaneously to the external aqueous phase, inducing the immediate precipitation of the polymer. After nanoparticle formation, the solvent is eliminated and the suspension concentrated under reduced pressure [42].

PLGA nanoparticles containing 14% (w/w) PVA and encapsulating the antitubercular drugs rifampicin, isoniazid, and pyrazinamide, were produced by Pandey et al. by a solvent evaporation technique. Nanoparticle sizes varied between 190 and 290 nm and associated the drugs with efficacies between 57 and 68%. Drug-loaded nanoparticle suspensions were shown to be efficiently aerosolized with a nebulizer; 96% of the aerosolized particles were in the respirable fraction, and the resultant aerosol droplets presented a mass mean aerodynamic diameter (MMAD) of approximately 1.9 μm. Therefore, the nanoparticle formulation was considered suitable for delivering the encapsulated drugs into the deep pulmonary regions [138].

Nanoparticles consisting of polyvinyl alcohol (PVA)-grafted-PLGA were produced using the method of nanoprecipitation (PVA/PLGA ratios = 1:10 and 1:20), encapsulating coumarin-6 as a model drug. The obtained particle size was approximately 100 nm, and the encapsulation efficiency was around 37%. Nanoparticle suspensions were nebulized without further processing using three different nebulizers. The aerosol patterns were compared to those of 0.9% NaCl and 5% glucose solution, which were used as controls. When using nebulization as the aerosol generation process, nanoparticles are known to be efficiently incorporated in the respirable fraction of aerosolized droplets (when compared to larger particles) because the size of nanoparticles perfectly fits the droplet size range (1–5 μm) [140]. Therefore, as expected, the generated aerosols were generally considered to be within this respirable fraction, and the presence of nanoparticles did not negatively affect the aerosol droplet size in a clinically relevant manner when compared to the used controls. This result indicates the suitability of the nanoparticles for pulmonary administration using nebulization. However, the technique of aerosol generation (jet, ultrasonic, and piezo-electric nebulizer) was shown to influence the aggregation of nanoparticles during the aerosolization process. Only jet and ultrasonic nebulizers resulted in adequate aerosol droplets for lung delivery [97], which suggests that the adequate nebulization technique should be cautiously selected to maximize the therapeutic effect. Moreover, the same authors proposed the production of nanoparticles containing PVA-grafted-PLGA with a backbone of diethylaminopropylamine (DEAPA-PVA-g-PLGA), with some also comprising carboxymethylcellulose (CMC) in concentrations ranging from 0 to 400 μg CMC/mg polymer. The main advantage of this system is that the amphiphilic properties of the polymer DEAPA-PVA-g-PLGA made nanoparticles preparation by the solvent displacement method possible without adding the usual surfactant stabilizer required for the preparation of the first system mentioned [96]. This is of crucial importance for pulmonary application because it is known that the inhalation of high amounts of synthetic surfactants may affect the surface tension of the pulmonary surfactant, thus resulting in inflammation or impaired natural functions [46]. The referred nanoparticles had sizes ranging between 70 and 250 nm; and their zeta potential was dependent on the CMC concentration, being strongly positive when no CMC was present and decreasing gradually, reaching accentuated negative values when the formulation comprised 400 μg CMC/mg polymer. The point where zeta potential changed from positive to negative was 50 μg CMC/mg polymer. Although cell association was low, the anionic nanoparticles were the only ones internalized by the A549 cells, an alveolar epithelial cell line, and were the most stable during nebulization. Therefore, anionic nanoparticles are expected to be the most suitable for aerosol therapy [96]. Unfortunately, an explanation for these particle/cell interaction patterns was not provided.

As already commented on, Mo and Lim prepared PLGA nanoparticles conjugated with wheat germ agglutinin (WGA) by the solvent evaporation method. These nanoparticles, with a size around 250 nm, were efficiently taken up by the A549 cells in a time-, temperature-, and concentration-dependent saturable process. Nanoparticle internalization was confirmed by confocal microscopy, and fluorescein isothiocyanate-bovine serum albumin (FITC-BSA)-loaded PLGA nanoparticles were used as control. The conclusion was that the high internalization of the WGA-PLGA nanoparticles was preceded by a specific interaction with WGA-binding receptors in the cells and was mediated by caveolae-dependent endocytic pathways [44]. In a subsequent study, isopropyl myristate was further added to the WGA-PLGA nanoparticles, which encapsulated paclitaxel, a chemotherapeutic drug, with an efficiency of 66%. The addition of isopropyl myristate resulted in the formation of pores and channels in the nanoparticles, therefore facilitating the drug release. The release profile showed an initial burst effect in the first five hours, followed by a slower release for five days, which resulted in the release of 40% paclitaxel. Furthermore, studies in A549 cells resulted in a five-fold increase in drug action (also at five hours), compared to the conventional commercial formulation of paclitaxel. The high antiproliferation activity of these nanoparticles was attributed to more efficient cellular uptake via WGA receptor-mediated endocytosis. Moreover, once in the cytoplasm, isopropyl myristate facilitated the release of the loaded paclitaxel, thereby contributing to a stronger effect of the drug [139].

Another approach for surface modification was the alteration of PLGA nanospheres with chitosan, a natural polymer. (For further characterization of chitosan, consult the next section on polysaccharides.) The nanospheres were prepared by the nanoprecipitation method. Produced nanoparticles efficiently encapsulated the peptide elcatonin and had a size of approximately 650 nm. Nanoparticles were successfully aerosolized with a nebulizer, resulting in aerosol droplets with a geometrical diameter of 6.5 μm, which resulted in a respirable fraction of 51% [114].

So far, few *in vivo* studies have been performed with polyester-based nanoparticles for pulmonary delivery. Pandey et al. evaluated PLGA nanoparticles containing antitubercular drugs, developed as referred to above. Using a nebulizer, these nanoparticles were efficiently aerosolized to guinea pigs, and plasmatic drug levels were evaluated using a solution of the free drug administered orally as a control. Following nebulization, drugs could be detected in the plasma from 6 hours up to 144 hours (rifampicin) and 192 hours (isoniazid and pyrazinamide), contrary to what was observed after oral administration in which case the drugs were detected only until 12 hours. Figure 4 displays plasma versus time profiles of isoniazid following nebulization of drug-loaded nanoparticles and oral administration of the free drug in solution. The PVA content (approximately 15%) was reported to provide stability by forming a barrier to the diffusional release of the drugs, resulting in a sustained release [138].

In another *in vivo* study, surface-modified PLGA nanospheres with chitosan, which were aerosolized with a nebulizer to guinea pigs, had a slower elimination rate from the lung than the unmodified particles. Moreover, chitosan

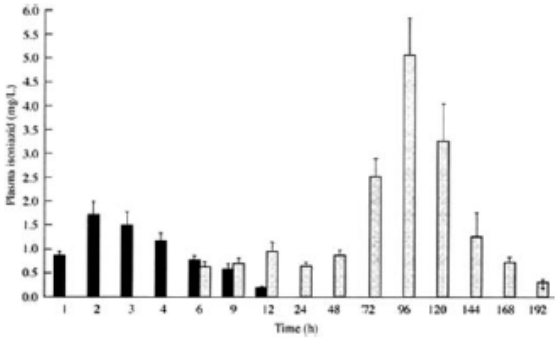

Figure 4. Plasma profile of isoniazid following the nebulization of drug-loaded PLG-NP and oral administration of parent drug. Values are mean ± S.D., n = 6–8. Black bars, oral isoniazid; grey bars, nebulized isoniazid-loaded PLG-NP. Reprinted with permission from [138], R. Pandey et al., *J. Antimicrob. Chemother.* 52, 981 (2003). © 2003, The British Society for Antimicrobial Therapy.

modification resulted in a prolonged and stronger hypocalcemic effect of elcatonin. Figure 5 shows blood calcium levels versus time following pulmonary administration of drug-loaded modified and unmodified nanospheres. The observed behavior of the chitosan-modified nanospheres was attributed to the mucoadhesive properties of chitosan as well as to its ability to open the intercellular tight junctions [114].

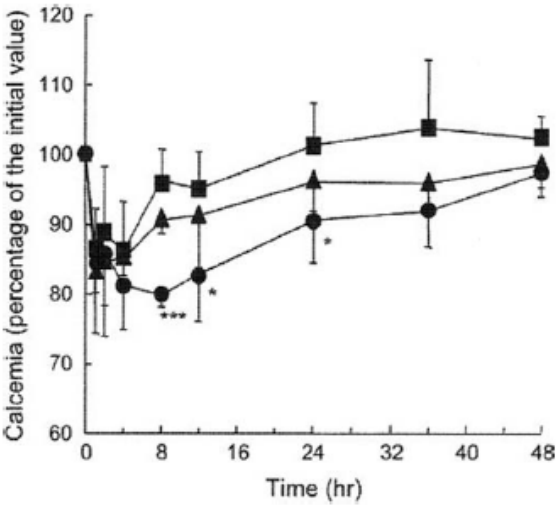

Figure 5. Profiles of the blood calcium level after pulmonary administration of the elcatonin-loaded nanosphere suspension (100 IU/kg) to male guinea pigs (6 weeks). (■) Elcatonin solution; (▲) noncoated PLGA nanospheres; (●) chitosan-coated PLGA nanospheres. Data are presented as the means ± S.D. (n = 5). ***$p<0.001$, *$p<0.05$ compared with elcatonin solution. Reprinted with permission from [114], H. Yamamoto et al., *J. Control. Release* 102, 373 (2005). © 2005, Elsevier.

6.1.2. Nanoparticles of Acrylic Polymers

Regarded as nontoxic and highly biocompatible, acrylate derivatives are currently components of drug delivery systems developed for many routes of administration [141–142]. In fact, the first nanoparticulate systems containing cyanoacrylates were reported in the 1970's and in the early 1980's. Couvreur et al. developed biodegradable poly (alkylcyanoacrylate) (PACA) nanoparticles by a simple polymerization reaction [42]. Since then, these nanoparticles have been the object of intensive research in the area of polymeric colloidal drug carriers, and many applications have emerged in the field of drug delivery [142], including delivery via the pulmonary route. The technique of emulsion polymerization, which is still used, consists of the emulsification of droplets of water-insoluble monomers in an external aqueous and acidic phase that contains a stabilizer, under magnetic stirring. The monomers polymerize relatively fast by an anionic polymerization mechanism, with a polymerization rate dependent on the pH of the medium. At acidic pH, between 2 and 4, the reaction is relatively slow, yielding nanospheres with a narrow-size distribution (frequently 200 nm, and, in some cases, less than 50 nm) [42, 143].

Brzoska et al. produced nanoparticles composed of polybutylcyanoacrylate (PBCA) or polyhexylcyanoacrylate (PHCA) using the previously described technique. The nanoparticles had sizes between 110 and 240 nm. However, they were shown to be highly toxic to a primary culture of airway epithelial cells as well as to the 16HBE14o- cell line [144]. This observation pointed out that care should be taken when using these polymers by the pulmonary route. However, to our knowledge, this is a unique study evaluating the toxicity of these polymers in pulmonary cell lines; further studies are needed to confirm the suggested toxicity. In addition, it is important to take into account that cell cultures are very susceptible to external factors that are not always easily controlled. The best way to confirm the safety of these polymers should be the performance of *in vivo* studies that allow the accurate evaluation of the lung tissue, evidencing eventual damage caused by the polymers.

Insulin-loaded PBCA nanoparticles were produced by emulsion polymerization, with a mean size around 250 nm. Insulin was associated with 80% efficiency, and, upon intratracheal administration of the nanoparticle suspension to normal rats, peptide doses of 10 or 20 IU/kg reached a reduction in serum glucose levels comparable to that obtained with a solution with the same insulin amount, however, achieving more prolonged effects. The duration of glucose levels below 80% of basal was considered a criterion to evaluate the formulation's efficacy. As can be observed in Figure 6a, with the dose of 10 IU/kg, the PBCA nanoparticles formulation reached a minimum glucose level of 30% at four hours, while the solution reached the minimum value of 20% at the same time interval. However, the 80% blood glucose level was reached after 8 hours for the solution and at 16 hours for the nanoparticles. When using 20 IU/kg (Figure 6b), the blood glucose level reached minimum points of 14% at eight hours for the nanoparticles and 4% at six hours for the respective insulin solution. Again, the recuperation to normal levels was faster when the solution was administered (80% at 12 hours for the solution and at 20 hours for the nanoparticles). These studies registered the possibility that administering nanoparticles, which may achieve similar, if not better, reductions in the glucose levels as with administration of solution with the same insulin amount, results in a more prolonged effect, thus indicating the controlled release of insulin from the nanoparticles [145]. The intratracheal administration of a suspension is not a method that could be used in humans; therefore, it is not feasible for clinical trials. The correct method for nanoparticle administration as a suspension would be nebulization. This sort of study is not reported, and the authors do not refer to the nanoparticles' stability, an important issue concerning the administration and storage of suspensions.

6.1.3. Lipidic Nanoparticles

The excellent potential of using lipids to prepare drug delivery pulmonary carriers has been shown in the previous section. Solid lipid nanoparticles (SLN) were recently proposed as novel drug delivery systems. First reported by Müller's group from Berlin in the 1990's for intravenous administration due to their biocompatibility, they have been repeatedly proposed as interesting approaches in drug delivery because they provide low cytotoxicity and controlled drug release due to the solid lipid matrix [146–147]. Recently, they were proposed in the pulmonary field to act as colloidal carriers for cytotoxic drugs intended for lung

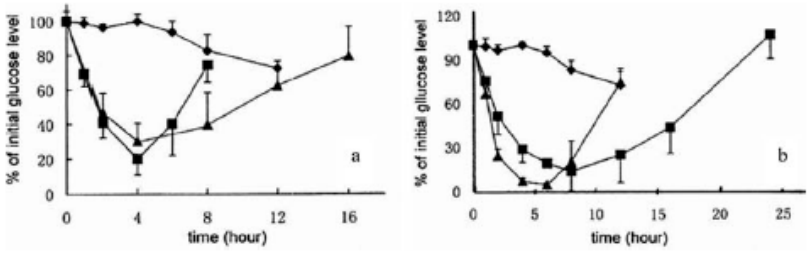

Figure 6. Hypoglycemic effect of a single intratracheal administration of a) insulin-loaded nanoparticles of 10 IU·kg^{-1} (▲) and insulin solution of 10 IU·kg^{-1} (■); b) insulin-loaded nanoparticles of 20 IU·kg^{-1} (■) and insulin solution of 20 IU·kg^{-1} (▲) to normal rats fasted overnight. The glucose concentration at time zero served as the basis for comparison (%). Results are means for 5 or 6 animals. The control (◆) is phosphate buffer solution (pH 7). Reprinted with permission from [145], Q. Zhang et al., *Int. J. Pharm.* 218, 75 (2001). © 2001, Elsevier.

cancer treatment as well as radiolabeled agents for lymphoscintigraphy. In this manner, solid lipid nanoparticles composed of glyceryl behenate containing a radiolabel (99mTc) were produced by the melted homogenization technique, resulting in a mean size around 200 nm. Upon nebulization to rats, gamma scintigraphic images showed a significant uptake of the radiolabeled SLN into the lymphatics, rendering them suitable as carriers to be applied in either imaging techniques or lung therapy [148].

Dickinson et al. developed a formulation of lecithin-based nanoparticles using water/lecithin/propanol/iso-octane microemulsions containing 40–45% (w/w) of surfactant (lecithin/propanol). Nanoparticles were frozen and freeze-dried, obtaining a size smaller than 100 nm, and salbutamol was used as the model drug. These nanoparticles were efficiently dispersed in co-solvent modified HFA-227, a pMDI propellant, due to the presence of the surfactant. Upon aerosolization from this device, the mass mean aerodynamic diameter (MMAD) and fine particle fraction, which were 1–1.5 μm and 55–65%, respectively, were found to be suitable for systemic pulmonary administration of drugs [149].

6.2. Nanoparticles Made of Natural Hydrophilic Materials

6.2.1. Protein-based Nanoparticles

Proteins, such as gelatin and albumin, are natural hydrophilic polymers, with evident advantages from a manipulation (avoidance of organic solvents) and drug transport point of view. The major drawbacks of these materials are the easy degradation and the potential antigenicity when administered by the parenteral route. Nevertheless, information on their antigenicity by pulmonary route is still scarce, therefore further *in vivo* toxicity studies will have to be performed to assess the safety of carriers based on these polymers. Nanoparticles based on albumin and gelatin are usually prepared by a desolvation technique. This method consists of dissolving the protein in water, subsequently desolvating with a solvent such as alcohol or acetone. Finally, cross-linking with glutaraldehyde takes place, leading to the formation of colloidal particles [42]. Brzoska et al. produced gelatin and human serum albumin (HSA) based nanoparticles using the above described desolvation technique. Having a size around 240–280 nm, they were assayed using a primary culture of airway epithelial cells and the 16HBE14o- cell line with no observed toxicity. Confocal microscopy analysis showed that gelatin nanoparticles and HSA nanoparticles were incorporated into airway epithelium cells in a concentration- and temperature-dependent manner. At 4°C there was no uptake, in contrast to what happens at 37°C, indicating that nanoparticle penetration is an active endocytic process. Taking these features into account, the referred nanoparticles (HSA and gelatin-based) were considered to be highly suitable drug or gene carriers via the pulmonary route [144].

6.2.2. Nanoparticles of Polysaccharides

Using an ionic gelation technique [150], our group has developed chitosan/tripolyphosphate (CS/TPP) nanoparticles, which were reported to be efficient carriers of several peptides through distinct routes of administration, including nasal and ocular routes, promoting their absorption as well [111–113]. This technique consists of the interaction between the positively charged chitosan amino group and the negatively charged phosphate groups of pentasodium tripolyphosphate (TPP). Recently, we have evaluated the cytotoxicity of chitosan nanoparticles in bronchial Calu-3 cells. Results showed that chitosan nanoparticles significantly decreased the cytotoxicity of the polymer, increasing the IC_{50} (concentration-inhibiting cell viability with 50%) about 10-fold compared to the CS solution.

Using the same technique, Huang et al. produced FITC-labeled CS/TPP nanoparticles with a mean size of approximately 200 nm and investigated their uptake by A549 cells, an alveolar cell line of human origin. Results showed a higher uptake of the chitosan nanoparticles compared to the chitosan solution. Moreover, uptake of the nanoparticles was concentration- and temperature-dependent, increasing with concentration and significantly reduced at 4°C compared to 37°C. This led the authors to conclude that internalization of nanoparticles by the cells occurs predominantly by adsorptive endocytosis initiated by non-specific interactions between nanoparticles and cell membranes, and is partially mediated by a clathrin-mediated process [130].

In recent years, there has been a boom of research into nonviral vectors intended for gene delivery, including cationic polymers, cationic lipids/liposomes, and, more recently, polymeric nanostructures. These nanostructures are gaining popularity because they are easily produced and scaled-up, there is no size limit on the DNA to be delivered, there are fewer immunological and safety implications, they offer the potential of sustained release of gene/gene products within the transfected cells [151–152], and can be targeted by the attachment of cell-specific ligands [153].

Among the materials used to obtain nanoparticulate carriers, polycationic polymers, particularly chitosan, have emerged as promising vehicles for nonviral plasmid DNA (pDNA) delivery [154–155], and, very recently, for *in vivo* delivery of small interfering RNA (SiRNA) used as a genetic vaccine against the respiratory syncytial virus infection [156]. Consisting of a simple chitosan-based gene delivery system, it is comprised of ionic complexes, i.e., polyplexes, which are mainly assembled through ionic interactions between the positively charged groups of chitosan and the negatively charged groups of pDNA. Moreover, the ability to form these polyplexes is dependent on chitosan structural parameters, i.e., the degree of deacetylation, and the molecular weight [155, 157–158]. Although these polyplexes are promising for mucosal pDNA delivery, they still suffer from several limitations such as undefined physical shapes, dissociation in the presence of anions, and a limited capacity to co-associate other functional molecules such as proteins to the polyplex structure, which could help overcome the cellular barriers for efficient gene transfer and expression. One strategy proposed to solve these limitations is based on the addition of a desolvating agent, which induces phase separation, and, consequently, the formation of coacervates, generally called nanospheres or nanoparticles [154, 159–161], whose transfection efficiency is comparable

to that of polyplexes. Another strategy to form defined chitosan nano-scale gene carriers is to hydrophobically modify chitosan, thus enabling it to self-assemble in aqueous solution [162–163].

Finally, to overcome the above mentioned limitations with polyplexes, Koping-Hoggard et al.have adopted the ionic-gelation technique, previously developed in our group for the encapsulation of peptides and proteins [111, 150], to incorporate pDNA and small oligonucleotides into chitosan nanoparticles. In this technique, the DNA molecule to be encapsulated is previously incorporated in the cross-linking TPP solution, and, in this case, the nanoparticle formation would not only be determined by electrostatic interactions between chitosan and DNA, but it would also be governed by the cross-linking agent. Just as expected, nanoparticles formed because of this process have a more compact structure, with controlled release properties that are expected to influence the performance of the system both *in vitro* and *in vivo*. A qualitative assessment of the *in vivo* efficiency of this system was obtained by administering nanoparticles loaded with pDNA encoding beta-galactosidase (pLacZ) intratracheally to mice, using naked pLacZ as a control. Nanoparticles made from low molecular weight chitosan resulted in a strong beta-galactosidase gene expression in mouse lungs 72 hours after administration, in contrast to the high molecular weight chitosan particles and naked plasmid [164].

7. LUNG DRUG DELIVERY CARRIERS COMBINING NANO- AND MICROPARTICLES

In recent years, we have been assisting in the appearance of very innovative drug delivery systems, which are, in fact, the combination of a few other systems. It was in the later 1990's when, to our best knowledge, the encapsulation of nanospheres inside microspheres was first reported in an attempt to improve the inhalation efficacy of nanospheres [133]. However, the basic idea of combining systems had appeared before with the encapsulation of particulate matter inside lipid vesicles [165–166]. The encapsulation of vesicles inside a second vesicle has also been reported [122]. Several research groups followed the idea toward a pulmonary drug delivery application, with the strong challenge of overcoming aerosolization and stability problems. Table 12 summarizes data on combined drug delivery systems developed for pulmonary administration, describing the composition of each of the integrated systems, the preparation methods, and the major findings.

Tsapis et al. developed a formulation comprised of nanoparticle-loaded microspheres using polystyrene nanoparticles. These nanoparticles were simply added to a mixture of DPPC, dimyristoylphosphatidylethanolamine (DMPE), and lactose and spray dried afterward. The resultant microspheres had adequate properties for pulmonary administration, with aerodynamic diameters ranging between 3–5 μm and the ability to be readily dissolved into a nanoparticle suspension upon contact with an aqueous medium [63]. Sham et al. developed a similar formulation, preparing lactose microspheres containing either gelatin or cyanoacrylate nanoparticles (obtained by desolvation and emulsion polymerization, respectively) by spray drying. The presented microspheres also yielded aerosols with aerodynamic characteristics suitable for efficient pulmonary delivery; their aerodynamic diameter was around 3 μm, which resulted in fine particle fraction of 40%. The nanoparticles were also recovered from the microspheres without significant changes in their size or zeta potential after being dissolved in an aqueous medium [167]. Another formulation of microspheres encapsulating nanoparticles was proposed by Cook et al., who prepared terbutaline sulfate nanoparticles by emulsification and subsequently spray dried using hydrogenated palm oil as an excipient in an attempt to achieve a sustained release of the drug. The microspheres were adequate for pulmonary administration because they had an aerodynamic diameter of 3.9 μm and exhibited a fine particle fraction of 47% and mass mean aerodynamic diameter (MMAD) of 3.9 μm. Moreover, a sustained release of the drug was achieved [168].

Unfortunately, all of these works were dependent on the utilization of organic solvents during the preparation of the formulations (either in the nanoparticles formation process or during their microencapsulation), and the presence of any organic traces in these microspheres could exert a very damaging effect on the pulmonary epithelium. Therefore,

Table 12. Description of combined microencapsulated nanoparticle systems adequate for pulmonary administration.

Nanoparticle composition	Nanoparticle preparation method	Microsphere composition	Microsphere preparation method	Major findings	Ref.
Polystyrene	Commercially supplied	DPPC, DMPE, lactose	Spray-drying	Aerodynamic diameters between 3 and 5 μm	[63]
Gelatin Cyanoacrylate	Desolvation Emulsion polymerization	Lactose	Spray-drying	40% of the particles in the respirable fraction and MMAD around 3 μm	[167]
Terbutaline sulfate	Emulsification	Hydrogenated Palm Oil	Spray-drying	47% of the particles in the respirable fraction and MMAD of 3.9 μm. Sustained release of the drug was achieved	[168]
CS-TPP	Ionic gelation	Mannitol	Spray-drying	Aerodynamic diameter of 2–3 μm. Spray-drying had no effect on insulin release from nanoparticles	[77]

CS: chitosan; DMPE: dimiristoylphosphatidylethanolamine; DPPC: dipalmitoylphosphatidylcholine; MMAD: mass mean aerodynamic diameter; TPP: tripolyphosphate

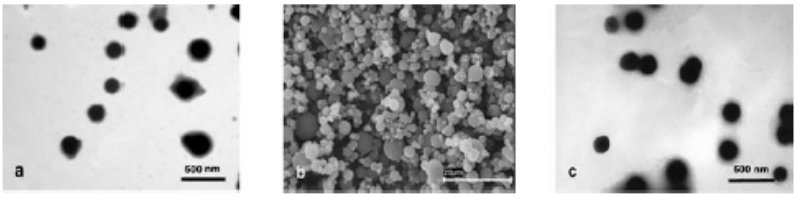

Figure 7. Microphotographs of CS/TPP nanoparticles and mannitol microspheres containing CS/TPP nanoparticles obtained by transmission electron microscopy (TEM) and scanning electron microscopy (SEM) respectively: a) fresh CS/TPP nanoparticles, b) microspheres containing mannitol/nanoparticles theoretical ratio of 80/20, and c) recovered CS/TPP nanoparticles. Reprinted with permission from [77], A. Grenha et al., *Eur. J. Pharm. Sci.* 25, 427 (2005). © 2005, Elsevier.

we accepted the challenge of producing such a formulation comprising chitosan nanoparticles, prepared by the previously mentioned ionic gelation method developed in our group, encapsulated in mannitol microspheres and prepared using only hydrophilic polymers and an entirely aqueous medium. To obtain these microspheres, chitosan nanoparticles were produced and mixed with a mannitol aqueous solution to obtain different mannitol (Ma)/nanoparticles (NP) ratios (Ma/NP = 50/50–95/5). Finally, the nanoparticles suspension was spray dried, obtaining dry powders that presented optimal properties for lung delivery with aerodynamic diameters varying between 2 and 3 μm. Figure 7 displays images of fresh nanoparticles (a), microparticles obtained after spray drying mannitol/nanoparticles suspension (b), and nanoparticles recovered from microspheres (c). In fact, this recovering process was easily performed *in vitro* upon microspheres' contact with an aqueous medium, and the spray-drying process did not have a negative effect on the nanoparticles' size, zeta potential, or insulin release profile (Fig. 8) because significant alterations on these parameters were not registered [77]. Specific analysis of the surface and internal structure of the system, which were performed using confocal microscopy and surface analysis techniques such as X-ray photoelectron spectroscopy (XPS) and time-of-flight secondary ion mass spectrometry (TOF-SIMS), demonstrated that the nanoparticles were homogeneously distributed in the microspheres. Furthermore, these microspheres were biocompatible with two different pulmonary cell lines of human origin (bronchial Calu-3 and alveolar A549). In fact, no significant toxic effects were observed in either cell line upon incubation with the formulations for as long as 48 hours. Furthermore, uptake studies suggested that nanoparticle internalization did not occur, but suggested the presence of cell membrane association. Considering all of these data and especially the absence of toxicity and the adequate aerodynamic properties, the presented system could represent a promising tool for the pulmonary administration of therapeutic macromolecules as powders. However, the performance of *in vivo* studies is a critical step that could definitely attest to the system suitability for lung delivery. Preliminary *in vivo* studies (n = 3) were already carried out with insulin-loaded microspheres (mannitol/nanoparticles ratio = 80/20). The efficacy of the system was assessed by measuring the hypoglycemic responses following intratracheal administration of the microspheres powder (16.7 IU/kg) to anesthetized rats. The curves corresponding to plasma glucose concentrations are shown in Figure 9, in which the decrease in glucose levels caused by the microspheres was compared to that of a control insulin solution (17.9 IU/kg). As can be seen, although the insulin control solution has a slightly higher dose of insulin, the administration of microspheres resulted in a stronger hypoglycemic effect during the first two hours, and the glucose level decreased to a greater extent ($P < 0.05$) than with the control insulin. In fact, the control insulin solution led to a minimum glucose level of 38% at 60 minutes, whereas the administered microspheres containing nanoparticles yielded a minimum glucose level of 8% at the same assay time (60 minutes).

Encouraged by these favorable results and considering the unique properties of hyaluronic acid (HA) reported in the literature relative to their choice for pulmonary administration [75], our group is currently developing a similar carrier composed of hyaluronic acid/chitosan nanoparticles prepared by ionic cross-linking encapsulated in mannitol microspheres. Finally, we are further developing a novel delivery system for pulmonary administration that is a combination of three different systems. It consists of coating chitosan nanoparticles with a lipid layer and

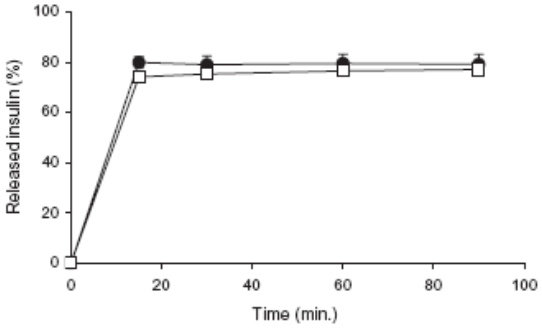

Figure 8. Release profile of insulin from (●) nanoparticles (CS/TPP = 6:1) and (□) microspheres (mannitol/nanoparticles = 80/20, solids content = 2.1%, CS/TPP = 6:1), in PBS pH 7.4 at 37°C (insulin = 30% w/w based on CS; mean ± SD, n = 3). Reprinted with permission from [77], A. Grenha et al., *Eur. J. Pharm. Sci.* 25, 427 (2005). © 2005, Elsevier.

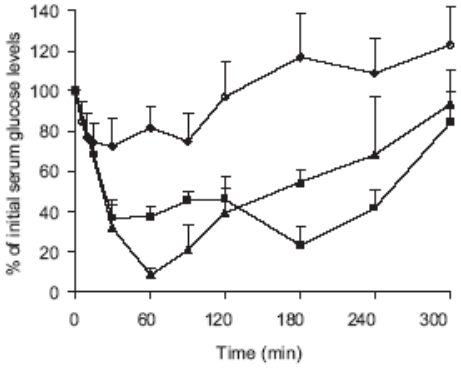

Figure 9. Hypoglycemic effect following intratracheal administration of (◇) a control PBS solution pH 7.4; (■) a control insulin solution (dose 17.9 U/kg) in PBS pH 7.4; and (▲) microspheres mannitol/nanoparticles = 80/20 (dose 16.7 U/kg).

microencapsulating it afterward in mannitol microspheres, which present suitable properties for lung delivery.

As demonstrated, many investigation efforts have been directed to the pulmonary field to overcome some problems previously referred to such as stability, aerosolization patterns, etc., resulting in the development of some new nanoparticulate-based technologies. However, the lack of *in vivo* studies is still strongly noticed in this field to ensure the feasibility of these delivery systems for a pulmonary application.

8. MAIN REMARKS

It is clear from the preceding comments that drug administration through the pulmonary route represents an excellent and alternative opportunity for some new molecules as well as for some others that did not gather good results through other routes. Special mention should be paid to the encouraging results related to the absorption of peptides and proteins. However, many challenges have to be faced from now on, and drugs will only be successfully administered through the lung when drug carriers have such properties that enable them to overcome distinct barriers such as difficult accessibility, aerodynamic specificities, and mucociliary clearance. In this manner, nanoparticles and microparticles have been proposed as carriers for pulmonary administration using a wide range of polymers and materials because they can offer efficient and controlled delivery as well as protection of the encapsulated molecules.

ACKNOWLEDGMENTS

This work was supported by the Spanish Government (CICYT, SAF2002-03314) (Cofinanced by FEDER Funds). The Predoctoral fellowship to Ana Grenha from Fundação para a Ciência e Tecnologia, Portugal (SFRH/BD/13119/2003) is highly appreciated.

REFERENCES

1. M. J. Alonso, *Biomed. Pharmacother.* 58, 168 (2004).
2. P. L. Smith, *J. Control. Release* 46, 99 (1997).
3. J. L. Cleland, A. Daugherty, and R. Mrsny, *Curr. Opin. Biotechnol.* 12, 212 (2001).
4. H. Takeuchi, H. Yamamoto, and Y. Kawashima, *Adv. Drug Deliv. Rev.* 47, 39 (2001).
5. D. A. Edwards, A. Ben-Jebria, and R. Langer, *J. Appl. Physiol.* 84, 379 (1998).
6. A. Clark, *Drug Deliv. Syst. Sci.* 2, 73 (2002).
7. H. M. Courrier, N. Butz, and T. F. Vandamme, *Crit. Rev. Ther. Drug Carrier Syst.* 19, 425 (2002).
8. J. S. Patton, *Adv. Drug Deliv. Rev.* 19, 3 (1996).
9. G. Taylor and I. Kellaway, in *Drug Delivery and Targeting. For Pharmacists and Pharmaceutical Scientists,* A. Hillery, A. Lloyd, and J. Swarbrick, Eds., Taylor & Francis, New York (2001), p. 269.
10. B. Fawcett, in *Tratado de Histología,* B. Fawcett and D. W. Fawcett, Eds., Interamericana McGraw-Hill, Madrid (1995), p. 765.
11. L. P. Gartner and J. L. Hiatt, *Histología: Texto y Atlas,* Interamericana McGraw-Hill, Madrid (1997).
12. E. E. Schneeberger and R. D. Lynch, in *Fluid and Solute Transport in the Airspaces of the Lungs,* R. M. Effros and H. K. Chang, Eds., Marcel Dekker, New York (1994), p. 1.
13. F. Geneser, *Histología: Sobre Bases Biomoleculares,* Editorial Medica Panamericana, Madrid (2000).
14. X. Yang, K. A. Joseph, C. J. Malanga, and Y. Rojanasakul, *Int. J. Pharm.* 195, 93 (2000).
15. F. Ahsan, I. P. Rivas, M. A. Khan, and A. I. Suárez-Torres, *J. Control. Release* 79, 29 (2002).
16. E. R. Jacobs and T. E. DeCoursey, in *Fluid and Solute Transport in the Airspaces of the Lungs,* R. M. Effros and H. K. Chang, Eds., Marcel Dekker, New York (1994), p. 151.
17. H. G. Burkitt, B. Young, and J. W. Heath, *Histología Funcional Wheater,* Churchill Livingstone, Madrid (1993).
18. A. Rios, M. E. Gordillo, C. Bocanegra, and J. A. Maldonado, in *Administración de Medicamentos: Teoría y Práctica,* B. S. Ramos and M. D. Aznar, Eds., Diaz de Santos, Madrid (1994), p. 131.
19. P. Gehr, F. H. Y. Green, M. Geiser, V. I. Hof, M. M. Lee, and S. Schurch, *J. Aerosol Med.* 9, 163 (1996).
20. K. McDonald and G. Martin, *Int. J. Pharm.* 201, 89 (2000).
21. I. J. Smith and M. Parry-Billings, *Pulm. Pharmacol. Ther.* 16, 79 (2003).
22. I. J. Smith, *Drug Deliv. Syst. Sci.* 2, 63 (2002).
23. H. Okamoto, H. Todo, K. Iida, and K. Danjo, *Kona* 20, 71 (2002).
24. H. Schulz, *Pharm. Sci. Technol. Today* 1, 336 (1998).
25. J. Hanes, M. Dawson, Y. Har-el, J. Suh, and J. Fiegel, in *Pharmaceutical Inhalation Aerosol Technology,* A. J. Hickey, Ed., Marcel Dekker, New York (2004), p. 489.
26. J. Heyder, J. Gebhart, G. Rudolf, C. F. Schiller, and W. Stahlhofen, *J. Aerosol Sci.* 17, 811 (1986).
27. N. R. Labiris and M. B. Dolovich, *Br. J. Clin. Pharmacol.* 56, 588 (2003).
28. A. R. Clark, in *Pharmaceutical Inhalation Aerosol Technology,* A. J. Hickey, Ed., Marcel Dekker, New York (2004), p. 571.
29. S.-A. Cryan, *AAPS J.* 7, E20 (2005).
30. M. Sakagami and P. R. Byron, *Clin. Pharmacokinetics* 44, 263 (2005).
31. J. S. Patton and R. M. Platz, *Adv. Drug Deliv. Rev.* 8, 179 (1992).
32. Z. Shen, Q. Zhang, S. Wei, and T. Nagai, *Int. J. Pharm.* 192, 115 (1999).
33. H. G. Folkesson, M. A. Matthey, B. R. Westrom, K. J. Kim, B. W. Karlsson, and R. H. Hastings, *J. Appl. Physiol.* 80, 1431 (1996).
34. D. R. Gill, L. A. Davies, I. A. Pringle, and S. C. Hyde, *Cell. Mol. Life Sci.* 61, 355 (2004).

35. L. Garcia-Contreras, T. Morçöl, S. J. D. Bell, and A. J. Hickey, *AAPS PharmSci*. 5, 1 (2003).
36. M. A. Myers, D. A. Thomas, and L. Stranb, *Exp. Lung Res.* 19, 1 (1993).
37. A. Yamamoto, S. Okumura, Y. Fukuda, M. Fukui, K. Takahashi, and S. Muranishi, *J. Pharm. Sci.* 86, 1144 (1997).
38. L. Heinemann, W. Klappoth, K. Rave, B. Hompesch, R. Linkeschowa, and T. Heise, *Diabetes Care* 23, 1343 (2000).
39. H. O. Alpar, S. Somavarapu, K. N. Atuah, and V. W. Bramwell, *Adv. Drug Deliv. Rev.* 57, 411 (2005).
40. M. Sakagami, K. Sakon, W. Kinoshita, and Y. Makino, *J. Control. Release* 77, 117 (2001).
41. K. Yamada, M. Odomi, N. Okada, T. Fujita, and A. Yamamoto, *J. Pharm. Sci*. 94, 2432 (2005).
42. M. J. Alonso, in *Microparticulate Systems for the Delivery of Proteins and Vaccines,* S. Cohen and H. Bernstein, Eds., Marcel Dekker, New York (1996), p. 203.
43. C. Evora, I. Soriano, R. A. Rogers, K. M. Shakesheff, J. Hanes, and R. Langer, *J. Control. Release* 51, 143 (1998).
44. Y. Mo and L.-Y. Lim, *J. Pharm. Sci*. 93, 20 (2004).
45. A. Hussain, J. J. Arnold, M. A. Khan, and F. Ahsan, *J. Control. Release* 94, 15 (2004).
46. M. Suzuki, M. Machida, K. Adachi, K. Otabe, T. Sugimoto, M. Hayashi, and S. Awazu, *J. Toxicol. Sci*. 25, 49 (2000).
47. H. Todo, H. Okamoto, K. Iida, and K. Danjo, *Int. J. Pharm*. 220, 101 (2001).
48. A. Portero, C. Remuñan-Lopez, and H. M. Nielsen, *Pharm. Res.* 19, 169 (2002).
49. C. Prego, M. Garcia-Fuentes, D. Torres, and M. J. Alonso, *J. Control. Release* 101, 151 (2005).
50. D. Teijeiro-Osório, C. Remuñán-López, and H. M. Nielsen, *Proc. 32nd Ann. Meet. Exp. Control. Release Soc.* #378. Miami, FL (2005).
51. S. Kobayashi, S. Kondo, and K. Juni, *Pharm. Res.* 11, 1239 (1994).
52. Y. Tabata and I. Ikada, *Biomaterials* 9, 356 (1998).
53. D. A. Edwards, J. Hanes, G. Caponetti, J. Hrkach, A. Ben-Jebria, M. L. Eskew, J. Mintzes, D. Deaver, N. Lotan, and R. Langer, *Science* 276, 1868 (1997).
54. A. Ben-Jebria, D. Chen, M. L. Eskew, R. Vanbever, R. Langer, and D. A. Edwards, *Pharm. Res*. 16, 555 (1999).
55. R. Vanbever, A. Ben-Jebria, J. Mintzes, R. Langer, and D. A. Edwards, *Drug Dev. Res.* 48, 178 (1999).
56. R. Vanbever, J. Mintzes, J. Wang, J. Nice, D. Chen, R. Batycky, R. Langer, and D. A. Edwards, *Pharm. Res*. 16, 1735 (1999).
57. C. Dunbar, G. Scheuch, K. Sommerer, M. DeLong, A. Verma, and R. Batycky, *Int. J. Pharm*. 245, 179 (2002).
58. A. I. Bot, T. E. Tarara, D. J. Smith, S. R. Bot, C. M. Woods, and J. G. Weers, *Pharm. Res.* 17, 275 (2000).
59. L. Dellamary, T. E. Tarara, D. J. Smith, C. H. Woelk, A. Adractas, M. L. Costello, H. Gill, and J. G. Weers, *Pharm. Res*. 17, 168 (2000).
60. A. I. Bot, D. J. Smith, S. R. Bot, L. Dellamary, T. E. Tarara, S. Harders, W. Phillips, J. G. Weers, and C. M. Woods, *Pharm. Res.* 18, 971 (2001).
61. S. Steiner, A. Pfützner, B. R. Wilson, O. Harzer, L. Heinemann, and K. Rave, *Exp. Clin. Endocrinol. Diabetes* 110, 10 (2002).
62. A. Pfützner, A. E. Mann, and S. S. Steiner, *Diabetes Technol. Ther.* 4, 589 (2002).
63. N. Tsapis, D. Bennet, B. Jackson, D. A. Weitz, and D. A. Edwards, *Proc. Nat. Acad. Sci*. 99, 12001 (2002).
64. V. A. Philip, R. C. Mehta, M. K. Mazumder, and P. P. DeLuca, *Int. J. Pharm*. 151, 165 (1997).
65. M. M. El-Baseir and I. W. Kellaway, *Int. J. Pharm*. 175, 135 (1998).
66. R. Sharma, D. Saxena, A. K. Dwivedi, and A. Misra, *Pharm. Res*. 18, 1405 (2001).
67. S. Suarez, P. O'Hara, M. Kazantseva, C. E. Newcomer, R. Hopfer, D. N. McMurray, and A. J. Hickey, *J. Antimicrob. Chemother*. 48, 431 (2001).
68. S. Suarez, P. O'Hara, M. Kazantseva, C. E. Newcomer, R. Hopfer, D. N. McMurray, and A. J. Hickey, *Pharm. Res*. 18, 1315 (2001).
69. N. Bandi, S. P. Ayalasomayajula, D. S. Dhanda, J. Iwakawa, P.-W. Cheng, and U. B. Kompella, *J. Pharm. Pharmacol*. 57, 851 (2005).
70. S. Pandit, C. Martin, and H. O. Alpar, *J. Drug Deliv. Sci. Technol.* 15, 281 (2005).
71. H. Zhou, Y. Zhang, D. L. Biggs, M. C. Manning, T. W. Randolph, U. Christians, B. M. Hybertson, and K. Ng, *J. Control. Release* 107, 288 (2005).
72. R. O. Williams, M. K. Barron, M. J. Alonso, and C. Remuñan-Lopez, *Int. J. Pharm*. 174, 209 (1998).
73. K. Morimoto, H. Katsumata, T. Yabuta, K. Iwanaga, M. Kakemi, Y. Tabata, and Y. Ikada, *J. Pharm. Pharmacol*. 52, 611 (2000).
74. R. Alcock, J. A. Blair, D. J. O'Mahony, A. Raoof, and A. V. Quirk, *J. Control. Release* 82, 429 (2002).
75. K. Surendrakumar, G. P. Martin, E. C. M. Hodgers, M. Jansen, and J. A. Blair, *J. Control. Release* 91, 385 (2003).
76. Y. C. Huang, M. K. Yeh, S.-N. Cheng, and C. H. Chiang, *J. Microencapsul*. 20, 459 (2003).
77. A. Grenha, B. Seijo, and C. Remuñan-Lopez, *Eur. J. Pharm. Sci.* 25, 427 (2005).
78. Y. C. Huang, A. Vieira, K. L. Huang, M. K. Yeh, and C. H. Chiang, *J. Biomed. Mater. Res.* 75A, 283 (2005).
79. C. Bosquillon, C. Lombry, V. Préat, and R. Vanbever, *J. Control. Release* 70, 329 (2001).
80. H. Steckel and H. G. Brandes, *Int. J. Pharm*. 278, 187 (2004).
81. B. G. Jones, P. A. Dickinson, M. Gumbleton, and I. W. Kellaway, *J. Pharm. Pharmacol*. 54, 1065 (2002).
82. V. Sanna, N. Kirschvink, P. Gustin, E. Gavini, I. Roland, L. Delattre, and B. Evrard, *AAPS PharmSciTech*. 5, 1 (2003).
83. P. O'Hara and A. J. Hickey, *Pharm. Res*. 17, 955 (2000).
84. M. Sakagami, W. Kinoshita, K. Sakon, J. Sato, and Y. Makino, *J. Control. Release* 80, 207 (2002).
85. V. Codrons, F. Vanderbist, R. K. Verbeeck, M. Arras, D. Lison, V. Préat, and R. Vanbever, *J. Pharm. Sci*. 92, 938 (2003).
86. K. Tomoda, S. Kojima, M. Kajimoto, D. Watanabe, T. Nakajima, and K. Makino, *Colloids Surf. B Biointerfaces* 45, 1 (2005).
87. Y. F. Maa, P. A. Nguyen, T. Sweeney, S. J. Shire, and C. C. Hsu, *Pharm. Res*. 16, 249 (1999).
88. M. Skiba, F. Bounoure, C. Barbot, P. Arnaud, and M. Skiba, *J. Pharm. Pharm. Sci.* 8, 409 (2005).
89. O. C. Chidavaenzi, G. Buckton, F. Koosha, and R. Pathak, *Int. J. Pharm*. 159, 67 (1997).
90. Y. F. Maa and S. J. Prestrelski, *Curr. Pharm. Biotechnol*. 1, 283 (2000).
91. K. Koushik and U. B. Kompella, *Drug Deliv. Technol.* 4, 40 (2004).
92. C. Elvira, A. Fanovich, M. Fernández, J. Fraile, J. San Román, and C. Domingo, *J. Control. Release* 99, 231 (2004).
93. H. Schiavone, S. Palakodaty, A. Clark, P. York, and S. T. Tzannis, *Int. J. Pharm*. 281, 55 (2004).
94. A. R. C. Duarte, M. S. Costa, A. L. Simplício, M. M. Cardoso, and C. M. Duarte, *Int. J. Pharm.* 308, 168 (2006).
95. D. E. Perrin and J. P. English, in *Handbook of Biodegradable Polymers*, A. J. Domb, J. Kost, and D. M. Wiseman, Eds., Harwood Academic Publishers, New York (1997), p. 3.
96. L. A. Dailey, E. Kleemann, M. Wittmar, T. Gessler, T. Schmehl, C. Roberts, W. Seeger, and T. Kissel, *Pharm. Res*. 20, 2011 (2003).

97. L. A. Dailey, T. Schmehl, T. Gessler, M. Wittmar, F. Grimminger, W. Seeger, and T. Kissel, *J. Control. Release* 86, 131 (2003).
98. M. Schnabelrauch, S. Vogt, Y. Larcher, and I. Wilke, *Biomol. Eng.* 19, 295 (2002).
99. V. Codrons, F. Vanderbist, B. Ucakar, V. Préat, and R. Vanbever, *J. Pharm. Sci*. 93, 1241 (2004).
100. S. M. McAllister, H. O. Alpar, Z. Teitelbaum, and D. B. Bennett, *Adv. Drug Deliv. Rev.* 19, 89 (1996).
101. R. Mitra, I. Pezron, Y. Li, and A. K. Mitra, *Int. J. Pharm*. 217, 25 (2001).
102. S. I. Rennard, G. Basset, D. Lecossier, K. M. O'Donnell, P. Pinkston, G. P. Martin, and R. G. Crystal, *J. Appl. Physiol.* 60, 532 (1986).
103. L. Dellamary, D. J. Smith, A. Bloom, S. R. Bot, G. R. Guo, H. Deshmuk, M. Costello, and A. I. Bot, *J. Control. Release* 95, 489 (2004).
104. K. Makino, H. Yamamoto, K. Higuchi, N. Harada, H. Ohshima, and H. Terada, *Colloid Surf. B Biointerfaces* 27, 33 (2003).
105. T. Nagai and Y. Machida, in *Bioadhesive Drug Delivery Systems,* V. Lenaerts and R. Gurny, Eds., CRC Press, Boca Raton, FL (1990), p. 169.
106. S. Hirano, H. Seino, Y. Akiyama, and I. Nonaka, *Polym. Mat. Sci. Eng.* 59, 897 (1988).
107. M. Dornish, A. Hagen, E. Hansson, C. Peucheur, F. Vedier, and O. Skaugrud, in *Advances in Chitin Science,* A. Domard, G. A. F. Roberts, and K. M. Varum, Eds., Jacques Andre publisher, Lyon (1997), p. 664.
108. C. M. Lehr, J. A. Bouwstra, E. H. Schacht, and H. E. Junginger, *Int. J. Pharm*. 78, 43 (1992).
109. P. Artursson, T. Lindmark, S. S. Davis, and L. Illum, *Pharm. Res.* 11, 1358 (1994).
110. G. Borchard, H. L. LuBen, G. A. De Boer, J. C. Verhoef, C. M. Lehr, and H. E. Junginger, *J. Control. Release* 39, 131 (1996).
111. R. Fernández-Urrusuno, P. Calvo, C. Remuñán-López, J. L. Vila-Jato, and M. J. Alonso, *Pharm. Res*. 16, 1576 (1999).
112. R. Fernández-Urrusuno, D. Romani, P. Calvo, J. L. Vila-Jato, and M. J. Alonso, *STP Pharm. Sci.* 9, 429 (1999).
113. A. de Campos, A. Sanchez, and M. J. Alonso, *Int. J. Pharm*. 224, 159 (2001).
114. H. Yamamoto, Y. Kuno, S. Sugimoto, H. Takeuchi, and Y. Kawashima, *J. Control. Release* 102, 373 (2005).
115. R. A. A. Muzzarelli, in *The Polysaccharides,* G. O. Aspinall, Ed., Academic Press, Orlando, FL (1985), p. 417.
116. R. A. A. Muzzarelli, *Cell. Mol. Life Sci*. 53, 131 (1997).
117. H. Okamoto, S. Nishida, H. Todo, Y. Sakakura, K. Iida, and K. Danjo, *J. Pharm. Sci.* 92, 371 (2003).
118. Y. C. Huang, M. K. Yeh, and C. H. Chiang, *Int. J. Pharm*. 242, 239 (2002).
119. M. Bivas-Benita, K. E. van Meijgaarden, K. L. Franken, H. E. Junginger, G. Borchard, T. H. Ottenhoff, and A. Geluk, *Vaccine* 22, 1609 (2004).
120. M. Huang, E. Khor, and L.-Y. Lim, *Pharm. Res*. 21, 344 (2004).
121. H. Okamoto, M. Aoki, and K. Danjo, *J. Pharm. Sci*. 89, 1028 (2000).
122. D. McPhail, L. Tetley, C. Dufes, and I. F. Uchegbu, *Int. J. Pharm*. 200, 73 (2000).
123. A. R. Pohlmann, V. Weiss, O. Mertins, N. P. Silveira, and S. S. Guterres, *Eur. J. Pharm. Sci.* 16, 305 (2002).
124. K. A. Janes, P. Calvo, and M. J. Alonso, *Adv. Drug Deliv. Rev.* 47, 83 (2001).
125. S. A. Agnihotri, N. N. Mallikarjuna, and T. M. Aminabhavi, *J. Control. Release* 100, 5 (2004).
126. M. J. Alonso and A. Sanchez, in *Carrier-based Drug Delivery,* S. Svenson, Ed., American Chemical Society, New York (2004), p. 283.
127. P. Jani, G. W. Halbert, J. Langridge, and A. T. Florence, *J. Pharm. Pharmacol*. 42, 821 (1990).
128. M. P. Desai, V. Labhasetwar, G. L. Amidon, and R. J. Levy, *Pharm. Res*. 13, 1838 (1996).
129. S. Schurch, P. Gehr, V. Im Hof, M. Geiser, and F. H. Y. Green, *Respir. Physiol.* 80, 17 (1990).
130. M. Huang, M. Zengshuan, E. Khor, and L.-Y. Lim, *Pharm. Res.* 19, 1488 (2002).
131. S. Akhtar and K. J. Lewis, *Int. J. Pharm*. 151, 57 (1997).
132. S. Rudt and R. H. Müller, *J. Control. Release* 22, 263 (1992).
133. Y. Kawashima, T. Serigano, T. Hino, H. Yamamoto, and H. Takeuchi, *Pharm. Res.* 15, 1748 (1998).
134. Y. Kawashima, H. Yamamoto, H. Takeuchi, S. Fujioka, and T. Hino, *J. Control. Release* 62, 279 (1999).
135. H. Kikuchi, H. Yamauchi, and S. Hirota, *Chem. Pharm. Bull*. 39, 1522 (1991).
136. T. R. Desai, R. E. W. Hancock, and W. H. Finlay, *Eur. J. Pharm. Sci*. 20, 459 (2003).
137. W. F. Wolkers, H. Oldenhof, F. Tablin, and J. H. Crowe, *Biochim. Biophys. Acta*. 1661, 125 (2004).
138. R. Pandey, A. Sharma, A. Zahoor, S. Sharma, G. K. Khuller, and B. Prasad, *J. Antimicrob. Chemother.* 52, 981 (2003).
139. Y. Mo and L.-Y. Lim, *J. Control. Release* 107, 30 (2005).
140. O. N. M. McCallion, K. M. G. Taylor, M. Thomas, and A. J. Taylor, *Int. J. Pharm*. 133, 203 (1996).
141. M. Dittgen, M. Durrani, and K. Lehmann, *STP. Pharm. Sci*. 7, 403 (1997).
142. E. Fattal, M. T. Peracchia, and P. Couvreur, in *Handbook of Biodegradable Polymers,* A. J. Domb, J. Kost, and D. M. Wiseman, Eds., Harwood Academic Publishers, New York (1997), p. 183.
143. B. Seijo, E. Fattal, L. Roblot-Treupel, and P. Couvreur, *Int. J. Pharm*. 62, 1 (1990).
144. M. Brzoska, K. Langer, C. Coester, S. Loitsch, T. O. F. Wagner, and C. V. Mallinckrodt, *Biochem. Biophys. Res. Commun*. 318, 562 (2004).
145. Q. Zhang, Z. Shen, and T. Nagai, *Int. J. Pharm*. 218, 75 (2001).
146. C. Schwarz, W. Mehnert, J. S. Lucks, and R. H. Müller, *J. Control. Release* 30, 83 (1994).
147. R. H. Müller, K. Madre, and S. Gohla, *Eur. J. Pharm. Biopharm*. 50, 161 (2000).
148. M. A. Videira, M. F. Botelho, A. C. Santos, L. F. Gouveia, J. J. P. Lima, and A. J. Almeida, *J. Drug Target*. 10, 607 (2002).
149. P. A. Dickinson, S. W. Howells, and I. W. Kellaway, *J. Drug Target*. 9, 295 (2001).
150. P. Calvo, C. Remuñan-Lopez, J. L. Vila-Jato, and M. J. Alonso, *J. Appl. Polym. Sci.* 63, 125 (1997).
151. A. Vila, A. Sanchez, C. Perez, and M. J. Alonso, *Polym. Adv. Technol*. 13, 851 (2002).
152. G. Carlesso, E. Kozlov, A. Prokop, D. Unutmaz, and J. M. Davidson, *Biomacromolecules* 6, 1185 (2005).
153. S. P. Vyas, A. Singh, and V. Sihorkar, *Crit. Rev. Ther. Drug Carrier Syst*. 18, 1 (2001).
154. M. Kumar, A. K. Behera, R. F. Lockey, J. Zhang, G. Bhullar, C. P De la Cruz, L. C. Chen, and K. W. Leong, *Hum. Gene Ther.* 13, 1415 (2002).
155. M. Koping-Hoggard, K. M. Varum, M. Issa, S. Danielsen, B. E. Christensen, B. T. Stokke, and P. Artursson, *Gene Ther*. 11, 1441 (2004).
156. W. Zhang, H. Yang, X. Kong, S. Mohapatra, H. San Juan-Vergara, G. Hellermann, S. Behera, R. Singam, R. F. Lockey, S. S. Mohapatra, *Nat. Med.* 11, 56 (2005).
157. F. C. MacLaughlin, R. J. Mumper, J. Wang, J. M. Tagliaferri, I. Gill, M. Hinchcliffe, and A. P. Rolland, *J. Control. Release* 56, 259 (1998).
158. M. Koping-Hoggard, I. Tubulekas, C. Y. Guan, K. Edwards, M. Nilsson, K. M. Varum, and P. Artursson, *Gene Ther.* 8, 1108 (2001).

159. K. W. Leong, H. Q. Mao, V. L. Truong-Le, K. Roy, S. M. Walsh, and J. T. August, *J. Control. Release* 53, 183 (1998).
160. M. Kumar, X. Kong, A. K. Behera, G. R. Hellermann, R. F. Lockey, and S. S. Mohapatra, *Genet. Vaccines Ther.* 1, 3 (2003).
161. A. Bozkir and O. M. Saka, *Drug Deliv.* 11, 107 (2004).
162. K. Y. Lee, I. C. Kwon, Y. H. Jo, and S. Y. Jeong, *J. Control. Release* 51, 213 (1998).
163. H. S. Yoo, J. E. Lee, H. Chung, I. C. Kwon, and S. Y. Jeong, *J. Control. Release* 103, 235 (2005).
164. M. Köping-Höggard, N. Csaba, and M. J. Alonso (submitted).
165. S. G. Antimisiaris, P. Jayasekera, and G. Gregoriadis, *J. Immunol. Methods* 166, 271 (1993).
166. J. Arrault, C. Grand, W. C. K. Poon, and M. E. Cates, *Europhys. Lett.* 38, 625 (1997).
167. J. O. Sham, Y. Zhang, W. H. Finlay, W. H. Roa, and R. Löbenberg, *Int. J. Pharm.* 269, 457 (2004).
168. R. O. Cook, R. K. Parnu, and I. W. Kellaway, *J. Control. Release* 104, 79 (2005).

Anexo II

Glucomannan: a Promissing Polysaccharide for Biopharmaceutical Purposes

M. Alonso-Sande, D. Teijeiro-Osorio, C. Remuñán-López, M. J. Alonso

Abstract

Over the last decades, polysaccharides have gained increasing attention in the biomedical and drug delivery fields. Among them, glucomannan (GM), has become a particularly attractive polymer. In this paper, we review the physicochemical and biological properties which are determinant for the exploitation of GM as a biomaterial. These properties include the structural organization, molecular weight, solubility, viscosity, gelling properties and degradation behaviour. Moreover, herein we analyze the possibilities to combine GM with other hydrophilic polymers, as well as the preparation of semisynthetic derivatives of GM, which may be of interest in the pharmaceutical context. Finally, we discuss the specific applications of GM in the drug delivery field.

Key words: Glucomannan; polysaccharides; gelation; colloidal systems; nanoparticles**;** nanocomplexes; drug delivery.

Introduction

Natural polysaccharides, as well as their derivatives, have been classically used in pharmaceutical formulations as solubilizers or adhesives. Over the last years, the evolution of these polysaccharides from the concept of "pharmaceutical excipient" to "bioactive material" has raised their potential utility in the design of drug delivery carriers. This conceptual change has, partially, been motivated by the recent emphasis in the design of biomimetic and intelligent drug delivery nanostructures, which can be recognized and assimilated in the body (1-4). In fact, polysaccharides can be used as ligands in order to facilitate the interaction of a nanostructure with a specific biological surface (5,6). As a consequence of these new potential applications, the number of publications dealing with the use of polysaccharides for drug delivery has remarkably increased over the last 10 years (see **Fig. 1**).

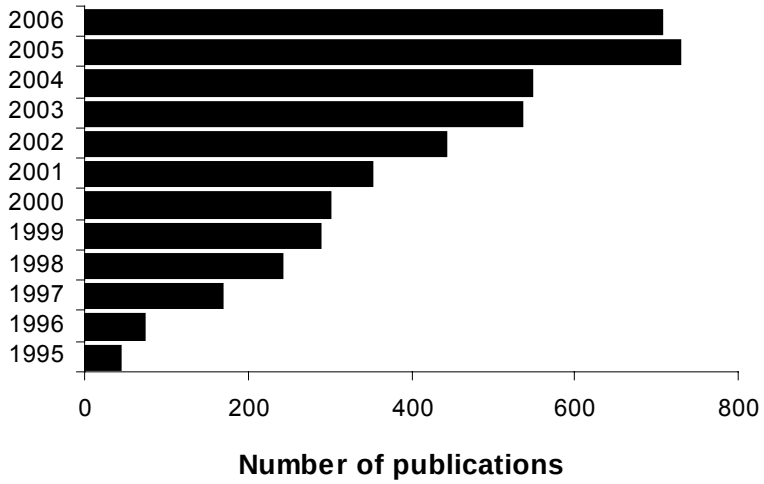

Figure 1. Number of scientific publications published on the topic of hydrophilic polysaccharides in the drug delivery field as function of the publication year. Taken from CAPLUS and MEDLINE (*SCIFINDER SCHOLAR2006 Edition*). Keywords entered: Polysaccharides and Drug Delivery.

A very promising polysaccharide, which has been lately incorporated into the drug delivery field is glucomannan (GM) (7-11). GM is a hydrocolloidal polysaccharide consisting in β-1,4 linked mannose and glucose residues (12). Despite of its potential in drug delivery, most of the review articles about GM have been focused on its chemical and physicochemical properties, such as chemical structure, molecular weight, gelation behaviour, and ability to interact with other polymers, such as carregeenan or xanthan (13,14). Just a few recent reports have considered only the pharmaceutical and therapeutic applications of GM (15,16). In this paper, we review the critical aspects about GM, closely related with its promising utility in the design and development of new drug delivery systems.

1. Glucomannan: Origin and Structure

Glucomannan (GM) is a polysaccharide of the mannan family, very abundant in nature, specifically in softwoods (hemicellulose), roots, tubers and many plants bulbs (17-23). Despite the variety of sources, the most commonly used type of GM is named Konjac GM, which is extracted from tubers of *Amorphophallus konjac* (24,25). Irrespective of its origin, GM is composed of β-1,4 linked D-mannose and D-glucose monomers (**Fig. 2**) (12). However, the mannose/glucose monomer ratio may vary depending on the original source of GM. For example, it has been reported that Konjac GM has a molar ratio of around 1.6:1, whereas GMs extracted from Scotch pine and orchid tubers have ratios of 2.1:1 and 3.6:1, respectively (20,26). These values should be taken cautiously given the variability observed depending on the studies and, in particular, on the analytical procedures.

In addition to the variable glucose/mannose ratio, the different types of GM may differ in their acetylation degree. The typical acetylation degree values are 5-10 %. On the other hand, it is known that native GM can be easily acetylated with acetic anhydride in presence of a catalyst (27-29).

Despite the information about the GM chemical structure, additional work is needed in order to fully understand how its structure and composition affect its physicochemical and pharmaceutical behaviour.

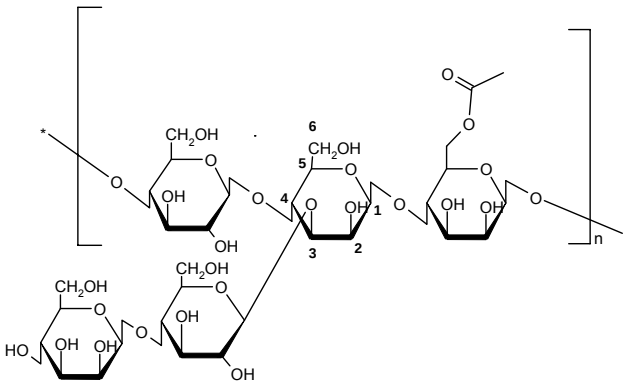

Figure 2. Chemical structure of GM

2. Physicochemical Properties

2.1. Solubility

Although GM is a hydrophilic molecule, its solubility in water is reduced due to the formation of strong hydrogen bonds after purification or drying processes (30,31). Among the parameters that affect the aqueous solubility of GM, the acetylation degree appears to be particularly important. More specifically, it has been described that the presence of acetyl groups in the GM inhibits the formation of intramolecular hydrogen bonds, thus improving the GM solubility (29). Moreover, a number of GM derivatives (discussed in section 4) have been synthesized in order to increase the GM aqueous solubility. This versatile solubility behavior could be of special interest for a variety of pharmaceutical applications that will be later described.

2.2. Molecular weight

The molecular weight (Mw) of GM has been determined by light scattering, viscosimetry and Gel Permeation Chromatography (GPC). One of the main problems in the determination of GM Mw relies on its limited water solubility. In fact, some of Mw studies have been performed with GM which has been chemically modified in order to increase its solubility in water or others solvents (30). Mark-Howinks parameters were fixed according to $\eta = 3.8 \cdot 10^{-2} \times M_w^{0.723}$ for a solution of konjac GM in water at 25 ± 0.5ºC (32).

The most frequently used and commercially available GM has a Mw in the range of $1.9 \cdot 10^6$ and $1 \cdot 10^4$ (30,33,13,14). Nevertheless, there is also the possibility to depolymerise GM in order to obtain low Mw GM. This strategy may offer interesting possibilities in the pharmaceutical field. In fact, it is known that the polymer Mw has an influence on the physicochemical characteristics of the drug delivery systems (34, 10), as well as on their efficacy *in vitro* and *in vivo*. As an example, polymeric nanoparticles based on low Mw chitosan showed higher transfection efficiency *in vitro* and *in vivo*, than those prepared with high Mw chitosan (35,36).

Among the techniques described until now to decrease the GM Mw, acid, alkaline and enzyme hydrolysis are the most important (19,37,12,38,39).

It is well known that certain enzymes can convert polysaccharides into oligosaccharides. The complete degradation of the GM backbone requires the action of β- mannanase, β-mannosidase and β- glucosidase (40-42).

β-mannanase is of special interest in polysaccharides degradation because it catalyzes the random cleavage of β-D-1,4-mannopyranosyl linkages. The breakdown of these linkages in GM leads to mannobiose and mannotriose (43-50). The ability of β-mannanase to degrade the GM backbone depends on several factors, such as the number and distribution of the substituents on the backbone

and the ratio of glucose to mannose (51). This enzyme is in bacteria (*Bacillus* sp., *Aeromonas* sp., *Penicillium* sp., *Pseudomonas* sp. or *Vibrio* sp.) (52-57) fungi (*Streptomyces* sp., *Tyromices* sp., *Trichosporum* sp., *Sclerotium* sp. and *Aspergillus* sp.) (58-62,50), as well as in plants (*Amorphophallus konjac*) (40), in animals (63,49) and in the colonic region of humans (64,65).

The enzyme β-mannosidase, which catalyzes the removal of D-mannose residues from β-1, 4-linked manno-oligosaccharides, leads to the conversion of GM into D-mannose (43,66). As in the case of mannanase, this enzyme is present in many microorganisms, plants and animal tissues (67).

Finally, the degradation by β- glucosidase occurs only at a terminal glucose unit and stops at terminal oxidized residues or mannose units (68) (**Fig. 3**).

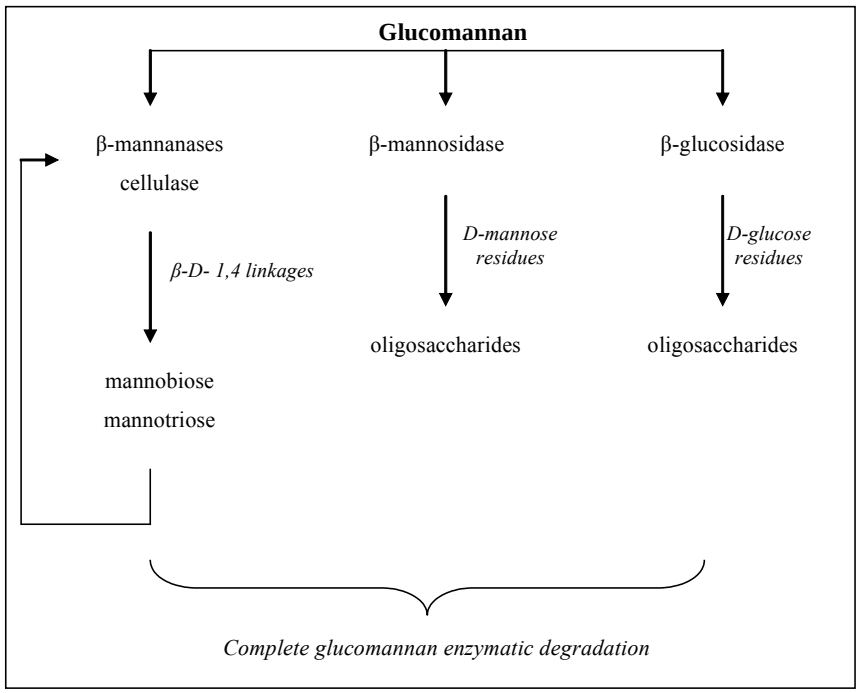

Figure 3. Scheme of the enzymatic degradation of GM

With respect to the influence of GM properties on its enzymatic degradation, some studies have shown that the acetyl groups inhibit β-mannanase and β-mannosidase activity (62,69).

2.3. Gelation properties

The knowledge of the GM gelation mechanism, as well as the variables that affect this process, are useful in the design and understanding of the mechanism of formation of GM-based delivery systems. GM gels can be prepared by heating a GM solution containing alkaline compounds or higher amounts of neutral salt (33,70). The gelation process occurs due to the interaction of the GM acidic moieties with alkalis (71). This interaction induces structural changes in the GM molecules, which facilities the establishment of hydrogen bonds and hydrophobic interactions between the GM chains and, consequently, leading to the formation a network gel structure (**Fig. 4**) (27,33,14,71,29).

There are a number of parameters which affect the GM gelation behaviour and, thus, the properties of the final gel structure. These parameters are the GM acetylation degree, the GM Mw, the temperature and also the concentration of both GM and the alkali involved in the gelation process (see **Table 1**). The specific influence of each parameter is described as follows.

Since acetylation hinders the aggregation of GM, the increase in the GM acetylation degree leads to a delay the gelation process (71,29). On the contrary, gelation is favoured when the Mw, alkali concentration or the temperature increases. This is due to enhancement of the interactions between GM chains (14), but also because the formation of hydrogen bonds in the junction zones requires energy (27,71,14,29).

At low GM concentrations, the formation of the GM gel is impaired by the distance between molecules. In this situation a previous deacetylation process is required in order to facilitate the approximation of the GM molecules. However, at

high GM concentrations the proximity of GM molecules promotes the interaction between them, favouring the formation of the network (33,27,14,71,29).

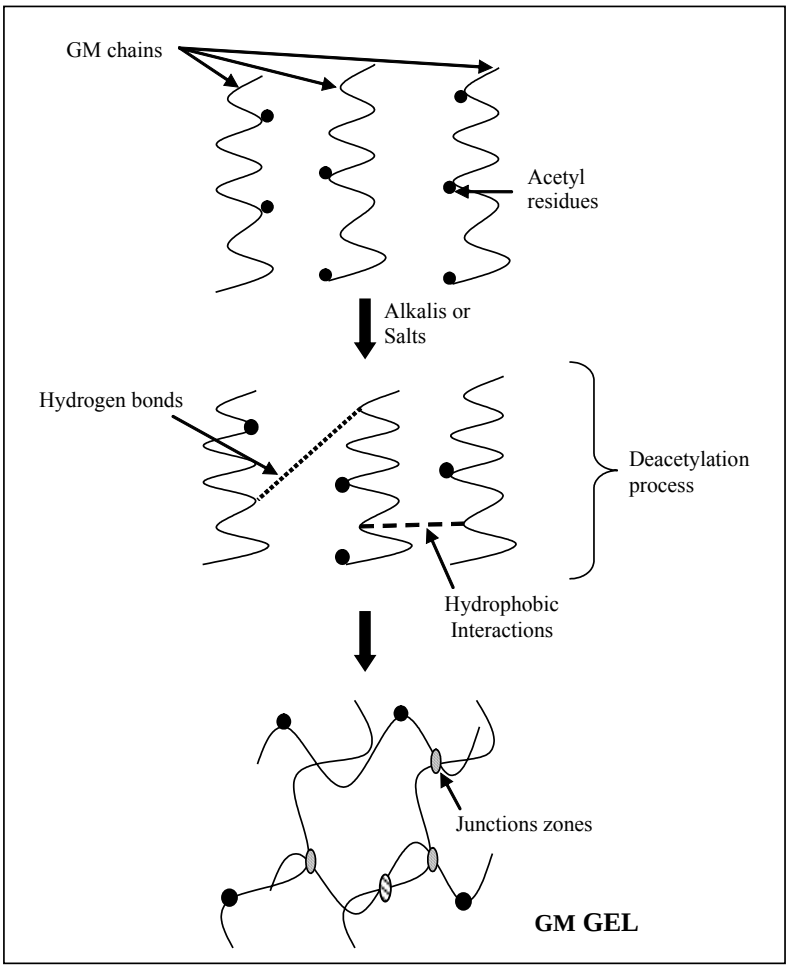

Figure 4. Scheme of gelation mechanism of GM

Table 1. Influence of different variable on the gelation mechanism of GM

Variable	**Gelation Mechanism**	
↓ acetylation degree	↑ formation of hydrogen bonds	Promote the formation of GM gel
↑ GM Mw	↑ number of junction zones ↑ length of connecting chains	
↑ GM concentration	↑ number of molecules ↑ proximity between molecules	
↑ temperature	↑ formation of hydrogen bonds	
↑ alkali concentration	↑ deacetylation process ↑ formation of hydrogen bonds	

3. Interaction of glucomannan with other polymers

The possibility to combine GM with other polymer increases its versatility in the drug delivery field. In fact, the interaction of GM with other polysaccharides has been extensively investigated in order to produce new gels with improved gelling properties (72-74).

Carrageenan, Xanthan, Acetan, Gellam gum, alginate or chitosan are some examples of polysaccharides which could be combined with GM (75,31,76,14,24,25).

3.1. Interaction with kappa carrageenan

Kappa carrageenan forms thermoreversible gels and its gelation depends on the temperature, concentration of counterions or other polysaccharides. More specifically, its interaction with GM gives thermo-reversible gels (75), whose

structure is affected by the GM Mw (31) and also by the addition of a small amount of sugars (13).

The potential of these hydrogels for drug delivery applications has been suggested (77). However, so far we have not found any evidence of this potential in the literature.

3.2. Interaction with Xanthan

Xanthan gum does not naturally gel at any concentration, however gelification can be induced by temperature, ionic strength of the solution, the pH and the nature of electrolyte (K^+, Cs^+, Na^+, NH_4^+, Ba^{2+}, Mg^{2+}, Ca^{2+}). The interaction with GM is ruled by a preferred stoichiometry, where the ratio Xanthan:GM is 1:2 (78,79, 80).

It has been recently reported the application xanthan-GM gels and solutions as drug delivery systems of macromolecules and low Mw drugs (80-82).

3.3. Interaction with Acetan (xylinan)

The polysaccharide acetan, secreted by the bacterium *Acetobacter xylinum*, has a similar chemical structure to xanthan (83,84). It has been reported that deacetylation of acetan provides stability to the molecule and improves the establishment of intermolecular binding with GM (85,86,76), obtaining transparent thermoreversibe gels at sufficiently high polymer concentrations and theoretical deacetylated acetan/GM ratios above 6/4 (76).

From our knowledge there are no references on the utility of acetan-GM complexes for drug delivery. However, taking into account the similar chemical structure reported for xanthan and acetan, comparable applications could be given to these both polymers and to their combination with GM.

3.4. Interaction with Gellan gum

The interaction of gellan gum with GM molecules is promoted with increasing concentration of cations, such as sodium or calcium. However, an excessive salt

content leads to a separation phase, caused by the formation of aggregates of gellam gum helices with different thermal stabilities (87,14).

With regard to the drug delivery applications of gellam gum-GM mixtures, the only report found in the literature refers to blend films as releasing active agents systems for food packaging purposes (88).

3.5. Interaction with Alginate

Previous studies have shown that the interaction between GM and alginate is mediated by hydrogen binding and electrostatic interactions (24,8). This interaction has been the basis for the formation of GM-alginate beads intended for the controlled delivery of proteins (8). In this work it was shown that the introduction of GM led to the formation of stronger and more stable gels than those composed only of alginate.

3.6. Interaction with Chitosan

Using IR and X-Ray spectroscopy it was found that the interaction between chitosan and GM is due to the formation of intermolecular hydrogen bonds between the amine groups of chitosan and the hydroxyl and carboxymethyl groups of GM (25, 8).

The combination of GM with chitosan has been reported to offer an interesting potential in the drug delivery field. In fact, films, beads, micro and nanoparticles have been prepared, based on the combination of these polymers, and presented as new drug and protein carriers (25,8,11,10,9,89,90, 91). These specific applications will be described in detail at the end of this review article.

4. Glucomannan Derivatives

The poor water solubility of GM (30,31,68) together with its specific advantages (14,13,65) has motivated active research towards the formation of GM derivatives of different solubility. Indeed, most frequently the chemical modification of GM has been intended to obtain derivatives with improved solubility properties and/or enhanced capacity to interact with other polymers (**Table 2**).

Table 2. Characteristics of semisynthetic GM derivatives

Derivative	**Main Characteristics**
Dicarboxy-GM	Negative charge Higher water solubility
Carboxymethylated-GM	Negative charge Higher water solubility
Methylated-GM	Non charge Higher water solubility
Tosylated-GM	Non charge Higher solubility in organic solvents
Palmitoyl-GM	Non charge Water in oil emulsifier
Benzoyl-GM	Non charge Higher solubility in polar solvents

4.1. Dicarboxy-GM

Matsumura et al. (92) proposed the preparation of dicarboxy-GM, a negatively charged derivative, which presents carboxylic groups between the sugar residues and at C-3 position. This chemical modification has resulted in an important increase in GM water solubility, and also in its ability to interact with positively charged polymers. These new features are very attractive for the design of new drug carriers. On the other hand, this chemical modification may also affect its biological activity.

For example, Ohya and co-workers have found that the inherent ability of GM to stimulate macrophages could be modulated by varying the dicarboxy substitution degree (5,68).

4.2. Methylated-GM

The methylation of GM (**Fig. 5**) has also been intended to increase the water solubility of this polysaccharide. This modification was first proposed by Kishida et al. in 1979 in order to improve the reologycal properties of GM (93,94).

Up until now, no pharmaceutical or medical application has been specifically reported for this derivative; however, it could be induced that the increase of GM water solubility could promote its use as a pharmaceutical excipient.

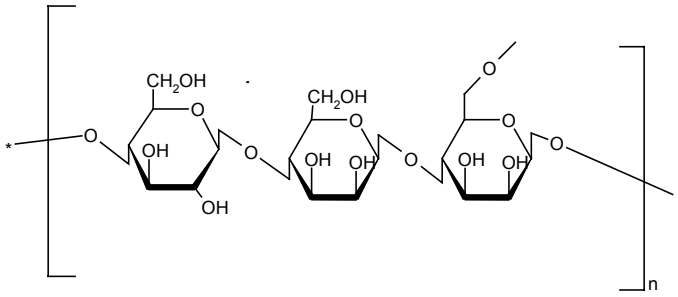

Figure 5. Chemical structure of methylated-GM

4.3. Carboxymethylated-GM

A high degree of substitution (DS) (DS>0.1), in carboxymethylated-GM (**Fig. 6**), leads to a soluble product in water. This derivative is a negatively charged polyelectrolyte, which is susceptible of interacting with positively charged polymers by electrostatic attraction (95,96,68).

A biomedical application of this derivative has been reported by Du et al. (9,89,90). They prepared polyelectrolyte chitosan- Carboxymethylated-GM nanoparticles by simple mixing of both polymers using sonication.

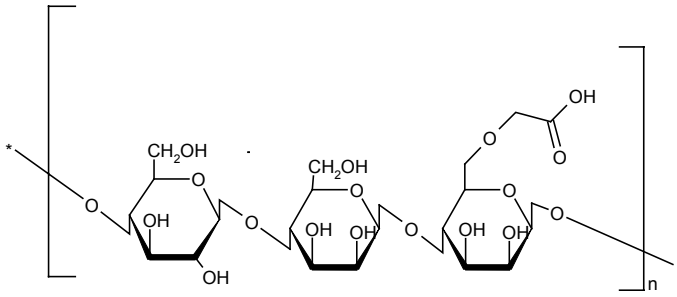

Figure 6. Chemical structure of carboxymethylated-GM

4.4. Tosylated-GM

A few years ago, Takechi et al. synthesized tosylated-GM (**Fig. 7**), with the idea of improving the solubility of GM in a variety of organic solvents (97). Although this derivative could offer certain advantages in pharmaceutical technology, the most attractive use of this derivative is as a precursor in polysaccharide chemistry. Indeed, the tosyl group is a good leaving group, allowing the easy modification in this position (97).

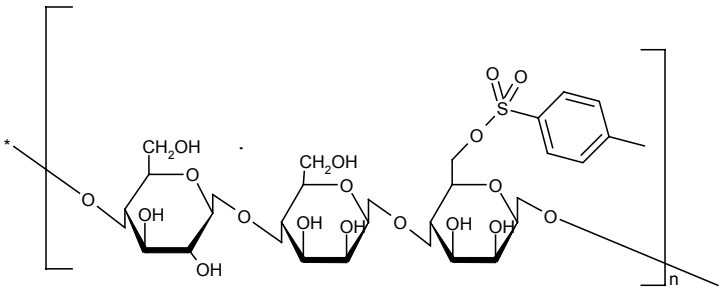

Figure 7. Chemical structure of tosylated-GM

4.5. Palmitoyl-GM

Various degrees of palmitoylated GM were prepared by Tian and colleagues following a heterogeneous method previously reported by Fujii (98). This synthesis was based on similar work on chitosan (99) and cellulose (100). It was found that palmitoylated-GM may work as a water in oil (w/o) and oil in water (o/w) emulsifier, being active at very low concentrations (0.1-0.01%) (101). Despite this specific application, no references were found reporting the use of palmitoylated-GM in the drug delivery field.

4.6. Benzoyl-GM

Benzoyl-GM (**Fig. 8**) with a degree of substitution of 1.6 is highly soluble in polar solvents. This derivative plays an important role in films coating, enhancing the mechanical properties and water resistively of the coated films (102). The use of benzoyl-GM has been reported for the preparation of coating films (103,104); however, no reference has been published about its use in the drug delivery field.

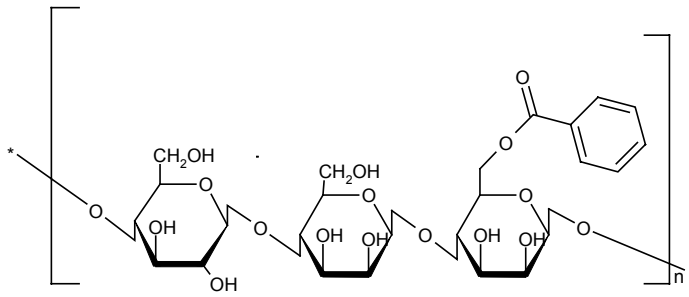

Figure 8. Chemical structure of benzoyl-GM

4.7. Glucomannan grafted acrylic acid

The preparation of the GM grafted acrylic acid co-polymer was performed by free radical polymerization, leading to the introduction of the acrylic acid at the C1 position. The application of this derivative was aimed at the preparation of hydrogels for colonic drug delivery. The combination of both ingredients was chosen in order to obtain a more selected release at the colonic level. This hypothesis was supported by the biodegradation behaviour of GM and pH dependence of acrylic acid (121).

4.8. Natural derivatives of glucomannan

Finally, besides the chemically synthesized derivatives of GM, there is a class of natural derivatives of GM, such as those obtained from the bacteria *Candida utilis*. This variety of GM is characterized by the presence of phosphate groups, a high content in mannose (mannose:glucose ratio 11.4:1) and α-1,6 linkages in the main backbone. Moreover, in contrast to the ordinary GM, the phosphorylated derivative presents low molecular weight (around 150 KD) and high solubility in water and polar solvents, such as acetone and ethanol.

The negative charge of this derivative is a very attractive characteristic for its application in the pharmaceutical field. For example, our group has extensively investigated the formation and drug delivery applications of nanoparticles, made of chitosan and phosphorylated GM (10,11).

5. Biopharmaceutical applications

Traditionally, the use of konjac flour has been related with food applications. Indeed, Konjac GM is a health product widely used in Asian countries and the United States for its unique properties. This thickening agent presents an extraordinary water absorption capacity, a unique viscosifying action and a synergistic behaviour with others gums. In fact, Konjac GM has been used to improve the bread texture, as a dietary fibre…etc. However, over the last years this polymer has gained increasing importance in the biomedical and pharmaceutical fields (**Table 3**). More specifically, these applications include:

Table 3. GM biomedical and pharmaceutical applications

Applications		**Advantages**
Biomedical	Obesity	Weight loss
	Cholesterol	Decrease LDL cholesterol levels
	Diabetes type 2	Decrease the carbohydrate absorption
	Cancer	Antitumor activity against sarcoma-180 solid tumor
Pharmaceutical	Pharmaceutical forms	Sustained release profiles
		Increase of stability
		Improve the interaction between polymers
		Enhance protein association
	Coating	Antiseptic coating
	Targeting	Recognize mannose receptors

5.1. Glucomannan as a bioactive polymer

GM can not be considered as a drug, however, some biological effects described in the literature suggest its potential as a bioactive polymer. For example, GM has been found to decrease the serum glucose levels following oral administration to diabetes type 2 rats. This hypoglycemic effect was attributed to the inhibition of carbohydrate absorption (105,106,107) and also to the decrease of the postprandial insulin flow (108). On the other hand, some studies performed in rodents have suggested the activity of GM as a growth inhibitor of solid tumors, such as sarcoma (109,110,111). Unfortunately, this effect and the corresponding mechanism of action have not been evaluated in further detail.

5.2. Pharmaceutical applications of glucomannan

GM has been investigated as a pharmaceutical excipient in tablets, films, beads and hydrogels, due to its gelling, solubility and biodegradable properties (7,8,25). Interestingly, recent work in this field has highlighted the potential of GM for the targeting of nanocarriers to specifics receptors, i.e. the mannose receptors on the cell surface (112). This mannose receptor is a 180 kDa transmembrane protein with five domains, able to recognize several sugars, such as mannose (113). This hypothesis is supported by previous reports which have shown that the presence of mannose residues on the particle's surface increases their uptake by the M cells (114,5) and macrophages (6), where the mannose receptors are overexpressed.

Glucomannan-based films

A number of recent articles have described the preparation of films made of GM or its derivatives in combination with other polymers (115,88, 116,117,118,95,119,25,24,120). Among them, GM-methylcellulose and GM-poly(acrylic)acid films have been found particularly promising for drug delivery (115, 88). The role of GM in these films is the modulation of their swelling properties and, hence, their ability to control drug release.

Glucomannan-based beads

Beads made of GM in combination with others polymers have been prepared in order to be used for protein delivery (8). The results have shown that the incorporation of GM into the alginate beads causes, not only the modification of the particle surface, but also the different disposition of the components inside the network. The resulting beads exhibited an improved protein loading capacity and also a pH-dependent swelling behaviour.

Glucomannan-based hydrogels

Due to the fact that GM is degraded by the enzymes secreted by the colonic bacteria, some authors have underlined the potential of GM-based hydrogels for

colonic drug delivery (117,118,121). These hydrogels were prepared using combinations of GM with acrylic acid or sodium tripolyphosphate. In addition, in order to achieve a selective colonic drug delivery, GM hydrogels were also formed using azo polymers as cross-linkers. It was concluded that GM is responsible of the enzymatic degradation of hydrogels, and thus, for the resulting drug release from the systems.

The formation of hydrogels from oxidized- konjac GM and chitosan was very recently reported (115). In this gels GM works as a crosslinker agent for chitosan, thus improving the controlled release properties of the resulting hydrogels.

Glucomannan-based microparticles

We have recently developed GM and chitosan-GM microparticles intended for pulmonary drug delivery using the spray-drying technique. The results showed that the morphology and surface appearance of the microspheres, as well as their densities and aerodynamic diameters, are closely dependent on their composition (presence and amount of GM) (**Fig. 9**). Furthermore, studies performed on well-differentiated Calu-3 cells showed the ability of these chitosan-GM microspheres to closely interact with the mucus layer, remaining adhered to the epithelium (122).

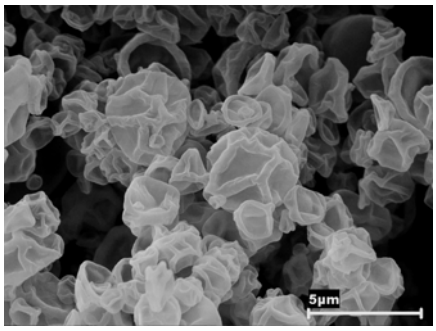

Figure 9. SEM photograph of GM microspheres

Glucomannan-based nanoparticles

Nanoparticles made of carboxymethylated GM and chitosan have been prepared by electrostatic interaction between the negative carboxylic groups of carboxymethylated GM and the positive amino groups of chitosan, followed by a sonication step (89). These nanoparticles exhibit a positive charge, and a size that can be modulated within the range of 50-1200 nm, depending on the polymer concentration. Additionally, these nanoparticles elicited an ability to entrap and release bovine serum albumin (BSA) (9,89,90). The introduction of GM in these formulations was intended to increase their stability and their controlled release properties.

Similarly, in our lab, we have developed a new protein particulate carrier made of GM and chitosan. The difference with the above mentioned nanoparticles, relies on the preparation technique, which, in our case was based on an ionotropic gelation process (10). These nanoparticles are obtained spontaneously by the simple mixing of the components. These very mild conditions make this approach very attractive for the association of delicate macromolecules to the nanoparticles. The interaction between both polymers, GM and chitosan, is expected to be driven by hydrophobic interactions and hydrogen bonds. Moreover, the presence of TPP (sodium tripolyphosphate) helps to build up the nanostructure, resulting in round and homogenous nanoparticles.

As expected, these nanoparticles exhibited an improved stability in ionic media and a delayed protein release (10,11). This delay could be explained by the higher crosslinking degree of chitosan nanogels impaired by the presence of GM (8,10,7). Furthermore, the results from our group have shown that the introduction of GM in the nanoparticles has led to a facilitated interaction with the intestinal epithelium both *in vitro* and *in vivo* (123,124). In summary, GM-chitosan nanoparticles offer attractive features as carriers for transmucosal drug delivery applications (**Fig. 10**).

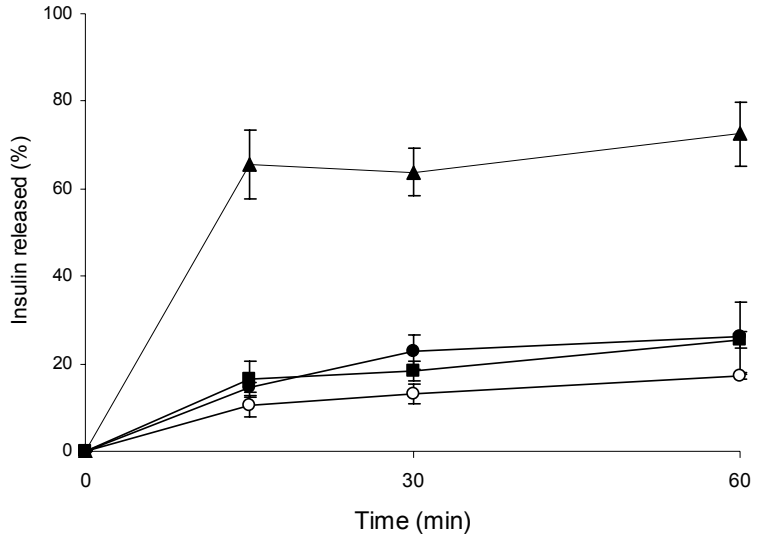

Figure 10. Release profiles from Insulin loaded Chitosan-GM nanoparticles. Insulin release profiles of CS/TPP (CS/TPP ratio: 6/1) (▲);CS/TPP/GM (CS/TPP/GM ratio: 6/1/1.8) (loading 29%) (■); CS/TPP/GM (CS/TPP/GM ratio: 6/1/1.8) (loading 15%) (●) and CSreac/TPP/GM (CSreac/TPP/GM ratio: 6/1/1.8) (loading 15%) (○) nanoparticles in artificial gastric juice (pH: 1.2) for 1 hour at 37ºC (mean ± SD, n = 4).

6. *In vivo* degradation of glucomannan

Tradicionally, konjac GM has been considered a polymer non susceptible to biodegradation in the human body. However, recently a number of GM-degrading enzymes have been identified in some microorganisms which are present in the human gut flora such as *Aerobacter mannanolyticus*, *Clostridium butyricum* and *Clostridium beijerinckii*. These bacteria produce endo-β-mannanase, an enzyme that catalyzes the cleavage of the β-1,4 linkages of GM to produce mainly the disaccharides β-1,4-D-mannobiose, cellobiose and 4-O-β-D-glucopyranosyl-D-glucopyranosyl-D-mannopyranose. These intermediate products are finally degraded to glucose and/or mannose by intestinal bacteria. Additionally, the monosaccharides serve as a carbon source for the proliferation of intestinal

bacteria, which ferment them into short-chain fatty acids (mainly acetic, propionic and butyric acid) (**Fig. 11**). These fermentative products can be absorbed across the intestinal wall and metabolized efficiently (64,65). In fact, it is known that short-chain fatty acids are rapidly absorbed from the colon of humans (124,125). Consequently, these results indicate that GM is a biodegradable polymer, which degradation products are natural compounds present in the human body.

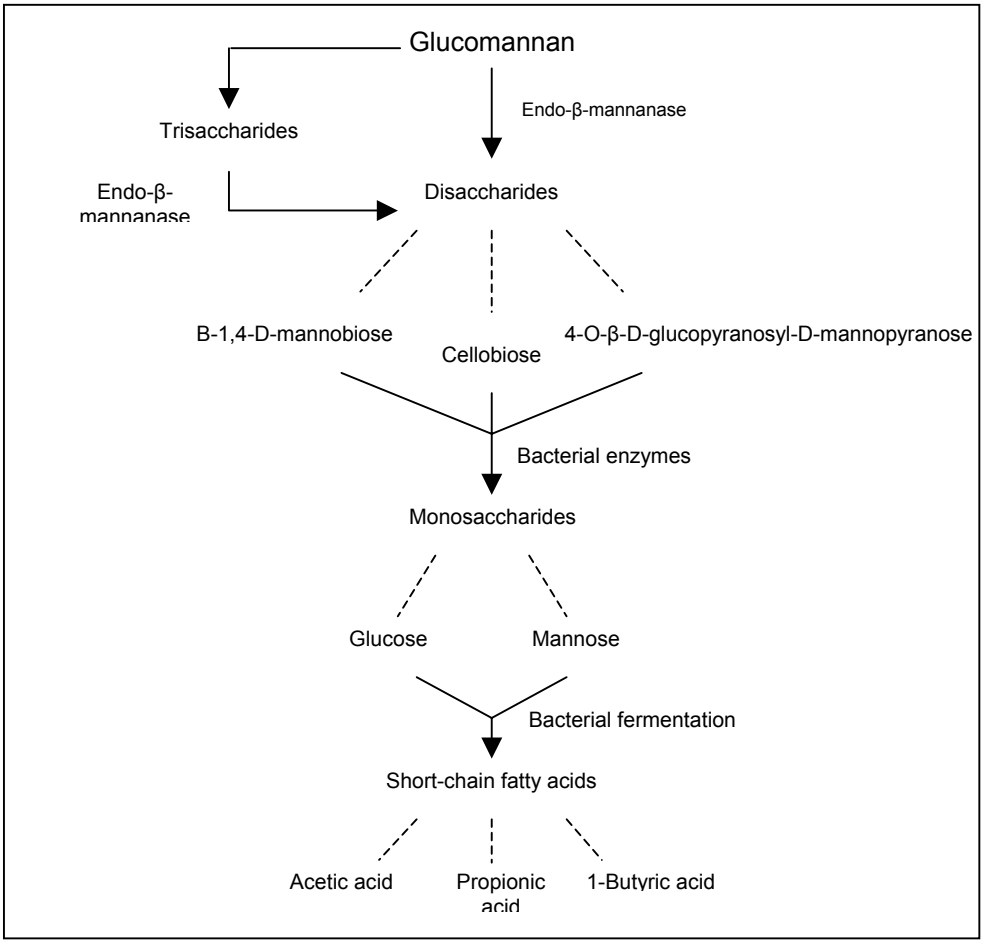

Figure 11. Scheme of the *in vivo* degradation of GM

7. Toxicity of Glucomannan

It is well known that GM has been traditionally used as a food additive in China and Japan, most specifically as a dietary fibre and, hence, considered good for health (14). Despite this long-use tradition, the results of the toxicity studies are very promising but still limited. For example, several authors have found no evidence of toxicity in rats after the long-term feeding of rats with a GM dose equivalent to an intake of 500 mg/kg body weight per day (126,127). Other authors have performed more detailed toxicity studies aimed at identifying signs of toxicity such as oral toxicity, sensitization studies in the skin, sub-acute and sub-chronic intestinal toxicity studies, cell-ageing, embryocitoxicity and genotoxicity studies (128,129). Interestingly, none of these studies has revealed significant signs of toxicity and only minor effect such as diarrhoea, abdominal pain and flatulence were reported at doses higher than 5g/day (130,131, 132).

Finally, concerning the regulatory aspects, in 1996 the European Commision in its "Report of the scientific committee for food" (41st series) considered that even when the GM toxicity studies were no enough to establish and Acceptable Daily Intake (ADI) "the use of konjac gum as an additive at intended levels up to 1% in food is acceptable provided that the total intake from all sources did not exceed 3g/day".

8. Conclusion

The polysaccharide GM and the family of related polymers present very attractive characteristics from the biopharmaceutical point of view. Over the last years a number of GM-based drug delivery systems, intended for their administration by different routes, have been designed. More specifically, hydrogels, beads, micro and nanoparticles made of GM or its derivatives have been obtained and evaluated for their ability to associate and deliver drugs. Even if the interest of the pharmaceutical field for GM is still recent, a general conclusion is that GM is a promissing and versatile polysaccharide for the preparation of new drug delivery systems.

Acknowledgements

The authors would like to thank the Spanish Ministry of Education (SAF2003-08765-C03-03; SAF2002-03314) for the financial support of some of the work included in this review. M. Alonso Sande acknowledges the Spanish Government her Predoctoral grant (FPU-MEC).

References

[1] J.-M. de la Fuente, S. Penades, Glyconanoparticles: types, síntesis and applications in glycoscience, biomedicina and material science, Biochim. Biophys. Acta 1760 (2006) 636--651.

[2] M.-J. Alonso, A. Sanchez, Biodegradable nanoparticles as new transmucosal drug carriers, ACS Symposium Series 879 (2004) 283--295.

[3] K.-A. Janes, P. Calvo, M.-J. Alonso, Polysacharide colloidal particles as delivery systems of macromolecules, Adv. Drug Del. Rev. 47 (2001) 83--97.

[4] R. Challa, A. Ahuja, J. Ali, R.-K. Khar, Cyclodextrins in drug delivery: an updated review, AAPS Pharm. Sci. Tech. 6 (2005) 329--357.

[5] H. Tomizawa, Y. Aramaki, Y. Fujii, T. Hara, N. Suzuki, K. Yachi, H. Kikuchi, S. Tsuchiya, Uptake of phosphatidylserine liposomes by rats Peyer's patches following intraluminal administration, Pharm Res. 4 (1993) 549--552.

[6] Z. Cui, C-H. Hsu, R.-J. Mumper, Physical characterization and macrophage cell uptake of mannan-coated nanoparticles, Drug Dev. Ind. Pharm. 6 (2003) 689--700.

[7] M. Nakano, K. Takikawa, T. Arita, Release characteristics of dibucaine dispersed in konjac gels, J. Biomed. Mater. Res. 13 (1979) 811--819.

[8] K. Wang, Z. He, Alginate-konjac glucomannan-chitosan beads as controlled release matrix, Int. J. Pharm. 244 (2002) 117--126.

[9] J. Du, R. Sun, S. Zhang, L.-F. Zhang, Ch.-D. Xiong, Y.-X.Peng, Novel polyelectrolyte carboxymethyl konjac glucomannan-chitosan nanoparticles for drug delivery. I. Physicochemical characterization of the carboxymethyl konjac, Biopolymers 18 (2005) 1--8.

[10] M. Alonso-Sande, M. Cuña, C. Remuñán-López, D. Teijeiro-Osorio, J.-L. Alonso-Lebrero, M.-J. Alonso, Formation of new glucomannan-chitosan

nanoparticles and study of their ability to associate and deliver proteins, Macromolecules 39 (2006) 4152--4158.

[11] M. Cuña, M. Alonso-Sande, C. Remuñan-López, J.-P. Pivel, J.-L. Alonso-Lebrero, M.-J. Alonso, Development of phosphorylated glucomannan-coated chitosan nanoparticles as nanocarriers for protein delivery, J. Nanosci. Nanotechnol. 8 (2006) 2887--2895.

[12] M. Maeda, H. Shimahara, N. Sugiyama, Detailed examination of the branched Structure of konjac glucomannan, Agric. Biol. Chem. 44 (1980) 245--252.

[13] V. Davé, S.-P. McCarthy, Review of konjac glucomannan, J. Env. Polym. Degrad. 4 (1997) 237--241.

[14] K. Nishinari, Konjac Glucomannan, Developments in Food Science 41 (2000) 309--330.

[15] A. Gonzalez-Canga, N. Fernandez Martinez, A.-M. Sahagun, J.-J. García Vieitez, M.-J. Diez Liebana, A. -P. Calle Pardo, L.-J. Castro Robles, M. Vega Sierra, Glucomannan: properties and therapeutic applications, Nutricion Hospitalaria 19 (2004) 45--50.

[16] Y. Zhang, B. Xie, X. Gan, Advance in the applications of konjac glucomannan and its derivatives, Carbohydr. Polym. 60 (2005) 27--31.

[17] H.-O. Bouveng, T. Iwasari, B. Lindberg, H. Meier, Studies on Glucomannans from Norwegian Spruce. 4. Enzymic Hydrolysis Acta Chem. Scand. 17 (1963) 1796--1797.

[18] T. -E. Timell, Wood Hemicelluloses: Part I, Adv. Carbohydr. Chem. 19 (1964) 247--302.

[19] Y. Nozawa, Y. Hiraguri, Y. Ito, Studies on the acid stability of neutral monosaccharides by gas chromatography with reference to the analysis of

sugar components in the polysaccharides, J. Chromatogr. 45 (1969) 244--249.

[20] G. Franz, Biosynthesis of salep mannan, Phytochem. 10 (1973) 2369--2373.

[21] L. Kenne, K.-G. Rosell, S. Svensson, Distribution of the O-acetyl groups in pine glucomannan, Carbohydr Res. 1 (1975) 69--76.

[22] O. Ishrud, M. Zahid, U.-A. Viqar, Y.-J. Pan, Isolation and structure analysis of a glucomannan from the seeds of Libian dates, Agric. Food Chem. 8 (2001) 3772--3774.

[23] D. I. Rhodes, B.-A. Stone, Proteins in walls of wheat aleurone cells, J. Cereal Sci. 1 (2002) 83--101.

[24] Ch. Xiao, S. Gao, L. Zhang, Blend films from konjac glucomannan and sodium alginate solutions and their preservative effect, J. Appl. Polym. Sci. 3 (2000) 617--626.

[25] Ch. Xiao, S. Gao, H. Wang, L. Zhang, Blend films from chitosan and konjac glucomannan solutions, J. Appl. Polym. Sci. 4 (2000) 509--515.

[26] A.-J. Buchala, G. Franz, H. Meier, Glucomannan from the tubers of Orchis morio, Phytochem. 13 (1974) 163--166.

[27] K. Maekaji, Determination of acidic component of konjac mannan, Agric. Biol. Chem. 42 (1978) 177--178.

[28] B. Koroskenyi, S.-P. McCarthy, Synthesis of acetylated konjac glucomannan and effect of degree of acetylation on water absorbency, Biomacromolecules 2 (2001) 824--826.

[29] S. Gao, K. Nishinari, Effect of deacetylation rate on gelation kinetics of glucomannan, Colloids and Surfaces B: Biointerfaces 38 (2004) 241--249.

[30] N. Kishida, S. Okimasu, T. Kamata, Molecular weight and intrinsic viscosity of konjac glucomannan, Agric. Biol. Chem. 42 (1978) 1645--1650.

[31] K. Kohyama, H. Lida, K. Nishinari, A mixed system composed of different molecular weights konjac glucomannan and kappacarrageenan: large deformation and dynamic viscolastic study, Food Hydrocolloids-Oxford 7 (1993) 213--226.

[32] Y. Guang, L. Zhang, Y. Chihiro, M. Ikuya, I. Miki, O. Kunihiko, Blend membranes from cellulose/konjac glucomannan cuprammonium solution, J. Membr. Sci. 139 (1998) 47--56.

[33] E. M. Ozu, I.C. Baianu, L.S. Wei, Physical and chemical properties of glucomannan gels and related polysaccharides, Phys. Chem. Food Processes 2 (1993) 487--517.

[34] C. Schatz, J.M. Lucas, C. Viton, A. Domard, C. Pichot, T. Delair, Formation and properties of positively charged colloids based on polyelectrolyte complexes of biopolymers, Langmuir 20 (2004) 7766--7778.

[35] M. de la Fuente, B. Seijo, M. J. Alonso, Proc. 33rd Meeting of the Controlled Release Society, Viena 2006.

[36] N. Csaba, M. Kopping-Hoggard, E. Fernández-Megia, R. Novoa-Carballal, M.J. Alonso, 5th World Meeting on Pharmaceutics, Biopharmaceutics and Pharmaceutical Technology, Geneve, Switzland 2006.

[37] K. Kato, T. Watanabe, K. Matsuda, Studies on the chemical structure of konjac mannan, II, isolation and characterization of oligosaccharides from the enzymatic hydrolyzate of the mannan, Agr. Biol. Chem. 34 (1970) 532--539.

[38] H. Chiura, M. Lizuka, T. Yamamoto, A glucomannan as an extracellular product of Candida utilis. II. Structure of a glucomannan: characterization of oligosaccharides obtained by partial hydrolysis, Agric. Biol. Chem. 46 (1982) 1733--1742.

[39] J.-A. Hansson, N. Hartler, Alkaline degradation of pine glucomannan, Holzforschung 24 (1970) 54-59.

[40] N. Sugiyama, H. Shimahara, T. Andoh, M. Takamoto, Mannan and related compounds. II. Konjac-mannanase from the tubers of Amorphophallus konjac, Agric. Biol. Chem. 1 (1973) 9--17.

[41] H. Shimahara, H. Suzuki, N. Sugiyama, K. Nisizawa, Partial purification of β-mannanase from the konjac tubers and their substrate specificity in relation to the structure of konjac glucomannan, Agric. Biol. Chem. 39 (1975) 293--299.

[42] R.P. de Vries, J. Visser, Aspergillus enzymes involved in degradation of plant cell wall polysaccharides, Microbiol. Mol. Biol. Rev. 65 (2001) 497--522.

[43] T. Reese, Y. Shibata, β-Mannannases of fungi, Can. J. Microbiol. 11 (1965) 167--183.

[44] K.W. Eriksson, M. Winell, Purification and characterization of a fungal β-mannanase, Acta Chem. Scand. 22 (1968) 1924--1934.

[45] N. Yamazaki, M. Sinner, H.H. Drietrichs, Isolation and properties of β-1,4-mannanase from Aspergillus niger, Holzforschung 4 (1976) 101--109.

[46] B.V. McCleary, N.K. Mathesen, Action patterns and substrate-binding requirements of β-D-mannanase with mannosaccharides and mannan-type polysaccharides, Carbohydr. Res. 119 (1983) 191--219.

[47] A. Civas, R. Eberhard, P. le Dizet, F. Petek, Glycosidases induced in Aspergillus tamarii. Secreted α-D-galactosidase and β-D-mannanase, Biochem. J. 219 (1984) 857--863.

[48] L. Viikari, A. Kantelinen, J. Sundquist, M. Linko, Xylanases in bleaching: from an idea to the industry, FEMS Microbiol. Rev. 13 (1994) 335--350.

[49] L. Viikari, M. Tenkanen, J. Buchert, M. Rättö, M. Bailey, M. Siika-Ako, M. Linko, Hemicellulases for industrial applications, in: Saddler J.N. (Ed.), Biotechnology in Agriculture, Bioconversion of Forest and Agricultural Plant Residues, C.A.B. International, Wallingford, 1993, pp. 131--182.

[50] P. Ademark, A. Varga, J. Medve, V. Harjunpaa, T. Drakenberg, F. Tjerneld, H. Stålbrand, Softwood hemicellulose-degrading enzymes from Aspergillus niger: purification and properties of a β-mannanase, J. Biotechnol. 63 (1998) 199--200.

[51] B.V. McCleary, Comparison of endolytic hydrolases which depolymerise 1,4-β-D-mannan, 1,5-alpha-L-arabinan and 1,4-beta-D-galactan, in: G.F. Leatham, M.E. Himmel (Eds.), Enzymes in Biomass Conversion, ACS Symposium Series 460, American Chemical Society, Washington D.C., 1991, chapter 34.

[52] S. Emi, J. Fukumoto, T. Yamamoto, Crystallization and some properties of mannanase, Agric. Biol. Chem. 36 (1972) 991--1001.

[53] T. Akino, N. Nakamura, K. Horikoshi, Characterization of three β-mannanases of an alkalophilic Bacillus sp., Agric. Biol. Chem. 52 (1988) 773--779.

[54] T. Araki, Purification and characterization of an endo- β-mannanase from Aeromonas sp. F-25, J. Fac. Agr. Kyushu Univ. 27 (1983) 89--98.

[55] I. Kusakabe, G.G. Park, N. Kumita, T. Yasui, K. Murakami, Specificity of β-mannanase from Penicillium purpurogenum for konjac glucomannan, Agric. Biol. Chem. 2 (1988) 519--524.

[56] L. Yamaura, T. Matsumoto, M. Funatsu, Y. Funatsu, Purification and some properties of endo-1,4-β-D-mannanase from Pseudomonas sp. PT-5, Agric. Biol. Chem. 54 (1990) 2425--2427.

[57] Y. Tamaru, T. Araki, H. Amagoi, H. Mori, T. Morishita, Purification and characterization of an extracellular β-(1,4)-mannanase from a Marine Bacterium, Vibrio sp. strain MA-138, Appl. Environ. Microbiol. 61 (1995) 4454--4458.

[58] R. Takahashi, I. Kusakabe, S. Kusama, Y. Sakurai, K. Muramaki, A. Maekawa, T. Suzuki, Structures of glucomanno-oligosaccharides from hydrolitic products of konjac glucomannan produced by a β-mannanase from Streotomyces sp., Agric. Biol. Chem. 48 (1984) 2943--2950.

[59] M. Ishihara, K. Shimizu, Hemicellulases of brown rotting fungus Tyromices palustris. IV. Purification and some properties of an extracellular mannanase, Mozukai Gakkaishi 12 (1980) 811--818.

[60] K. Shimizu, M. Ishihara, Isolation and characterization of oligosaccharides from the hydrolysate of larch wood glucomannan with endo-β-mannanase, Agric. Biol. Chem. 47 (1983) 949--955.

[61] Y. Oda, T. Komaki, K. Tonomura, Purification and properties of extracellular β-mannannases produced by Enteroccocus casseliflavus FL2121 isolated from decayed konjac, J. Ferment. Bioengin. 76 (1993) 14--18.

[62] G.M. Guebitz, M. Hayn, W. Steiner, Mannan-degrading enzymes from Sclerotium rolfsii: characterization and synergism of two endo-β-mannanases and a β-mannosidase, Bioresource Technol. 58 (1996) 127--135.

[63] R.F.H. Dekker, G.N. Richards, Hemicellulases: their occurrence, purification, properties, and mode of action, Adv. Carbohydr. Chem. Biochem. 32 (1976) 277--352.

[64] N. Nakajima, Y. Matsuura, Purification and characterization of konjac glucomannan degrading enzyme from anaerobic human intestinal bacterium, Clostriduim butyricum-Clostridium beijerinkii group, Biosci. Biotech. Biochem. 61 (1997) 1739--1742.

[65] Y. Matsuura, Degradation of konjac glucomannan by enzymes in human feces and formation of short-chain fatty acids by intestinal anaerobic bacteria, J. Nutrit. Sci. Vitamin. 44 (1998) 423--436.

[66] P. Ademark, J. Lundqvist, P. Hägglund, M. Tenkanen, N. Torto, F. Tjerneld, H. Stålbrand, Hydrolytic properties of a β-mannosidase purified from Aspergillus niger, J. Biotechnol. 75 (1999) 281--289.

[67] P.M. Dey, Biochemistry of plant galactomannans, Adv. Carbohydr. Chem. Biochem. 35 (1978) 341--376.

[68] Y. Ohya, K. Ihara, M. Jun-ichi, S. Tomoko, O. Tatsuro, Preparation and biological properties of dicarboxy-glucomannan: enzymatic degradation and stimulating activity against cultured macrophages, Carbohydr. Polym. 25 (1994) 123--130.

[69] M. Tenkanen, Action of Trichoderma reesei and Aspergillus oryzae esterases in the deacetylation of hemicelluloses, Biotechnol. Appl. Biochem. 27 (1998) 19--24.

[70] S.E. Case, J.A. Knopp, D.D. Hamann, S.J. Schwartz, Characterisation of gelation of konjac mannan using lyotrophic salts and rheological measurements, in: G.O. Phillips, P.A. Willliams, D.J. Wedlock (Eds.), Gums and stabilisers for the food industry 6, IRL Press, Oxford, 1992, pp. 489–500.

[71] L. Huang, R. Takahashi, S. Kobayashi, T. Kawase, K. Nishinari, Gelation behaviour of native and acetylated konjac glucomannan, Biomacromolecules 3 (2002) 1296--1303.

[72] P.A. Williams, D.H. Day, M.J. Langdon, G.O. Phillips, K. Nishinari, Synergistic interaction of xanthan gum with glucomannans and galactomannans, Food Hydrocol. 4 (1991) 489--493.

[73] P.A. Williams, S.M. Clegg, D.H. Day, G.O. Phillips, K. Nishinari, Food polymers, gels and colloids, Special publication-Royal Society of Chemistry 82 (1991) 339--348.

[74] P.A. Williams, S.M. Clegg, M.J. Langdon, K. Nishinari, L. Piculell, Investigation of the gelation mechanism in κ-carrageenan/konjac mannan

mixtures using differential scanning calorimetry and electron spin resonance spectroscopy, Macromolecules 26 (1993) 5441--5446.

[75] K. Kohyama, K. Nishinari, New application of konjac glucomannan as a texture modifier, Japan Agricultural Research Quarterly 31 (1997) 301--306.

[76] M.J. Ridout, P. Cairns, G.J. Brownsey, V. J. Morris, Evidence for intermolecular binding between deacetylated acetan and the glucomannan konjac mannan, Carbohydr. Res. 309 (1998) 375--379.

[77] U. Bertram, R. Bodmeier, In situ gelling, bioadhesive nasal inserts for extended drug delivery: In vitro characterization of a new nasal dosage form, Eur. J. Pharm. Sci. 27 (2006) 62--71.

[78] M. Tako, Synergistic interaction between xanthan and konjac glucomannan in aqueous media, Biosci. Biotechnol. Biochem. 56 (1992) 1188--1192.

[79] G. Paradossi, E. Chiessi, A. Barbiroli, D. Fessas, Xanthan and glucomannan mixtures: synergistic interactions and gelation, Biomacromolecules 3 (2002) 498--504.

[80] F. Alvarez-Manceñido, K. Braeckmans, S.C. De Smedt, J. Demeester, M. Landin, R. Martínez-Pacheco, Characterization of diffusion of macromolecules in konjac glucomannan solutions and gels by fluorescence recovery after photobleaching technique, Int. J. Pharm. 19 (2006) 37--46.

[81] F. Alvarez-Manceñido, M. Landin, I. Lacik, R. Martinez-Pacheco, Konjac glucomannan and konjac glucomannan/xanthan gum mixtures as excipients for controlled drug delivery systems. Diffusion of small drugs, Int. J. Pharm. In press 2007.

[82] A.A. Agoub, A.M. Smith, P. Giannouli, R.K. Richardson, E.R. Morris, Melt-in-the-mouth" gels from mixtures of xanthan and konjac glucomannan under acidic conditions: A rheological and calorimetric study of the mechanism of synergistic gelation, Carbohydr. Polym. 69 (2007) 713--724.

[83] R.O. Couso, L. Lelpi, M.A. Dankert, A xanthan-gum-like polysaccharide from Acetobacter xylinum, J. Gen. Microbiol. 8 (1987) 2123--2135.

[84] P.E. Jansson, J. Lindberg, K.M.S. Wimalasiri, M.A. Dankert, Structural studies o facetan, an exopolysaccharide elaborated by Acetobacter xylinum, Carbohydr. Res. 245 (1993) 303--310.

[85] C. Ojinnaka, E.R. Morris, V.J. Morris, G. J. Brownsey, Effect of acetyl substituents on the conformational stability and functional interactions of acetan polysaccharide, Gums Stab. Food Ind. 7 [Proceedings of the International Conference], 7th (1994) 15--26.

[86] C. Ojinnaka, G.J. Brownsey, E.R. Morris, V.J. Morris, Effect of deacetylation on the synergistic interaction of acetan with locust bean gum or konjac mannan, Carbohydr. Res. 305 (1998) 101--108.

[87] E. Miyoshi, T. Takaya, K. Nishinari, Effects of glucose, mannose and konjac glucomannan on the gel-sol transition in gellan gum aqueous solutions by rheology and DSC, Polymer Gels and Networks 6 (1998) 273--290.

[88] B. Li, J.F. Kennedy, J.L. Peng, X. Yie, B.J. Xie, Preparation and performance evaluation of glucomannan–chitosan–nisin ternary antimicrobial blend film, Carbohydr. Polym. 65 (2006) 488--494.

[89] J. Du, R. Sun, S. Zhang, T. Govender, L.F. Zhang, Ch.D. Xiong, Y.X. Peng, Novel polyelectrolyte carboxymethyl konjac glucomannan-chitosan nanoparticles for drug delivery, Macromol. Rapid. Commun. 25 (2004) 954--958.

[90] J. Du, S. Zhang, R. Sun, L.F. Zhang, Ch.D. Xiong, Y.X. Peng, J. Biomed. Mater. Res. Part B: Appl. Biomater. 72B (2005) 299--304.

[91] G. Zhou, Y. Li, L. Zhang, Y. Zuo, J.A. Jansen, Preparation and characterization of nano-hydroxyapatite/chitosan/konjac glucomannan composite, J. Biomed. Mater. Res. A 13 (2007).

[92] S. Matsumura, M. Nishioka, S. Yoshikawa, Enzymically degradable poly(carboxylic acid) derived from polysaccharide, Macromol. Chem. Rapid. Commun. 12 (1991) 89--94.

[93] N. Kishida, Relationship between the quality of konjac flour and the molecular matter nature of konjac mannan, Agric. Biol. Chem. 11 (1979) 2391--2392.

[94] K.P. Shatwell, I.W. Sutherland, S.B. Ross-Murphy, I.C.M. Dea, Influence of acetyl substituent on the interaction of xanthan with plant polysaccharides III. Xanthan-konjac mannan systems, Carbohydr. Polym. 14 (1991) 131--147.

[95] H. Zheng, Y.M. Du, Preparation and characterization of chitosan/carboxymethylated konjac glucomannan blend films, Wuhan Univ. J. Nat Sci. 7 (2002) 107--112.

[96] S. Kobayashi, S. Tsujihata, N. Hibi, Y. Tsukamoto, Preparation and rheological characterization of carboxymethyl konjac glucomannan. Food Hydrocolloids. 16 (2002) 289--294.

[97] K. Takechi, K.I. Furuhata, Synthesis and nucleophilic substitution of tosylated konjac glucomannan, Sen'i Gakkaishi 55 (1999) 315--322.

[98] S. Fujii, H. Kumagai, M. Noda, Preparation of poly(acyl)chitosans, Carbohydr. Res. 2 (1980) 389--393.

[99] S. Grant, H.S. Blair, G. Mckay, Deacetylation effects on the dodecanoyl substitution of chitosan, Polym. Comm. 7 (1990) 267--268.

[100] A.K. Sircar, D.J. Stanonis, C.M. Conrad, Cellulose propionylpropionate as a side product in the reaction of cotton cellulose with propionyl chloride, J. Appl. Polym. Sci. 9 (1967) 1683--1692.

[101] B. Tian, D. Changming, L. Chen, Preparation of konjac glucomannan ester of palmitic acid and its emulsification, J. Appl. Polym. Sci. 67 (1998) 1035--1038.

[102] L. Yongshang, L. Zhang, Interfacial structure and properties of regenerated cellulose films coated with superthin polyurethane benzoyl konjac glucomannan coating, Ind. Engineering Chem. Res. 5 (2002) 1234--1241.

[103] Y. Lu, L. Zhang, Interfacial structure and properties of regenerated cellulose films coated with superthin polyurethane/benzoyl konjac glucomannan coating, Ind. Engineering Chem. Res. 41 (2002) 1234--1241.

[104] Y. Lu, L. Zhang, X. Zhang, Y. Zhou, Effects of secondary structure on miscibility and properties of semi-IPN from polyurethane and benzyl konjac glucomannan, Polym. 44 (2003) 6689--6696.

[105] C.Y. Huang, M.Y. Zhang, S.S. Peng, J.R. Hong, X. Wang, H.J. Jiang, F.L. Zhang, Y.X. Bai, J.Z, Liang, Y.R. Yu, Effect of Konjac food on blood glucose level in patients with diabetes, Biomed. Environ. Sci. 2 (1990) 123--131.

[106] V. Vuksan, D.J.A. Jenkins, P. Spadafora, J.L. Stevenpiper, R. Owen, E. Vidgen, F. Brighenti, R. Josse, L.A. Leiter, C. Bruce-Thompson, Konjac-mannan (Glucomannan) improves glycemia and other associated risk factors for coronary heart disease in type 2 diabetes, Diabetes Care 22 (1999) 913--919.

[107] V. Vuksan, J.L. Stevenpiper, R. Owen, J.A. Swilley, P. Spadafora, D.J.A. Jenkins, E. Vidgen, F. Brighenti, R. Josse, L.A. Leiter, X. Zheng, R. Novokmet. Beneficial effects of viscous dietary fiber from konjac-mannan in subjects with the insulin resistence syndrome, Diabetes Care 23 (2000) 9--14.

[108] M.F. McCarthy, Glucomannan minimizes the postprandial insulin surge: a potential adjuvant for hepatothermic therapy, Medical Hypotheses 6 (2002) 487--490.

[109] S. Suzuki, M. Suzuki, H. Hatsukaiwa, H. Sunayama, T. Suzuki, M. Uchiyama, F. Fukuoka, Antitumor activity of polysaccharides. III. Growth-

inhibitory activity of purified mannan and glucan fractions from Baker's yeast against sarcoma-180 solid tumor, Gann. 60 (1969) 273--277.

[110] S. Suzuki, M. Suzuki, T. Matsumoto, Y. Okawa, Growth inhibition of sarcoma-180 solid tumor by the cells of regional lymph node and spleen from mice administered with yeast polysaccharides, Gann. 62 (1971) 343--352.

[111] D. Chorvatovicova, E. Machova, J. Sandula, G. Kogan, Rotective effect of the yeast glucomannan against cyclophosphamide-induced mutagenicity, Mutation Res. 444 (1999) 117--122.

[112] P.D. Stahl, J.S. Rodman, M.J. Miller, P.H. Schlesinger, Evidence for receptor-mediated binding of glycoproteins, glycoconjugates, and lysosomal glycosidases by alveolar macrophages, Proc. Natl. Acad. Sci. 3 (1978) 1399--1403.

[113] P.D. Stahl, R.A.B. Ezekowitz, The mannose receptor is a pattern recognotion receptor involved in the host defense, Curr. Op. Immunology. 10 (1998) 50--55.

[114] M. Takada, T. Yuzurita, K. Katayama, K. Iwamoto, J. Sunamoto, Increased lung uptake of liposomes coated with polysaccharides, Biochim. Biophisic. Acta. 802 (1984) 237--244.

[115] H. Yu, A. Huang, C. Xiao, Characteristics of konjac glucomannan and poly(acrylic acid) blend films for controlled drug release, J. Appl. Polym. Sci. 100 (2006) 1561--1570.

[116] X. Ye, J.F. Kennedy, B. Li, B.J. Xie, Condensed state structure and biocompatibility of the konjac glucomannan/chitosan blend films, Carbohydr. Polym. 64 (2006) 532--538.

[117] Ch. Liu, Ch. Xiao, Characterization of konjac glucomannan–quaternized poly(4-vinyl-N-butyl) pyridine blend films and their preservation effect, J. Appl. Polym. Sci. 93 (2004) 1868--1875.

[118] Z.L. Liu, H. Hu, R.X. Zhuo, Konjac glucomannan-graft-acrylic acid hydrogels containing azo crosslinker for colon-specific delivery, J. Polym. Sci. Part A: Polym. Chem. 42 (2004) 4370--4378.

[119] C. Xiao, L. Weng, L. Zhang, Improvement of physical properties of crosslinked alginate and carboxymethyl konjac glucomannan blend films, J. Appl. Polym. Sci. 84 (2002) 2554--2560.

[120] L. Cheng, A. Abd Karim, M.H. Norziah, C.C. Seow, Modification of the microstructural and physical properties of konjac glucomannan-based films by alkali and sodium carboxymethylcellulose, Food Res. Int. 35 (2002) 829--836.

[121] L.G. Chen, Z.L. Liu, R.X. Zhuo, Synthesis and properties of degradable hydrogels of konjac glucomannan grafted acrylic acid for colon-specific drug delivery, Polym. 46 (2005) 6274--6281.

[122] D. Teijeiro-Osorio, C.J. Lamela, H.M. Nielsen, C. Remuñán-López, Preparation and characterization of chitosan/glucomannan microspheres for pulmonary delivery of macromolecules, *submitted*.

[123] M. Alonso-Sande, A. des Rieux, Y.J. Schneider, C. Remuñán-López, M.J. Alonso, V. Préat, Uptake Studies of Chitosan and Chitosan-Glucomannan Nanoparticles in Human Intestinal FAE Model, Proc. 33rd Meeting of the Controlled Release Society, Vienna 2006.

[124] M. Alonso-Sande, C. Remuñán-López, J.L. Alonso-Lebrero, M.J. Alonso. Chitosan-glucomannan nanoparticles as carriers for oral adminitration of insulin: Effect of glucomannan type and insulin loading Proc.. 32nd Meeting of the Controlled Release Society, Miami 2005.

[125] A.M. Dawson, C.D. Holdsworth, Absorption of short chain fatty acids in man, J. Webb. Proc. Soc. Exp. Biol. Med. 117 (1964) 97--100.

[126] H. Ruppin, S. Bar-Meir, K.H. Soergel, C.M. Wood, M.G. Schmitt, Absorption of short-chain fatty acids by the colon, Gastroenterology 78 (1980) 1500--1507.

[127] S.S. Peng, M.Y. Zhang, Y. Z. Zhang, Z.H. Wu, Long-term animal feeding trial of the refined konjac meal. II. Effects of the refined konjac meal on the aging of the brain, liver and cardiovascular tissue cells in rats, Biomed. Environ. Sci. 8 (1995) 80--87.

[128] M.Y. Zhang, S.S. Peng, Y.Z. Zhang, Z. H. Wu, Long-term animal feeding trial of the refined konjac meal. I. Effects of the refined konjac meal on the calcium and phosphorus metabolism and the bone in rat, Biomed. Environ. Sci. 8 (1995) 74--79.

[129] F. Konishi, Y. Shidoji, T. Oku, N. Hosoya, Mode of rat cecal enlargement induced by a short-term feeding on glucomannan, Jap. J. Exp. Med. 54 (1984) 139--142.

[130] Technical and Scientific dossier submittred by FMC Europe NV 1995, Belgium.

[131] K. Doi, M. Matsuura, A. Kawara, T. Tanaka, S. Baba, Influence of Dietary Fiber (konjac Mannan) on Absorption of Vitamin B12 and Vitamin E, Tohoku J. Exp. Med. 141 (1983) 677--681.

[132] K. Doi, M. Matsuura, A. Kawara, R. Uenoyama, S. Baba, Effect of glucomannan (konjac fiber) on glucose and lipid metabolism in normal and diabetic subjects, Int. Congress Series 549 (1982) 306--312.

[133] Y. Saito, K. Yoshida, Effect of dietary fiber on urinary thiamin excretion in humans, Hum. Nutr.: Food Sci. Nutr. 41F (1987) 63--70.

Anexo III

Formation of New Glucomannan-Chitosan Nanoparticles and Study of their Ability to Associate and Deliver Proteins

M. Alonso-Sande, M. Cuña, C. Remuñán-López, D. Teijeiro-Osorio,
J.L. Alonso-Lebrero, M. J. Alonso

4152 *Macromolecules* **2006,** *39,* 4152−4158

Formation of New Glucomannan−Chitosan Nanoparticles and Study of Their Ability To Associate and Deliver Proteins

María Alonso-Sande,[†] Margarita Cuña,[†] Carmen Remuñán-López,[†] Desirée Teijeiro-Osorio,[†] José L. Alonso-Lebrero,[‡] and María J. Alonso*,[†]

Department of Pharmaceutical Technology, Faculty of Pharmacy, University of Santiago de Compostela, Spain, and R&D Department, Industrial Farmacéutica Cantabria SA, Spain

Received January 30, 2006; Revised Manuscript Received April 10, 2006

ABSTRACT: The purpose of this work was to investigate the factors involved in the formation of a new type of nanoparticle made of hydrophilic polysaccharides, chitosan (CS), and glucomannan (GM) and to study their potential for the association and delivery of proteins. Two different types of glucomannan were used (non-phosphorylated Konjac GM (KGM) and phosphorylated GM), and two different approaches were adopted for the preparation of the nanoparticles. These procedures involved the interaction of CS and GM in the presence or absence of sodium tripolyphosphate, which acted as an ionic cross-linking agent for CS. Using both approaches, it was possible to obtain nanoparticles with a size in the range from 200 to 700 nm and a variable zeta potential (from −2 to +39 mV), depending on the formulation conditions. Despite the mild forces involved in their formation, by adjusting the process variables, it was also possible to obtain nanoparticles that remain stable upon dilution with phosphate buffer saline. The nanoparticles exhibited a great capacity for the association of the model peptide insulin and the immunomodulatory protein P1, reaching association efficiency values as high as 89%. Moreover, the release of the peptide/protein could be modulated by varying the composition of the system. Consequently, the results presented here suggest that chitosan−glucomannan nanoparticles are promising carriers for the oral administration of peptides and proteins.

1. Introduction

A major recent challenge confronted in pharmaceutical sciences has been the development of effective delivery systems especially adapted for transmucosal administration of peptides and proteins.[1] Indeed, the efficacy of these active macromolecules is strongly hampered not only by their chemical and physical instability but also by the high metabolic activity and the limited permeability of the mucosal barriers.[2] As a consequence, the future of these molecules as therapeutic agents clearly depends on the design of appropriate vehicles for their delivery to the body. Several strategies have been explored so far to overcome these limitations, among which the design of biodegradable poly(lactic acid−glycolic acid) PLGA nanoparticles has attracted considerable interest.[3] However, an inconvenience of these particles is that their preparation requires the use of aggressive conditions (organic solvents, sonication, etc.) that compromise the stability of the encapsulated molecules. In addition, the degradation of these particles occurs over long periods of time, a situation that contributes to the degradation of the encapsulated protein.

An interesting alternative to hydrophobic nanoparticles is that made of hydrophilic polymers such as the polysaccharide CS. CS has a well-documented biocompatibility and low toxicity;[4,5] it adheres to the mucosal surfaces[6] and has the capacity of promoting the permeation of macromolecules through well-organized epithelia (nasal, intestinal, ocular, buccal).[7−10] The potential of CS for this specific application has been further reenforced by its demonstrated ability to form colloidal particles which entrap macromolecules through a number of mechanisms, including ionic cross-linking, desolvation, or ionic complexation.[11] In this respect, we have recently reported the preparation of CS nanoparticles via a mild ionotropic gelation procedure with the counterion sodium tripolyphosphate (TPP).[12,13] These nanoparticles have shown a high capacity for the association of macromolecules such as insulin, BSA, tetanus toxoid, and diphtheria toxoids. Moreover, in vivo experiments have evidenced their potential as nasal carriers for peptides and antigens.[8,14]

Based on this previous information, the aim of this paper was to develop a new nanoparticulate system, made of CS and GM, exhibiting adequate properties for the oral administration of peptides and proteins. The polysaccharide GM—either in a noncharged form (KGM) or negatively charged form (phosphorylated GM)—was chosen as a second ingredient for the nanoparticles formation because of its ability to interact with CS. Moreover, an interesting characteristic of GM relies on its ability to interact favorably with some biological surfaces which are particularly rich in mannose receptors, such as the M-cells overlying the Peyer's patches[15] and macrophages.[16] In addition, it has been reported that the addition of GM to CS gels may help in enhancing the stability of the resulting systems in the gastrointestinal fluids.[17,18] Therefore, based on this previous information, our hypothesis was that the nanoparticles made of CS and GM would be adequate vehicles for the delivery of peptides/proteins across the intestinal epithelium and, in particular, through the M-cells overlying Peyer's patches.

In light of these considerations, we first aimed at finding the adequate conditions for the formation of the particles and, second, we investigated their potential for the association and release of proteins. For this latter purpose, we chose insulin and an immunomodulatory protein (P1). P1 is a mixture of polypeptides which have shown the ability to up-regulate natural and specific cell-mediated immune mechanism, thus having application in therapeutic treatment of intra- and extracellular infections and as vaccination adjuvant.[19]

† University of Santiago de Compostela.
‡ Industrial Farmacéutica Cantabria SA.
* To whom correspondence should be addressed: Ph 00 34 981 563100-14885; Fax 00 34 981 547148; e-mail ffmjalon@usc.es.

10.1021/ma060230j CCC: $33.50
Published on Web 05/17/2006

2. Materials and Methods

2.1. Materials. Chitosan (CS) in the form of hydrochloride salt [Protasan Cl 110; supplier's specifications: intrinsic viscosity at 25 °C = 10 mPa, M_w = 110 kDa, deacetylation degree = 87%] was provided by Pronova Biopolymer (Norway). Konjac glucomannan (KGM) [RX-L; supplier's specifications: intrinsic viscosity at 25 °C = 15000 ± 5000 mPa] was purchased by Shimizu Chemical Co. (Japan). Phosphorylated GM [supplier's specifications: mannose = 84%, glucose and phosphate groups = 7 ± 3%, M_w = 150 kDa] and P1 [immunomodulatory mixture of proteins; supplier's specifications: M_w = 8−12 kDa, isoelectric point (IP) = 3−9] were kindly supplied by Industrial Farmacéutica Cantabria (Madrid, Spain). Bovine insulin [supplier's specifications: M_w = 5.8 kDa, IP = 5.3], pentasodium tripolyphosphate (TPP), and glycerol were purchased from Sigma Chemical Co. (Spain). Ultrapure water [Milli-Q Plus, Millipore Ibérica, Spain] was used throughout. All other reagents were analytical grade.

2.2. Preparation of Polymer Solutions. CS solutions (2 or 3 mg/mL) were prepared by dissolving the polymer in either purified water or acetic acid 1% (v/v) for 2 h under magnetic stirring. The pH of the CS solutions was adjusted to 4.8 by adding NaOH (10 M). Phosphorylated GM was dissolved in pure water at the concentration of 23 mg/mL, obtaining a final pH of 7.1. Non-phosphorylated KGM was first dispersed in water; then, the suspension was centrifuged, and the supernatant was freeze-dried and dissolved at 1 mg/mL in 10 mM Na_2HPO_4 (pH: 8.26) to obtain a clear solution (viscosity of 1% (w/v) solution in water at 25 °C = 1291 ± 36 mPa·s; experimentally determined with a Oswald's viscosimeter). Finally, TPP was directly dissolved in pure water at the concentrations of 0.84 or 3.3 mg/mL, depending on the formulation.

2.3. Preparation of Nanoparticles. We adopted two different approaches for the preparation of the nanoparticles. First, we prepared nanoparticles made of solely CS and GM (CS-KGM and CS-phosphorylated GM nanoparticles) upon mixing the aqueous solutions of both polymers. In a second approach, we prepared CS/TPP-GM nanoparticles by a previously described ionotropic gelation method within CS and TPP,[12] which here was modified to incorporate either KGM or phosphorylated GM into the nanoparticles structure.

Preparation of CS−GM Nanoparticles. CS−phosphorylated GM nanoparticles of 6/4.6 and 6/13.8 theoretical CS/phosphorylated GM ratios were formed spontaneously upon the incorporation of prefixed volumes (0.2 and 0.6 mL) of the phosphorylated GM solution (23 mg/mL in pure water, pH 7.1) onto 3 mL of the CS solution (2 mg/mL in pure water, pH 4.7) under magnetic stirring at room temperature. As indicated above, CS was directly dissolved in pure water or in acetic acid solution 1% (v/v) followed by raising the pH up to 4.8 by adding NaOH 10 M. On the other hand, CS−KGM nanoparticles of 6/4.6, 6/6, 6/12, 6/13.8, 6/18, and 6/24 theoretical CS/KGM ratios were obtained upon the addition of 1.15 and 6 mL of the KGM (non-phosphorylated) solution to 0.5 mL of the CS solution (3 mg/mL, in pure water, pH 4.75). Thereafter, the nanoparticles were purified by centrifugation (10000*g*, 40 min, 4 °C; Beckman Avanti 30, Beckman) using a bed made of 20 μL of glycerol. The supernatants were discarded, and the nanoparticles reconstituted in 100−200 μL of pure water.

Preparation of CS/TPP-GM Nanoparticles. Nanoparticles of a 6/1 theoretical CS/TPP ratio were formed spontaneously upon the incorporation of 1.2 mL of TPP solution (0.84 mg/mL) into 3 mL of a CS aqueous solution (2 mg/mL) under mild magnetic stirring, at room temperature. These nanoparticles were used as control.

For the preparation of CS/TPP−phosphorylated GM and CS/TPP−KGM, the polymer solutions were prepared as indicated before. CS/TPP−phosphorylated GM nanoparticles of 6/1/2.3 and 6/1/4.6 theoretical CS/TPP/phosphorylated GM ratios were obtained by incorporating 100 and 200 μL of a phosphorylated GM aqueous solution (23 mg/mL) to 1.2 mL of the TPP (0.84 mg/mL) aqueous phase before the nanoparticles formation. CS/TPP-KGM nanoparticles of 6/1/1.2, 6/1/1.8, 6/1/2.3, 6/1/3, and 6/1/4.6 theoretical CS/TPP/KGM ratios were formed upon the addition of a mixture of KGM and TPP (KGM = 1 mg/mL, 1.2−4.6 mL; TPP = 3.3. mg/mL, 0.3 mL) into 3 mL of CS solution (2 mg/mL) under magnetic stirring at room temperature. Thereafter, the nanoparticles were purified as described before.

2.4. Association of Insulin and P1 Protein to the Nanoparticles. Insulin was dissolved at a concentration of 5 mg/mL in NaOH 0.01 M (pH 11), and P1 protein was dissolved at 7.7 mg/mL in 10 mM phosphate buffer (pH 6.6). Then the insulin and P1 protein solutions (0.6 and 0.3 mL, respectively) were added to the TPP and/or GM solutions for the CS/TPP−GM and CS−GM formulations, respectively. Protein theoretical loadings were calculated to obtain CS/insulin and CS/P1 protein ratios of 2/1−2.4/1 and 1.6/1−2.2/1, respectively, which correspond to theoretical loadings of 20−22% (w/w) for insulin and 16−21% (w/w) for protein P1. The nanoparticles containing insulin and P1 protein were prepared according to the procedures indicated before.

2.5. Determination of Process Yield. For the calculation of the nanoparticles production yields, the nanoparticles suspension were centrifuged (10000*g*, 4 °C, 40 min), and the supernatant was discarded. The tubes containing the sediments were freeze-dried for 24 h, and the difference of the theoretical solids weights and the actual freeze-dried nanoparticles weights were obtained (n = 3). The yield of the process was calculated as follows:

$$\text{process yield (\%)} = \frac{\text{nanoparticles weight}}{\text{total solids (CS + TTP + GM) weight}} \times 100$$

2.6. Characterization of Nanoparticles. The morphological examination of the nanoparticles was performed by transmission electron microscopy (TEM) (CM12 Philips, Eindhoven, The Netherlands). The samples were stained with 2% w/v phosphotungstic acid for 10 s, immobilized on copper grids with Formvard, and dried overnight for viewing by TEM.

The measurements of size and zeta potential of the nanoparticles were performed by photon correlation spectroscopy and laser Doppler anemometry, respectively, with a Zetasizer 3000HS (Malvern Instruments, Malvern, UK). For the determination of the zeta potential, samples were diluted in 1 mM KCl and measured in automatic mode (placed in the electrophoretic cell where a potential of ±150 mV was established). The zeta potential values were calculated from the mean electrophoretic mobility values using the Smoluchowski's equation. For size analysis, samples were diluted in water and measured for a minimum of 18 s. Raw data were subsequently correlated to mean hydrodynamic size by cumulative analysis ($n \geq 6$).

2.7. Evaluation of Nanoparticles Stability. The stability of the nanoparticles was investigated in phosphate buffer saline (PBS) pH 7.4 at room temperature. Aliquots of fresh suspensions of nanoparticles were diluted with PBS, reaching a concentration 1 mg/mL, and the evolution of size was assessed using photon correlation spectroscopy (Zetasizer 3000HS, Malvern Instruments, UK) for 2 h at room temperature (n = 4).

2.8. Determination of Protein Loading Capacity of Nanoparticles. The quantity of insulin and P1 protein entrapped in the nanoparticles was calculated by the difference between the total protein incorporated in the nanoparticles formation medium and the quantity of nonentrapped protein remaining in the aqueous suspending medium. Association efficiencies of the nanoparticles were determined upon their separation from aqueous suspension medium by centrifugation (10000*g*, 4 °C, 40 min). Insulin and P1 protein were analyzed in the supernatant by Micro BCA protein assay at 562 nm (Pierce, Rockford, IL). Calibration curves were made with corresponding solutions of blank nanoparticles (n = 4).

The protein association efficiency and protein loading capacity of the nanoparticles were calculated as follows:

$$\text{association efficiency (\%)} = \frac{\text{total protein (mg)} - \text{free protein (mg)}}{\text{total protein (mg)}} \times 100$$

$$\text{loading capacity (\%)} = \frac{\text{total protein (mg)} - \text{free protein (mg)}}{\text{nanoparticles weight}} \times 100$$

2.9. In Vitro Release Studies. The releases of insulin and P1 protein from the nanoparticles were determined by incubating the nanoparticles in 1.5 and 1 mL (1−0.5 mg of nanoparticles), respectively, of pH 7.4 phosphate buffer (PBS) at 37 °C (P-Selecta, Hotcold-M, Spain) under mild horizontal agitation (Promax 1020, Heidolph, Germany). At appropriate time intervals, the individual samples were filtered and supernatants isolated, and released protein was evaluated by the Micro BCA protein assay (Pierce, Rockford, IL). A calibration curve was made at each time interval using nonloaded nanoparticles ($n = 4$).

3. Results and Discussion

3.1. Formation and Characterization of Nanoparticles. In this work, we report the preparation and characterization of new nanoparticulate systems consisting of two polysaccharides, CS and GM (Figure 1), which were obtained under exceptionally mild conditions. As stated in the Introduction, we have previously reported the development of CS nanoparticles based on the ionic cross-linking of CS with a counterion such as TPP.[12] The intra- and intermolecular linkages created between the negative groups of TPP and the positively charged amino groups of CS were responsible for the success of the process. These nanoparticles have shown a potential for nasal administration of proteins.[8,14] In the present work, the introduction of GM as a second ingredient in the nanoparticulate formulation was expected to open new possibilities for their interaction with biological surfaces.[15] With this idea in mind, we have developed a number of approaches for the preparation of nanoparticles containing CS and GM, based on mixing aqueous phases at room temperature. These approaches involve (i) mixing an aqueous phase containing CS with an aqueous phase that contains the cross-linking agent TPP (formation of CS/TPP nanoparticles) followed by their coating with GM or alternatively (ii) mixing an aqueous phase containing CS with an aqueous phase that contains GM with or without the cross-linking agent TPP. In a previous article we reported the results corresponding to the first approach and the efficient association of proteins to the nanoparticles.[20] In this work, we present the results corresponding to the second alternative. The GM used to form the nanoparticles was either KGM, obtained from *Amorphophallus konjac,* or phosphorylated GM, isolated from the cell wall of *Candida utillis.* As previously reported, both polysaccharides, CS and GM, were expected to interact through intermolecular hydrogen bonds in addition to the electrostatic interactions.[17,18] However, the phosphate groups (negatively charged) of phosphorylated GM were expected to facilitate the ionic interaction of this GM with the positively charged CS molecules. The differences in the chemical structure of both types of GM are shown in Figure 1.

CS−GM Nanoparticles. To begin, we conducted a study in order to identify the adequate processing conditions for the formation of nanoparticles made of solely CS and GM (phosphorylated or not). Taking into account the negative charge of the phosphorylated GM, it was expected that, under the appropriate conditions, it could electrostatically interact with CS, leading to the formation of CS-phosphorylated GM nanoparticles. In fact, nanoparticles with 6/4.6 and 6/13.8 theoretical CS/phosphorylated GM ratios were obtained upon mixing a CS solution (in water or acetic acid), with an aqueous solution of phosphorylated GM. The physicochemical properties of fresh CS−phosphorylated GM nanoparticles are shown in Table 1. Higher process yields were obtained for the nanoparticles

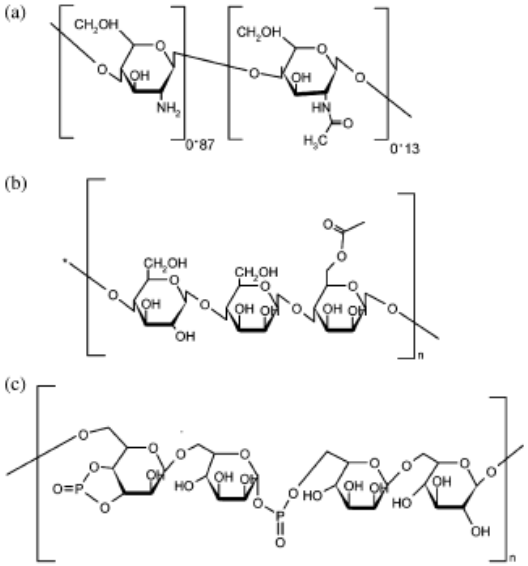

Figure 1. Chemical structure of (a) CS, (b) KGM, and (c) phosphorylated GM polymers.

Table 1. Physicochemical Properties of CS−Phosphorylated GM Nanoparticles Prepared with Different CS/Phosphorylated GM Theoretical Ratios (Mean ± SD, $n = 6$)

CS/phosphorylated GM (w/w)	process yield (%)	size (nm)	ζ potential (mV)
6/4.6[a]	22 ± 5	252 ± 15	+31.25 ± 1.0
6/13.8[a]	20 ± 3	183 ± 02	+30.5 ± 0.2
6/4.6[b]	45 ± 3	300 ± 12	+33.6 ± 1.0
6/13.8[b]	54 ± 3	185 ± 04	+33.2 ± 0.8

[a] CS was dissolved in pure water (final pH: 4.8). [b] CS was dissolved in acetic acid and neutralized up to pH 4.8 by adding NaOH (10 M) prior to mixing with phosphorylated GM.

prepared using CS solutions in acetic acid as compared to those obtained with CS solutions in water. This could be related to the higher ionic strength created by the presence of sodium acetate (the CS acetic acid solution was neutralized with NaOH). Several authors have described the effect of ionic strength on the conformation of the CS chains, which is related with the variation of the electrostatic charges along the polymer chains.[21,22] Furthermore, the ionic strength has a significant effect on the intrinsic viscosity (particularly at low salt levels), increasing polymer chain flexibility,[23] which could improve the interaction between both polymers (CS and phosphorylated GM). On the other hand, the results of the process yield shown in Table 1 indicate that an increase in the amount of phosphorylated GM led to the formation of a greater number of particles. This effect, only apparent for the formulations prepared in the presence of sodium acetate, could be attributed to the nanoparticles formation mechanism. As indicated above, the ionic strength may improve hydrophobic polymer−polymer interaction and, hence, increase the incorporation of GM into the nanoparticles.

The results in Table 1 also indicate that the nanoparticles have a size ranging from approximately 180 to 310 nm, depending on polymer composition (CS/phosphorylated GM ratio): an increase in the content of phosphorylated GM led to a smaller size. This size reduction could be explained by the compaction of the nanoparticles structure following the CS−anionic GM interaction. Decreasing the amount of phosphory-

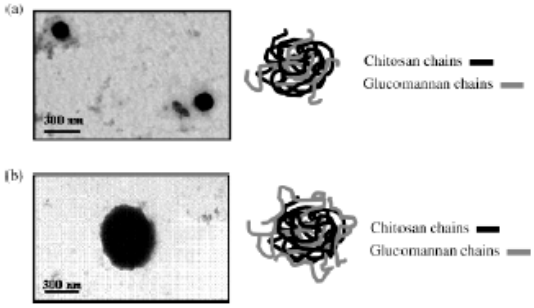

Figure 2. TEM microphotographs and expected structure of CS/GM nanoparticles made with different compositions. Nanoparticles polymer composition: (a) CS/phosphorylated GM(6/4.6) (× 75K); (b) CS/KGM (6/6) (× 60K).

Table 2. Physicochemical Properties of CS−KGM Nanoparticles Prepared with Different CS/KGM Theoretical Ratios (Mean ± SD, $n = 12$)

CS[a]/KGM (w/w)	process yield (%)	size (nm)	ζ potential (mV)
6/6	45 ± 2	745 ± 36	−0.8 ± 0.4
6/12	44 ± 4	611 ± 19	−0.4 ± 0.4
6/13.8	40 ± 2	588 ± 20	−1.65 ± 1.1
6/18	36 ± 2	493 ± 03	−2.2 ± 0.1
6/24	28 ± 4	488 ± 20	−2.1 ± 0.2

[a] CS was dissolved in water.

lated GM implies a reduction in the number of anions that are available to neutralize the amino groups of CS and, hence, to condense the polymer into tight particles.[24] Interestingly, despite the effect of the GM content on the size of the particles, the positive values of zeta potential (above +30 mV) were not substantially affected by the CS/phosphorylated GM ratio. This could be explained by the important positive charge density of CS as compared to that of phosphorylated GM. In fact, while around 87% of amino groups are expected to be positively charged in each CS molecule, only 7% of the OH groups of the phosphorylated GM were phosphorylated. This conclusion agrees with that reported by Du et al.,[25] who found that the superficial charge of CS/carboxymethyl GM nanoparticles were not influenced by the GM content. Illustrations of the expected and obtained structure for CS−phosphorylated GM nanoparticles by TEM are presented in Figure 2a.

In the first step of this work we assumed that the presence of the phosphate group in the phosphorylated GM would be critical in the formation of the nanoparticles; however, as illustrated in Figure 2b, CS−GM nanoparticles could also be obtained upon mixing of CS and KGM (non-phosphorylated) solutions in adequate conditions. More specifically, nanoparticles could be obtained with CS/KGM theoretical ratios from 6/6 to 6/24. In this case, the mechanism of nanoparticles formation is probably due to the already mentioned intermolecular hydrogen bonds within the hydroxyl groups of KGM and the free amino groups of CS.[17] As shown in Table 2, the highest process yields were obtained for the nanoparticles from 6/6 to 6/13.8 theoretical CS/KGMratios. A further increase in the amount of KGM and, hence, in theoretical total solids content led to a decrease in the process yield. This could be attributed to the fact that there is an excess of KGM, which cannot be integrated into the nanoparticle structure.

As noted for CS-phosphorylated GM nanoparticles, the increase of the KGM content led to the condensation of the nanostructure and hence to the reduction of the particle size. However, the size of CS−KGM nanoparticles (470−800 nm)

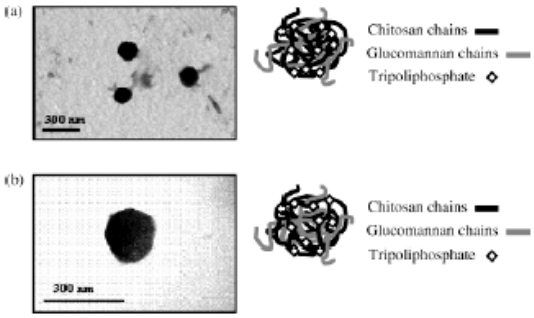

Figure 3. TEM microphotographs and expected structure of CS/TPP/GM nanoparticles made with different compositions. Nanoparticles polymer composition: (a) CS/TPP/phosphorylated GM (6/1/4.6) (× 75K); (b) CS/TPP/KGM (6/1/1.8) (× 260K).

was larger than that of the particles containing phosphorylated GM (Table 1). This result could be related to the different interaction forces between the two interacting species (CS and KGM), leading to a lower degree of compaction of the resulting nanostructure. This interpretation is in agreement with that given by Xu et al.[26] for the larger size of CS/TPP/PEG nanoparticles as compared to CS/TPP−sodium alginate nanoparticles. They attributed these differences to the weaker interaction between CS and PEG in comparison with the interaction of CS with sodium alginate. Nevertheless, although a different interaction could be expected for phosphorylated and non-phosphorylated KGM with CS, we cannot discard the potential influence of the GM molecular weight, which was much smaller for phosphorylated GM than for the non-phosphorylated KGM. In fact, it has been widely reported that the particle size of colloids, made by complexation of two polysaccharides, is highly influenced by the molecular weight of the initial components.[12,24,27]

With regard to the results of the surface charge, in contrast with those obtained for CS−phosphorylated GM nanoparticles (Table 1), the zeta potential values of the CS−KGM nanoparticles were neutral irrespective of the CS/KGM ratio. The neutral charge of the particles can only be explained by a shield effect of the KGM molecules (without charge) surrounding the positively charged CS molecules (see illustration in Figure 2b). This specific organization may be related to the formation process of the nanoparticles. In fact, we observed that whereas CS−phosphorylated GM nanoparticles formed spontaneously, CS−KGM nanoparticles need more time for their formation (15 min). This kinetics of particle formation and the structural organization of the two polysaccharides could be related not only to the different charge of both varieties of GM but also to their molecular weight. Furthermore, similar structures were described by Schatz et al.[27] for the formation of CS complexes with high molecular weight dextran sulfate. In actuality, they reported the formation of particles consisting in a hydrophobic core, made of CS and dextran sulfate, and a large hydrophilic shell of uncomplexed dextran sulfate segments.

CS/TPP−GM Nanoparticles. A substantial difference of these particles as compared to those described above is the incorporation of an ionic cross-linking agent, TPP, for CS. The TEM photographs of the CS/TPP−phosphorylated GM and CS/TPP−KGM nanoparticles are shown in parts a and b of Figure 3, and their physicochemical properties are depicted in Tables 3 and 4, respectively. The results in Table 3 show that the incorporation of phosphorylated GM into the nanoparticles did not cause a significant modification in the particle size or in process yield. These results could be explained because the

Table 3. Physicochemical Properties of CS/TPP−Phosphorylated GM Nanoparticles Prepared with Different CS/TPP/Phosphorylated GM Theoretical Ratios (Mean ± SD, $n = 6$)

CS[a]/TPP/phosphorylated GM (w/w/w)	process yield (%)	size (nm)	ζ potential (mV)
6/1/0[b]	35 ± 4	297 ± 25	+38.9 ± 0.3
6/1/2.3	31 ± 8	250 ± 24	+32.2 ± 2.0
6/1/4.6	39 ± 7	302 ± 26	+15.2 ± 1.7

[a] CS was dissolved in water. [b] Control (CS/TPP nanoparticles, without GM).

Table 4. Physicochemical Properties of CS/TPP−KGM Nanoparticles Prepared with Different CS/TPP/KGM Ratios (Mean ± SD, $n = 6$)

CS[a]/TPP/KGM (w/w/w)	process yield (%)	size (nm)	ζ potential (mV)
6/1/1.2	24 ± 2	318 ± 5	+31.4 ± 0.4
6/1/1.8	21 ± 8	304 ± 9	+29.6 ± 0.6
6/1/2.3	24 ± 4	303 ± 8	+25.3 ± 2.4
6/1/3	49 ± 8	465 ± 11	+14.1 ± 1.2

[a] CS was dissolved in water.

low amount of phosphorylated GM incorporated into the nanoparticle. In contrast, phosphorylated GM content strongly affected the zeta potential, which went from +38.9 to +15.2 mV. This surface charge reduction, which was not seen in the particles without TPP (Table 1), could be due to the different mechanism of particles formation. In this case, TPP is involved in the particle formation by ionic cross-linking; consequently, phosphorylated GM molecules may be consumed not only in particle formation but also in the neutralization of the free positive amino groups remaining in the CS/TPP nanoparticles (see illustration in Figure 3a).

From the comparison of the results in Tables 1 and 3, we can conclude that similar sizes were obtained for CS/TPP−phosphorylated GM and CS−phosphorylated GM nanoparticles with the same 6/4.6 CS/phosphorylated GM theoretical ratio. In contrast, the presence of TPP caused an increase of the yield (22 ± 5% vs 39 ± 7%), which could be explained by the presence of both types of counterion, TPP and phosphorylated GM, involved in the formation of more particles.

CS/TPP−KGM nanoparticles were obtained with several amounts of non-phosphorylated KGM. The physicochemical characteristics of the formulations are depicted in Table 4. For low KGM contents (CS/TPP/KGM: 6/1/1.2, 6/1/1.8, and 6/1/2.3), the sizes were around 300 nm; however, a significant increase in size was observed for a CS/TPP/KGM theoretical ratio of 6/1/3. Moreover, when the amount of KGM increases up to above the ratio of 6/1/4.6, large microparticles, other than nanoparticles, were formed (data not shown). This increase in the size, originated by the addition of important amounts of KGM, could be related to the entrapment of a greater amount of KGM within the particles gelled by the action of TPP. This explanation agrees with the more important process yield and the significant reduction of the surface change as the KGM content increased.[13] An illustration of the obtained structure by TEM is provided in Figure 3b. From the comparison of the results summarized in Tables 2 and 4 (corresponding to nanoparticles obtained with non-phosphorylated KGM, in the absence or presence of TPP, respectively), it can be concluded that the presence of TPP contributes to the formation of more compacted systems, of reduced particle size. This could be attributed to the different mechanism involved in the nanoparticle formation. In fact, the presence of TPP might lead to a more organized structure in which TPP reacts with CS, and KGM is incorporated into the network (Figure 3b). Furthermore,

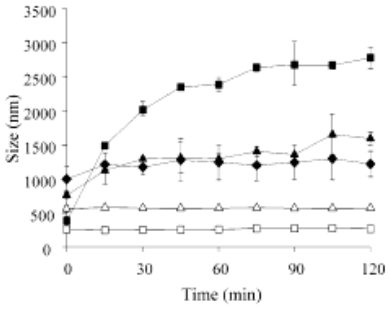

Figure 4. Evolution of the nanoparticles size following their incubation in PBS pH 7.4 up to 2 h at room temperature (mean ± SD, $n = 4$). Nanoparticles polymer composition: (▲) CS/phosphorylated GM (6/4.6); (◆) CS/phosphorylated GM (6/13.8); (■) CS/TPP/phosphorylated GM (6/1/4.6); (△) CS/KGM (6/6); (□) CS/TPP/KGM (6/1/1.8).

this organization of the polymers in the presence of TPP could also explain the positive charge of CS/TPP−KGM nanoparticles compared to CS−KGM ones (Table 2). Finally, the differences on the process yield obtained for both types of nanoparticles (CS/TPP−KGM and CS−KGM nanoparticles) could be related with the higher KGM content in CS−KGM formulations.

3.2. Stability Study of the Nanoparticles. An important goal when designing colloidal drug carriers, especially those prepared by mild ionic cross-linking processes, is to achieve an acceptable stability in high ionic strength media, similar to those present in the organism. In this regard, several authors have described that the combination of different polysaccharides, such as CS, GM, or alginate, could help to maintain the integrity of the resulting systems.[18,28,29] In the present work, we evaluated the stability behavior of the CS−GM and CS/TPP−GM systems, made with phosphorylated GM and non-phosphorylated KGM, in PBS pH 7.4. Under the experimental conditions of this study, we observed that the nonmodified CS/TPP nanoparticles suffered aggregation, followed by precipitation, immediately upon dilution with PBS. In contrast, the results presented in Figure 4 show that both non-phosphorylated KGM and phosphorylated GM have a positive effect in preserving the original size of the nanoparticles. However, it should also be noted from these results that, irrespective of the presence of TPP, the nanoparticles containing non-phosphorylated KGM were totally stable, whereas those containing phosphorylated GM suffered a certain increase in their size. The different stability of the nanoparticles containing phosphorylated GM and non-phosphorylated KGM could be justified by the different forces involved in the association of the two polymers with CS. As indicated above, the interaction of phosphorylated GM with CS is supposed to be driven by ionic forces, whereas that of KGM should be driven mainly by hydrophobic and hydrogen binding forces[17] which are less labile in high ionic force media.

On the other hand, in Figure 4 it can be seen that the incorporation of TPP in the CS−phosphorylated GM nanoparticles led to a further increase in their particle size upon incubation in PBS. Although no clear explanation can be given to this result, one could speculate about the possibility of a competition between TPP and phosphorylated GM for the CS amino groups, leading to the formation of poorly stable nanoparticles with a low GM content. Additionally, there is the possibility that the incorporation of TPP leads to the formation of a less compact and more swellable structure upon incubation in ionic media.

3.3. Association of Insulin and P1 Protein to the Nanoparticles. In a previous work, we have shown the feasibility of

Table 5. Process Yield and Association Efficiencies of Insulin-Loaded CS and CS−GM Nanoparticles (Mean ± SD, $n = 4$)

formulation	CS/TPP/GM (w/w)	process yield (%)	assoc efficiency (%)
CS/TPP	6/1/0	49 ± 2	83 ± 2
CS/phosphorylated GM	6/0/4.6	35 ± 6	37 ± 3
CS/TPP/phosphorylated GM	6/0.7/4.6	46 ± 2	75 ± 3
CS/KGM	6/0/6	48 ± 3	69 ± 6
CS/TPP/KGM	6/1/1.8	67 ± 8	88 ± 1

Table 6. Process Yield and Association Efficiencies of P1 Protein-Loaded CS and CS−GM Nanoparticles (Mean ± SD, $n = 4$)

formulation	CS/TPP/GM (w/w)	process yield (%)	assoc efficiency (%)
CS/TPP	6/1/0	24 ± 0.4	27 ± 3
CS/phosphorylated GM	6/0/4.6	39 ± 5	37 ± 4
CS/TPP/phosphorylated GM	6/1/4.6	60 ± 2	15 ± 6
CS/KGM	6/0/6	36 ± 4	11 ± 3
CS/TPP/KGM	6/1/1.8	30 ± 4	31 ± 3

CS−GM nanoparticles, obtained by GM coating of previously obtained CS/TPP nanoparticles, for the entrapment of P1 protein.[20] The results showed that the association efficiency was not dependent on the phase (CS or TPP) in which the protein was incorporated; however, it was very positively affected by the previous dissolution of the protein in phosphate buffer. Working with acidic proteins, i.e., insulin, BSA, tetanus toxoid, we have shown that their association to CS nanoparticles was improved by dissolving them into the alkaline TPP phase.[8,13,24] This was attributed to a facilitated ionic interaction between the protein (negatively ionized at high pH) and the positively charged CS molecules and also to the differences of solubility of the associated proteins at the different pHs. We decided to dissolve insulin and P1 protein in NaOH (0.01 M) and 10 mM phosphate buffer (pH 6.6), respectively, and to add them to TPP and/or GM solutions, which thereafter were mixed with the CS solution.

The results in Table 5 show that insulin was associated efficiently to all the developed formulations. In addition, it can be noted that the presence of TPP has a positive effect on the insulin association (37 and 69% vs 83, 75, and 88% for CS−phosphorylated GM, CS−KGM and CS/TPP, CS/TPP−KGM, CS/TPP−phosphorylated GM, respectively). This effect could be simply related to the increase of the pH in the medium where the protein was incorporated due to the presence of TPP. In fact, the pH of the TPP solution containing either phosphorylated GM or non-phosphorylated KGM was from 8.6 to 9.0, whereas that of the same solutions without TPP varied between 7.1 and 8.2. This dependence of the association efficiency of insulin to CS nanoparticles with the formulation pH was also reported by Ma et al.[30] In the more basic medium insulin is more negatively charged, and hence, its possibility to ionically interact with CS is improved.[31] Despite previous reports about the competition between polymers and proteins in their association to CS,[13,32] under the experimental conditions assayed, the association efficiency of insulin was not affected by the presence of KGM (comparison of formulations CS/TPP and CS/TPP−KGM). This may be due to the fact that there are enough free amine groups available in the CS molecules for the interaction with insulin. However, we found this competition for higher KGM content (data not shown).

According to the results depicted in Table 6, in general, P1 protein was less efficiently associated with the nanoparticles than insulin. Bearing in mind that one of the mechanisms of protein association to CS/TPP nanoparticles is mediated by protein−CS electrostatic interactions,[12] the different attachment of insulin and P1 could be explained on the basis of their different isoelectric point (IP) and ionization degree in the protein solutions. The IP of insulin is 5.3; however, P1 protein is a mixture of polypeptides with IP varying within 3 and 9. Thus, in the processing conditions of this study, insulin is negatively charged and, consequently, able to interact ionically with CS ($pK_a = 6.5$). In contrast, P1 protein is less negatively ionized, and hence, its ionic interaction with CS is reduced.

With regard to the association of P1 protein, as previously observed for insulin, there were no significant differences between the protein association to CS/TPP and CS/TPP−KGM nanoparticles (27 ± 3 and 31 ± 3, respectively). This indicates that non-phosphorylated KGM does not compete with the protein for CS in CS/TPP−KGM nanoparticles with theoretical ratio 6/1/1.8. However, as expected, the incorporation of higher amounts of non-phosphorylated KGM led to a decrease on the association efficiency (until a value of 10%, data not shown). This finding suggests that the competition between P1 protein and non-phosphorylated KGM occurs, only, for high KGM contents. This competition effect between protein P1 protein and GM was more pronounced in the case of phosphorylated GM. Indeed, the incorporation of higher amounts of phosphorylated GM to the nanoparticles resulted in a decrease in P1 protein association efficiency from 37% to 22%. This value was further reduced in the presence of TPP (37 vs 15%), indicating that a competition may occur as well between P1 and TPP. Consequently, overall these results suggest that the interaction of the fraction of P1, negatively charged, with CS may be interfered by TPP and GM.

In summary, as expected, insulin association is strongly influenced by the pH of the medium, being more important when the pH increases. In contrast, the association of P1 protein is not significantly affected by the pH, but by the presence of phosphorylated GM and TPP.

3.4. In Vitro Release of Insulin and P1 Protein from the Nanoparticles. Previous studies have shown that insulin is very rapidly released from the CS nanoparticles upon incubation at pH 7.4 PBS. These results suggested that the mechanism of release was a simple dissociation of the protein from the particles. More specifically, it was assumed that the presence of high ion concentrations in the media interfered with the electrostatic interactions that retained the protein within the nanoparticles, causing its fast release. In this study we aimed to investigate whether the presence of GM could affect this dissociation process. The formulations selected to perform these studies were CS−phosphorylated GM and CS−KGM nanoparticles with theoretical ratios of 6/4.6 and 6/6, respectively, and CS/TPP−phosphorylated GM and CS/TPP−KGM nanoparticles with theoretical ratios of 6/1/4.6 and 6/1/1.8, respectively. CS/TPP (6/1) nanoparticles were used as controls. The profiles plotted in Figure 5 reveal that insulin release was slower from the formulations containing non-phosphorylated KGM as compared to those without GM or containing phosphorylated GM. These results correlate well with those from the stability study and also suggest that the nanoparticles without GM or containing phosphorylated GM are more susceptible to the swelling or disassociation of the individual components. Moreover, the higher M_w and the lower solubility of KGM as compared to phosphorylated GM could make more difficult the diffusion of the peptide through the polymer networks into the release medium.[18,33] On the other hand, it can be noted that the presence of TPP in the CS−phosphorylated GM formulations reduces the release rate. This could be understood by the restricted

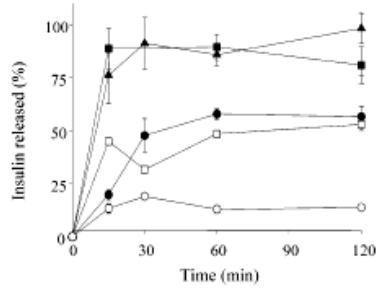

Figure 5. Release profiles of insulin from the nanoparticles in PBS pH 7.4 at 37 °C (CS/insulin: 2.4−2/1; mean ± SD, n = 4). Nanoparticles polymer composition: (▲) CS/TPP (6/1); (●) CS/TPP/phosphorylated GM (6/1/4.6); (■) CS/phosphorylated GM (6/4.6); (□) CS/KGM (6/6); (○) CS/TPP/KGM (6/1/1.8).

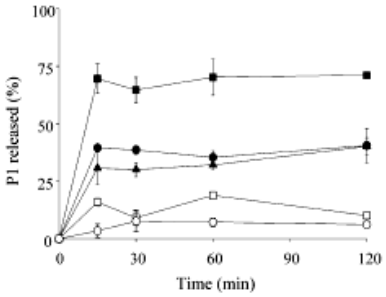

Figure 6. Release profiles of P1 protein from the nanoparticles in PBS pH 7.4 at 37 °C (CS/P1: 2.2−1.6/1; mean ± SD, n = 4). Nanoparticles polymer composition: (▲) CS/TPP (6/1), (●) CS/TPP/phosphorylated GM (6/1/4.6), (■) CS/phosphorylated GM (6/4.6), (□) CS/KGM (6/6) and (○) CS/TPP/KGM (6/1/1.8).

diffusion of the peptide through a highly CS cross-linked network, when it is ionically cross-linked with TPP, and reinforced by the presence of phosphorylated GM. Similar findings were found by Xu et al. for BSA loaded modified CS nanoparticles: the inclusion of PEG or sodium alginate gave slower release profiles.[26]

As in the case of insulin, the release of P1 protein was more rapid from the nanoparticles containing phosphorylated GM than from those made of non-phosphorylated GM (Figure 6). However, in this case, the release of P1 from CS nanoparticles occurred more slowly than insulin. This could be related to the molecular weight of P1 and the different interaction forces polymer−protein, which have been reported to affect the diffusion of proteins through the gelified nanostructure.[12] For this protein, the fastest release was observed for the formulation CS−phosporylated GM, which did not contain TPP. This result could be explained by the improved diffusion of P1 protein through a less cross-linked structure.

Overall, the in vitro protein release results suggest that there are possibilities of modulating the release rate of insulin and P1 protein by selecting the GM type and the GM and TPP content.

4. Conclusions

The preparation of various nanoparticulate systems composed of the hydrophilic polymers CS and GM is reported. These nanoparticles are formed under very mild conditions, and they have an excellent capacity for the association of the model proteins insulin and P1 protein. The protein release can be modulated by adequately selecting the type and content of GM. Furthermore, the nanoparticles are stable in pH 7.4 phosphate buffer. These interesting features make these nanoparticles very promising vehicles for oral administration of peptides and proteins and, more specifically, for their targeting to the M cells of Payer's patches.

Acknowledgment. This work was financed by the Spanish Government (FEDER 1FD97-2363, MCYT-AK22) and Industrial Farmacéutica Cantabria S.A. The first author acknolowledges the grant from the Spanish Government (FPU-MEC).

References and Notes

(1) Fix, J. A. *Pharm. Res.* **1996**, *13*, 1760−1764.
(2) Lipka, E.; Crison, J.; Amidon, G. L. *J. Controlled Release* **1996**, *39*, 121−129.
(3) Blanco, D.; Alonso, M. J. *Eur. J. Pharm. Biopharm.* **1998**, *45*, 285−294.
(4) Hirano, S.; Seino, H.; Akiyama, Y.; Nonaka, I. In *Progress in Biomedical Polymers*; Gebelein, C. G., Dunn, R. L., Eds.; Plenum Press: New York, 1990; p 283.
(5) Domish, M.; Hagen, A.; Hansson, E.; Pecheur, C.; Verdier, F.; Skaugrud, Ø. In *Advances in Chitin Science*; Domard, A., Roberts, G. A. F., Vårum, K. M., Eds.; Jacques Andre Publishers: Lyon, 1997; p 664.
(6) Lehr, C. M.; Bouwstra, J. A.; Schacht, E. H.; Junginger, H. E. *Int. J. Pharm.* **1992**, *78*, 43−48.
(7) Borchard, G.; Luessen, H. L.; De Boer, G. A.; Coos Verhoef, J.; Lehr, C. M.; Junginger, H. E. *J. Controlled Release* **1996**, *39*, 131−138.
(8) Fernández-Urrusuno, R.; Calvo, P.; Remuñán-López, C.; Vila-Jato, J. L.; Alonso, M. J. *Pharm. Res.* **1999**, *16*, 1576−1581.
(9) De Campos, A.; Sanchez, A.; Alonso, M. J. *Int. J. Pharm.* **2001**, *224*, 159−168.
(10) Portero, A.; Remuñan-López, C.; Mørck Nielsen, H. *Pharm. Res.* **2002**, *19*, 169−174.
(11) Janes, K. A.; Calvo, P.; Alonso, M. J. *Adv. Drug Delivery Rev.* **2001**, *47*, 83−97.
(12) Calvo, P.; Remuñán-López, C.; Vila-Jato, J. L.; Alonso, M. J. *J. Appl. Polym. Sci.* **1997**, *63*, 125−132.
(13) Calvo, P.; Remuñán-López, C.; Vila-Jato, J. L.; Alonso, M. J. *Pharm. Res.* **1997**, *14*, 1431−1436.
(14) Vila, A.; Sanchez, A.; Janes, K.; Behrens, I.; Kissel, T.; Vila Jato, J. L.; Alonso, M. J. *Eur. J. Pharmacol. Biopharm.* **2004**, *57*, 123−131.
(15) Tomizawa, H.; Aramaki, Y.; Fujii, Y.; Kara, T.; Suzuki, N.; Yachi, K.; Kikuchi, H.; Tsuchiya, S. *Pharm. Res.* **1993**, *10*, 549−552.
(16) Cui, Z.; Hsu, Ch.; Mumper R. J. *Drug Dev. Ind. Pharm.* **2003**, *29*, 689−700.
(17) Xiao, Ch.; Gao, S.; Wang, H.; Zhang, L. *J. Appl. Polym. Sci.* **2000**, *76*, 509−515.
(18) Wang, K.; He, Z. *Int. J. Pharm.* **2002**, *244*, 117−126.
(19) Paulesu, L.; Pessina, G. P.; Nocoletti, C.; Boccanera; M.; Cassone, A. *Immunol. Lett.* **1991**, *27*, 231−235.
(20) Cuña, M.; Alonso-Sande, M.; Remuñán-López, C.; Pivel, J. L.; Alonso-Lebrero, J. L.; Alonso, M. J. *J. Nanosci. Nanotechnol.*, in press.
(21) Schazt, C.; Pichot, C.; Delair, T.; Viton; C.; Domard, A. *Langmuir* **2003**, *19*, 9896−9903.
(22) Tsaih, M.; Chen, R. H. *J. Appl. Polym. Sci.* **1999**, *73*, 2041−2050.
(23) Signini, R.; Desbrières, J.; Campana Filho, S. P. *Carbohydr. Polym.* **2000**, *43*, 351−357.
(24) Janes, K.; Alonso, M. J. *J. Appl. Polym. Sci.* **2003**, *88*, 2769−2776.
(25) Du, J.; Sun, R.; Zhang, S.; Govender, T.; Zhang, L. F.; Xiong, Ch. D.; Peng, Y. X. *Macromol. Rapid Commun.* **2004**, *25*, 954−958.
(26) Xu, Y.; Du, Y.; Huang, R.; Gao, L. *Biomaterials* **2003**, *24*, 5015−5022.
(27) Schatz, C.; Domard, A.; Viton, C.; Pichot, C.; Delair, T. *Biomacromolecules* **2004**, *5*, 1882−1892.
(28) Thu, B.; Bruheim, P.; Espevik, T.; Smidsroed, O.; Soon-Shiong, P.; Skjak-Braek, G. *Biomaterials* **1996**, *17*, 1031−1040.
(29) Vila, A.; Sánchez, A.; Tobío, M.; Calvo, P.; Alonso, M. J. *J. Controlled Release* **2002**, *78*, 15−24.
(30) Ma, Z.; Yeoh, H. H.; Lim, L. Y. *J. Pharm. Sci.* **2002**, *91*, 1396−1404.
(31) Yoshida, H.; Nishihara, H.; Kataoka, T. *Biotechnol. Bioeng.* **1994**, *43*, 1087−1093.
(32) Xu, Y.; Du Y. *Int. J. Pharm.* **2003**, *250*, 215−226.
(33) Nakano, M.; Takikawa, K.; Arita, T. *J. Biomed. Mater. Res.* **1979**, *13*, 811−819.

MA060230J

Anexo IV

Development of Chitosan Sponges for Buccal Administration of Insulin

A. Portero, D. Teijeiro-Osorio, C. Remuñán-López, M. J. Alonso

Available online at www.sciencedirect.com
ScienceDirect
Carbohydrate Polymers 68 (2007) 617–625
Carbohydrate Polymers
www.elsevier.com/locate/carbpol

Development of chitosan sponges for buccal administration of insulin

Ana Portero, Desirée Teijeiro-Osorio, María J. Alonso, Carmen Remuñán-López *

Department of Pharmacy and Pharmaceutical Technology, Faculty of Pharmacy, University of Santiago de Compostela, Campus Sur, 15782-Santiago de Compostela, Spain

Received 4 May 2006; received in revised form 20 July 2006; accepted 27 July 2006
Available online 20 September 2006

Abstract

This paper describes the development of a new highly porous, flexible device for buccal peptide administration by a very simple and mild casting/freeze-drying procedure. It consists of a mucoadhesive chitosan layer containing the peptide drug and an impermeable protective layer made of ethylcellulose. This structure was expected to provide unidirectional drug release to the mucosa and avoid loss of drug due to washout with saliva. Insulin release was modulated by varying some formulation variables (chitosan salt type and M_w, chitosan solution pH, insulin dose). The main factor affecting insulin release was its diffusion across the matrix, this being related to the water uptake/swelling and dissolution properties of chitosan and the viscosity of the gel formed upon hydration. In addition, an electrostatic interaction could occur between chitosan amino groups and the insulin carboxylic groups. Preliminary mucoadhesion studies showed that the affinity of chitosan sponges to mucin surfaces was related to the swelling and solubility properties of the different salts of chitosan.

Keywords: Bilayered drug delivery device; Buccal peptide administration; Chitosan; Insulin; Mucoadhesive sponge

1. Introduction

The successful exploitation of the new generation of peptides and proteins as therapeutic agents clearly depends on the availability of non-invasive transmucosal (nasal, pulmonary, buccal, peroral) drug delivery systems. These systems must be able to protect the associated macromolecule against enzymatic degradation and promote its passage across the epithelial barriers. The buccal route is a subject of growing interest for systemic delivery of high molecular weight (M_w) drugs because of its numerous advantages, including the bypass of the hepatic first-pass metabolism and gastrointestinal degradation, typically observed following oral administration. Additionally, it has rich blood supply, good accessibility for self-medication, patient compliance and safeness, since the drug device can be removed whenever desired (Hoogstraate & Wertz, 1998; Merkle, Anders, Wermerskirchen, Raehs, & Wolany, 1991). In contrast, the main limitation of the buccal route is the necessity of using penetration enhancers due to the low permeability of the buccal mucosa to high M_w drugs. In practice, drug absorption enhancement is generally accompanied by mucosal damage. Nevertheless, this local irritation is followed by the rapid cellular recovery inherent to the buccal epithelium (Merkle & Wolany, 1992).

An ideal buccal systemic drug delivery system requires intimate contact with the buccal mucosa in order to maintain its position in the mouth for a desired period of time; this can obviously be achieved by using mucoadhesive polymers. Furthermore, the device itself or its components should promote the permeation of the macromolecule across the mucosa, and protect it from environmental degradation (Veuillez, Kalia, Jacques, Deshusses, & Buri, 2001).

Among the mucoadhesive polymers, which are being explored as absorption enhancers across the mucosal

* Corresponding author. Tel.: +34 981 563100x15045; fax: +34 981 547148.
E-mail address: ffcarelo@usc.es (C. Remuñán-López).

0144-8617/$ - see front matter © 2006 Elsevier Ltd. All rights reserved.
doi:10.1016/j.carbpol.2006.07.028

surfaces, chitosan (CS) is gaining increasing importance due to its good biocompatibility, biodegradability and its favorable toxicological properties (Hirano, Seino, Akiyama, & Nonaka, 1990). CS is degraded by lyzozyme enzyme, that is highly present in the human body tissues and secretions (Muzzarelli, 1997; Varum, Myhr, Hjerde, & Smidsrod, 1997) and its degradation is dependent on the polymer degree of deacetylation (the higher the deacetylation degree, the lower is the degradation) and on the *N*-acetylglucosamine groups distribution along the CS chains (Tomihata & Ikada, 1997). Furthermore, it has also been demonstrated in mice that CS and its degradation products are quickly eliminated by the kidney following intraperitoneal administration to mice, thus overcoming accumulation in the body (Onishi & Machida, 1999). The evidence of the ability of CS to enhance the penetration of macromolecules across several mucosal barriers has been shown not only for CS solutions (Artursson, Lindmark, Davis, & Illum, 1994) but also for CS nanoparticles (Fernández- Urrusuno, Calvo, Remuñán-López, Vila-Jato, & Alonso, 1999). Furthermore, the permeability enhancing effect of CS was recently shown in an *in vitro* model of the human buccal epithelium (Portero, Remuñán-López, & Nielsen, 2002) and in porcine buccal mucosa (Senel et al., 2000). From a technological point of view, it is important to note that CS has excellent film-forming properties as well as a potential for controlling the release of drugs (Remuñán-López & Bodmeier, 1996a, 1996b). For all these reasons, CS has been widely proposed for increasing adhesion of drug delivery systems to oral mucosa and enhancing drug penetration across it (Senel et al., 2002). In spite of this, only a few studies have so far been performed on its usefulness as a vehicle for buccal peptide/protein administration (Langoth, Kalbe, & Bernkop-Schnürch, 2005, 2006; Portero et al., 2002; Senel et al., 2000).

We have previously reported the preparation of mucoadhesive bilayered tablets that are adequate for buccal administration of low M_w drugs (Remuñán-López, Portero, Vila-Jato, & Alonso, 1998b). However, further experiments aimed at investigating its potential application for high M_w drugs, confirmed a limited diffusivity of the macromolecules through these compact matrixes, thus presenting inadequate release patterns (Remuñán-López, Lorenzo-Lamosa, Vila-Jato, & Alonso, 1998a).

The use of CS-based porous matrixes has been reported for different applications, such as for periodontal bone regeneration (Park et al., 2000), matrices for culturing pancreatic islets (Cui, Kim, Imamura, Ion, & Inoue, 2001) or wound dressing structures, in which antibiotics and analgesics could be included (Foda, El-laithy, & Tadros, 2004; Mi, Shyu, Wu, Shyong, & Huang, 2001). However, there are no reports concerning the use of the CS sponges as peptide/protein carriers.

In this article, we describe the development of a porous mucoadhesive bilayered device based on CS intended for buccal systemic delivery of high M_w drugs. Insulin was chosen as a model of peptide drug.

2. Materials and methods

2.1. Materials

The following chemicals were obtained from commercial suppliers and used as received: chitosan (CS) (medium M_w, 150 kDa; deacetylation degree = 87%) and CS glutamate (medium M_w, 150 kDa and high M_w, 350 kDa; deacetylation degree >80%) (*Pronova Lab., Norway*); bovine insulin, dibutylphthalate (*Sigma Chemical Co., Spain*); ethylcellulose (Ethocel 10, standard premium) (*Dow Chemical, USA*); tartaric acid (*Probus, Spain*); citric acid (*Vorquímica, Spain*); hydrochloric acid (*Carlo Elba, France*) and Micro BCA (*Pierce, Rockford Illinois, USA*). Ultrapure water (MilliQ Plus, *Millipore Ibérica, Spain*) was used throughout. All other reagents were of analytical grade and used without further purification.

2.2. Preparation of the mucoadhesive buccal bilayered devices

Bilayered sponges (diameter = 12 mm, thickness = 6 mm) were prepared by a very simple casting/freeze-drying technique. Briefly, 1 g of a 2% w/w polymer solution in water (CS glutamate) or in tartaric or citric acid 3% w/v (CS base), with pH varying from 2 to 6 (pH was adjusted by adding HCl or NaOH) was mixed with insulin (5%, 8.75% and 12.5% w/w based on CS) which had previously been dissolved in a minimal amount of HCl 0.01 M (200 μl HCl/mg insulin). The resulting mixture was poured into a cylindrical mold of adequate size, frozen at −20 °C and freeze-dried (*Labconco freeze-drier, Labconco Co., USA*) to eliminate the solvent, obtaining the CS/insulin mucoadhesive layer. Then, an ethylcellulose solution in acetone containing the plasticizer dibutylphthalate (30% w/w based on polymer) was cast onto it and the solvent evaporated at room temperature obtaining the backing film on the sponge. Sponges were stored in a dessicator at 2–8 °C until used. The preparation method of the devices is illustrated in Fig. 1.

2.3. Viscosity measurements

CS glutamate was dissolved in Milli-Q water with pH varying from 2 to 6, and CS base in tartaric or citric acid 3% w/v by mechanical agitation, and centrifuged (*Sigma 2-15, Sigma, Spain*) at 6000*g* for 15 min in order to remove insoluble impurities. The total polymer concentration was fixed at 2% w/w in all samples and their viscosities were determined at 25 °C using a Cannon-Fenske viscosimeter (*Afora, Spain*). All samples were analyzed nine times.

2.4. Turbidity measurements

CS glutamate solutions (5 g, 1% w/w) at pH 2, 4 and 6 were mixed with 2.5 mg of insulin previously dissolved in

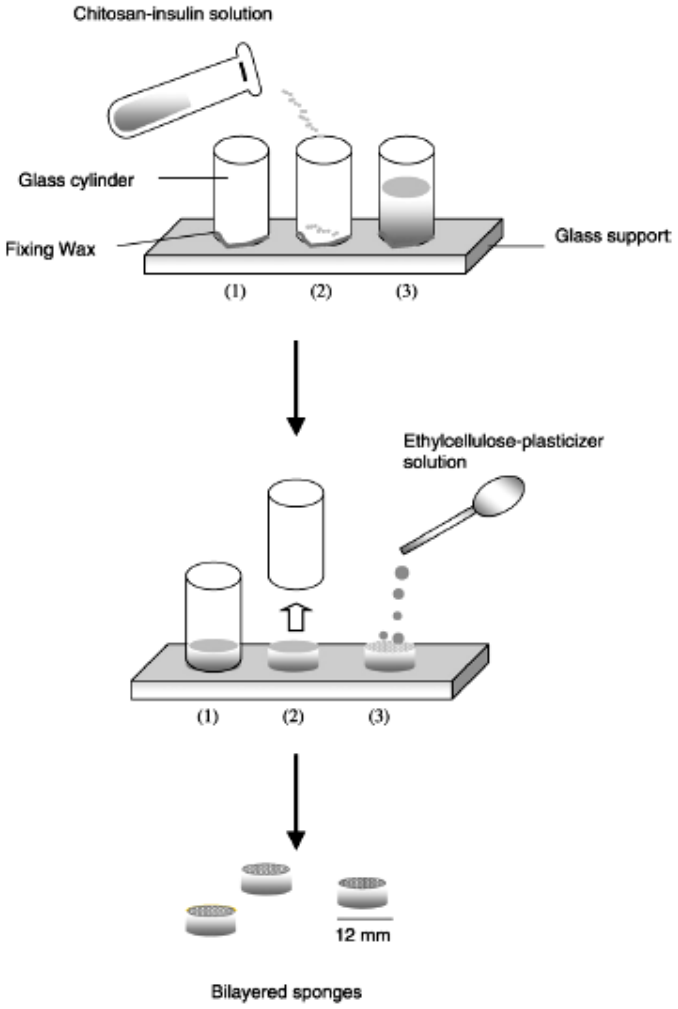

Fig. 1. Preparation method of bilayered chitosan/ethylcellulose sponges.

250 μl of HCl 0.01 M. The mixtures were shaken vigorously and left for 15 min before measuring their turbidities (absorbance at 420 nm) (*Shimadzu RF 5001 PC, Tokyo, Japan*). The turbidities of CS solutions without insulin and insulin solutions without the polymer at the same pH values were also recorded as controls. Afterwards, the samples were centrifuged at 30,000*g* for 40 min. (*Beckman Avanti™30 centrifuge, Beckman, Spain*), the insoluble precipitates were separated and the turbidities and pH of the supernatants were determined. The pellet was resuspended in Milli-Q water and then recentrifuged. The washed precipitates were finally freeze-dried and weighted (*HM-202, AND instruments, Oxford, UK*). Analysis of six replicates was conducted.

2.5. Scanning electron microscopy (SEM)

The surface morphology and cross-sections of the devices were examined by SEM (*JSM-640, Tokyo, Japan*). They were coated under an argon atmosphere with gold–palladium (*Sputter coater, Balzers SCD 004, Liechtenstein*) to achieve a film of 20 nm thickness and then observed with a scanning electron microscope (*SEM., JSM-6400, Tokyo, Japan*).

2.6. Determination of insulin content

Insulin content was determined following incubation of the devices in tubes containing 0.5 M HCl for 6 h under

magnetic stirring at room temperature. The supernatants were filtered (*Durapore Millex®-HV, low protein binding, Millipore, Spain*) and the extracted insulin was spectrophotometrically assayed at 277 nm (*Shimadzu RF 5001 PC, Tokyo, Japan*). Blank sponges were also incubated and the supernatants filtered and used as blanks in order to avoid CS interference at this wavelength. All samples were analyzed in triplicate.

2.7. In vitro release studies

The *in vitro* drug release studies were performed at 23 °C using *Franz-Chien* type vertical diffusion cells (*Vidrafoc, Spain*) whose receptor sides were filled with 5.6 ml of phosphate buffer pH 7.4 and maintained under magnetic stirring ($n = 4$–6). Low protein adsorption membranes (*Durapore® Membrane filters 0,45 μm HV, Millipore, Spain*) were placed between the two cells as supports of the delivery devices, and these were situated on top of them on the donor sides. The release studies of insulin were purposely conducted at 23 °C rather than at 37 °C to minimize the insulin self-aggregation tendency (Sluzky, Klibanov, & Langer, 1992). Samples were withdrawn at predetermined time intervals and replaced with fresh medium. The samples were filtered and insulin released assayed by Micro-BCA protein assay at 562 nm. The pH of the release medium as well as the pH inside the polymer matrix after the release process were recorded (*Crison, microph 2001, Spain*).

2.8. Swelling studies

The water uptake capacity of sponges was determined gravimetrically. Previously weighed CS sponges were incubated in phosphate buffer pH 7.4 at 23 °C, as described before in the in vitro release studies section. After 6 h, the devices were withdrawn, blotted with paper to eliminate excess water and immediately weighed at room temperature on an electronic balance (*HM-202, AND instruments, Oxford, UK*). Then, the sponges were freeze-dried and the weight of the dry devices recorded.

The water uptake was calculated from the relative weight gain according to the following equation:

$$\text{Weight change(mg/mg device)} = (W_6 - W_0)/W_0$$

where W_0 is the initial weight of each sponge and W_6 is the weight of the swollen device after 6 h. Analysis of 3 replicates was conducted.

The percentage of remaining weight of each sponge after 6 h, which is an indication of its solubility, was calculated from:

$$\text{Remaining weight}(\%) = (W_{6F} \times 100)/W_0$$

where W_{6F} is the weight of the sponge after 6 h incubation in the release medium and further freeze-drying and W_0 is the initial weight of each sponge. Analysis of 3 replicates was conducted.

2.9. Preliminary mucoadhesion studies

Mucoadhesive capacity of the sponges was evaluated by applying them to mucin films which were previously obtained by casting aqueous mucin dispersions on Petri dishes and further solvent evaporation at 40 °C. The system was maintained in desiccators at 100% relative humidity at room temperature (20–25 °C) for different time periods. Afterwards, sponges were manually removed from the mucin films and the detachment forces were qualitatively estimated.

2.10. Statistical evaluation

All data are expressed as the mean ± standard deviation (SD). Statistical differences were investigated by a one-way analysis of variance (ANOVA) with the Pairwise Multiple Comparisson Procedures (Student-Newman-Keuls method) for multiple comparisons (SigmaStat program; Jandel Scientific, Version 3.0). Differences were considered to be significant at a level of $P < 0.05$.

3. Results and discussion

The main goal of this work was to develop a mucoadhesive device adequate for buccal peptide administration, insulin being used as model peptide. We designed a bilayered system that consists of a mucoadhesive CS layer containing the peptide drug and an impermeable protective layer made of ethylcellulose and the plasticizer dibutylphthalate (Fig. 2).

The hypothesis behind the design of this system is that it will increase peptide permeation by releasing it at the absorption site for a prolonged period of time owing to the mucoadhesive properties of CS. Indeed, we have recently found that CS glutamate is able to increase the permeability of large hydrophilic compounds across an *in vitro* model of the buccal mucosa (the TR146 cell culture model) at minimally harmful CS concentrations (Portero et al., 2002). Additionally, the bilayered structure is expected to provide unidirectional peptide delivery to the absorptive mucosa and avoid loss of drug with saliva. With this

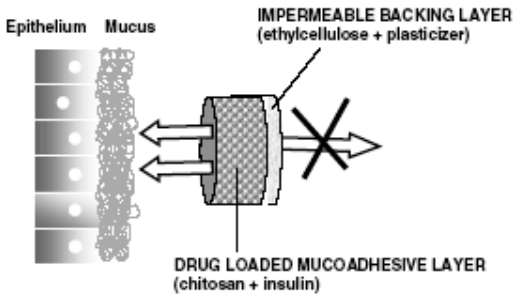

Fig. 2. Structure of the chitosan/ethylcellulose bilayered devices.

idea in mind, we first evaluated the utility of the previously developed bilayered tablets (Remuñán-López et al., 1998b) for insulin formulation and further release. We have already reported that these bilayered tablets have mucoadhesive properties and deliver adequately low M_w drugs in a unidirectional way. However, insulin *in vitro* release from the devices was found to be extremely slow, only 5% of the peptide being delivered after 10 h of study. This poor release behavior was attributed to the limited diffusivity of the high M_w molecules through compact matrixes (Merkle et al., 1991; Remuñán-López et al., 1998a). Therefore, we designed a very porous system, that we have called sponge, and compared the *in vitro* properties of both systems. The sponges were obtained by a very simple and mild casting/freeze-drying technique, in which no heat or vigorous agitation is involved. Flexible and easily manageable CS sponges could be formed without plasticizers. This is very advantageous bearing in mind that the addition of plasticizers would increase the hygroscopicity of the system thereby compromising the stability of the peptide. A critical point while developing new peptide formulations is to assess the stability of the peptide following its incorporation into the device. With this purpose in mind, we extracted the insulin from the sponges with HCl and found that it was possible to recover the total amount (90–100%) of insulin incorporated into the system.

Preliminary studies indicated that insulin release from sponges was significantly faster than from tablets. The noticeable differences found in their release behaviors could be explained by the markedly different internal structure of both devices. SEM pictures revealed that the sponge has a very porous structure (Fig. 3a), which strongly contrasts with the compact non-porous surface of the tablet. When placed in the aqueous medium, the sponge rapidly absorbs water, facilitating insulin diffusion and release. In contrast, the tablet erodes gradually, leading to a slow peptide delivery. Taking into account that the buccal epithelium behaves like a barrier to drug permeation, the porous system was selected as a more appropriate drug delivery system for macromolecules and was further investigated. Furthermore, it is important to mention that the CS (hydrophilic) was easily covered by EC (hydrophobic), and that a perfect binding between the mucoadhesive and the backing layer was achieved as is clearly demonstrated by SEM of sponges cross-sections (Fig. 3b).

In an attempt to control insulin release from the sponges, we investigated a number of variables in the formulation process. The results show that the *in vitro* release properties of the sponges can be easily controlled by simply modifying the formulation variables, such as the pH of the polymer solution prior to freeze-drying (pH 2, 4, 6), the M_w (medium M_w, 150 kDa, and high M_w, 300 kDa), the type of CS salt (glutamate, tartrate and citrate) and the insulin content (1, 1.75, 2.5 mg). The profiles depicted in Fig. 4 indicate that insulin release from the sponges obtained using the pH 2 CS solution was significantly faster

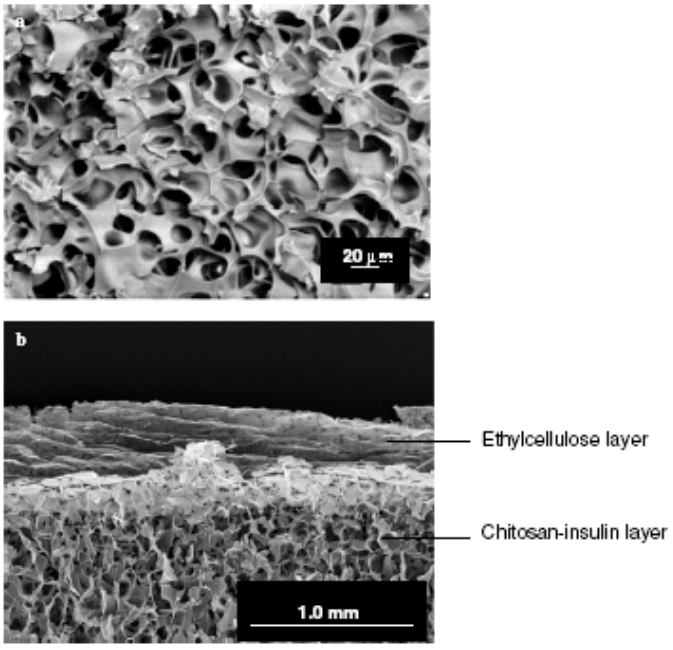

Fig. 3. Scanning electron micrographs of (a) the chitosan surface of a sponge and (b) a cross-section of a bilayered chitosan/ethylcellulose device.

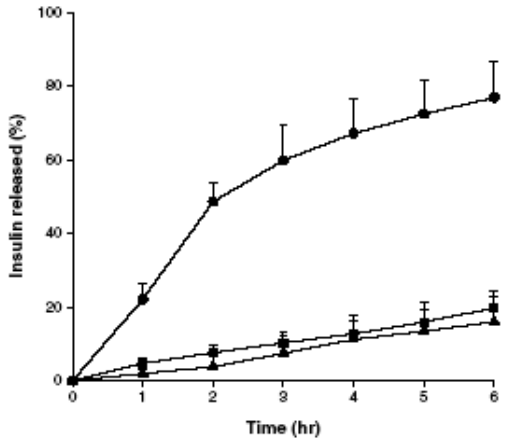

Fig. 4. Effect of the pH of the chitosan-insulin mixture prior to the freeze-drying process on insulin release from the sponges in pH 7.4 phosphate buffer (medium M_w chitosan glutamate; 1 mg insulin): (●) pH 2, (■) pH 4 and (▲) pH 6 (mean ± SD; $n \geq 4$).

($P < 0.05$) than from those made using pH 4 and pH 6 solutions. It is important to note that there were no important differences either in the pH of the release medium or in the local internal pH of the CS glutamate sponges made from CS solutions at the different pH values (Table 1). This unexpected behavior could be related to the high volatility of the acid (HCl) used to adjust the pH values of the different CS glutamate solutions, which could have been eliminated during the freeze-drying process. Consequently, the differences in drug release could not be explained by the variations in CS and insulin solubility as a function of the pH inside or outside the sponges.

On the other hand, the viscosity data corresponding to CS glutamate solutions at the different pH values, also depicted in Table 1, show (for the same M_w sponges) a significant ($P < 0.05$) increase of the CS viscosity as the pH was increased from 2 to 6. This increase was less pronounced for pH 6 compared to pH 4 due to the precipitation process suffered by CS at the higher pH. In all cases, this increase in the CS viscosity, related to the pH value, could explain the slower insulin release found for sponges obtained from pH 4 and 6 solutions.

However, it is our hypothesis that the effect of the CS solution pH prior to freeze-drying on drug release could be mainly related to the establishment of electrostatic interactions between peptide and polymer. It is interesting to note that, in the preformulation experiments, we observed that, when insulin was added to the CS solutions at pH 4 and 6, the mixture became cloudy, whereas this phenomenon was not apparent for CS solutions at pH 2. Furthermore, the higher the pH value, the more intense was the turbidity of the CS-insulin mixture. These observations suggest that an electrostatic interaction could occur between insulin and CS upon mixing. In fact, CS is positively charged across the pH range used in this work, whereas the charge on the insulin molecules is pH dependent; insulin has a net positive charge at a pH below its isoelectric point – which is approximately 5.3 – and it has a net negative charge at any pH above it. Therefore, at pH 2 where insulin has a predominantly positive charge, ionic interactions should not be expected. Oppositely, at pH 6, the carboxylic groups of insulin will be ionized (negatively charged) and consequently its ionic interaction with the positively charged amine groups of CS will be favored.

This information was confirmed by measuring the turbidity (absorbance at 420 nm) of CS solutions, insulin solutions and CS-insulin solutions mixtures at those pH values (2, 4 and 6). Results in Fig. 5 show that the turbidity of CS-insulin mixtures gradually increases when raising the pH values of the solution from 2 to 6. In addition, turbidity measurements gave us information about the solubility of both CS and insulin. The absorbance at 420 nm for CS solutions at pH 2 and 4 was similar, but a decrease in turbidity at pH 6 was observed. This behavior can be explained by the fact that, at pH 6, the CS solution begins to precipitate, which leads to a decrease in turbidity. On the contrary, at pH 6, the insulin solution becomes milky, but sedimentation was not appreciable and, consequently, a higher absorbance at 420 nm was found, probably as a result of the increase in pH that could bring insulin to its isoelectric precipitation zone (pH: 4.5–6.5) (Brange & Langkær, 1993). It must be pointed out that the influence

Table 1
Effect of the chitosan type of salt, molecular weight and pH of the polymer solution before freeze-drying on the weight of sponges, viscosity of polymer solutions, and pH inside and outside sponges, swelling capacity and sponge weight remaining after the drug release study (mean ± SD)

Chitosan salt	pH	M_w (kDa)	Sponge weight (mg)[a]	Viscosity (cSt)[b]	pH of release medium[a]	pH of swollen sponge[a]	Swelling (mg water/mg dry device)[a]	Sponge weight remaining (%)[a]
Glutamate	2	350	23.5 (1.16)	260.41 (15.31)	ND	ND	ND	ND
	2	150	23.80 (2.30)	12.22 (0.05)	7.24 (0.04)	6.45 (0.01)	13.26 (0.26)	20.7 (2.27)
	4	150	24.87 (1.56)	20.33 (0.20)	7.29 (0.02)	6.66 (0.01)	14.66 (3.25)	44.50 (8.05)
	6	150	23.52 (0.53)	15.23 (3.39)	7.37 (0.00)	6.40 (0.02)	6.40 (0.49)	62.57 (6.53)
Citrate	2	150	67.92 (3.42)	238.99 (7.53)	7.22 (0.02)	3.08 (0.05)	11.27 (3.61)	35.15 (11.10)
Tartrate	2	150	65.78 (4.21)	205.62 (3.47)	7.18 (0.03)	2.97 (0.08)	10.91 (4.09)	21.10 (5.51)

ND: not determined.
[a] $n = 3$–6.
[b] $n = 9$.

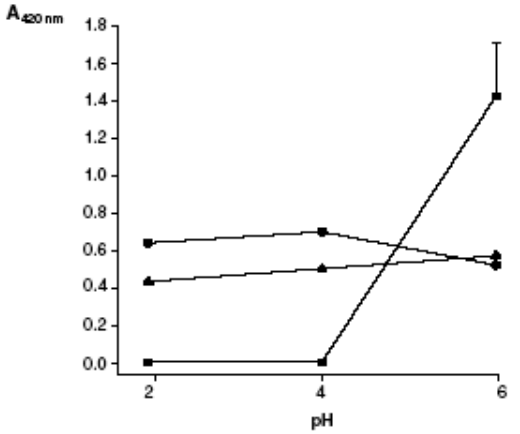

Fig. 5. Effect of the pH of the (●) chitosan solutions, (■) insulin solutions and (▲) chitosan-insulin mixtures on their absorbance values at 420 nm (mean ± SD; $n \geqslant 4$).

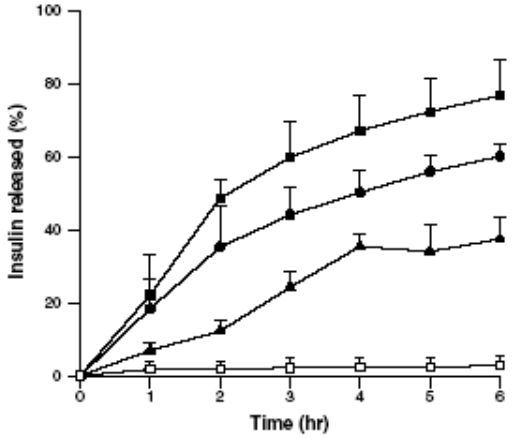

Fig. 6. Effect of the chitosan type of salt and M_w on insulin release from the chitosan sponges in pH 7.4 phosphate buffer (pH 2; 1 mg insulin): (■) medium M_w chitosan glutamate, (●) medium M_w chitosan tartrate, (▲) medium M_w chitosan citrate and (□) high M_w chitosan glutamate (mean ± SD; $n \geqslant 4$).

of pH on turbidity of the CS-insulin mixtures was less pronounced than for each species, individually. This could indicate a stabilizing effect of the polymer, as a result of a probable interaction, against the precipitation/aggregation tendencies of the insulin observed at the higher pH in the absence of CS.

Indeed, there was a clear effect of the initial pH of the CS solution on the percentage of the remaining weight (insoluble fraction of the sponge) of the different devices following incubation in the release medium, which was found to be significantly ($P < 0.05$) higher when the initial pH value was increased (Table 1). In fact, it was observed that after 6 h of incubation in the aqueous release medium, the percentage of remaining weight (insoluble fraction of the sponge) of sponges prepared at pH 2 was around 21% compared to the 45% and 63% observed for the sponges made from pH 4 and 6, respectively. Additionally, the initial pH of the CS-insulin mixtures affected the swelling capacity of the sponges. In this respect, the most noticeable reduction on the swelling properties of CS was found for CS glutamate sponges made at pH 6. It has been previously reported that the type of CS salt has an influence on the solubility and swelling/gelling properties of CS (Chen, Lin, & Yang, 1994; Kienzle-Sterzer, Rodríguez-Sánchez, & Rha, 1982). In fact, we found not only that the swelling properties of the sponges made from the different salts of CS at pH 2 could be ranked: CS glutamate > CS citrate > CS tartrate, but also that for the same CS M_w and initial pH of the CS solution, the viscosity of the polymer solution was a function of the acid used as a solvent (Table 1). Therefore, a strategy to control the peptide delivery from the CS matrixes consists of changing the type of acid used to dissolve the polymer prior to the freeze-drying step in the sponge preparation process. As expected and judging from the results in Fig. 6, the type of acid used to dissolve CS influenced insulin release from the sponges, the release rate ranking being: CS glutamate > CS tartrate > CS citrate. This behavior concurs with the observation that CS glutamate sponges were more soluble than those made of tartrate or citric acid, since less remaining weight was recovered. Furthermore, it was noticeable that CS citrate and tartrate sponges swelled rapidly leading to a very viscous gel-like barrier which hindered the release of the drug. The citrate CS sponges, which were the less soluble ones, exhibited slower peptide release.

Indeed, it was found that upon exposure of the sponges to the release medium, a local variable pH was created inside the sponges, this being dependent on the type of acid used as a solvent of CS, as it is shown in Table 1. This could be a factor to take into account due to the well-known pH-dependent solubility of both CS and insulin (Brange & Langkær, 1993; Rinaudo & Domard, 1989). However, in our opinion, besides the previous arguments, the key factor affecting the insulin release from sponges of different type of salts of CS is the viscosity of the CS gels resulting after hydration of the different CS salts, as it can be seen in Table 1. Note that citric and tartaric acids led to near a 20-fold increase in viscosity, in comparison to the glutamic salt of CS, a fact that greatly influences peptide diffusion through the CS gel. These results agree with those previously reported by Remuñán-López et al. (1998a) and Nigalaye, Adusumilli, and Bolton (1990) who found that CS citrate retarded the release rate of drugs from both microparticles and tablets due to its high viscosity and gel forming capacity. On the other hand, the same type of explanation could be applied to analyze the great influence of CS M_w on insulin release from sponges. As

expected, the lower the CS M_w and, hence, CS viscosity, the faster the peptide diffusion through the swollen polymer. A similar effect has already been described for bovine serum albumin release from a microparticulate system (Remuñán-López et al., 1998a) which was also predictable based on the relationship between M_w and viscosity (Adusumilli & Bolton, 1991).

With respect to the influence of the insulin dose incorporated in the device on the in vitro release results, Fig. 7 shows that low-dose insulin sponges release a significantly higher ($P < 0.05$) percentage of their content than high-dose devices. This could be due to the fact that insulin is closely bound to CS and, as a consequence, the total amount of peptide released is not strictly dependent on the total amount of peptide included in the device, as would be the case if the peptide particles were only physically dispersed in the polymer matrices. In addition, the increase in insulin dose results in a subsequent decrease in the amount of CS on the total device weight. This could lead to limited water penetration into the CS matrix, and thus, to a decrease in the percentage of insulin released. All these in vitro release studies led us to conclude that the sponges designed are versatile in terms of their release properties and that this behavior can be modulated by adequately selecting the formulation parameters.

It is well known that the mucoadhesive properties of CS are mediated by the ionic interaction between its positive amino groups and the negatively charged sialic acid in mucus, which covers the moist surface of the buccal epithelium (Lehr, Bouwstra, Schacht, & Junginger, 1992). For mucoadhesion to occur, an intimate polymer–mucosa contact must take place as a result of a good wetting of the sponge surface with saliva. Afterwards, interpenetration of the chains of the mucoadhesive with those of the mucus must occur. In a preliminary mucoadhesion study, we determined the affinity of the different sponges to the surface of a mucin film. We observed that (data not shown) for sponges made from CS solutions at pH 2, the CS citrate sponges adhered more strongly to the mucin than the tartrate and glutamate ones, the latter being found to overhydrate, loosing its structure. This could be explained by differences in viscosity and swelling properties of the various sponges as we have demonstrated before. For the glutamate salt sponges, the higher the pH, the greater the mucoadhesion. This was also related to the major integrity of sponges made from pH 4 and 6 solutions as was noted before. Unfortunately, it was not possible to quantify the force necessary to separate the mucoadhesive device and the mucin substratum by standardized methods because the polymer–mucin adhesion forces were stronger than those existing within the polymer matrix, hence leading to sponge fracture and, a part of the sponge (CS layer) remaining adhered to the mucin membrane. However, it is evident from this preliminary study that the mucoadhesive capacity of CS sponges to the mucin surface is great and that the intensity of the adhesion is mainly affected by the swelling capacity of the device, as previously demonstrated (Needleman & Smales, 1995; Remuñán-López et al., 1998b). In addition to the permeabilising effect of CS on buccal mucosa (Portero et al., 2002), the demonstrated capacity of these CS sponges to adhere to a mucosal surface and to control insulin delivery by changing several formulation variables highlights the potential of the developed bilayered sponges for buccal peptide delivery.

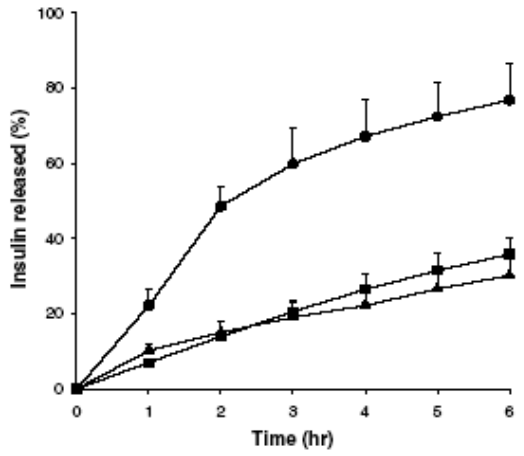

Fig. 7. Effect of drug content on insulin release from the chitosan sponges in pH 7.4 phosphate buffer (medium M_w chitosan glutamate, pH 2): (●) 1 mg, (▲) 1.75 mg and (■) 2.5 mg (mean ± SD; $n \geqslant 4$).

In conclusion, we have designed a bilayered mucoadhesive porous device based on CS, which allows the efficient unidirectional delivery of insulin. When placed in contact with a mucin membrane, the sponge remains strongly adhered to it. The water uptake/swelling and dissolution properties and consequently, the mucoadhesive properties as well as insulin release from the sponges can be modulated by selecting the M_w, type of CS salt and pH of the CS-insulin mixtures prior to freeze-drying. The system developed offers exciting opportunities for the buccal administration of peptide and protein drugs.

Acknowledgments

This work was financed by The Spanish Government (CICYT, SAF 2002-03314, FEDER cofinanced) and The *Xunta de Galicia* (PGIDT00PXI20315PR). The Pre-doctoral grant to A. Portero from the *Gobierno Vasco* is acknowledged.

References

Adusumilli, P., & Bolton, S. (1991). Evaluation of chitosan citrates complexes as matrices for controlled release formulations using a 3^2 full factorial design. *Drug Development and Industrial Pharmacy, 17*, 1931–1945.

Artursson, P., Lindmark, T., Davis, S. S., & Illum, L. (1994). Effect of chitosan on the permeability of monolayers of intestinal epithelial cells (Caco-2). *Pharmaceutical Research, 11*, 1358–1361.

Brange, J., & Langkær, L. (1993). Insulin structure and stability. In Y. J. Wang & R. Pearlman (Eds.), *Stability and characterization of protein and peptide drugs: case histories* (pp. 315–350). New York: Plenum Press.

Chen, R. H., Lin, J. H., & Yang, M. H. (1994). Relationships between the chain flexibilities of chitosan molecules and the physical properties of their casted films. *Carbohydrate Polymers, 24*, 41–46.

Cui, W. X., Kim, D. H., Imamura, M., Ion, S. H., & Inoue, K. (2001). Tissue-engineered pancreatic islets: culturing rat islets in the chitosan sponge. *Cell Transplantation, 10*, 499–502.

Fernández-Urrusuno, R., Calvo, P., Remuñán-López, C., Vila-Jato, J. L., & Alonso, M. J. (1999). Enhancement of nasal absorption of insulin using chitosan nanoparticles. *Pharmaceutical Research, 16*, 1576–1581.

Foda, N. H., El-laithy, H. M., & Tadros, M. I. (2004). Optimization of biodegradable sponges as controlled release drug matrices. I. Effect of moisture level on chitosan sponge mechanical properties. *Drug Development and Industrial Pharmacy, 30*, 369–379.

Hirano, S., Seino, H., Akiyama, I., & Nonaka, I. (1990). Chitosan – a biocompatible material for oral and intravenous administrations. In C. G. Gebelein & R. L. Dunn (Eds.), *Progress in biomedical polymers* (pp. 283–289). New York: Plenum Press.

Hoogstraate, A. J., & Wertz, P. W. (1998). Drug delivery via the buccal mucosa. *Pharmaceutical Science & Technology Today, 1*, 309–316.

Kienzle-Sterzer, C. A., Rodríguez-Sánchez, D., & Rha, C. (1982). Mechanical properties of chitosan films: effect of solvent acid. *Makromolecular Chemistry, 183*, 1353–1359.

Langoth, N., Kahlbacher, H., Schöffman, G., Schmerold, I., Schuh, M., Franz, S., et al. (2006). Thiolated chitosans: Design and in vivo evaluation of a mucoadhesive buccal peptide drug delivery system. *Pharmaceutical Research, 23*, 573–580.

Langoth, N., Kalbe, J., & Bernkop-Schnürch, A. (2005). Development of a mucoadhesive and permeation enhancing buccal delivery system for PACAP (pituitary adenylate cyclase-activating polypeptide). *International Journal of Pharmaceutics, 296*, 103–111.

Lehr, C. M., Bouwstra, J. A., Schacht, E. H., & Junginger, H. E. (1992). In vitro evaluation of mucoadhesive properties of chitosan and some other natural polymers. *International Journal of Pharmaceutics, 78*, 43–48.

Merkle, H. P., Anders, R., Wermerskirchen, A., Raehs, S., & Wolany, G. (1991). Buccal routes of peptide and protein drug delivery. In V. H. L. Lee (Ed.), *Peptide and protein drug delivery* (pp. 741–767). New York: Marcel Dekker, Inc.

Merkle, H. P., & Wolany, G. (1992). Buccal delivery for peptide drugs. *Journal of Controlled Release, 21*, 155–164.

Mi, F. L., Shyu, S. S., Wu, Y. B., Shyong, J. Y., & Huang, R. N. (2001). Fabrication and characterization of a sponge-like asymmetric chitosan membrane as a wound dressing. *Biomaterials, 22*, 163–173.

Muzzarelli, R. A. A. (1997). Human enzymatic activities related to the therapeutic administration of chitin derivatives. *Cellular and Molecular Life Sciences, 53*, 131–140.

Needleman, G., & Smales, F. C. (1995). In vitro assessment of bioadhesion for periodontal and buccal drug delivery. *Biomaterials, 16*, 617–624.

Nigalaye, G., Adusumilli, P., & Bolton, S. (1990). Investigation of prolonged drug release from matrix formulations of chitosan. *Drug Development and Industrial Pharmacy, 16*, 449–467.

Onishi, H., & Machida, Y. (1999). Biodegradation and distribution of water-soluble chitosan in mice. *Biomaterials, 20*, 175–182.

Park, Y. L., Lee, Y. M., Park, S. N., Sheen, S. Y., Chung, C. P., & Lee, S. J. (2000). Platelet derived growth factor releasing chitosan sponges for periodontal bone regeneration. *Biomaterials, 21*, 153–159.

Portero, A., Remuñán-López, C., & Nielsen, H. M. (2002). The potential of chitosan in enhancing peptide absorption across the TR146 cell culture model – an in vitro model of the buccal mucosa. *Pharmaceutical Research, 19*, 169–174.

Remuñán-López, C., & Bodmeier, R. (1996a). Mechanical and water vapor transmission properties of polysaccharide films. *Drug Development and Industrial Pharmacy, 22*, 1201–1209.

Remuñán-López, C., & Bodmeier, R. (1996b). Effect of formulation and process variables on the formation of chitosan-gelatin coacervates. *International Journal of Pharmaceutics, 135*, 63–72.

Remuñán-López, C., Lorenzo-Lamosa, M. L., Vila-Jato, J. L., & Alonso, M. J. (1998a). Development of new chitosan-cellulose multicore microparticles for controlled drug delivery. *European Journal of Pharmaceutics and Biopharmaceutics, 45*, 49–56.

Remuñán-López, C., Portero, A., Vila-Jato, J. L., & Alonso, M. J. (1998b). Design and evaluation of chitosan/ethylcellulose mucoadhesive bilayered devices for buccal drug delivery. *Journal of Controlled Release, 55*, 143–152.

Rinaudo, M., & Domard, A. (1989). Solution properties of chitosan. In G. Skjak-Brak (Ed.). *Chitin and chitosan: sources, chemistry, biochemistry, physical properties and applications* (pp. 71–86). Amsterdam: Elsevier.

Senel, S., Kremer, M. J., Kas, S., Wertz, P. W., Hincal, A. A., & Squier, C. A. (2000). Enhancing effect of chitosan on peptide drug delivery across buccal mucosa. *Biomaterials, 21*, 2067–2071.

Senel, S., Kremer, M. J., Wertz, P. W., Hill, J. R., Kas, S., Hincal, A. A., et al. (2002). Chitosan for intraoral peptide delivery. In C. Muzzarelli (Ed.), *Chitosan in pharmacy and chemistry* (pp. 77–84). Ancona: Atec Edizioni.

Sluzky, V., Klibanov, A. M., & Langer, R. (1992). Mechanism of insulin aggregation and stabilization in agitated aqueous solutions. *Biotechnology and Bioengineering, 40*, 1–9.

Tomihata, K., & Ikada, Y. (1997). In vitro and in vivo degradation of films of chitin and its deacetylated derivatives. *Biomaterials, 18*, 567–575.

Varum, K. M., Myhr, M. M., Hjerde, R. J. N., & Smidsrod, O. (1997). In vitro degradation rates of partially *N*-acetylated chitosans in human serum. *Carbohydrate Research, 299*, 99–101.

Veuillez, F., Kalia, Y. N., Jacques, Y., Deshusses, J., & Buri, P. (2001). Factors and strategies for improving buccal absorption of peptides. *European Journal of Pharmaceutics and Biopharmaceutics, 51*, 93–109.

El trabajo experimental contenido en la presente tesis ha sido financiado por el ***Ministerio de Educación*** *(CI-CYT, SAF2002-03314),* ***fondos FEDER****,* ***Xunta de Galicia*** *(PGIDIT03PXIC20301PN: Incentivo del proyecto SAF 2002-03314),* ***Programa Marie Curie*** *(European Community Program "Improving the Human Research Potential and the Socio-Economic Knowledge Base", HPMT-CT-2001-00403), y el* ***Proyecto Europeo NanoBiosaccharides*** *(European Commission within the 6th Framework program - Contract nr. 013882).*

El principal objetivo de este trabajo ha sido el desarrollo de sistemas micro- y nanoparticulares compuestos por polisacáridos y destinados a la administración pulmonar y nasal de macromoléculas terapéuticas, tales como péptidos, proteínas y ADN. Se prepararon microsferas de quitosano y quitosano/glucomanano mediante un proceso de atomización, cuyas características morfológicas y aerodinámicas, así como su capacidad de asociar y liberar insulina (molécula modelo) resultan adecuadas para su administración por vía pulmonar. El potencial de dichas formulaciones se ha visto reforzado por los resultados obtenidos en los diferentes estudios realizados *in vitro* en cultivos celulares, que demuestran su efecto promotor de la absorción de macromoléculas, su reducida citotoxicidad y su capacidad bioadhesiva. Por otra parte, utilizando una técnica de gelificación iónica extremadamente suave, se prepararon nanopartículas compuestas por quitosano y derivados aniónicos de ciclodextrina, en cuya estructura fue posible incorporar eficazmente macromoléculas (insulina y ADN). Dichos sistemas demostraron una excelente capacidad de atravesar barreras celulares y mucosas (nasal). Finalmente, y como prueba de concepto del potencial de estas nanopartículas, se realizaron estudios de expresión genética *in vitro* utilizando un modelo de epitelio nasal/bronquial, así como estudios *in vivo* (administración nasal), que condujeron a la obtención de prometedores resultados en cuanto a eficiencia de transfección y descenso de los niveles de glucemia, respectivamente.

The main objective of the present work was the development of micro- and nanoparticulate systems made of polysaccharides, intended for pulmonary and nasal delivery of therapeutic macromolecules, such as peptides, proteins and DNA. Chitosan and chitosan/glucomannan microspheres, whose morphological and aerodynamic characteristics as well as capacity to associate and release insulin (model molecule) resulted adequate for being administered by the pulmonary route, were prepared by spray-drying. The potential of these formulations was reinforced by the results obtained in the different *in vitro* studies performed in cell cultures, demonstrating their ability to enhance the permeation of macromolecules, reduced cytotoxicity and bioadhesion. On the other hand, nanoparticles consisting of chitosan and anionic cyclodextrin derivatives were prepared by the extremely mild ionic gelification technique and macromolecules (i.e. insulin and DNA) were entrapped into the nanostructure very efficiently. These systems evidenced their excellent capability to overcome cellular and mucosal barriers (i.e. nasal). Finally, as a proof-of-concept of the potential of these nanoparticles, *in vitro* gene expression studies (nasal/bronchial epithelium model) and *in vivo* studies (nasal administration) were performed, obtaining promissing results with regard to transfection efficiency and decrease of glucose levels, respectively.